

NOTTINGHAM   
TRENT UNIVERSITY

**Flexural Behaviour of Enhanced  
Foamed Concrete Beams Reinforced  
with GFRP Bars**

By

**Nadir Alkurdi**

BEng, MSc (Honours) Civil Eng

Thesis submitted to Nottingham Trent University in fulfilment of  
the requirements for the degree of Doctor of Philosophy School of  
Architecture, Design and the Built Environment

**July 2021**

## DECLARATION

This thesis has been submitted to Nottingham Trent University (NTU) for the degree of PhD. I declare that the work in this thesis was carried out following the regulations of NTU and it is original except where indicated by specific reference. The research reported in this thesis was conducted at Nottingham Trent University between April 2017 and July 2021. Any views expressed in this thesis are those of the author and in no way represents the university.

Nadir Alkurdi (July 2021)

## LIST OF PUBLICATIONS

### JOURNAL PAPERS:

- Alkurdi, N.M., Mohammad, F.A., Klalib, H.A., 2020. Mechanical properties and direct tensile strength of waste toner foamed concrete. J. Adv. Civ. Eng. Pract. Res. 11, 11.
- Alkurdi, N.M., Mohammad, F.A., Klalib, H.A., 2021. Flexural behaviour of foamed concrete beam reinforced with GFRP bars. (Under internal review)

### CONFERENCE PAPERS:

- Alkurdi, N.M., Mohammad, F.A., Klalib, H.A., 2019. Direct and indirect tensile strength testing for foamed concrete. School of Architecture, Design and the Built Environment, Nottingham Trent University. (School conference)

[Check the link: https://www.researchgate.net/profile/Nadir-Alkurdi](https://www.researchgate.net/profile/Nadir-Alkurdi)

## ABSTRACT

Concrete is the second most widely consumed substance on earth after water. However, normal-weight concrete is a relatively heavy construction material with a density of  $2400 \text{ kg/m}^3$ , which adds extra load on structures, resulting in larger foundations and structural elements section. The second issue is reinforcement corrosion, which has been one of the main durability problems in reinforced concrete. Therefore, there is a need for lightweight reinforced concrete that resists corrosion. This research aims to produce sustainable lightweight concrete reinforced with non-corrosive bars, which has the potential to be used in structural applications. The use of Foamed Concrete (FC) reinforced with Glass Fibre Reinforced Polymer (GFRP) bars in structural elements will reduce permanent actions on structures and foundations, contributes to more sustainable, energy-efficient construction and cost reduction by reducing structural elements size, labour and energy during transportation and construction stages, reinforcement corrosion repair and maintenance.

To investigate and develop the mechanical properties and structural behaviour of FC to be suitable for structural applications, 876 specimens classified into six different densities (800, 1000, 1200, 1400, 1600 and  $1800 \text{ kg/m}^3$ ) were tested. For each concrete density, four mixes were designed including the control mix and three different additives: metakaolin, silica fume and waste toner. The waste toner additive was collected from used printer cartridges. The experimental programme was considered to introduce a modified direct tensile test, where splitting and flexural tests were conducted to confirm its reliability. Full scale beams made of normal/ foamed concrete reinforced with steel/GFRP bars were tested experimentally, theoretically and numerically using Finite Element Modelling FEM.

The waste toner additive improved the FC mechanical properties by 30%. The bond between FC and GFRP bars was found to be 95% of normal weight concrete and steel bars. With the same total reinforcement amount of GFRP and steel bars, the ultimate flexural capacity of the GFRP reinforced foamed concrete beam was 87% of that in the steel-reinforced concrete beam, but the deflection

and maximum crack width were larger than those of steel-reinforced concrete beams under the same service load levels. The results from FEM, showed good agreement with the experiment results. The theoretical equations developed in this study reasonably predicted the failure moments of the steel/GFRP reinforced. These results are promising and point to the significant potential of developing eco-friendly lightweight concrete reinforced with lightweight and anti-corrosive reinforcement bars.

**KEYWORDS:** Foamed concrete (FC); Waste toner; Mechanical property development; Sustainability, Fibre Reinforced Polymer bars (GFRP); Flexural behaviour.

## ACKNOWLEDGEMENT



In the name of ALLAH, the Most Gracious and the Most Merciful

First and foremost, all praise is to ALLAH for endowing me with health, patience, strength, countless blessings, the opportunity and knowledge to complete this PhD successfully.

I would like to thank all my beloved family, especially my mother and father who I am indebted to, for taking care and supporting me with prayers and patience during the completion of my studies which would have been impossible for me to complete alone. I have been fortunate to have parents who always cared for me, encouraged me and gave me guidance, endless love, and comforting hands while preparing me for my future. May Allah bless you all with joy and happiness.

The completion of this thesis would not have been possible without the support and encouragement of many people. I express my sincere gratitude to all those who have helped me succeed. It is impossible to list everyone here, but several people deserve special mention. First of all, I acknowledge and thank, with sincere gratitude and appreciation both my supervisors, Dr Mohammad Fouad and Dr Hynda Klalib for their exceptional supervision, encouragement, continuous guidance, feedback, freedom and constant interest in my research area. I hope this partnership has been as memorable and enjoyable for you as it has been for me. I also acknowledge the financial support from the Libyan Ministry of Higher Education and Sabratha University.

I would like to further extend my thanks to the technical laboratory staff members who I always went to with unusual demands which they found miraculous solutions. A massive thanks to Julian Robinson, David Nix, Judith Kipling, Matt Garlick, Dave Edwards, William Zindoga, who assisted in all material preparing and testing, and for all their valuable assistance in the laboratory. Also, special thanks go to Dr Bubaker Shakmak, Dr Ahmad Ghaladanci for their assistance in formatting and using FEM and Mendeley software. I would also like to thank Hynda for the useful discussions, encouragement and priceless advice. Finally, I would like to express special thanks to all my fellow PhD researchers in the School of ADBE. Also, many thanks to Abdalhakem Alkhdashi, Ahmad Ghaladanci for their support.

Far from academic, special appreciation to my friends for their invaluable support during this four-year study including Uncle Rasheed, Abdullah Ragra, Abdalhakem Alkhdashi, Ahmad Ghaladanci, Ramadan with whom I have shared many memorable moments. Your friendship makes my life a wonderful experience. Your support is irreplaceable in the context of this work.

Finally, I want to express my deepest gratitude towards all those people who have played a part in my life so far but not mentioned.

A big thank you to all of you.

Nadir Alkurdi (July 2021)

# Table of Contents

<b>DECLARATION .....</b>	<b>II</b>
<b>LIST OF PUBLICATIONS .....</b>	<b>III</b>
<b>ABSTRACT .....</b>	<b>IV</b>
<b>ACKNOWLEDGEMENT .....</b>	<b>VI</b>
<b>TABLE OF CONTENTS .....</b>	<b>VIII</b>
<b>LIST OF FIGURES .....</b>	<b>XIII</b>
<b>LIST OF TABLES.....</b>	<b>XVIII</b>
<b>LIST OF ABBREVIATIONS .....</b>	<b>XX</b>
<b>LIST OF NOTATIONS .....</b>	<b>XXIII</b>
<b>CHAPTER 1 .....</b>	<b>1</b>
<b>INTRODUCTION.....</b>	<b>1</b>
1.1    RESEARCH MOTIVATION .....	1
1.2    LIGHTWEIGHT CONCRETE .....	3
1.2.1    Foamed Concrete (FC) .....	3
1.3    FOAMED CONCRETE IN STRUCTURAL APPLICATIONS .....	5
1.4    FIBRE-REINFORCED POLYMER (FRP) .....	6
1.5    GLASS FIBRE REINFORCED POLYMER (GFRP) .....	6
1.6    PROBLEM STATEMENT.....	7
1.7    AIM, OBJECTIVES, AND METHODOLOGY .....	8
1.7.1    Aim .....	8
1.7.2    Objectives .....	8
1.8    SCIENTIFIC NOVELTY .....	9
1.9    SCOPE OF RESEARCH .....	9
1.10    METHODOLOGY.....	10
<b>CHAPTER 2 .....</b>	<b>12</b>
<b>LITERATURE REVIEW .....</b>	<b>12</b>
2.1    INTRODUCTION.....	12
2.1.1    Lightweight Concrete .....	13
2.2    CELLULAR OR AERATED CONCRETE .....	14
2.3    FOAMED CONCRETE .....	15
2.3.1    Specifications.....	17
2.3.2    Developments .....	19

2.4	ADVANTAGE OF FRESH FOAMED CONCRETE .....	20
2.5	ADVANTAGE OF HARDENED FOAMED CONCRETE .....	21
2.6	LIGHTWEIGHT FOAMED CONCRETE CURRENT APPLICATIONS .....	21
2.7	PRODUCTION OF FOAMED CONCRETE .....	26
2.7.1	Constituent Materials.....	26
2.7.2	Mix Design and Procedure .....	31
2.7.3	Preparation of Foamed Concrete .....	32
2.8	PROPERTIES OF FOAMED CONCRETE .....	33
2.8.1	Fresh Properties .....	33
2.8.2	Hardened Properties .....	35
2.9	REINFORCED CONCRETE.....	41
2.10	GLASS FIBRE REINFORCED POLYMER (GFRP) BARS .....	42
2.10.1	Developments of Fibre Reinforced Composite Materials .....	43
2.10.2	Constituent Materials.....	44
2.10.3	Production and Manufacturing Process .....	45
2.10.4	Properties of FRP Reinforcement .....	46
2.10.5	GFRP bar Mechanical Properties .....	48
2.10.6	Durability .....	52
2.10.7	Current Use of GFRP in Structures.....	53
2.11	EXISTING FRP RC DESIGN GUIDELINES .....	53
2.12	FLEXURAL BEHAVIOUR OF FRP REINFORCED CONCRETE MEMBERS.....	54
2.12.1	Bond Behaviour of FRP Reinforcement .....	54
2.12.2	Deflection of FRP RC Members.....	57
2.12.3	Shear Capacity in FRP RC Members.....	60
2.12.4	Moment of Resistance of FRP RC Members .....	62
2.13	SUMMARY.....	64
<b>CHAPTER 3 .....</b>		<b>65</b>
<b>FOAMED CONCRETE DEVELOPMENT: EXPERIMENTAL PROGRAMME.....</b>		<b>65</b>
3.1	INTRODUCTION.....	65
3.2	MATERIALS.....	66
3.2.1	Cement .....	66
3.2.2	Silica Fume (SF).....	67
3.2.3	Metakaolin (MK).....	67
3.2.4	Waste Toner .....	69
3.2.5	Fine Aggregate.....	70
3.2.6	Water.....	70
3.2.7	Foaming Agents (surfactants).....	71
3.3	MIX DESIGN .....	72

3.3.1	Examples of Mix Design .....	73
3.4	EXPERIMENTAL CONCRETE PRODUCTION .....	74
3.4.1	Foam Production .....	74
3.4.2	Foamed Concrete Production .....	75
3.4.3	Preparation of Forms and Sampling .....	76
3.5	CURING .....	76
3.6	TEST PROGRAMME .....	77
3.6.1	Fresh State and Early Age Tests .....	77
3.6.2	Hardened Concrete Tests .....	81
3.7	GFRP MECHANICAL PROPERTIES TESTING .....	90
3.7.1	Bond Behaviour .....	92
3.8	SUMMARY .....	96
<b>CHAPTER 4 .....</b>		<b>100</b>
<b>FOAMED CONCRETE DEVELOPMENT: RESULTS AND ANALYSIS .....</b>		<b>100</b>
4.1	INTRODUCTION .....	100
4.2	MECHANICAL PROPERTIES .....	100
4.2.1	Compressive Strength .....	100
4.2.2	Flexural Strength (Modulus of Rupture) .....	106
4.2.3	Splitting Tensile Strength .....	109
4.2.4	Direct Tensile Strength .....	113
4.2.5	Shear Strength .....	117
4.2.6	Stress-Strain Relationship and Modulus of Elasticity .....	120
4.3	BOND BEHAVIOUR FROM PULL-OUT AND BEAM TESTS .....	125
4.4	SUMMARY .....	135
<b>CHAPTER 5 .....</b>		<b>137</b>
<b>FLEXURAL BEHAVIOUR OF GFRP REINFORCED FOAMED CONCRETE BEAMS .....</b>		<b>137</b>
5.1	INTRODUCTION .....	137
5.2	FULL-SCALE BEAM FLEXURAL TESTING .....	137
5.2.1	Materials Properties .....	137
5.2.2	Test Specimens and Preparations .....	139
5.2.3	Beam Properties and Assumptions .....	139
5.3	THEORETICAL DERIVATIONS OF REINFORCED CONCRETE BEAM .....	140
5.3.1	Material Characteristics .....	141
5.3.2	Normal Concrete Beam Reinforced with Steel (NC+S) .....	146
5.3.3	Foamed concrete beam reinforced with steel (FC+S) .....	152
5.3.4	Normal Concrete Beam Reinforced with GFRP (NC+GFRP) .....	157
5.3.5	Foamed Concrete Reinforced with GFRP (FC+GFRP) .....	161

5.4	SUMMARY OF THE ULTIMATE MOMENTS OF RESISTANCE .....	165
5.5	RESULT AND ANALYSIS .....	166
5.5.1	Load-Deflection Response.....	166
5.5.2	Concrete and Reinforcement Load - Strain Response.....	167
5.5.3	Bending Moment.....	169
5.5.4	Crack Propagation and Failure Modes .....	172
5.6	SUMMARY.....	175
<b>CHAPTER 6.....</b>		<b>177</b>
<b>FINITE ELEMENT MODELLING OF GFRP REINFORCED FOAMED CONCRETE BEAMS.....</b>		<b>177</b>
6.1	INTRODUCTION.....	177
6.2	FINITE ELEMENT METHOD .....	177
6.3	NONLINEAR FINITE ELEMENT ANALYSIS .....	179
6.4	ABAQUS OVERVIEW .....	180
6.5	FE MODELLING OF CONCRETE IN ABAQUS.....	181
6.6	FE MODELLING OF REINFORCEMENT IN ABAQUS .....	184
6.6.1	Smearred Model .....	184
6.6.2	Discrete Model .....	184
6.6.3	Embedded Model .....	185
6.7	ELEMENT TYPES.....	186
6.7.1	Concrete .....	186
6.7.2	Reinforcement.....	187
6.8	MATERIALS PROPRIETIES.....	188
6.8.1	Concrete .....	189
6.8.2	Reinforcement Rebar .....	190
6.9	GEOMETRY .....	190
6.10	MESHING .....	191
6.11	LOADING AND BOUNDARY CONDITIONS.....	192
6.12	LOAD STEPPING AND FAILURE DEFINITION FOR FE MODEL .....	193
6.13	METHODS FOR NON-LINEAR SOLUTION .....	194
6.14	NUMERICAL MODELLING RESULTS .....	195
6.14.1	Load-Deflection Analysis .....	196
6.14.2	Strain Distribution of Beam Section. ....	198
6.14.3	Moment Resistance of RC Beam .....	200
6.14.4	Cracking Pattern and Failure Mode.....	201
6.15	SUMMARY.....	206
<b>CHAPTER 7.....</b>		<b>207</b>
<b>CONCLUSIONS AND RECOMMENDATIONS .....</b>		<b>207</b>
7.1	OVERVIEW .....	207

7.2	CONCLUSIONS .....	207
7.3	RECOMMENDATIONS FOR FUTURE WORK .....	209
	<b>REFERENCES.....</b>	<b>211</b>
	<b>APPENDIX A: FOAMED CONCRETE MIX DESIGN.....</b>	<b>227</b>
	<b>APPENDIX B: GLASS FIBER REINFORCED POLYMER GFRP PROPERTIES .....</b>	<b>229</b>
	<b>APPENDIX C: STRESS BLOCK CALCULATIONS EXAMPLE .....</b>	<b>230</b>

## List of Figures

Figure 1-1: Normal weight concrete disadvantages (Heavyweight and reinforcement corrosion)(www.nist.gov) .....	2
Figure 1-2: Research flowchart .....	11
Figure 2-1: Different methods to produce Lightweight concrete (Newman and Choo, 2003) .....	14
Figure 2-2: Lightweight concrete main types.....	15
Figure 2-3: The main components of fomed concrete .....	16
Figure 2-4: Foamed concrete production using the pre-foamed method(Alkurdi et al., 2020) .....	17
Figure 2-5: Some of the lightweights foamed concrete applications (www.dr-luca.com, 2009) .....	22
Figure 2-6: Produce Foam from water, foaming agents and compressed air (EAB Associated, 2001) .....	31
Figure 2-7: Strength density variation for mixes with different c/s ratios (Nambiar and Ramamurthy, 2006b) .....	37
Figure 2-8: Elastic modulus of foamed concrete graphical definition .....	40
Figure 2-9: The most common types of FRP bars ((Benmokrane et al., 2021).....	43
Figure 2-10: Aberfeldy Footbridge (Reinforced with GFRP bars) .....	44
Figure 2-11: Basic material components of FRP composite .....	44
Figure 2-12: Stress-strain relationship for resin, fibres, FRP composite (reproduced from ISIS Canada, 2007) .....	45
Figure 2-13: Pultrusion process for FRP bars .....	46
Figure 2-14: GFRP R–glass bars (Worner, 2015) .....	46
Figure 2-15: Stress-strain curves for typical reinforcing bars .....	50
Figure 2-16: Mechanism of shear and flexural resistance of FRP bar .....	51
Figure 2-17: Structural applications of concrete reinforced with GFRP bars .....	53
Figure 2-18: Tension stiffening mechanism .....	55
Figure 2-19: Bond stress along the length of the bar .....	56
Figure 2-20: Mechanisms of flexural bars crossing a crack .....	60

Figure 3-1: Portland cement and additives materials.....	70
Figure 3-2: Foam making products showing (a) foaming agent (b) foaming machine and (c) foam: .....	72
Figure 3-3: Foam production and use in foamed concrete showing (A) Foam generator (B) Foam (C) Foam mixed with raw concrete .....	75
Figure 3-4: Foamed concrete production showing (A) dry materials (B) dry materials in rotary drum (belly mixer) (C) foam added to the wet mix (D) foamed concrete product. .	76
Figure 3-5: The form preparation and casting showing (A) Form preparation, (B) Foamed concrete in a cube form, (B) Foamed concrete is cast in cylinders, cube and prism form, (D) Demoulded foamed concrete cubes.....	76
Figure 3-6: Foamed concrete beams, prism, cylinders and cubes are sealed for curing. ...	77
Figure 3-7: Dimensions of modified Marsh cone.....	78
Figure 3-8: Designed wet, measured wet and fully dried densities of foamed concrete. ..	81
Figure 3-9: Compression test for cubes and cylinders.....	82
Figure 3-10: Static Modulus of Elasticity test .....	84
Figure 3-11: Four points load flexural test.....	85
Figure 3-12: Splitting tensile (Brazilian) test .....	86
Figure 3-13: Direct tensile test shown (A) Test setup, (B) prism casting, (C) Direct tension applied on the prism and (D) Failed prisms. ....	87
Figure 3-14: Direct tensile test for foamed concrete .....	88
Figure 3-15: Modified direct shear test setup for formed concrete.....	89
Figure 3-16: Shear test shows (A) test setup (B) shear test and (C) shear cracks under loading. ....	90
Figure 3-17: Direct tensile test setup for GFRP bar .....	91
Figure 3-18: Pull-out test specimen .....	92
Figure 3-19: Pull-out test shows (A) specimens casting, (B) specimens curing, (C) pull-out test, (D) failed specimens.....	93
Figure 3-20: Beam bond test specifications and dimensions .....	94
Figure 3-21: Beam bond test preparing and testing.....	95
Figure 4-1: Effect of cement content on compressive strength .....	102
Figure 4-2:The effect of density on the compressive strength.....	103
Figure 4-3: Compressive strength/ density ratio with Density .....	104

---

Figure 4-4: The effect of additives on compressive strength (in 1:1.5 c/s ratio mix) .....	105
Figure 4-5: Compressive strength of different design mix .....	106
Figure 4-6: Effect of density and additives on flexural Strength .....	108
Figure 4-7: Relationship between flexural strength and 28-day compressive strength of FC18Ton, NWC, LWC and FC .....	109
Figure 4-8: Effect of density and additives on FC splitting tensile strength .....	111
Figure 4-9: Compressive and splitting tensile strength relationship. ....	112
Figure 4-10: Relationship between splitting tensile strength and 28 days compressive strength of LWCA and FC .....	113
Figure 4-11: Direct tensile testing for foamed concrete.....	114
Figure 4-12: Load - displacement for FC specimens under direct tension .....	115
Figure 4-13: Effect of density and additives on direct tensile strength.....	116
Figure 4-14: Tensile strength from direct and indirect tension testes .....	117
Figure 4-15: Effect of density and additives on FC shear strength .....	119
Figure 4-16: Shear and compressive strength relationship in foamed concrete .....	120
Figure 4-17: The stress-strain relationships of normal and foamed concrete .....	121
Figure 4-18: Effect of density and additives on FC modulus of elasticity from direct compression .....	123
Figure 4-19: Relationship between compressive strength and modulus of elasticity of NWC, SSC and FC.....	124
Figure 4-20: Distribution of bond stress between cracks .....	125
Figure 4-21: Typical modes of failures that occurred experimentally.....	127
Figure 4-22: Effect of density on the bond strength.....	128
Figure 4-23: Effect of additives on bond strength .....	129
Figure 4-24: Effect of bar size on bond strength .....	130
Figure 4-25: Effect of bar material on bond strength .....	131
Figure 4-26: Experimental and theoretical bond strength for steel and GFRP bars.....	133
Figure 5-1: Full scale beams flexure test preparations (A) GFRP and steel reinforcement (B) Strain gage on reinforcement (C) Beams ready for casting (D) Concrete beam testing ...	138
Figure 5-2: Full-scale beams casting, curing and testing .....	139
Figure 5-3: Full-scale beam model under four-point load test.....	140
Figure 5-4: Typical short-term stress-strain curve for concrete .....	142

---

Figure 5-5 Parabolic –rectangular stress-strain diagram for concrete in compression as per EC2.....	143
Figure 5-6 Design stress-strain diagram for reinforcing steel.....	145
Figure 5-7 Design stress-strain diagram for reinforcing steel and GFRP .....	146
Figure 5-8 Parabolic-rectangular design stress block for the ultimate limit state- EC2 (Normal concrete reinforced with steel) .....	147
Figure 5-9: Parabolic-rectangular design stress block for the ultimate limit state- EC2 (Foamed concrete reinforced with steel) .....	152
Figure 5-10: Parabolic-rectangular design stress block for the ultimate limit state- EC2 (Normal concrete reinforced with GFRP).....	157
Figure 5-11: Parabolic-rectangular design stress block for the ultimate limit state- EC2 (Foamed concrete reinforced with GFRP).....	161
Figure 5-12: Midspan Load-deflection response .....	167
Figure 5-13: The load-strain relationship for concrete and reinforcement for all beams.	168
Figure 5-14: Concrete and reinforcement Load-strain relationships .....	169
Figure 5-15: Bending moment-deflection for normal concrete reinforced with steel.....	170
Figure 5-16: Bending moment-deflection for foamed concrete reinforced with steel.....	170
Figure 5-17: Bending moment-deflection for normal concrete reinforced with GFRP.....	171
Figure 5-18: Bending moment-deflection for foamed concrete reinforced with GFRP ....	172
Figure 5-19: Crack pattern and failure mode of NC+S beam .....	173
Figure 5-20: Crack pattern and failure mode of FC+S beam.....	174
Figure 5-21: Crack pattern and failure mode of NC+GFRP beam .....	174
Figure 5-22: Crack pattern and failure mode of FC+GFRP beam.....	175
Figure 6-1: Nonlinear finite element solution procedures for reinforced concrete beams .....	180
Figure 6-2: Definitions of the stress-strain curves of the concrete damage model in ABAQUS (Bitiusca and Clausen, 2016) .....	183
Figure 6-3: Smearred formulations for reinforced concrete.....	184
Figure 6-4: Shared nodes between concrete elements and reinforcement elements .....	185
Figure 6-5: Embedded formulations for reinforced concrete .....	185
Figure 6-6: Embedded element technique applied for the reinforced concrete beams...	186

---

Figure 6-7: (A) Typical plane stress quadrilateral 4 node element (B) Typical 8 nodes linear brick element .....	187
Figure 6-8: ABAQUS mode of the concrete beams.....	187
Figure 6-9: Typical 2 nodes truss element .....	188
Figure 6-10: ABAQUS model of reinforcement.....	188
Figure 6-11: Typical uniaxial behaviour of plain concrete .....	189
Figure 6-12: Beam geometry and diminutions .....	191
Figure 6-13: Concrete beam meshing.....	192
Figure 6-14: Boundary condition notation in ABAQUS.....	192
Figure 6-15: Supports and applied loads on concrete beams .....	193
Figure 6-16: Steps in ABAQUS simulation .....	195
Figure 6-17: FEA ABAQUS mid-span deflection of GFRP and steel-reinforced beams.....	197
Figure 6-18: Load-deflection values (ABAQUS Vs Experiment) .....	198
Figure 6-19: Non-linear strain distribution along the depth of the beams .....	199
Figure 6-20: The stress in reinforcement at the ultimate applied load.....	200
Figure 6-21: The theoretical, experimental and ABAQUS moment capacity of the beams .....	201
Figure 6-22: Normal concrete reinforced with steel crack pattern and failure mode in ABAQUS.....	202
Figure 6-23: Foamed concrete reinforced with steel crack pattern and failure mode in ABAQUS.....	203
Figure 6-24: Normal concrete reinforced with GFRP crack pattern and failure mode in ABAQUS.....	204
Figure 6-25: Foamed concrete reinforced with GFRP crack pattern and failure mode in ABAQUS.....	205

## List of Tables

Table 1-1: Mechanical properties of normal and foamed concrete.....	4
Table 2-1: Main published specifications for foamed concrete in the UK.....	18
Table 2-2: The main researchers/universities developments in Foamed Concrete.....	20
Table 2-3 Applications of lightweight foamed concrete.....	23
Table 2-4: Table Surfactant types and properties (McCarthy, 2004) .....	30
Table 2-5: Typical properties including compressive strength of foamed concrete (Hamad, 2014). .....	37
Table 2-6: Typical coefficients of thermal expansion for GFRP compared with steel and concrete (Aydin, 2018).....	47
Table 2-7: Size designation and minimum guaranteed tensile strength of FRP round bars (Shakir Abbood et al., 2020).....	49
Table 2-8: Typical mechanical properties and bond strength of GFRP bar (Shakir Abbood et al., 2020).....	57
Table 2-9: Deflection design equations for FRP reinforced concrete members .....	58
Table 2-10: The shear design for FRP reinforced concrete elements without shear reinforcement .....	61
Table 3-1: Experimental research programme .....	66
Table 3-2: Chemical composition and main properties of cement and fillers, percentage by mass compound .....	68
Table 3-3: Absolute volume method for mix design.....	73
Table 3-4: Classification of foamed concrete flow ((Jones et al., 2003) .....	78
Table 3-5: The plastic (wet) and target dry density .....	80
Table 3-6: Summary of the experimental procedure to test and develop FC mechanical properties.....	97
Table 4-1: compressive strength for concrete mixes with different densities and different cement /sand ratios. ....	101
Table 4-2: Flexural strength for different FC mixes with densities (800-1800) kg/m <sup>3</sup> .....	107
Table 4-3: Splitting tensile strength for different FC mixes with densities (800-1800) kg/m <sup>3</sup> .....	110

---

Table 4-4: Shear strength for different Foamed Concrete mixes .....	118
Table 4-5: Modules of elasticity for different FC mixes .....	122
Table 4-6: Bond behaviour from Pull-out test .....	134
Table 5-1: The mechanical properties of GFRP and Steel reinforcing bar .....	138
Table 5-2: Beam materials properties.....	140
Table 5-3: The concrete characteristic strength classes (Eurocode 2, 2004) .....	143
Table 5-4: Summary of all beams ultimate moment of resistance.....	165
Table 5-5: The theoretical ultimate moment of resistance .....	166
Table 5-6: Structural performance and failure mode of the concrete beams .....	173
Table 6-1: The concrete damage plasticity parameters .....	183
Table 6-2: Elastic parameters of concrete .....	189
Table 6-3: Steel and GFRP rebar main properties.....	190

## List of Abbreviations

12Ton	Waste toner foamed concrete with a target plastic density of 1200 kg/m <sup>3</sup>
14MK	Metakaolin foamed concrete with a target plastic density of 1400 kg/m <sup>3</sup>
16Co	Control (No additives) foamed concrete with a target plastic density of 1600 kg/m <sup>3</sup>
18FS	Silica fume foamed concrete with a target plastic density of 1800 kg/m <sup>3</sup>
AAC	Autoclaved aerated concrete
ABS	Australian Bureau of Statistics
AC	Aerated concrete
ACI	American Concrete Institute
AEA	Air-entraining agent
AFRP	Aramid Fibre Reinforced Polymer
ASR	Alkali-silica reactivity
ASTM	The American Society for Testing and Materials
BCA	British Cement Association
BCM	Brittle Cracking Model
BFRP	Basalt Fibre Reinforced Polymer
BRE	British Research Establishment
BS	British Standard Institution
BS EN	British Standard European Norm
C	Concrete
CAC	Chemically Aerated Concrete
CDPM	Concrete Damaged Plasticity Model
XX	

CEM	Centre for Evaluation and Monitoring
CFRP	Carbon Fibre Reinforced Polymer
CTU	Concrete Technology Unit
FC	Foamed concrete
FC+GFRP	Foamed concrete reinforced with GFRP
FC+S	Foamed concrete reinforced with steel
FEM	Finite element method
FRP	Fibre Reinforced Polymer
GFRP	Glass Fibre Reinforced Polymer
HAUC	Highway Authorities and Utilities Committee
LWC	Lightweight concrete
LWFC	Lightweight foamed concrete
MK	Metakaolin
NAAC	Non-autoclaved concrete
NC+GFRP	Normal concrete reinforced with GFRP
NC+S	Normal concrete reinforced with steel
NWC	Normal weight concrete
SCC	Self-compacting concrete
SCM	Smearred Crack Model
SF	Silica fume
SFC	Structural Foamed Concrete
TRL	The Highways Agency and Transport Research Laboratory
UKWIR	UK Water Industry Research

WRAP      Waste & Resources Action Programme

---

## List of Notations

$[K]$	Assembled global stiffness matrix
$\{F\}$	Vector of applied nodal forces
$\{U\}$	Vector of global displacement
$A_b$	Reinforcement bar area
$A_f$	Area of longitudinal reinforcement
$b$	Width
$b_w$	Beam effective width
$C_c$	Compression force in concrete above the neutral axis
$d$	Effective depth
$d_c$	Concrete cover of an outermost bar
$D_{dry}$	Dry density of foamed concrete
$d_b$	Bar diameter
$D_{wet}$	Wet density of foamed concrete
$E$	Modulus of elasticity
$E_f$	Modulus of elasticity of FRP
$E_{fk}$	Characteristic modulus of elasticity of longitudinal reinforcement
$E_s$	Modulus of elasticity of steel longitudinal bars
$F$	Maximum load at the time of failure
$f'_c$	Concrete cylinder compressive strength
$f_{cd}$	Design compressive strength of concrete
$f_{ck}$	Characteristic value of concrete cylinder compressive strength

---

$f_{ck\ cube}$	Corresponding characteristic concrete cube strength
$f_f$	Tensile stress in longitudinal FRP bar
$f_{fd}$	Design tensile strength of FRP rebar
$f_{fk}$	Characteristic ultimate tensile strength of longitudinal reinforcement
$f_{fu}$	Ultimate tensile strength of longitudinal FRP reinforcement
$F_{max}$	Maximum pull-out force
$f_r$	Flexural strength of concrete
$f_{sp}$	Splitting tensile strength of concrete
$F_T$	Tensile force developed in an FRP bar
$f_t$	Direct tensile strength of concrete
$F_u$	Maximum load at the time of failure
$I_e$	Effective moment of inertia
$I_g$	Moment of inertia of the cross-section
$K_p$	1.0 for FRP bars with similar bond characteristics to that of steel
$L$	Length of specimen
$L_{cr}$	Moment of inertia of cracked section transformed to concrete
$M_1$	Mass of empty container
$M_2$	Combined mass of container and samples
$M_a$	Applied moment
$M_{cr}$	Cracking moment
$M_u$	Ultimate moment of resistance
$P_{max}$	Maximum pull-out load
$T$	Tension force in the reinforcing bar at balance

---

$v$	Volume of concrete produced by the batch
$V_c$	Shear strength of concrete
$V_f$	Shear force for FRP
$\omega$	Crack width measured at the extreme beam bottom level,
$W_{ct}$	Weight of cement in the batch
$W_{da}$	Weight of dry aggregate in the batch
$x$	Neutral axis depth
$X_{FRP}$	Neutral axis depth of concrete section reinforced with FRP bars
$X_{steel}$	Neutral axis depth of concrete section reinforced with steel bars
$\alpha$	Coefficient taking into account long term effects on the compressive strength and of unfavourable effects resulting from the way the load is applied
$\alpha_1$	Ratio of the average of characteristic compressive strength of concrete to the average compressive stress
$\alpha_2$	Ratio of the depth of the neutral axis to the centroid of the stress block from the compression face depth
$\alpha_3$	Ratio of the distance between and the neutral axis to the depth of the neutral axis
$\alpha_{cc}$	Coefficient taking account of long-term effects on the compressive strength and of unfavourable effects resulting from the way the load is applied
$\beta$	Ratio of distances to the neutral axis from the extreme beam bottom level and the centroid of longitudinal bars
$\beta_1$	Concrete strength factor
$\gamma_c$	Partial safety factor for concrete
$\epsilon_a$	Strain under the upper stress

---

$\epsilon_b$	Strain under the basic stress
$\epsilon_c$	Concrete compressive strain
$\epsilon_{cu}$	Concrete ultimate compressive strain
$\epsilon_f$	Tensile strain of longitudinal reinforcement
$\epsilon_{fd}$	FRP design tensile strain
$\epsilon_{fu}$	Ultimate tensile strain of longitudinal reinforcement
$\epsilon_{fw}$	Maximum allowable strain to be developed in the shear reinforcement
$\eta$	Factor defining effective strength of concrete
$\lambda$	Factor defining the effective height of compression zone
$\xi$	Ratio of neutral axis depth to the effective depth
$\rho_{dry}$	Target dry density
$\rho_f$	Reinforcement ratio for longitudinal reinforcement
$\rho_{bal}$	Balanced reinforcement ratio for longitudinal reinforcement
$\rho_m$	Target plastic density
$\sigma_a$	Upper loading stress
$\sigma_b$	Basic stress
$\tau$	Bond stress
$\tau_{b,max}$	Maximum bond strength
$\tau_{max}$	Ultimate shear strength of concrete
$\gamma$	Unit weight of concrete
$\gamma_c$	Safety factor for concrete at the Ultimate Limit State, for persistent and transient design situations

# Chapter 1

## Introduction

### 1.1 Research Motivation

Concrete has been considered by the construction industry as the most essential building material. It is widely used due to its many favourable characteristics such as workability, durability, adequate strength and the availability of its raw materials (water, cement and aggregates) (Mohammed and Hamad, 2014). Concrete by definition is a composite material made of aggregate particles and a binding medium, which can be moulded into any shape (Kosmatka, 2015). Reinforced concrete is a combination of reinforcement and concrete and finds application in various types of construction works. Reinforced concrete is used for construction, such as bridges, dams, piers, tall buildings and stadiums. It is most commonly used in domestic construction for the footings and foundations.

Deolalkar (2016) stated that concrete has been the second most widely consumed substance on earth after water in the last 30 years. Concrete structure with proper design and construction is preferable in terms of durability, economy and functionality compared to structures made from other structural materials, such as timber or steel. Concrete is the favoured construction material for a wide range of civil engineering structures such as bridges, roads and buildings (Tan et al., 2013). However, the use of normal concrete reinforced with steel in the future construction industry is facing obstacles due to:

- 1- Normal weight concrete is a relatively heavy construction material with a density of  $2400 \text{ kg/m}^3$ , with a weight/strength ratio of 4-5 times higher in concrete than that in steel. In a concrete structure, self-weight represents an enormous percentage of the total load of the structure.
- 2- Steel is often used as a reinforcing agent for concrete, and it is very energy-intensive. The steel industry generates between 7 and 9% of direct emissions from the global use of fossil fuel. 1.85 tonnes of  $\text{CO}_2$  were emitted for every tonne of steel produced (World Steel Association, 2020). Using GFRP bars to reinforce concrete instead of steel is more sustainable where it can reduce carbon dioxide production by about 30%.

Reinforcement corrosion has been one of the main durability problems in reinforced concrete. It is the chief factor in limiting the life expectancy of RC structures (Abedini et al., 2017). Figure 1-1 illustrates normal weight concrete reinforcement corrosion.

- 3- The inductive effect mainly affects the steel reinforcement embedded in concrete foundations in high-voltage power electronics systems, due to the rebar's high electric conductivity. Steel rebar could act as a Faraday cage in some reinforced concrete structures such as underground structures and tunnels, where the electromagnetic waves are blocked outside and inside the cage.



*Figure 1-1: Normal weight concrete disadvantages (Heavyweight and reinforcement corrosion)  
([www.nist.gov](http://www.nist.gov))*

Reduction in self-weight in concrete structures may be achieved by reducing the density of the concrete (Hama, 2017). The application of glass fibre bars GFRP could solve both issues; the reinforcement corrosion and electromagnetic interaction as it is corrosion-resistant and has low electric and nonmagnetic conductivity. Glass fibre bars GFRP provides the same handling properties, bond characteristics and load-bearing capacity as reinforcing steel whilst achieving even higher performance in terms of strength and durability (Abedini et al., 2017).

## 1.2 Lightweight Concrete

Concrete might be classified into three types regarding its density, which are normal weight, heavyweight and lightweight concrete. Neville (2011) stated that the practical density range of lightweight concrete is 300- 1800 kg/m<sup>3</sup>, which may be achieved by replacing some of the solid materials with air voids (bubbles) locating in three possible locations, which are:

- In the aggregate particles (lightweight aggregate concrete).
- Among the coarse aggregate particles by excluding fine aggregate (no- fines concrete).
- In the cement paste (cellular concrete), which can be divided according to the method of production into two main types: Autoclaved aerated concrete (AAC) and foamed concrete (LWFC).

Lightweight concrete can be classified in terms of density and its application according to ACI 213R-87 into three classes, which are: (1) low-density concrete with a density between 300 and 800 kg/m<sup>3</sup> used mainly for non-structural purposes such as thermal insulation with a compressive strength between 1-5 MPa. (2) Semi-structural lightweight concrete with a density from 800 to 1400 kg/m<sup>3</sup>, with a compressive strength between 5 MPa and 17 MPa, used for non- and semi-structural purposes. (3) Structural lightweight concrete density greater than 1600 kg/m<sup>3</sup> which has a minimum compressive strength of 17 MPa (Jalal et al., 2017).

### 1.2.1 Foamed Concrete (FC)

Foamed concrete is a new generation of lightweight concrete, and nowadays it is the most used type of aerated and cellular concrete. Foamed concrete is manufactured either by:

- 1- A mix-foam method, in this method air-entraining agent (AEA) is added to the mix, which introduces air bubbles during the high-speed mixing process.
- 2- Pre-foamed method, in this method a stable pre-formed foam is added to the un-foamed mixture during the mixing process or by adding a foaming agent to mortar or cement paste (Neville, 2011). Thus, the mortar becomes lighter by incorporating small-enclosed air bubbles within the un-foamed mixture (Ramamurthy and Nambiar, 2009).

The construction industry in recent years has shown a significant interest in using foamed concrete (FC) as a construction material. It is light in weight, economic, easy to fabricate,

durable and environmentally sustainable (Ramamurthy and Nambiar, 2009). The use of FC has increased more rapidly than any other type of concrete product, with 1 million m<sup>3</sup> of FC used in the UK market alone every year (Ching, 2012). This growth in FC applications has attracted numerous researchers all over the world to explore new ideas and opportunities in its application. Mohammad (2011) stated that with the beginning of the 21<sup>st</sup> century a number of published articles on aerated and foamed concrete showed a clear increase compared to other types of concrete. However, there still no code of practice covers the design of FC because of the lack of studies on certain behaviour and characteristics of foamed concrete such as tensile strength, ultimate strain and bond with GFRP bars. Table 1-1 shows the mechanical properties of normal and foamed concrete. It should be noted that this research is focusing only on foamed concrete, which is manufactured by using the mix-foam method to introduce air bubbles with a size between 0.02 mm to 1.0 mm into the cement paste.

*Table 1-1: Mechanical properties of normal and foamed concrete (Amran et al., 2015a).*

<b>Mechanical properties</b>	<b>Normal concrete</b>	<b>Foamed concrete</b>
Density (kg/m <sup>3</sup> )	2400	300-2000
Compressive strength (MPa)	15-150	1-40
Modulus of elasticity (GPa)	25-75	1-15
Ultimate compressive strain	0.0035	0.0035-0.004
Thermal expansion coefficient °C <sup>-1</sup>	12 E-6	12 E-6

### 1.3 Foamed Concrete in Structural Applications

Due to its advantage of higher strength to weight ratio, Foamed concrete (FC) can be used in structural elements to decrease the self-weight of concrete structures resulting in a reduction in the size of beams, columns, walls, foundations and load-bearing elements (Jones and McCarthy, 2005). However, Jones *et al.*, (2005) cited that producing FC with similar or closer strengths to normal weight concrete and meeting other mechanical and durability requirements is still a challenge in the construction industry.

From sustainability and environmental point of view, FC is a self-compacting concrete (SCC). It helps productivity and reduces power and noise as it does not require vibration during compaction and placement. Also reduces the power needed for handling and installation in the case of precast concrete elements. All that resulting in a huge saving in the overall cost. FC is ideally suitable for precast concrete elements as larger units can be lifted, transferred and handled by down-sizing machinery, resulting in speed and economy in construction and maximizing the number of concrete elements on lorries without exceeding highway load limits, reducing transportation delivery costs (Ozlutas, 2015).

Functionally, using FC in structural elements such as roofs, floor slabs and walls provides excellent thermal insulation reducing costs of operation such as air-conditioning and heating. Furthermore, FC has good acoustic properties where it absorbs sound, unlike dense concrete that reflects sound. Moreover, FC is a non-combustible material and it is fire resistant (Hilal, 2015a). However, FC has low compressive strength compared to normal weight concrete, which shows the importance of increasing its strength using additives.

Structurally, the use of FC which is light in weight reduces structural element size, requires less reinforcing steel and reduces concrete volume leading to a reduction of overall structure weight. That makes the structure behaves better under seismic loads. Jones *et al.*, (2005) cited that FC is well-suited material for seismic design since the lateral forces on a structure during an earthquake are directly proportional to the structure's weight. A study in 1982 by (National Science Foundation) showed that reinforced FC columns under seismic loads performed better than similar strength columns made of normal weight concrete (Kudryakov *et al.*, 2015). With all of these advantages and improvements in FC, it

is not yet accepted as a structural material due to its low compressive strength compared to normal weight concrete and there is no official design codes or guidelines exist for its use structurally.

### 1.4 Fibre-Reinforced Polymer (FRP)

Fibre-reinforced polymer (FRP) refers to composite materials consisting of two phases: the matrix phase and the reinforcing phase. The matrix phase provides protection and support for fibres as well as transfers local stress. The reinforcing phase is short or long continuous fibre reinforcement, which is the load-carrying element of FRP and controls its stiffness and strength.

The reinforcement fibres can be aramid, carbon, or glass. Aramid fibre reinforced polymer (AFRP) is a polyamide that provides exceptional flexibility and high tensile strength. It is an excellent choice as a structural material for resisting high stresses and vibration (GangaRao et al., 2006). Carbon fibre reinforced polymer (CFRP) is produced from synthetic fibres through heating and stretching. It has high strength-to-weight ratios, high tensile strength, and low coefficient of thermal expansion. Glass fibre reinforced polymer (GFRP) is produced from silica-based glass compounds that contain several metal oxides. It has been used as an alternative to steel rebar because it offers high tensile and great corrosion resistance. The mechanical properties of GFRP composites depend on several factors including the types of fibre and resin matrix, fibre volume and orientation (Krasniqi et al., 2018).

### 1.5 Glass Fibre Reinforced Polymer (GFRP)

Glass fibre reinforced polymer (GFRP) bars have been developed for use as an alternative to steel reinforcing bars in various structural applications due to the main benefit of being cost-competitive, non-corrodible, high strength and stiffness to weight ratio, good fatigue properties, more control over thermal expansion and damping characteristics, high electromagnetic and chemical attack resistance (Kemp and Blowes, 2011).

Since the 80s, research has been carried out on fibre-reinforced polymer composites bars (GFRP) for use as a reinforcement material in concrete structures owing to the high

strength to weight ratio which is 8-10 times higher than that in steel, high resistance to harsh corrosive environments, decent health and safety advantage due to low weight and low maintenance requirements (Johnson, 2009).

Despite the significant amounts of research being carried out showing the suitability of GFRP, the adoption of reinforcement bars in concrete structures in the UK construction industry has been very slow compared to Japan and China (Hoffmann, 2016).

### 1.6 Problem Statement

FC has a lighter weight compared to conventional concrete. However, the low compressive strength of FC is recognised. Ramamurthy and Nambiar (2009) mentioned that the compressive strength of FC needs more improvement, the reinforcement bond and flexural strength still requires a better understanding and the mechanical properties and structural behaviour of the material required more investigations. (Markin et al., 2019) stated that FC is disregarded for use in structural applications and that further improvements of the material are required to reduce brittleness and increase strength and introduce innovative reinforcing systems that will lead to improved bond performance.

FC has a high volume of air between 10- 75% of the total volume, which makes the material very porous, therefore, steel bars need to be coated before being used with FC as it provides low reinforcement protection. Anti-corrosion coating reduces the bonding between concrete and steel bars. Dunn and Rooyen (2018) further explored the structural mechanics and bond behaviour of FC. However, it was concluded that both the bond behaviour and fracture energy of FC is considerably lower than normal-weight concrete and it was suggested that new materials might be added to the concrete to improve the bond or that another type of reinforcement bar be used rather than steel bars.

Sustainable development has become more and more significant in the 21<sup>st</sup> century and the concrete industry undoubtedly is not exceptional. The need for low-cost lightweight concrete made by using waste materials is in high demand.

## 1.7 Aim, Objectives, and Methodology

### 1.7.1 Aim

This research aims to produce lightweight reinforced foamed concrete with enhanced mechanical properties, which is suitable for structural purposes and investigate the flexural behaviour of FC beams reinforced with steel/GFRP experimentally, theoretically and numerically using Finite Element Method.

### 1.7.2 Objectives

In order to achieve the aim of the research, the study includes the following specific objectives:

- 1- To review the mechanical properties and current use of foamed concrete and the potential of FC to be developed using recycled materials
- 2- To produce a range of FC with target density ( $800-1800 \text{ kg/m}^3$ ) with different mix designs.
- 3- To investigate the mechanical properties (Compressive strength, tensile strength, flexural strength, modulus of elasticity and poisson's ratio) of the produced FC. A programme was set to improve the mechanical properties of the concrete, by testing concrete with different cement/sand ratios, water/cement ratios and adding different additives including waste materials to enhance its mechanical properties. This programme includes loads of casting and testing to produce FC with compressive strength higher than 25 MPa and other developed mechanical properties that make the material suitable for structural applications.
- 4- To investigating the bond behaviour of FC with steel and GFRP experimentally by using pull-out and beam tests.
- 5- To investigate the flexural behaviour experimentally including load-deflection, crack pattern and the mode of failure in simply supported beams.
- 6- To investigate the structural behaviour of full-scale beams numerically using Finite Element Analysis programme (**ABAQUS**) to simulate models and compare with the experimental results.

## 1.8 Scientific Novelty

To the author's best knowledge, yet there has not been any specific study to investigate and develop foamed concrete mechanical properties using direct and indirect methods and improve these properties by adding recycled materials such as Waste Toner as additive which make it more sustainable construction material, aiming to test the structural behaviour of the developed foamed concrete experimentally and numerically.

In addition, it is the first study to investigate the bond behaviour of enhanced foamed concrete and GFRP bars using different methods (Pull out and beam method). The research also studies the flexural behaviour of full scale foamed concrete beams reinforced with Glass Fibre Reinforced Polymer (GFRP) rebar. In this study, the improved mechanical properties of FC were applied in Finite Element Analysis programme (**ABAQUS**) for modelling and numerically analysis using the nonlinear method.

## 1.9 Scope of Research

This research concentrates on investigating the mechanical properties of FC and developing these properties to be suitable for structural use. The structural behaviour will be investigated experimentally and numerically using a Finite Element Analysis programme (**ABAQUS**) software.

This research is divided into four main phases; the first phase focusing on producing a range of mix-design trials, cast and tested to get the mechanical properties of FC. The second phase is all about the development of these mechanical properties so the material can be used in structural applications, including an experimental programme to investigate the bond behaviour between FC and steel/ GFRP.

In the third phase, full-scale beams of foamed concrete reinforced with steel and GFRP are tested to investigate the load-displacement, the moment of resistance, crack patterns and failure modes. In the fourth phase, a numerical analysis (Structural Simulation) using Finite Element Analysis programme (**ABAQUS**) of full-scale beams using the mechanical properties from phase two, then the results are compared with the experimental programme outcome in phase three.

## 1.10 Methodology

This research consists of the following tasks: see Figure 1-2.

**Task 1:** Critical literature review study to review the mechanical properties of foamed concrete and the potential of FC to be developed using recycled materials.

**Task 2:** Design mix trials by means of the absolute volumes method with density not exceeding  $2000 \text{ kg/m}^3$  to have a decent understanding of the mixing procedure (pre-foamed mix) with initial testing to establish a general picture of the materials properties, equipment and testing machine's ability in the laboratory.

**Task 3:** Produce a range of foamed concretes with a density between ( $800\text{-}1800 \text{ kg/m}^3$ ), with and without additives and different sand/cement and water/cement ratios. An intensive testing procedure took place in this task to investigate the mechanical properties of FC including (compressive strength, tensile strength, flexural strength, shear strength, stress-strain relation and modulus of elasticity)

**Task 4:** Study the effects of the density and additives on FC's mechanical properties and develop these properties to be suitable for structural use.

**Task 5:** Investigate the bond behaviour of FC with steel and glass fibre reinforced polymer (GRP) reinforcing bars using the pull-out test and beam bond test.

**Task 6:** Experimentally, study the flexural behaviour; load-displacement, moment capacity, crack patterns and modes of failure of full-scale simply supported beams reinforced with steel /GRP bars.

**Task 7:** Theoretical and numerical, investigation to study the flexural behaviour of simply supported beam using nonlinear finite element analysis programme (**ABAQUS**) to simulate the model and study its flexural behaviour by applying FC enhance mechanical properties.

**Task 8:** Finally compare the experimental results with numerical outcomes to evaluate the foamed concrete reinforced beams behaviour.

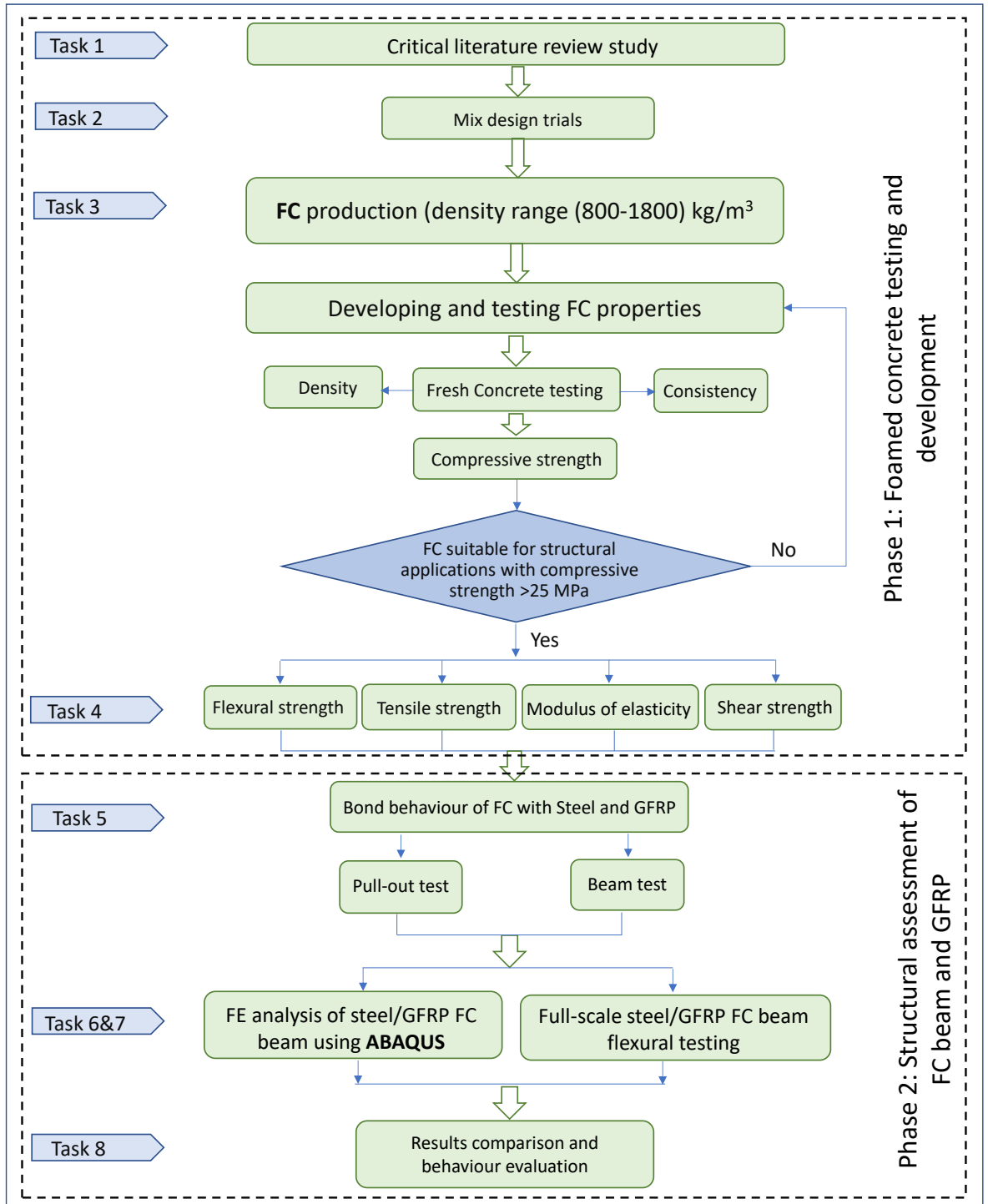


Figure 1-2: Research flowchart

## Chapter 2

# Literature Review

### 2.1 Introduction

This chapter provides a comprehensive review of the literature on lightweight foamed concrete, covers lightweight concrete main types, production methods, specifications, developments and current applications, as well as it covers foamed concrete constituent materials, mix design and fresh and hardened properties. This chapter also covers a wide-ranging review of the literature on alternative materials of steel bars such as GFRP bars that might be used as reinforcement in structural concrete elements to replace conventional steel reinforcement.

Since the last century, concrete has been the most extensively used construction material worldwide. It is widely used due to its many favourable characteristics such as workability, durability, adequate strength and the availability of its raw materials (cement, aggregates and water) (Jones et al., 2005a). However, Harmon (2010) stated that concrete needs to be developed to be used as future construction material and one of the properties that required improvement is concrete self-weight. One of the most successful methods to reduce the total load in a multi-storey concrete building is to reduce its self-weight by using light construction materials.

Lightweight concrete (LWC) is a light construction material with satisfactory strength and excellent thermal insulation. Therefore, LWC is not beneficial in reducing the total load from the structure only, but achieving energy conservation advantages and reducing air/heating -conditioning costs as well (Neville, 2011).

The FRP types, physical and mechanical properties, advantages and disadvantages and highlight the design philosophy and design guides as well. Investigated The applicability of the current design guides to predict the flexural behaviour of concrete structural members reinforced with GFRP.

### 2.1.1 Lightweight Concrete

Lightweight concrete (LWC) is not a new material, according to Brady and Jones (2001), LWC first patent and recorded use dates back to the early 1920s, limited scale production began in 1923 and, in 1924 Linde described its properties, production and applications.

Neville (2011) stated that the practical density range of LWC is 300- 2000 kg/m<sup>3</sup> which can be achieved by replacing some of the solid materials with air voids locating in three possible locations, which are:

- In the aggregate particles (lightweight aggregate concrete).
- Between the coarse aggregate particles by omitting fine aggregate (no- fines concrete).
- In the cement paste (cellular concrete), which can be divided according to the method of production into two main types: Autoclaved aerated concrete (AAC) and foamed concrete (LWFC), as shown in Figure 2-1.

Kumar and Tomar, (2018) mentioned that LWC can be produced with densities ranging from 350 to 1800 kg/m<sup>3</sup> and corresponding compressive strength between (1- 30) MPa. LWC has been used to enhance thermal insulation. However, a few types of LWC are used as structural materials such as lightweight aggregate concrete. Nowadays, huge demand in the modern construction industry for LWC to be used in structural applications, due to its advantage of lower thermal conductivity and higher strength/weight ratio (Hilal, 2015a). Hama (2017) stated that structural LWC with a density ranging from 1350 to 1850 kg/m<sup>3</sup> is found to have compressive strength exceeding 17 MPa after 28-day similar to normal weight concrete, which is primarily used to reduce the dead load in concrete members.

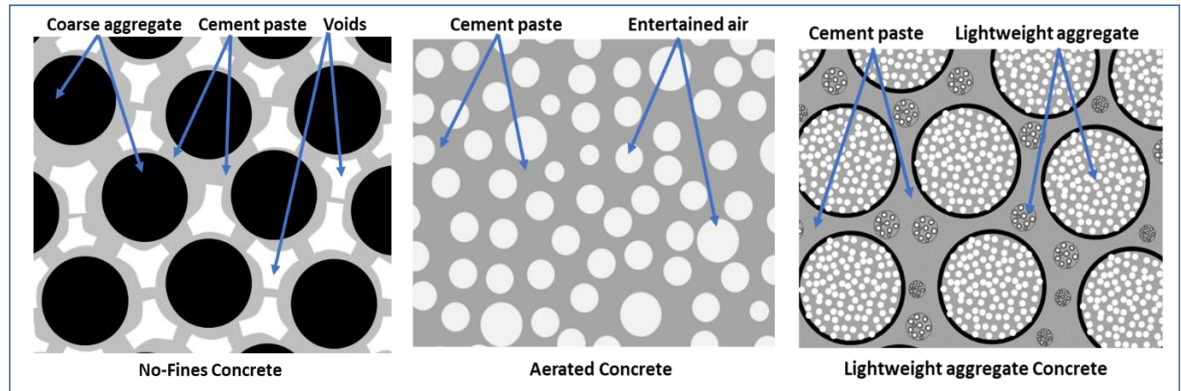


Figure 2-1: Different methods to produce lightweight concrete (Newman and Choo, 2003)

## 2.2 Cellular or Aerated Concrete

In 1997, the ACI committee 523.2R-96 mentioned that aerated or cellular concrete, can be defined as; lightweight material consisting of Portland cement, siliceous fine material such as sand, fly ash, and slag mixed with water to form a slurry that has a consistent cell or void structure. The use of mechanical incorporation of air or gas-releasing chemical reaction, resulting in macroscopic voids with size between 0.1 - 1 mm as a diameter (Gangatire and Suryawanshi, 2016).

Cellular (aerated) concrete might be produced in several ways including, see Figure 2-2: Lightweight concrete main types;

- 1- Chemically Aerated Concrete (CAC), might be produced by adding aluminium/ zinc powder to cement mortar to generate hydrogen or adding hydrogen peroxide ( $H_2O_2$ ) to the mix to generate oxygen or produce acetylene gas ( $C_2H_2$ ) by using calcium carbide ( $CaC_2$ ).
- 2- Autoclaved Aerated Concrete (AAC) when concrete is cured in steam at normal or high pressure in an autoclave, has higher strength, stability and volume compared to non-autoclaved concrete (NAAC). However, it is limited to specified mould and factory production.
- 3- Non-autoclaved concrete (NAAC), is a cellular concrete and Foamed concrete, it might be produced by mixing air-entraining agents with dry cement and sand mix in special high-speed mixers (pre-formed method) or using a foam generator and air compressor to generate foam and then adding a given quantity to cement-sand mortar in the mixer (mix-form method) (Jose et al., 2021).

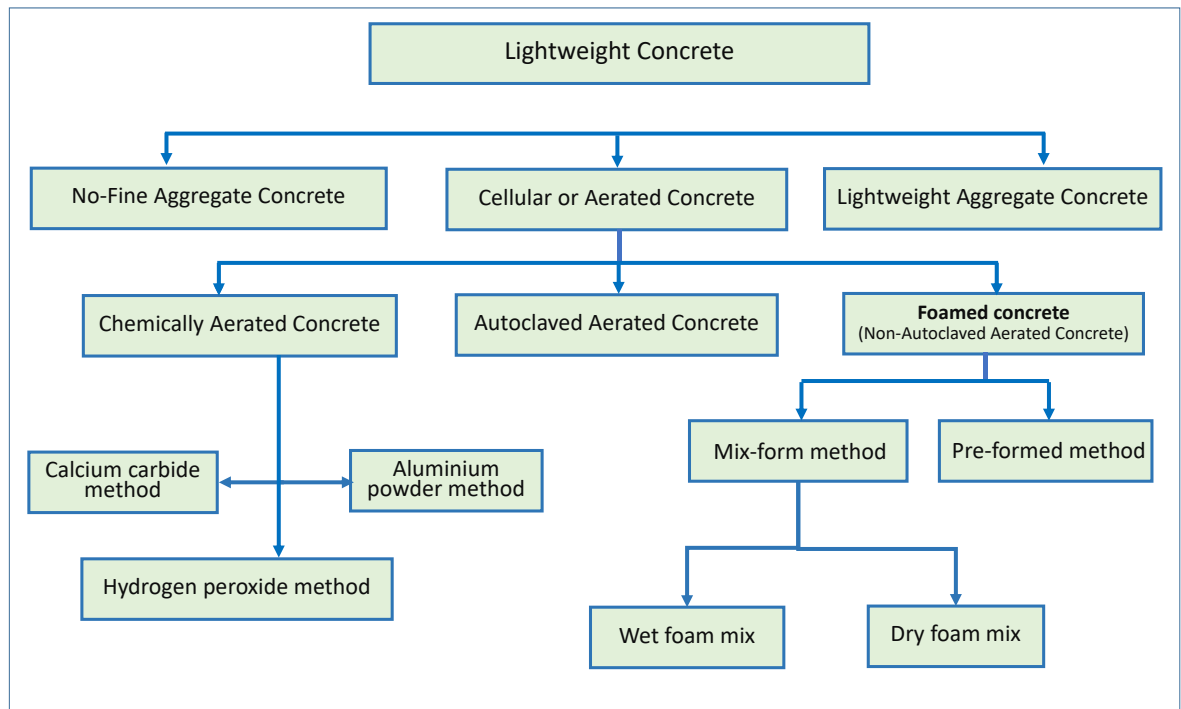


Figure 2-2: Lightweight concrete main types (Sldozian et al., 2021)

### 2.3 Foamed Concrete

Ching (2012) mentioned that the research activities related to foamed concrete preparation and technology dated back to 1923 when a foamed concrete patent was granted to J. A. Eriksson. Foamed concrete defines as lightweight concrete weighing from 200 to 1600 kg/m<sup>3</sup> (dry densities), having homogeneous void or cell structures containing no large aggregates, only fine sand (Jalal et al., 2017). Amran and Ali (2015) also defined foamed concrete as “a cementitious material, where the air is entrained by the mechanical incorporation of a preformed foam or admixture into a mortar”. However, The Concrete Society (2009) defined foamed concrete as “highly aerated mortar with air content greater than 20% by volume of mechanically entrained foam in the plastic mortar” (Mohammed and Hamad, 2014). Foamed concrete is a material consisting of either cement filler matrix (mortar) or only Portland cement paste, with a homogeneous pore structure created by entrained 0.1-1.0 mm size air voids (Ramamurthy and Nambiar, 2009), see Figure 2-3.

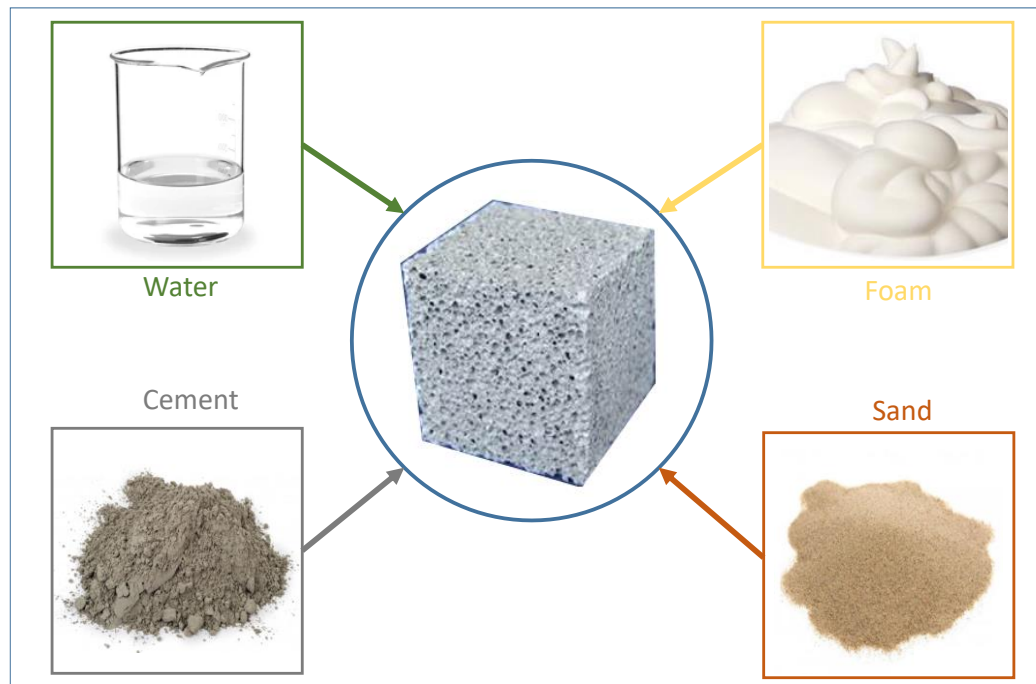


Figure 2-3: The main components of foamed concrete (Raj et al., 2019)

Saidani *et al.*, (2016) stated that creating pores inside foamed concrete may be achieved mechanically by mix foaming (mixing foaming agent with the matrix) or preformed foaming (preformed foam before being added to the mix). Foamed concrete may be cured either at ambient temperature, slightly raised temperature or even in high pressure and temperature environment (Sldozian et al., 2021). It is worthwhile mentioning that the foamed concrete investigated in this research has been manufactured using the preformed foaming method and cured at ambient temperature and pressure, see Figure 2-4.

Due to the presence of air voids, foamed concrete may have a number of advantages and be widely used in the construction industry as void filling material and sound, thermal insulation (Hilal et al., 2015). Foamed concrete with higher strength is used in semi-structural applications as well such as floor and roof screeding, road sub-bases, bridge abutments (Wahyuni, 2012). Additionally, some applications taking advantage of foamed concrete's ability to absorb energy such as roadway crash barriers, ballistic range targets and vehicle arresters on airport aprons (Hu et al., 2016).

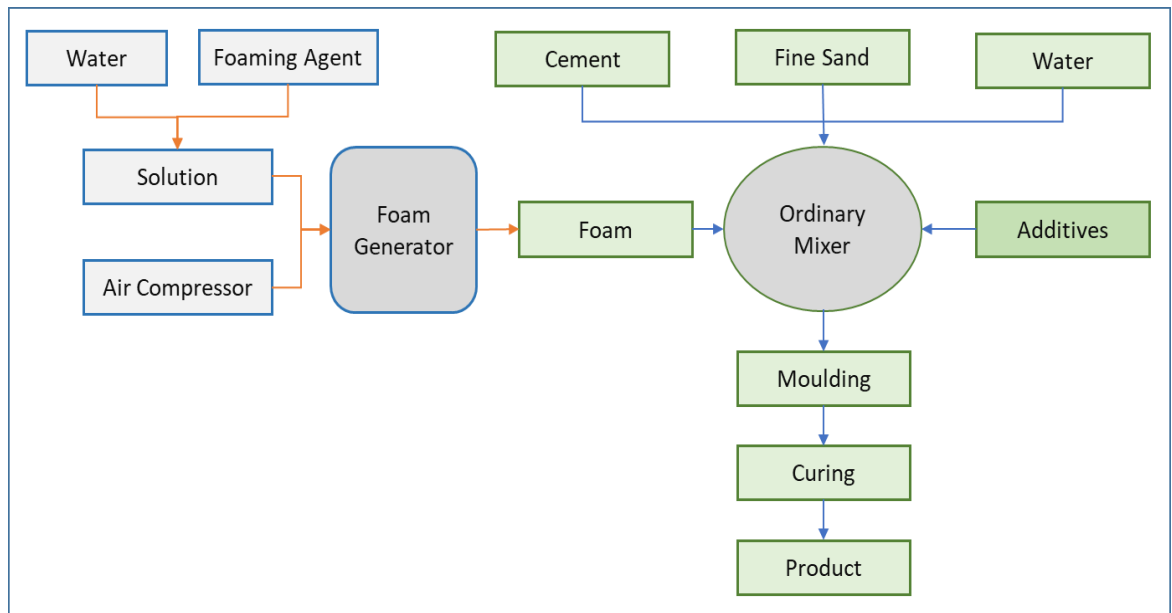


Figure 2-4: Foamed concrete production using the pre-foamed method (Alkurdi et al., 2020)

### 2.3.1 Specifications

British Cement Association in 1991 published the first report including specifications for the foamed concrete in the UK (BCA, 1991) (Ozlutas, 2015). More publications by BCA were followed between 1992 and 1995 contained further details on the advantages, properties, guidelines on strength and recommendations for applications. Foamed concrete first was recognised as a ground stabiliser and void fillings; therefore, the publications were aimed to specify the use of it for groundworks and trench reinstatement. However, in 1992 a major movement was made when the Highway Authorities and Utilities Committee (HAUC) drew a specification for the reinstatement of openings in Highways. The specification was approved as a Code of Practice in late 1992 included an Appendix entitled 'Foamed Concrete for Reinstatement', this Code of Practice took effect from January 1993 (Hilal, 2015b).

The Highways Agency and Transport Research Laboratory in 2001 with an assistant from Concrete Technology Unit (CTU) in Dundee University published an application guide AG39 titled "Specification for foamed concrete". The guideline covers quality control, properties, applications and acceptance criteria in more detail (Highways agency and TRL, 2001) (Young and Darlington, 2016). The UK Water Industry in 1995 published further specifications including the use of foamed concrete as reinstatement material and the use

of foamed concrete for insulated building foundations in 2004 (Mehta, 2017) and (Ozlutas, 2015). In Japan, an industrial standard was published (JIS A 1162:1973) titled Testing Methods for Volume Change of Cellular Concrete.

It should be mentioned that yet there is no single standard or code of practice to specify the properties, quality control and applications of foamed concrete as a structural material, Table 2-1 main published specifications for foamed concrete in the UK.

*Table 2-1: Main published specifications for foamed concrete in the UK (Hilal, 2015a).*

<b>Publishing Body/year</b>	<b>Title of the specification</b>	<b>Contents</b>
BCA /1991	Foamed concrete	Definition, properties, advantages
BCA /1994	Foamed concrete composition and properties Specification	Definition, properties, advantages, and potential applications
UKWIR /1995	Specification of foamed concrete	Use as a reinstatement material
HAUC (2010) 1st & 2nd Publications / 1992 & 2002	Specification for the reinstatement of openings in highways	General requirements for foamed concrete as an alternative reinstatement material
TRL- Brady et. al with contributions of University of Dundee /2001	TRL Report AG39 – Specification for foamed concrete	Constituents, production, properties, uses, a guideline for specifications, uses and quality control
WRAP /2005	Recycled and secondary aggregates in foamed concrete	Specification on the use of recycled and secondary aggregates in the production
WRAP /2007	Specification and quality control of foamed concrete incorporating RSA	Constituent materials, requirements, production control, and end-of-life and recycling of RSA foamed concrete
Concrete Society /2009	Concrete Guide 7 - Foamed concrete: application & specification	Case studies, practicalities, properties, quality control

### 2.3.2 Developments

Substantial improvements in foamed concrete materials, production processes, quality control and properties over the past 15 years, which have created wide choices for FC to be used in different construction applications (Ashrafian et al., 2020). Since the first production of foamed concrete, it has been used for ground stabilisation, trenches, filling voids, slabs, and road sub-base owing to the advantages of flow self-levelling, self-compacting, lightweight and low dimensional change (Hashim, 2014).

Contemporary technology has allowed the usage of foamed concrete on a bigger scale to study its behaviour accurately, furthermore, scientists and researchers can produce better FC quality by improving the quality of surfactants (foaming agents) (Hashim and Tantray, 2021). Several universities including Nottingham Trent University studied foamed concrete from different points of view and achieved some significant development see Table 2-2.

Shawnim and Mohammad, (2018) investigated the effect of toner as new material on enhancing permeability and compressive strength of foamed concrete (FC). The study aimed to develop FC through testing the reaction of toner with the cement, to produce a hydrophobic lightweight FC, and the current study aims to carry on the investigations.

Table 2-2: The main UK researchers/universities developments in Foamed Concrete (Hulusi et al., 2020).

<b>Researcher/University</b>	<b>Main Development</b>
Jones, M.R. and McCarthy (2004) / The University of Dundee	Development of thermally insulating foundations and evaluating several fresh properties of FC with plastic densities range from 1000 to 1400 kg/m <sup>3</sup>
Rao (2008) / The University of Dundee	Characterising 1000 and 1400 kg/m <sup>3</sup> foamed concretes produced with a wider range of recycled secondary aggregates (RSA) than fly ash and demolition fines. Developed foamed concrete with no/minimal primary aggregates with a plastic density of 500 kg/m <sup>3</sup>
Yerramala, (2008) / The University of Dundee	Evaluated the energy absorption potential of foamed concrete. Explored the recycling potential of RSA foamed concrete for utilising it as fine aggregate in new foamed concrete.
Othuman, (2010) The University of Manchester	Evaluate the thermal and mechanical properties of FC at high temperatures and structural performance of composite walling system with FC core.
Mohammad (2011) / The University of Dundee	Attempted to solve the stability issues in 300 kg/m <sup>3</sup> foamed concrete and gained further understanding of instability.
Hilal, (2015) / The University of Nottingham	A comprehensive study on Properties and microstructure of pre-formed foamed concretes.
Shawnim and Mohammad, (2018)/Nottingham Trent University	Foamed concrete development for structural purposes: An investigation to the viability of using alternative materials

Numerous materials may improve the physical, chemical and mechanical, properties of FC such as Silica fumes, Metakaolin, slag, rice husk ash and fly ash. Silica fumes and MK has been used in very recent years as filler replacement material to improve foamed concrete workability, quality, durability and strength with lower permeability (Lesovik et al., 2020).

## 2.4 Advantage of Fresh Foamed Concrete

The key advantages of fresh-foamed concrete are: It is not a hazardous material. Does not settle therefore, it does not require any compaction. It is reliable quality control material thus batches are easy to reproduce, small or large amounts can be placed rapidly. It is self-

compacting concrete (SCC), helps productivity and reduces power and noise, as it does not require vibration during compaction and placement. It can be placed easily by pouring and it can be pumped long vertical or horizontal distances. It is made on-site, thus the mix design can be optimised for site conditions if required (Yao et al., 2019)

### 2.5 Advantage of Hardened Foamed Concrete

Foamed concrete is a lightweight construction material. It has excellent load distribution characteristics. However, it is weak compared to normal weight concrete. It has high freeze and thaws damage resistance. It has excellent sound and thermal insulation properties, where the thermal conductivity of FC of density  $1800 \text{ kg/m}^3$  is less than 20% of the value of normal concrete. It is extremely fire resistant and well suited to applications where a fire is a risk (Rafey and Mulhem, 2016). The use of FC in construction reduces structural element size, less reinforcing bars and reduced concrete volume leads to a reduction of overall weight, which makes the structure behaves better under seismic loads. It reduces the power needed for handling and installation in the case of precast concrete elements. Furthermore, since the material is typically formed on-site, one cubic meter of the base mix can produce up to six cubic meters of FC, resulting in a reduction in CO<sub>2</sub> emission, embodied energy, manpower and transport cost to produce a given volume of material (Jones and McCarthy, 2005).

### 2.6 Lightweight Foamed Concrete Current Applications

Foamed concrete as a new generation of lightweight concrete, first was mostly used for applications for groundworks such as road sub-bases, high volume void fills, reinstatement of utility trenches, soil stabilisation, grouting tunnel walls and trench reinstatement. With the improvements in techniques and foaming agents, the use of foamed concrete has increased more rapidly than any other type of concrete. Foamed concrete currently has been extensively used for floor screed and insulation, sub-base in highways, precast blocks, prefabricated insulation boards, precast wall elements/panels, and cast-in-situ / cast-in-place walls (Jalal et al., 2017), see Figure 2-5.



*Figure 2-5: Some of the lightweights foamed concrete applications (www.dr-luca.com, 2009)*

More foamed concrete applications are shown in Table 2-3. It may be noticed that the current utilization of foamed concrete is limited to none and semi-structural purposes only such as thermal insulation, void filling, soil stabilisation, precast wall elements/panels. However, the use of foamed concrete in structural elements is very limited due to its low compressive strength.

Table 2-3 Applications of lightweight foamed concrete

Application	Dry Density Range (kg/m <sup>3</sup> )	Compressive Strength Range (MPa)	Advantages	Image
Roof Insulation Screed <a href="http://alliedfoamtech.com">http://alliedfoamtech.com</a>	300 - 600	1.0 – 3.0	Has excellent thermal insulation properties and Does not add significantly to the overall weight of the roof	
Road Sub-Base <a href="https://compositecellularconcrete.com">https://compositecellularconcrete.com</a>	300 - 1000	1.0 - 3.5	Reduce loads on weak underlying soils	
Raising Floor Level (Prabha et al., 2017)	400 - 1200	1.0 - 4.5	No compaction needed, less weight, High-performance void-filling, used for skin friction piles - Reduced foundation cost	

Chapter 2

<p>Decorative Panels www.fsiwi.com</p>	<p>&gt;1000</p>	<p>3.5 - 5.5</p>	<p>Enhance the appearance of buildings without adding much extra loading to the structure</p>	
<p>Trench Reinstatement www.rusmarinc.com/cellular-concrete</p>	<p>&gt;1200</p>	<p>4.5 - 5.5</p>	<p>Self-levelling, filling small cavities, easily to pump with low pressure over long distances</p>	
<p>Ground Stabilisation www.greenbuildingadvisor.com</p>	<p>600 - 1000</p>	<p>2.0 - 5.5</p>	<p>Reducing loading on burden soil imposes a little vertical stress on the substructure -</p>	
<p>Building blocks www.indiamart.com</p>	<p>400 - 1000</p>	<p>2.0 – 8.0</p>	<p>Foamed blocks are lightweight with excellent sound and thermal insulation properties.</p>	
<p>Void fill www.rusmarinc.com/cellular-concrete</p>	<p>300 - 1600</p>	<p>1.0 - 10.0</p>	<p>loading reduction on the basement floor and roof column piers</p>	

Chapter 2

<p>Harbour fill www.greenbuildingadvisor.com</p>	<p>400 - 1600</p>	<p>1.0 - 10.0</p>	<p>Used as impact layer due to its energy-absorbing properties</p>	
<p>Floor Slabs (Mohamad et al., 2014)</p>	<p>1200 - 1600</p>	<p>4.5 - 10.0</p>	<p>It can be pre-cast or cast in-situ. It is solid and light in weight.</p>	
<p>Bridge Abutments www.fsiwi.com</p>	<p>400 - 1650</p>	<p>1.5 - 10.0</p>	<p>Less overburden on the structure and underlying soils--dropping the thickness of the walls, and the size of the foundations, thus huge cost savings can be achieved</p>	
<p>Non-Structural Walls www.greenbuildingadvisor.com</p>	<p>800 - 1600</p>	<p>3.0 - 10.0</p>	<p>Foamed concrete walls are both lightweight and low in cost</p>	
<p>Semi-Structural Walls www.fsiwi.com</p>	<p>1200 - 1600</p>	<p>6.5 - 12.0</p>	<p>It is possible to build walls from pre-cast reinforced foamed concrete elements. It is lightweight and strong enough to take some load.</p>	

## 2.7 Production of Foamed Concrete

### 2.7.1 Constituent Materials

Foamed concrete is foamed cement slurry or mortar, where cement slurry is made from cement and water and mortar is cement, sand (fillers) and water. Foamed concrete does not contain any coarse aggregates and it is manufactured by adding preformed foam to mortar mass see Figure 2-1. Foamed concrete properties can be enhanced by adding some additives such as Silica Fume SF, Metakaolin MK and Toner. The final density of foamed concrete is controlled by the amount of added preformed foam to the mortar (Hashim and Tantray, 2021).

#### 2.7.1.1 Cement

The Ordinary Portland Cement CEM I 42.5N conforming to BS EN 197: Part 1: 2000) is the core cementitious element of foamed concrete. The total cement content by weight in foamed concrete is usually between 250- 500 kg/m<sup>3</sup>. However, to attain higher strengths, a cement content of more than 500 kg/m<sup>3</sup> has been used (Meera and Gupta, 2020). Other types of cement such as high strength and rapid hardening Portland cement (compliant with BS 915:1983) is used in foamed concrete to improve its strength at early hydration stages and ultimate strength values by several researchers (Awang and Noordin, 2014).

#### 2.7.1.2 Silica Fume SF

The silica fume (SF) used is conforming to BS EN 13263-1. Wang et al., (2020) stated that the addition of silica fume of up to 15 per cent by weight of cement improves the strength of foamed concrete only where the foam content is less than 30 per cent by size. Nevertheless, for higher foam contents mixes, the increase in strength was negligible. Silica fume can increase the compressive strength of the foamed concrete under special curing conditions up to 30 per cent (Bing et al., 2012). Mohammed and Hamad (2014) stated that in foamed concrete silica fume was found to have little effect on shrinkage. However, Ramamurthy and Nambiar (2009) mentioned that silica fume generates much heat of hydration, which is not favourable for foamed concrete as it may lead to significant temperature increases which may have an adverse effect.

### 2.7.1.3 Metakaolin MK

Metakaolin (MK) is a pozzolanic ultra-fine material, with a specific surface area in the range of  $4000 \text{ m}^2/\text{kg}$  to  $12000 \text{ m}^2/\text{kg}$ . MK is an extremely active and effective pozzolan for the partial replacement of cement in concrete (Neville, 1996). MK is normally produced by the calcination of kaolinitic clay at high temperatures reaching  $800^\circ\text{C}$  (Mehta, 2017). Chun *et al.*, (2007) stated that the presence of MK in concrete improves several physical and mechanical properties of the produced concrete such as increases workability, compressive and tensile strengths, durability, resistance to chemical attack and reduces permeability, effects of alkali-silica reactivity (ASR), shrinkage. Despite the fact MK has the potential to improve the mechanical and durability properties of concrete, its use is still limited due to its high cost (Huiskes *et al.*, 2016)

Craeye *et al.*, (2014) mentioned that the incorporation of MK, up to 25 per cent by weight of cement, has shown pore refinement to 60 per cent of the original pore size. Up to date, very limited literature has been published on the use of MK in foamed concrete, and all of these pieces of literature are recommending more investigation on the Mk effect on FC properties (Hama, 2017). In the phase of developing foamed concrete mechanical properties and structural behaviour in this research, MK was used as a replacement of cement of 20 per cent by weight.

### 2.7.1.4 Waste Toner

Waste Toner is a waste material taken from used laser printers. Printers in universities, schools and companies that print books, newspapers and magazines produce a tonnes of waste Toner every year, and the amount of money spent on its disposal is considerable. Toner is a newly introduced material to be added to foamed concrete, yet there is very limited data available or published information covering the use of the material in FC. The material comes in form of powder. In this research Toner is used as an additive to the mortar, at 5% of the binding cementitious material (cement) by weight.

Toner could be considered as a sustainable and cost-effective material, where the material is from old printer cartridges or might be collected from the expired and waste material which may come at no cost at all. Toner mainly includes the following additives for flow

and lubrication purposes; Iron oxide, ground sand, fluoropolymer powders, metal stearates e.g. zinc stearate, Fumed silica, magnetite, and carbon black (Young and Darlington, 2016).

### 2.7.1.5 Fine Aggregate

The natural siliceous sand used has a particle size of up to 4 mm and conforming to BS EN 12620 which is the most commonly used fine aggregate to produce foamed concrete. Coarse aggregate is not used in foamed concrete production as the fine air void's structure cannot support bigger size aggregate which may lead to segregation.

Based on previous studies, Aini *et al.*, (2017) noted that alternative fine aggregate materials such as chalk, Lime, incinerator bottom ash, crushed concrete, recycled glass and Lytag fines are possible be used in foamed concrete as waste or sustainable materials to reduce the density.

### 2.7.1.6 Water

The significance of water in normal concrete is well-documented. However, a brief review would help understand the role of water in foamed concrete. Water is an essential element in the production of concrete to wet the aggregate, precipitate chemical reactions with the cement, and lubricate the mixture for easy workability (Thatcher et al., 2002). Water proportion is normally added to the mix by weight based on the water/cement ratio. The mix of water with cement should comply with BS EN 1008 Mixing Water for Concrete. This standard covers the use of potable water and establishes a guide to reuse the water that is reclaimed or recovered from processes in the concrete industry. Highways Agency (HG) and the future of Transport (TRL) (2001) stated that it is fundamental to use potable water in foamed concrete, especially when the foaming agent is protein-based for the reason that organic contamination may have an adverse effect on the quality of the foam, and hence the concrete produced (Mohammad, 2011).

Kemp and Blowes (2011) mentioned that the effect of water proportion on some of the foamed concrete properties is different to its effects on normal concrete. Awang and Noordin, (2014) stated that the w/c ratio plays fewer roles on the strength of foamed concrete than normal concrete. However, Halverson *et al.*, (2014) found that the w/c ratio

is an important factor in foamed concrete, where too much water may lead to segregation and too little water may lead to disintegration. Aini *et al.*, (2017) stated that using a small proportion of water leads to water withdrawal from the foam and the foam degenerates quickly. However, it was suggested that the w/c ratio required to achieve acceptable workability in foamed concrete is ranging from 0.3 to 1 dependent on; type of binders used, the use of plasticizing agent, wet density targeted, strength required.

### 2.7.1.7 Foaming Agents (Surfactants)

Foaming agents (surfactants) are wetting agents needed to lower the surface tension of water to produce foam (Gangatire and Suryawanshi, 2016). Table 2-4 shows the main foaming agent types and properties used in foamed concrete. The surfactant is typically mixed with water with a ratio of 1/ (5-20), one part surfactant to be mixed with a range of 5 to 20 parts of water (Ghorbani et al., 2019). Protein-based or synthetic surfactants may be used to produce foam, both are formulated to produce air bubbles that are stable and able to resist the chemical and physical forces required in the process of making foamed concrete (Othuman Mydin, 2010).

Protein-based surfactants produce stable, strong, closed-cell foam, which easily blends into the mortar with little bubble breakdown and produces foamed concrete with a strength/density ratio of 50% to 100% higher compared to synthetic surfactants. However, protein-based surfactants are sensitive to the alkalinity of the mix and have a lower expansion ratio to solution volume to foam volume (Mehta, 2017).

Table 2-4: Table Surfactant types and properties (McCarthy, 2004)

Surfactant type	Example composition	Properties	Characteristics of foam produced	Applications in foamed concrete
<b>Synthetic</b>	Alkyl sulfates	Consistent, Stable and easy to formulate	Larger with opened cells due to lower strength & higher expansion	In higher FCs density, good for fast & large placing
<b>Protein</b>	keratin and Hydrolysed animal proteins	Stabilised, variable & highly refined	Firm texture, Stable, stronger, and smaller closed-cell bubbles.	In low FC density, when waterproofing & high strength are required

Synthetic surfactants are easy to formulate, stable and have consistent performance. On the other hand, the size of the produced bubble is larger, the cells are more open owing to higher expansion and the foamed concrete produced normally has lower strengths compared to foamed concrete produced using protein-based surfactants (Amran et al., 2015b).

#### 2.7.1.8 Foam

Lee *et al.*, (2014) stated that one of the key advantages of foamed concrete is the ability to control its density over a wide range, which may be achieved by adding a calculated amount of foam to the base mix. Foam is normally introduced to foamed concrete by two methods: the pre-formed method or by the mix-form method. According to (Mohammed and Hamad, 2014) the mix-form method is reported to be the most sustainable method, where a less foaming agent is required to produce foam and no chemical reactions involved. Dijk (2002) mentioned that the foam in the mix-form method should be stable enough and must be capable to resist the pressure of the base mix and remain stable during pumping, placement and curing.

The mix-form method is categorised as either dry foam or wet foam. Wet foam is generated by spraying a foaming agent and water solution over a fine mesh. This type of

foam has a bubble size ranging from 0.2 to 2 mm in diameter, therefore, it is not recommended for foamed concrete with ultra-low densities below  $800 \text{ kg/m}^3$ . Dry foam is generated by forcing foaming agent and water solution and compressed air through series of high-density restrictions, see Figure 2-6. Produced foam is very stable with a bubble size smaller than 1 mm diameter, thus it is suitable for high and low density foamed concretes (Kemp and Blowes, 2011). The quality and properties of foam generated to produce foamed concrete are critical (Hendriks et al., 2016). The foam quality is affected directly by its density, the foam-making process, the dilution factor of the agent and the blending process with the mortar.

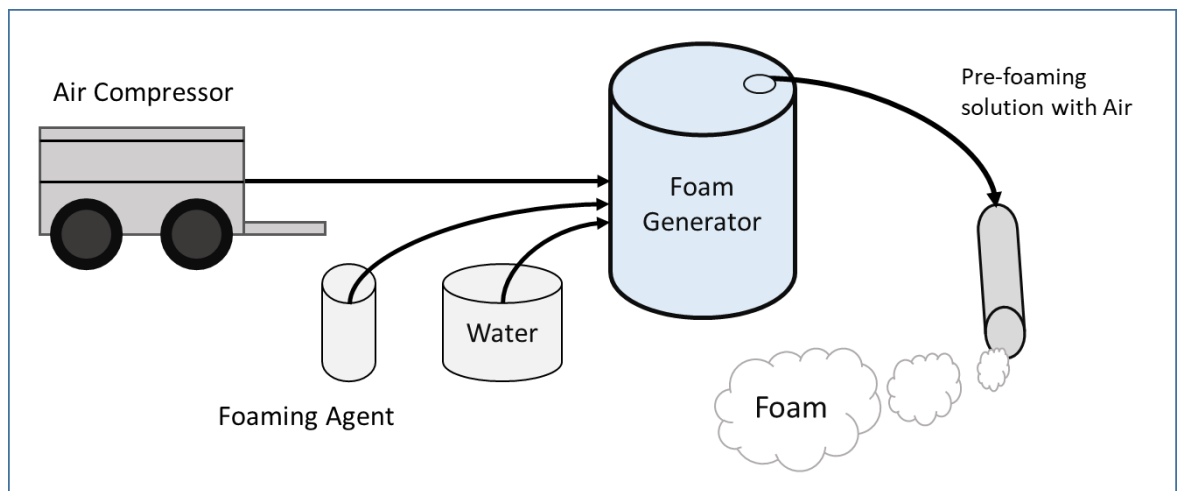


Figure 2-6: Produce Foam from water, foaming agents and compressed air (EAB Associated, 2001)

### 2.7.2 Mix Design and Procedure

Ghorbani *et al.*, (2019) stated that has not yet been a standard method to calculate the mixed proportions of foamed concrete. Unlike normal concrete mix design, the criterion in foamed concrete mix design is the target plastic density rather than target dry density. Conversely, some researchers such as (Gangatire and Suryawanshi, 2016) and (Ramamurthy and Nambiar, 2009) followed the same design method by specifying a target dry density.

The amount of foam required to achieve the target density (plastic/dry) is calculated by using the cement and fine aggregate contents, w/c ratio and specific density values of all corresponding constituents (including the foam). Additionally, when different cement/aggregate types are used such as fine/coarse fly ash, the mix design needs to be

tailored considering the higher water requirement of fly ash (Mohammed and Hamad, 2014).

In general, foamed concrete properties are depending on the proportions of its raw materials. According to Babbitt *et al.*, (2014) foamed concrete mix proportioning starts with the selection of its overall wet density, cement content, sand to cement, water to cement ratios, then the mix is designed by the absolute volumes method. For foamed concrete production, the mixing procedure adopted by several researchers such as (Hilal, 2015b) is as follows:

- Worked out the number of raw materials.
- Dry constituents are mixed in an ordinary mixer for a few minutes.
- Mixing water will be added in stages.
- After thorough mixing, the foam is added to the wet slurry. Although foam should be completely mixed with the mortar. Excessive mixing should be avoided due to the possibility of changes in consistency and density.

### 2.7.3 Preparation of Foamed Concrete

Habsya *et al.*, (2018) stated that the wet foamed concrete should be placed in two equal layers and tapping the sides of the mould lightly during the filling operation until the layer surface has settled to a plane. At that time, the top surface should be finished and covered with a plastic sheet to prevent evaporation. If to the extent that removal from moulds after 24 hours is concerned, foamed concrete specimens must not be removed from moulds if there is a risk of damage. Nevertheless, is recommended to remove specimens from moulds within 7 days after moulding in low FC density (less than  $800 \text{ kg/m}^3$ ) (Khaw, 2010).

Concerning curing, different methods have been adopted to prevent the loss of specimen moisture. According to both (Norasyikin Bt. Md., 2009) and (Hashim, 2014) for the first 24 hours after moulding, the specimens should be maintained at a temperature of  $21 \pm 5^\circ\text{C}$ . Then, they should be cured, for 7 days, under damp sand and wet burlap or similar materials with a temperature lower than that of the surrounding atmosphere. Then, they should be stored at a temperature of  $21 \pm 5^\circ\text{C}$  and relative humidity of  $50 \pm 25\%$  for 21 days. For foamed concrete specimens curing, (Thatcher *et al.*, 2002) and (Ramamurthy and

Nambiar, 2009) implemented moist curing method in a fog room at a temperature of  $25\pm 2^{\circ}\text{C}$  for 28 days. Nevertheless, (ASTM C496-96, 1996) cured FC specimens in a moist condition for 7 days and in the air at a temperature of  $25 \pm 2^{\circ}\text{C}$  for the remaining time. In initial views on foamed concrete potential as a structural material expressed by (Dong and Zhang, 2013), FC specimens were wrapped in cling film (sealed-cured and stored for 28 days at  $25\pm 2^{\circ}\text{C}$ ), the sealed-curing could reflect typical industry practice for FC elements. For curing specimens of structural lightweight concrete, (Amran et al., 2015b) reported that the unhardened specimen should be covered with a non-absorptive or nonreactive sheet, and then it should be stored in a moist room at  $23 \pm 2^{\circ}\text{C}$  with relatively high humidity. Whereas, for precast cellular concrete members, (Jones and McCarthy, 2005) stated that the concrete members are cured by atmospheric steam curing or by high-pressure steam (autoclaving) curing.

### 2.8 Properties of Foamed Concrete

This section covers foamed concrete properties in both, fresh and hardened states, as follows:

#### 2.8.1 Fresh Properties

Unlike normal weight concrete, Foamed concrete must not be vibrated or compacted since this would affect its design density. Nevertheless, both (Chun et al., 2007) and (Ramamurthy and Nambiar, 2009) reported that, in moulding, tapping on sides could be beneficial after mix placing to avoid large air bubbles trapped. Therefore, self-compatibility and flowability represent significant fresh state characteristics of foamed concrete and they are evaluated in terms of stability and consistency of the mix. The consistency of concrete is defined by its flowability and spreadability measurement. Generally, it is reduced by adding foam to the un-foamed mix depending on the volume and the design density (Norasyikin *et al.*, 2009). Foamed concrete consistency and stability are strongly affected by the water content in the base (un-foamed) mix and the amount of foam (Lee et al., 2014). Wahyuni (2012) reported that for a given FC mix: the flowability reduces when the foam is added, also, it reduces sharply with the increase of density. The likely reason for this might be that the bond between solid particles and bubbles in the mixture improves its stability

resulting in flowability reduction, despite the fact that there are more bubbles in the lower densities mixes.

Saidani *et al.*, (2016) stated that even supposing superplasticizers are used to achieve suitable flowability, they might affect the foam stability. The Marsh cone was used by Marata and Suzuki (1997) to determine foamed concrete followability by measuring the time required for a mix to flow through a March cone opening (Hilal, 2015a). Then, to consider the sand particles size effect on the flowability this test was modified by Chai (1999) by making the volume of afflux 1 L instead of 200 ml and the orifice diameter 12.5 mm instead of 8 mm. Furthermore, the slump flow test and the Brewer spread test as per BS 4551-1 were used for lightweight concrete. However, Ramamurthy and Nambiar (2009) used the ASTM hydraulic cement flow table for measuring spreadability. As described by Amran, Farzadnia and Ali (2015), the workability of both the un-foamed mix and foamed concrete can be quantified by the spreadability of a cylinder of material of 76.2 mm diameter and 152.4 mm height.

Based on the discussion above, the fresh properties of foamed concrete such as consistency and stability are affected by the water-solids ratio and the volume of foam. By assessing the stability of foamed concrete. Moreover, the workability and flowability can be measured by using the standard flow cone (ASTM C230-1998) or the modified Marsh cone test (Kumar *et al.*, 2018).

### 2.8.1.1 Wet Density

Almost all foamed concrete properties are affected by its designed density and consequently, they should be qualified by the density, which is significantly affected by the water content (A. Neville, 2011). Based on the previous studies, the density of foamed concrete is also affected by the type of fine aggregate, aggregate size, foam type, sand-cement ratio. According to Ramamurthy and Nambiar (2009), the replacement of sand with fly ash led to a reduction in concrete density and an increase in its strength. Thus, in order to achieve a specific design density of foamed concrete with fly ash, foam volume reduction is required to produce foamed concrete with the target density. In the literature, empirical relationships for the determination of foam concrete density are proposed. Jones and

McCarthy (2005) stated a useful method for calculating the approximate fully dry unit weight of foamed concrete as following:

$$D_{dry} = \frac{W_{da} + 1.2W_{ct}}{v} \quad \text{Equation 2-1}$$

Where:

$W_{da}$  Weight of dry aggregate in the batch, kg

$W_{ct}$  Weight of cement in the batch, kg

$v$  Volume of concrete produced by the batch, L

The  $1.2W_{ct}$  represents the weight of cement and water of hydration, where the water of hydration is 20% of the cement weight.

### 2.8.2 Hardened Properties

Compressive strength is the main property of concrete, it is found to decrease with a reduction in the mix density. It has been reported that water content, the method of pore formation, characteristics of ingredients, the specimen shape and size, and direction of loading all affect the strength of cellular concrete members (Krishna et al., 2021). Furthermore, the cement-sand ratio, method of curing, type of foaming agent and distribution of sand particles have also been reported as parameters affecting the strength of foam concrete (Tanveer *et al.*, 2017). Moreover, the foamed concrete compressive strength is also affected by the air void size and distribution, spacing, the void/paste ratio and the number of air voids. Hendriks and Belletti (2016), mentioned that the air pores structure has a great effect on the cellular concrete compressive strength. In a study on the effect of replacing large volumes of cement with fly ash on the strength of foam concrete, it has been reported that up to 50% of the cement could be replaced without any significant reduction in strength (Hashim, 2014).

#### 2.8.2.1 Density

Foam concrete is a low-density material ranging from 300 kg/m<sup>3</sup> to 1900 kg/m<sup>3</sup> hardened mortar or Portland cement paste containing a large number of introduced small air bubbles called entrained air (Mohammed and Hamad, 2014). Structural Foamed Concrete (SFC) has

a density ranging from 1200 kg/m<sup>3</sup> to 1900 kg/m<sup>3</sup>, lower concrete density may be specified for non-structural applications, compared to normal-weight concrete with a density in the range of 2240 kg/m<sup>3</sup> to 2400 kg/m<sup>3</sup>. For structural applications, the concrete strength should be greater than (17.0 MPa) according to (ACI 213R Committee, 2003).

Babbitt *et al.*, (2014) stated that wet density (Freshly Mixed Concrete Density) is always higher than the dry density of foamed concrete, FC's wet density starts decreasing after placed in an oven at 105 ± 2 °C for a period of time until reach constant weight. The equation below is applicable for foamed concrete density ranging from 1400-1900 kg/m<sup>3</sup>.

$$D_{dry} = \frac{D_{wet} - 105}{1.05} \quad \text{Equation 2-2}$$

Where:

$D_{dry}$  Dry density of foamed concrete, kg/m<sup>3</sup>

$D_{wet}$  Wet density of foamed concrete, kg/m<sup>3</sup>

### 2.8.2.2 Compressive Strength

According to Akinpelu *et al.*, (2018), concrete compressive strength is one of the key properties. Foamed concrete compressive strength is influenced by several factors but density is the most influencing factor, then the c/s ratio, the foaming agent used, type and particle size distribution of sand, method of pore formation, w/c ratio, characteristics of ingredients used and the method of curing. Figure 2-7 shows compressive strength density variation for mixes with different c/s ratios (Nambiar and Ramamurthy, 2006b).

Alsubari *et al.*, (2015) stated that the compressive strength of FC decreases dramatically with the increase in void diameter for dry density between 500 – 1200 kg/m<sup>3</sup>. However, the influence of air void diameter decreases for density higher than 1200 kg/m<sup>3</sup>. Table 2-5 shows typical properties including the compressive strength of foamed concrete (Hamad, 2014). With a minimum strength of 25 N/mm<sup>2</sup>, foamed concrete has the potential to be used as a structural material. (Hamad, 2014) showed compressive strength and density typical relationship in foamed concrete.

Table 2-5: Typical properties including compressive strength of foamed concrete (Hamad, 2014).

Dry density (kg/m <sup>3</sup> )	Compressive strength (MPa)	Modulus of elasticity E (GPa)
400	0.25-1.0	0.25-1.0
600	0.5-1.5	0.5-1.5
800	1.0-2.0	1.0-2.0
1000	2.0-4.0	1.5-2.5
1200	3.0-6.0	2.0-4.0
1400	4.0-8.0	3.0-6.0
1600	7.0-12.0	5.0-8.0
1800	10.0-15.0	7.0-12.0

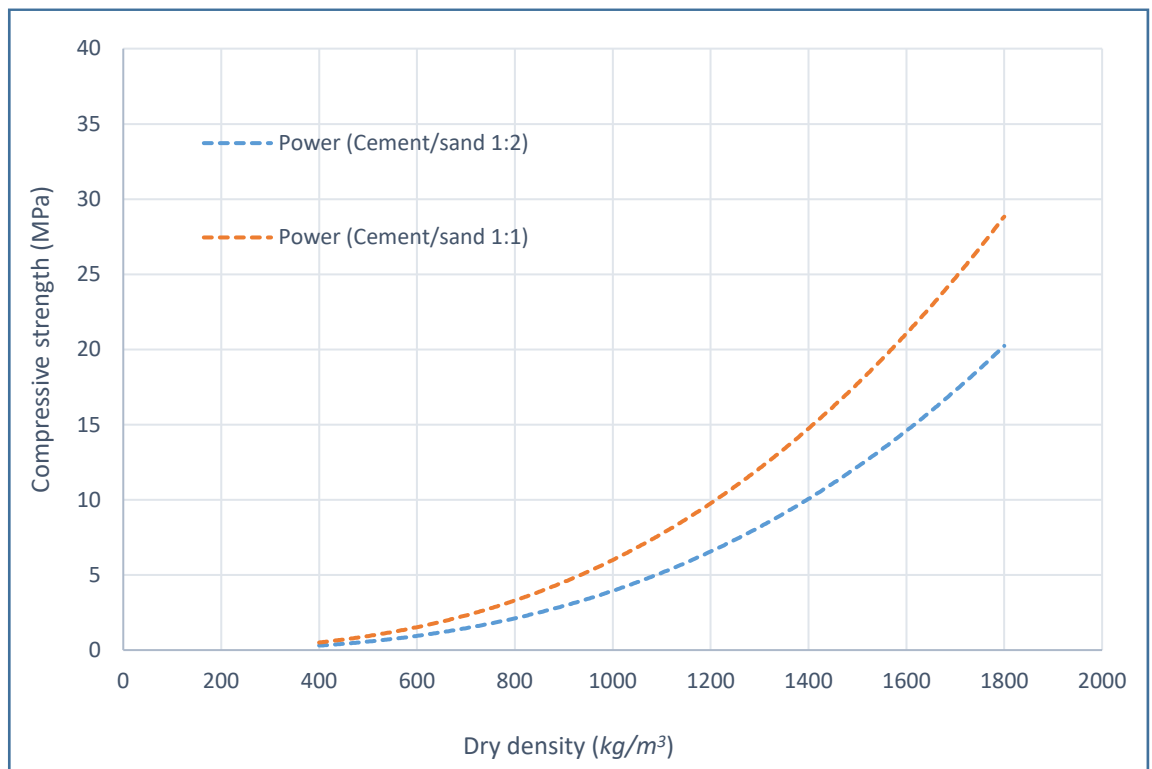


Figure 2-7: Strength density variation for mixes with different c/s ratios (Nambiar and Ramamurthy, 2006b)

### 2.8.2.3 Flexure and Splitting Tensile Strengths

Flexure and splitting tensile strengths of concrete are important parameters utilised in the analysis and design of concrete members. However, the classification of concrete in most

design codes of practice are often based on compressive strength, while other mechanical properties such as tensile strength, modulus of elasticity and Poisson's ratio are expressed as a function of the compressive strength.

A number of empirical models and theories have been developed to predict the splitting tensile strength of foamed concrete based on its compressive strength (Resan et al., 2020). American Concrete Institute (ACI) model did not cover lightweight concrete, but some studies based on ACI recommend a square root relationship between cylinder compressive strength and splitting tensile strength. Recent studies have also shown that the power of compressive strength varies between 0.4 and 0.6 (ASTM C496-96, 1996). Lee *et al.*, (2017) stated that splitting tensile strength is around 10% from cylinder compressive strength, and flexural strength of foamed concrete is 10-15% from cylinder compressive strength. Many equations exist to determine the modulus of rupture such as Equation 2-3 an equation given in ACI 318-05 (2004).

$$f_r = 0.62 \sqrt{f'_c} \quad \text{Equation 2-3}$$

Where:

$f_r$  Flexural strength, MPa

$f'_c$  Compressive strength, MPa

Foamed concrete splitting tensile strength is slightly lower than those of equivalent lightweight aggregate concrete and normal weight concrete. However, cement-sand based FC recorded a higher tensile strength than those that contain fly ash. The higher tensile strength contributes to improving the shear capacity between the paste phase and sand particles (Babbitt et al., 2014).

### 2.8.2.4 Shear Strength

The shear strength of concrete is presented by the shear friction or aggregate interlock. According to (KUM, 2011) the push-off specimen test is the way for measuring the direct shear strength of concrete. Where prism members comprised of two L-shaped blocks, connected in an inverted position to formulate the shear plane. In previous research, models of shear strength were suggested using different approaches, such as modified

compression field theory, distributed stress field model and shear strength based on the push-off specimen. Generally, the shear failure of the normal strength concrete member is brittle.

The increase in the shear strength of concrete is associated with the increase in material compressive strength. Nevertheless, concretes with higher strength are known to be more brittle than less strength concrete, representing a significant limitation for their wide-range application in innovative structural design. According to Wang *et al.*, (2013) shear strength in lightweight concrete can be predicted using Equation 2-4.

$$v_c = 0.5 \sqrt{f'_c} \quad \text{Equation 2-4}$$

Where:

$v_c$  Shear strength, MPa

$f'_c$  Compressive strength, MPa

### 2.8.2.5 Modulus of Elasticity

Modulus of elasticity is one of the essential factors in determining the structural behaviour of concrete. Modulus of elasticity can be defined as the ratio of uniaxial stress to the resultant axial strain (Muñoz, 2010). Modulus of elasticity is a direct measure of the concrete's stiffness properties. However, in concrete, it is highly variable from one mix to another. The Modulus of elasticity of foamed concrete is mainly affected by mix density, the concrete strength, type of aggregate and aggregate paste interface connection.

Modulus of elasticity of foamed concrete can be given in three ways, as shown in Figure 2-8. The Modulus of elasticity can be defined as the initial tangent modulus, where foamed concrete behaves linearly within 25-35% of ultimate concrete strength. The secant modulus is the stress-strain diagram slope from the origin to a specific point, typically taken at  $(0.45f'_c)$  (Roberts, 2015). Where the tangent modulus is the slope taken at any specified point along the curve.

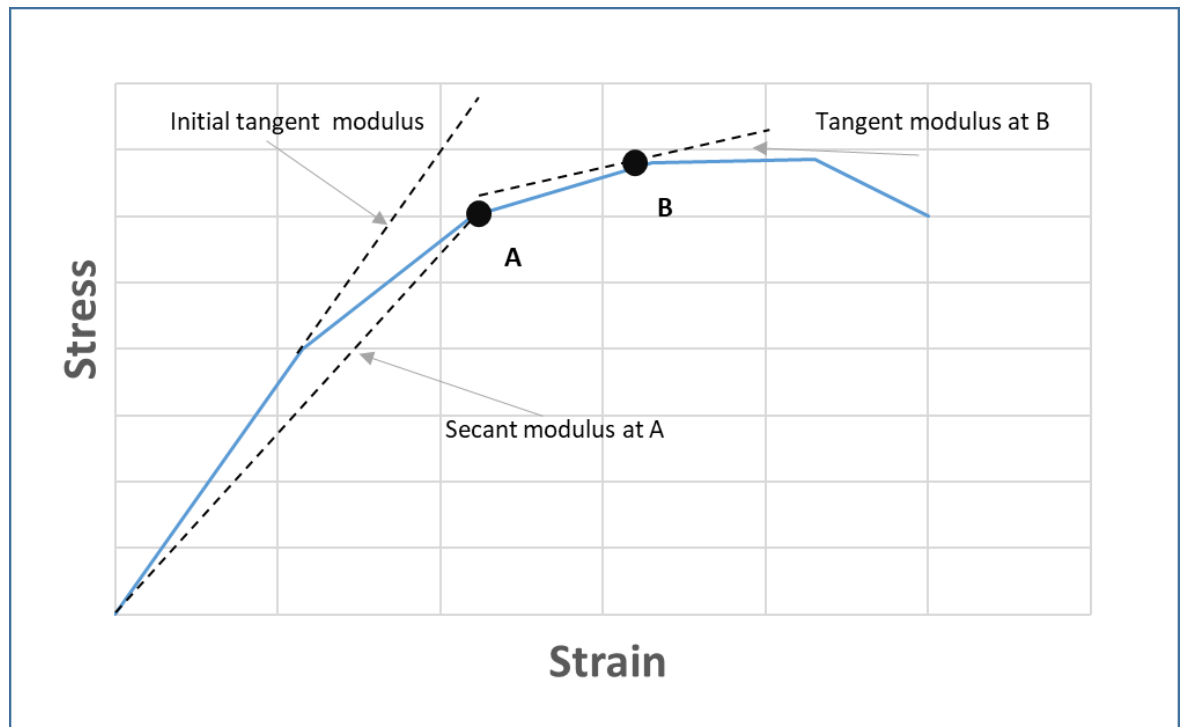


Figure 2-8: Elastic modulus of foamed concrete graphical definition (Khaw, 2010)

#### 2.8.2.6 Foamed Concrete Durability

The concrete durability is generally affected by the fluid transport through its pore system resulting in deterioration. The movement of aggressive liquids into concrete is depending on its permeation characteristics such as sorption, water absorption and permeability (Trevor and Gideon, 2018). This represents the most significant factors affecting the service life of a concrete structure (Jones and McCarthy, 2005). Therefore, one of the most important indicators of concrete long term durability is its permeability which is the ability of concrete to resist water and chemical migration such as salts, chlorides and other aggressive chemicals that can cause deterioration and crack in concrete (Amran et al., 2015b). Therefore and because the durability of concrete is governed by its resistance to being penetrated by external aggressive agents, the property of permeability seems to be a reliable estimator of its quality (Trevor, Gideon, 2018). Moreover, it is well known that transport properties are affected by the pore structure (Saidani et al., 2016).

Jones and McCarthy, (2005) studied the permeation characteristics, a relationship between porosity and water vapour permeability in foamed concrete and cement pastes. In the study, it was concluded that with the decrease of FC density, the water vapour permeability

increases. Jones and McCarthy, (2005) stated that in the case of FC the air voids that are entrained might be considered as an aggregate and their inclusion might decrease the permeability not only by obstructing flow nonetheless also because of microcracking absence at the interface between air voids and the mortar.

Amran et al., (2015) stated that the foamed concrete permeability coefficient is proportional to pore content. Furthermore, foamed concrete sorption is affected by the pore structure, filler type and mechanisms of permeation. Dong and Zhang (2013) stated that water absorption and sorptivity decrease with a reduction in density and primarily controlled by capillary porosity. This is since the foamed concrete water absorption is mostly influenced by the paste phase, in which the air voids are not involved in water absorption as their suction is weaker than that of capillary pores (Amran et al., 2015b).

Jones and McCarthy (2005) stated that foamed concrete provides good resistance to aggressive chemical attacks as well as good freeze-thaw resistance. Nevertheless, according to Hu *et al.*, (2016), generally higher porosity in concrete leads to a rise in permeability resulting in an increase in vulnerability to the effects of freezing and thawing. Falliano et al., (2020) stated that the increase in porosity of foamed concrete is associated with improved physical properties. However, it is accompanied by a significant reduction in mechanical performance. Concrete with low density appears to carbonate at a relatively higher rate but that is not a problem except the exposure to CO<sub>2</sub> is severe. It was found that depending on the curing method, autoclaved aerated concrete is more durable than normally cured aerated concrete (Lee et al., 2014).

### 2.9 Reinforced Concrete

Reinforced concrete (RC) is a versatile composite and one of the most widely used materials in modern construction. Concrete is a relatively brittle material that is strong under compression but weak in tension. Plain concrete (unreinforced) is unsuitable for many structures as it is relatively poor at withstanding stresses induced by vibrations, wind loading.

To increase the concrete overall strength, steel rods, wires, cables or mesh might be embedded in concrete before it sets. This reinforcement, often known as rebar, resists

tensile forces. By forming a strong bond together, the two materials are able to resist a variety of applied forces, effectively acting as a single structural element. Concrete can be reinforced using different materials such as hot rolled deformed steel bars, cold worked steel bars, prestress bars and fibre reinforced polymer (Engineering, 2005).

### 2.10 Glass Fibre Reinforced Polymer (GFRP) Bars

Steel bars have several disadvantages such as heavyweight and handling difficulties and corrosion. Fibre-reinforced polymer (FRP) bars have been developed as an alternative to steel reinforcement for various structural concrete applications. FRP bar is a structural bar made of continuous fibres held in a polymeric resin matrix. Together contribute to the consequential mechanical and physical properties which are required for specific structural applications (Kemp and Blowes, 2011).

The used fibres are continuous fibres with high stiffness and high strength. furthermore, they are lightweight material, non-corrosive nature, and particularly suited for harsh environments. The most common type of fibres for structural purposes are carbon, aramid, basalt and glass fibres. Currently, different types of FRP rebar for reinforced concrete structural elements are available, which are classified by fibre type as shown in Figure 2-9, Carbon Fibre Reinforced Polymer (CFRP) rebar, Basalt Fibre Reinforced Polymer (BFRP) rebar, Aramid Fibre Reinforced Polymer (AFRP) rebar Glass Fibre Reinforced Polymer (GFRP) rebar (Hoffmann, 2016).

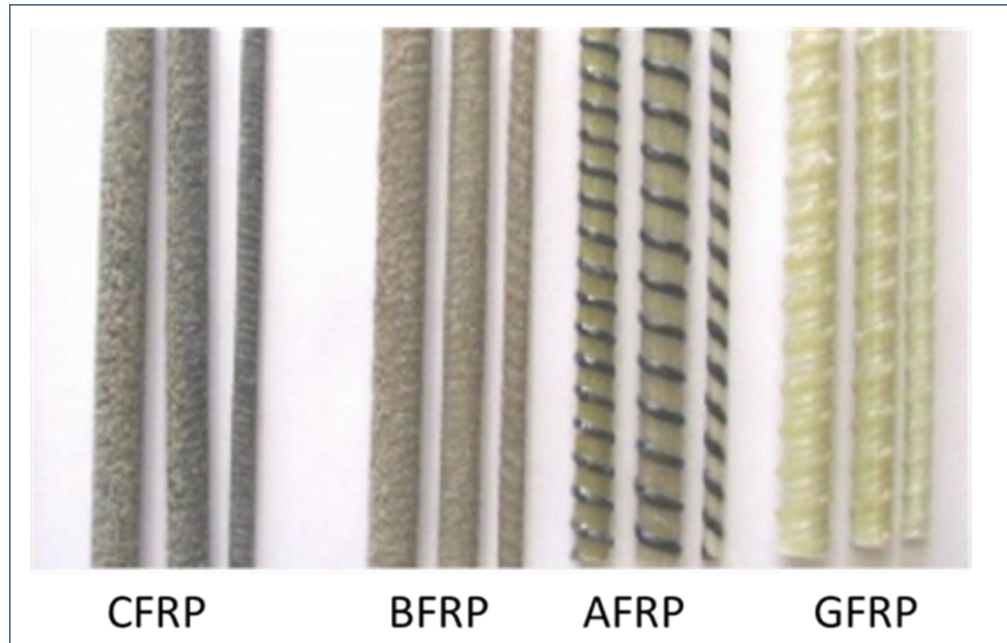


*Figure 2-9: The most common types of FRP bars (Benmokrane et al., 2021)*

The GFRP is becoming more frequently used for reinforcement of corrosion-prone concrete structures and was chosen in this study due to its lightweight, excellent corrosion resistance, high tensile strength to weight ratio and good non-magnetization properties (Worner, 2015). However, recent studies showed that GFRP reinforced concrete members behave differently from traditional steel-reinforced concrete structures since GFRP has a lower modulus of elasticity, different stress-strain relationship than steel, which cause a substantial decrease in the flexural stiffness of the member after cracking and, consequently, larger deformations under service conditions. Therefore, the design of GRP reinforced concrete members is often ruled by the serviceability limit state (Ng et al., 2020).

### 2.10.1 Developments of Fibre Reinforced Composite Materials

The development of FRP bars as reinforcement could be drawn back to the increased use of composites after the Second World War. However, it was not considered for use as reinforcement within concrete members until the 1960s. In the USA and Europe, the application of de-icing salts on highway bridges resulted in extensive corrosion of steel reinforcing bars in these structures. The construction material market demanded non-metallic reinforcement such as FRP. Fibre-reinforced polymer began to be considered as a common solution for corrosion problems and became a reinforcement that could be used on highway roads and bridges (Hickinbotham, 2016). The Aberfeldy Footbridge crosses the

Tay River in Scotland is considered the world's first major project using Fibre Reinforced Polymer (FRP) composites, see Figure 2-10.



Figure 2-10: Aberfeldy Footbridge (Reinforced with GFRP bars) (compositesuk.co.uk, 2015)

### 2.10.2 Constituent Materials

FRP are composite materials mainly consisting of two basic components: matrix (resin) and reinforcing fibres. The fibres are responsible for providing strength and carrying the load, which are preferably brittle, elastic, and have high tensile strength. The resin holding the fibres together, protecting the fibres from environmental and physical damage, provides a cohesive environment to transfer stresses between fibres, also provides lateral support for the fibres against local buckling (Hoffmann, 2016) as illustrated in Figure 2-11.

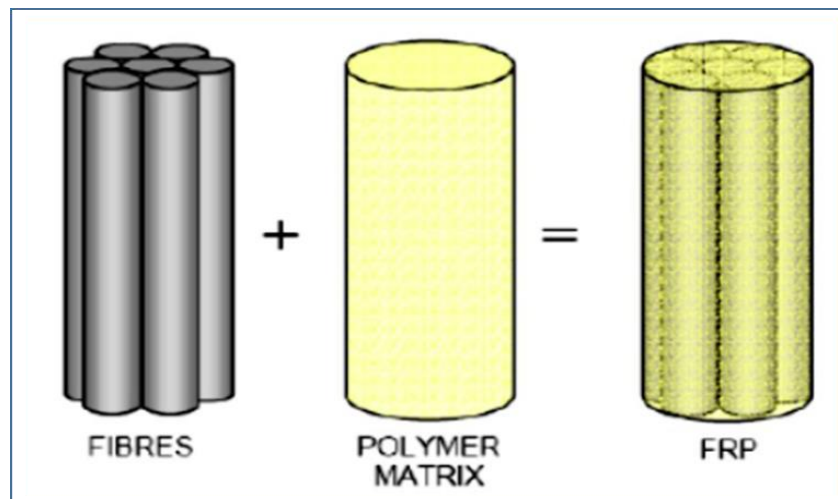


Figure 2-11: Basic material components of FRP composite ((Abedini et al., 2017)

Fibres are significantly stronger than the resin material and control the final mechanical properties such as strength and elastic modulus of the bar Figure 2-12 illustrates the stress-strain curve of the materials.

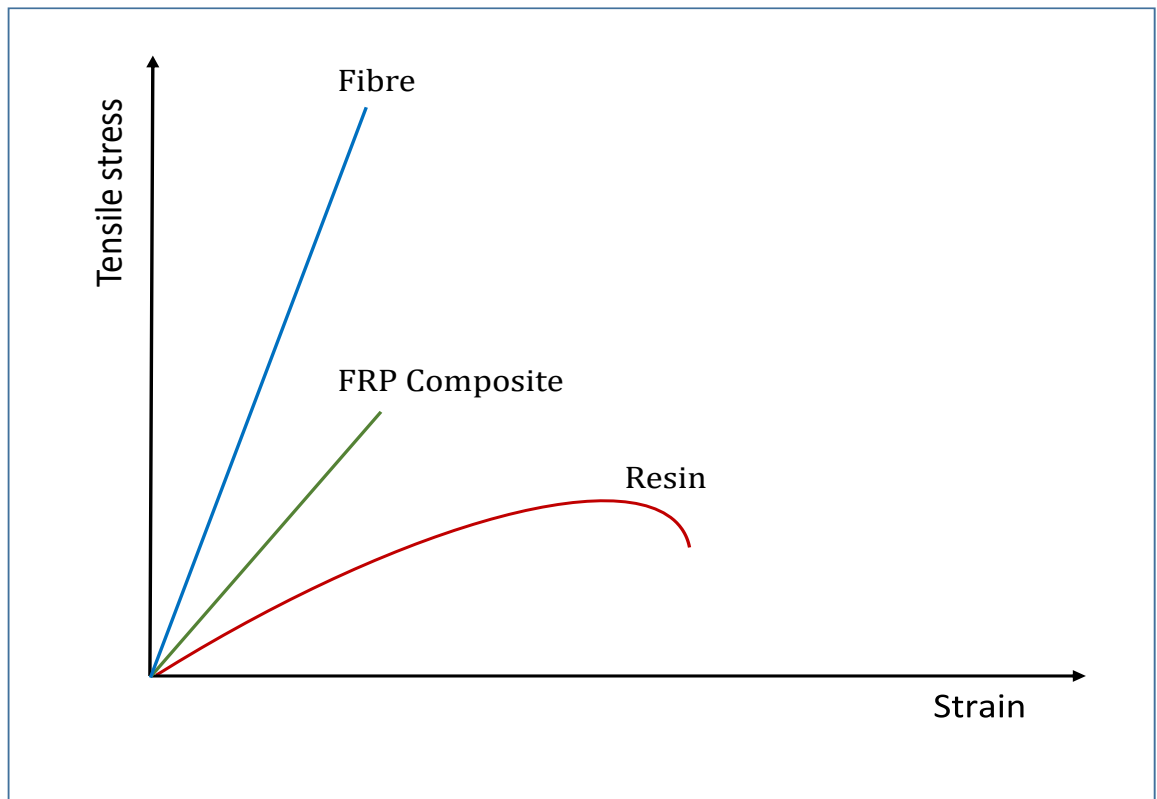


Figure 2-12: Stress-strain relationship for resin, fibres, FRP composite (reproduced from ISIS Canada, 2007)

### 2.10.3 Production and Manufacturing Process

Japan is one of the leading countries to invest heavily in FRP materials development and production to be used in construction, civil engineering and sports goods. The earliest guideline of FRP design for a structural application was published in Japan. However, China has become more involved in a large variety of composite products, and it is the largest producer and market all around the world (Pilakoutas et al., 2002).

Three common manufacturing processes for FRP materials, which are: Filament winding, Braiding and Pultrusion. Filament winding is a method whereby continuous fibres are impregnated with matrix resin and wrapped around a mandrel. The thickness of the fibre-volume fraction and wind angle is controlled. Heat lamps are used to cure the final product. This method is commonly used to produce tubes, pipes and storage tanks (Hoffmann, 2016).

Braiding is a method when interlocking two or more yarns to form an integrated structure. Pultrusion is a method for manufacturing continuous lengths of FRP bars that are of constant profile. A schematic representation of this technique is illustrated in Figure 2-13. Continuous strands of reinforcing material are drawn from glass roving bobbin, through a

resin pool, where they are saturated with resin, and then passed through several wiper rings and rapped by clothing into the entrance of a curing platform. The speed of pulling through the bars from the curing platform is governed by the required curing time. To ensure a good bond between the FRP bar and concrete, the surface of the bars is usually braided or sand-coated (Quayyum and Rteil, 2012).

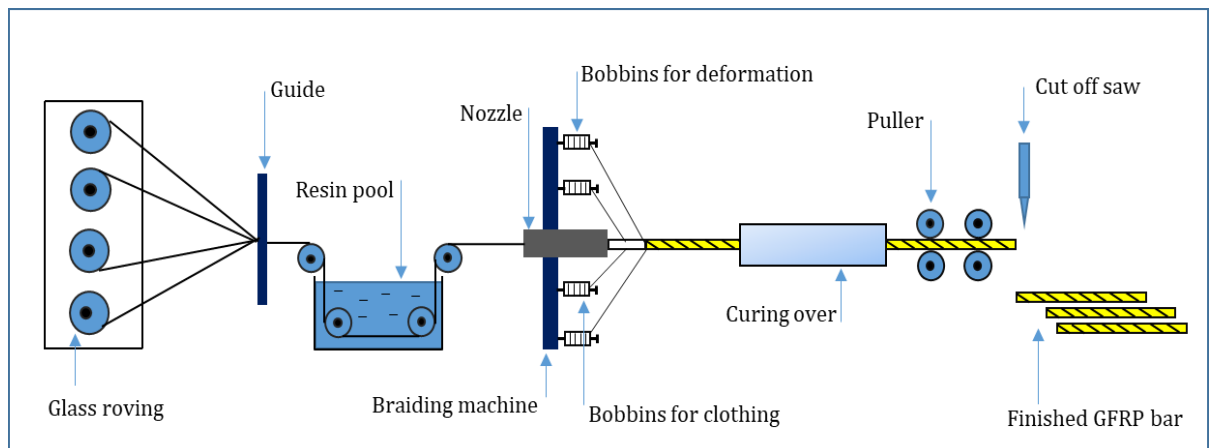


Figure 2-13: Pultrusion process for FRP bars (Benmokrane et al., 2021)

#### 2.10.4 Properties of FRP Reinforcement

Most types of Fibre-reinforced polymer have high tensile strength, high chemical resistance. For the above reasons and due to the good insulation properties of electricity and heat, GFRP is the most commonly used fibre in FRP composites products. Alkali-resistance A-glass, C-glass, electrical E-glass, high-strength S-glass and regular R-glass are the most common types of GFRP (Abedini et al., 2017). Figure 2-14 shows GFRP bars.



Figure 2-14: GFRP R-glass bars (Worner, 2015)

#### 2.10.4.1 Density

GFRP bar has a density of  $2.0 \text{ g/cm}^3$ , four-time lower than that of steel reinforcing bar which is  $8.0 \text{ g/cm}^3$ . The lightweight property in GFRP bars reduces transportation costs and makes handling the bars easier on the project site (Yoo et al., 2019).

#### 2.10.4.2 Thermal Properties

The coefficient of thermal expansion for GFRP bars varies in the transverse and longitudinal directions depending on the type of resin, glass and volume fraction of fibre. Table 2-6 shows the typical coefficients for thermal expansion for GFRP, steel and concrete. The GFRP longitudinal coefficient of thermal expansion is comparable to that of concrete, which means that thermal incompatibility is unlikely to cause any concern when designing GFRP reinforced concrete structures.

Nonetheless, the GFRP transverse coefficient of thermal expansion is two times greater than that of concrete which may lead to splitting cracks in a case where insufficient cover is provided. It was found that the ratio of normal concrete cover thickness to GFRP bar diameter must be greater than or equal to two. This makes it sufficient to avoid cracking concrete up to temperatures of  $+80^\circ\text{C}$ . However, the cover may be reduced if GRFP bars used to reinforce foamed concrete witch has higher thermal insulation properties than normal concrete (Aydin, 2018).

*Table 2-6: Typical coefficients of thermal expansion for GFRP compared with steel and concrete (Aydin, 2018)*

<b>Material &amp; Direction</b>	<b>CTE, x <math>10^{-6}</math> / <math>^\circ\text{C}</math></b>
GFRP longitudinal	8.0-12.0
GFRP transverse	21.0-23.0
Steel	11.0-13.0
Concrete	12.0

In case of fire GFRP bars embedded in concrete will not burn. However, the resin will soften due to the high temperatures. The tensile strength of GFRP starts to decrease when the temperature above 300°C due to a reduction in the bond between fibres. Foamed concrete proved to provide better fire protection to reinforcing bars than normal concrete (Othuman Mydin, 2010) which is one of the reasons that foamed concrete and GFRP combination was chosen in this study.

### 2.10.5 GFRP bar Mechanical Properties

#### 2.10.5.1 Tensile Behaviour

GFRP bar has a tensile strength of 2-4 times higher than that of mild steel reinforcing bars. However, GFRP material does not show any yielding behaviour under tensile stress and experience a sudden brittle failure at the ultimate loading point (Hosen et al., 2017). The GFRP ultimate strain is between 1.2 - 2%, which means a bar of one-meter length could stretch approximately 12- 20 mm before rupture. The tensile strength of GFRP bars may vary with changes in cross-section area, dropping by up to 15% proportionally as the diameter increases from 10 mm to 16 mm (Benmokrane et al., 2021).

The 16 mm bars used in the experimental part of this study have a guaranteed ultimate tensile strength of 1000 MPa. Table 2-7 shows the stress-strain curves for typical values of mild steel, Basalt Fibre Reinforced Plastics (BFRP), Carbon Fibre Reinforced Plastics (CFRP), Armed Fibre Reinforced Plastics (AFRP) and Glass Fibre Reinforced Plastics (GFRP) reinforcement. It is observed that the GFRP can take considerably more stress than mild steel. However, the strain in the GFRP is far greater than the steel for the same applied stress below the steel yield point, as shown in Figure 2-15.

*Table 2-7: Size designation and minimum guaranteed tensile strength of FRP round bars (Shakir Abboud et al., 2020)*

Bar size designation	Nominal diameter (mm)	Nominal area (mm <sup>2</sup> )	Minimum guaranteed tensile strength MPa			
			CFRP	AFRP	BFRP	GFRP
2	6.35	31.7	1902	1408	1242	1000
3	9.53	71.2	1571	1344	1186	955
4	12.70	126.6	1406	1280	1129	909
5	15.88	197.8	1323	1216	1073	864
6	19.05	284.9	1323	1152	1016	819
7	22.23	387.8	1306	1088	960	773
8	25.40	506.5	1298	1024	904	728
9	28.58	641.0	1282	960	847	682
10	32.25	816.9	1265	896	791	637

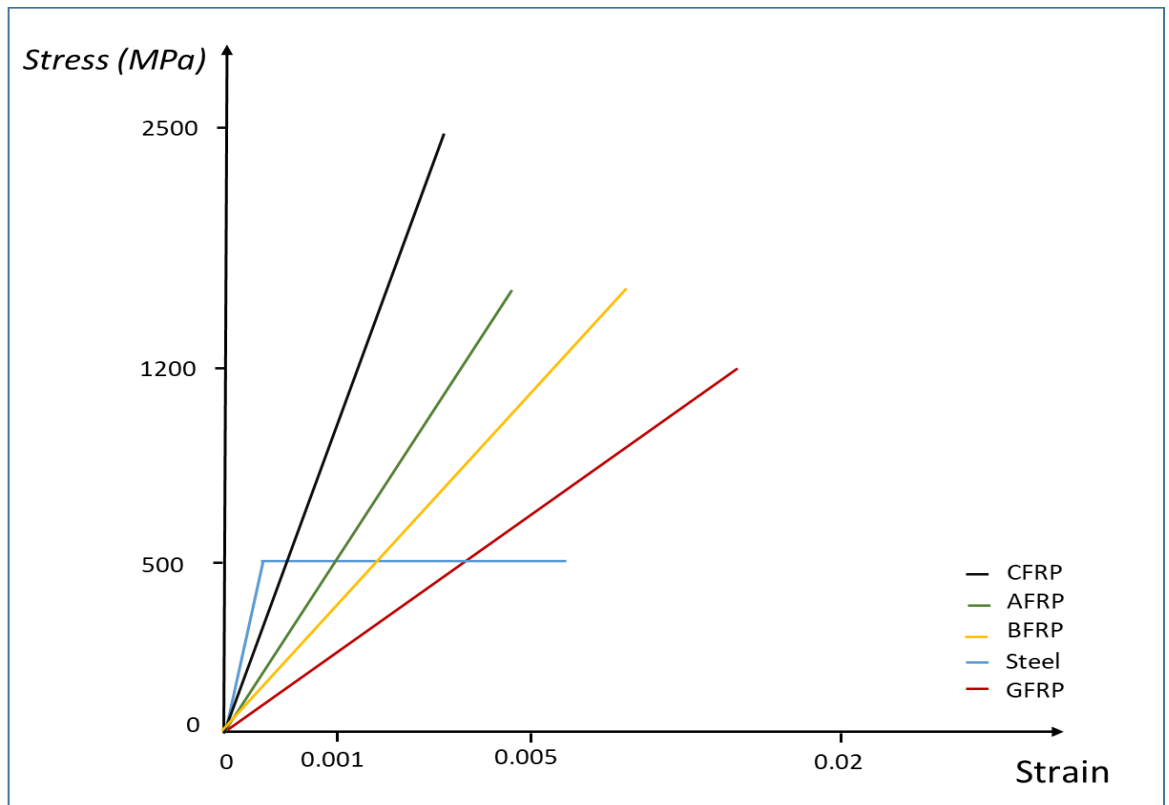


Figure 2-15: Stress-strain curves for typical reinforcing bars (Worner, 2015)

#### 2.10.5.2 Compressive Behaviour

Unlike steel, GFRP behaves differently under compression and tensile stresses. The compressive strength of GFRP bars is lower than its tensile strength, GFRP bars currently produced are not highly recommended for reinforcing concrete columns or any structural member where high compressive strength is required (ACI Committee 440, 2006). The compressive modulus of elasticity is approximately 80-85% for GFRP and CFRP of the tensile modulus of elasticity for the same bar (El-Nemr et al., 2018). Depends on the resin and fibre type, fibre volume fraction, GFRP bars compressive strength could reach up to 70% of its tensile strength. The main GFRP bars failure modes in longitudinal compression are transverse tensile fracture, micro-buckling of fibres, and shear failure of fibres without buckling (Ashour, 2006). Similar to typical flexural design with mild steel reinforcement all guidelines of concrete reinforced GFRP flexural design neglecting the compressive strength of the GFRP bars.

### 2.10.5.3 Shear Behaviour

FRP bars behaviour under transverse shear forces is mostly influenced by the properties of the matrix. FRP bars are weaker in transverse shear than steel. However, the shear strength of FRP can be improved by winding or braiding additional fibres in the direction transverse to the longitudinal one. The characteristic shear strength of FRP bars ranges between 30 to 50 MPa (Nanni et al., 2014). Failure of concrete elements reinforced with FRP due to shear accrue under combined stresses resulting from the applied bending moment and shear force as presented in Figure 2-16.

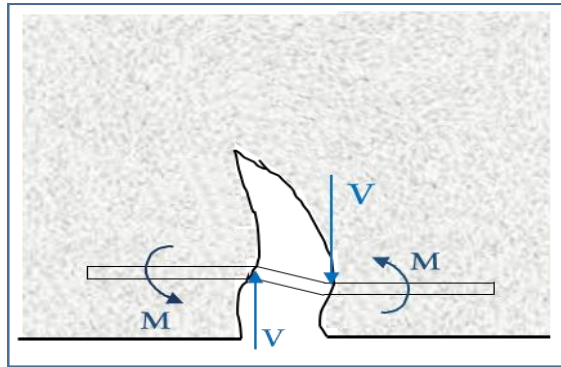


Figure 2-16: Mechanism of shear and flexural resistance of FRP bar

Several researchers (Kim et al., 2015), (Fico et al., 2008) and (Ashour, 2006) have studied the shear behaviour of FRP concrete members. Different approaches were investigated by considering the area, stiffness, and strength of reinforcement. It was demonstrated that shear capacity for FRP RC members could be predicted by introducing modifications to the equations proposed by (ACI-440, 2002) as shown in Equation 2-5.

$$V_{c,f} = \frac{2}{5} \sqrt{f'_c} \cdot b_w \cdot C \quad \text{Equation 2-5}$$

Where:

$f'_c$  Compressive strength of concrete, MPa

$b_w$  Beam's width, mm

$C = k \cdot d$

$d$  Effective depth of the beam, mm

Where:

$$k = \sqrt{(2\rho_f \eta_f + (\rho_f \eta_f)^2 - \rho_f \eta_f)} \quad \text{Equation 2-6}$$

$$\eta_f = \frac{E_f}{E_s} \quad \text{Equation 2-7}$$

In a GFRP bar, there is no reinforcement exists across layers of glass fibres. Therefore, the shear strength depends mostly on the polymer matrix of the bar. The shear strength of GFRP bars could be improved by offsetting the fibre direction from the longitudinal axis of the bar, which might be achieved by winding fibres transversely to the longitudinal axis of the bar (Kong et al., 2020). However, for applications where shear strength should be known, strength values need to be provided by the bar manufacturer.

#### 2.10.6 Durability

In the last three decades, the utilization of GFRP rebar has become a practical alternative to steel for reinforced concrete structures. Reasons behind the success of the worldwide use of GFRP in the construction industry are the relatively low cost, lightweight, high strength, non-corrosive and non-conductive. However, many factors may affect the durability of GFRP bars including ultraviolet exposure, elevated temperature, acidic conditions and long term exposure to alkaline (ACI-440, 2002). A study conducted by (Iqbal et al., 2021) found that a long term exposure to alkaline with a raised temperature up to 50°C show a minor reduction of the tensile strength of the GFRP bar less than 10% of the original tensile strength.

A comprehensive report by Benzecry et al., 2019, studied the durability of GFRP bars extracted from 11 concrete bridges with 15 to 20 years of service life. The bridge structures were visually inspected, and no signs of deterioration were detected. The tensile strength test indicated a reduction in GFRP bars tensile strength of only 2.1% over a period of 17 years in service. This study provides a positive indication of the long-term durability of GFRP bars as internal reinforcement for concrete structures.

### 2.10.7 Current Use of GFRP in Structures

GFRP is an anti-corrosion material. Hence, its applications are expected to be mostly in structures in or near the ground, near or in marine environments, in chemical industrial plants also in thin structural elements. GFRP bars first application as reinforcements in concrete structures were in Japan. Since 90's many projects made of concrete reinforced with GFRP were constructed and developed such as marine structures, bridges, bridge decks and ground anchors, Figure 2-17 shows some projects made of concrete reinforced with GFRP.



Figure 2-17: Structural applications of concrete reinforced with GFRP bars

Thousands of concrete structures such as bridges, parking garages and marine structures have been built of concrete reinforced with GFRP bars which shows the potential for GFRP reinforcement to be used in further applications. This has created the need to develop design procedures for the use of GFRP reinforcement. Japan, Europe, Canada and the USA have developed their design guidelines, in general, these guidelines have been developed by making modifications to the existing steel-reinforced concrete codes based on experimental testing of the material (Worner, 2015).

### 2.11 Existing FRP RC Design Guidelines

With the need to develop a procedure for FRP RC design, many design guidelines have been recently published for concrete elements reinforced with FRP. Four main design guidelines

for FRP RC structures were published in the last decades. The first was the Japanese guide (JMC, 1995; JSCE, 1997), then followed by the America guide (ACI 440–96, 1996; ACI 440–98, 1998; ACI440.1R, 2001; ACI440.1R–03, 2003; ACI440.1R–06, 2006, also the Canada guide (ISIS–01, 2001; ISIS- 07, 2007) and some studies based on the Eurocode (RILEM TC9-RC, 1983).

These design guidelines are mostly based on modifications of existing steel RC codes of practice, where the limit state design approach is predominantly adopted. These modifications are strongly influenced by the FRP reinforcement unconventional mechanical properties. Some empirical equations were developed based on experimental investigations of FRP reinforced concrete elements. However, the brittle linear-elastic behaviour of FRP reinforcement is the key influencing feature behind all of the existing design guidelines (Pilakoutas et al., 2002).

## 2.12 Flexural Behaviour of FRP Reinforced Concrete Members

### 2.12.1 Bond Behaviour of FRP Reinforcement

Marco (2015) stated that bond stress can be transferred through adhesion, friction or bearing on deformations of the reinforcing bar. Adhesion and friction normally have limited transferability due to Poisson's effect causing a reduction in bar diameter when the steel bar under tension force. Nevertheless, the majority of bond stress is developed through bearing on the deformation of the reinforcement bar. The bond stress is not constant with the length of the beam but follows the bending moment magnitudes.

To understand bond stress in concrete, crack development must be reviewed. For instance, when a concrete tensile stress capacity is exceeded in a loaded simply supported beam, for example, cracks in the concrete section start developing. In the cracked beam section, the beam portions between the cracks still carry tension force. However, with loading increases, the tensile stress in the concrete portions increases until the discrete portion of concrete's tensile capacity is reached, then secondary cracks start developing. Figure 2-18 shows the bond stress distribution for a central portion of a cracked beam (Pour et al., 2016).

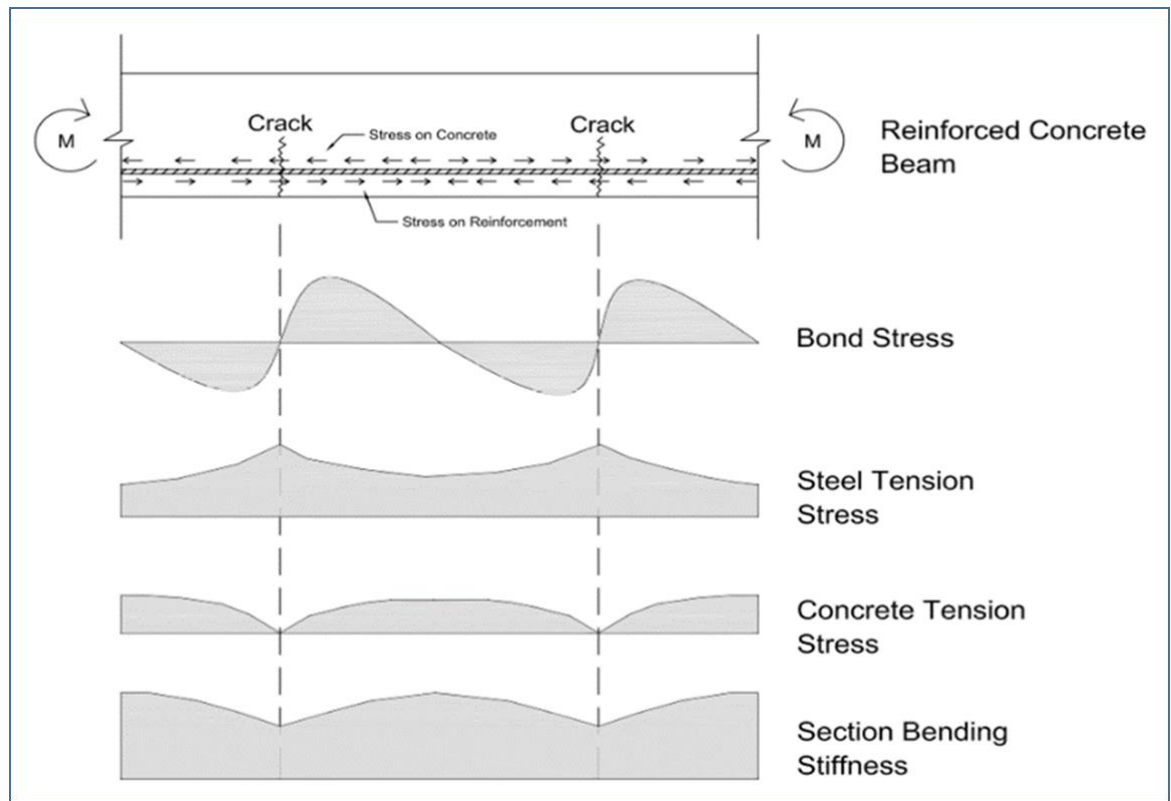


Figure 2-18: Tension stiffening mechanism

This action of bond stress distribution is important since the nonlinear displacement behaviour is considered. The increased rigidity attributable to these un-cracked portions and with loading increased, secondary cracks are developed, which termed tension stiffening (Silva et al., 2014).

The bond performance between FRP reinforcing bars and the surrounding concrete is different from that of steel reinforcing rebar. This is for the reason that FRP has different materials than steel which influence the interaction mechanisms with concrete. Moreover, FRP bars surface roughness plays a major role in bond performance with concrete. The surface roughness of FRP is controlled using fibres, epoxy or sand coating. Therefore, friction and chemical adhesion are the main bond mechanisms in concrete reinforced with FRP (Yan et al., 2016).

Some researchers (Marco, 2015), (Muñoz, 2010), (Hickinbotham, 2016) studied the bond behaviour between concrete and FRP in concrete structures. It was found that the failure mode and bond strength depend on concrete compressive strength, concrete cover and the embedment length of FRP bars in concrete. It was observed that the increase of

concrete compressive strength improves the bond, also the sufficient concrete cover provides a better bond. However, it was noticed that the bond strength decreases when the embedment length of FRP bars increases. This attributed to the non-linear distribution of bond stresses along the length of bars see Figure 2-19.

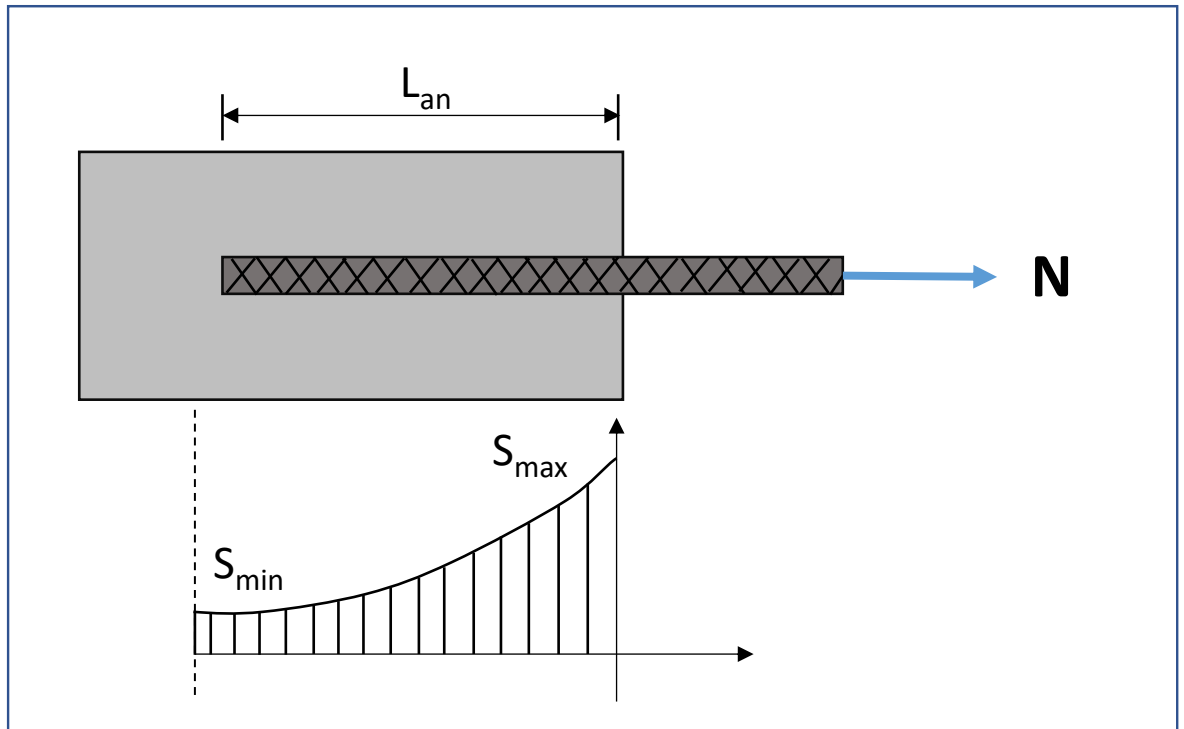


Figure 2-19: Bond stress along the length of the bar

Several types of test methods are available to determine the bond strength of FRP reinforcement in concrete structures such as pull-out and beam tests. According to a study conducted by (Muñoz, 2010) on concrete- FRP bond behaviour, where 88 samples were tested using the pull-out test. It was observed that the bar size may affect the bond strength with concrete. However, the surface treatment has a major effect on bond strength. For the bond reason, some manufacturers add a coating of sand and resin on the bar at the end of the manufacturing process to improve the bond with concrete. Table 2-6 shows, modulus of elasticity, tensile strength, ultimate tensile strain, shear strength, and bond strength of GFRP.

*Table 2-8: Typical mechanical properties and bond strength of GFRP bar (Shakir Abbood et al., 2020).*

<b>Property</b>	<b>GFRP</b>
Modulus of elasticity (MPa)	40-65
Tensile strength (MPa)	650-1200
Ultimate tensile strain (%)	1-2
Shear strength (MPa)	100-125
Bond strength (MPa)	8-12

### 2.12.2 Deflection of FRP RC Members

Concrete members reinforced with FRP behave differently from those reinforced with traditional steel rebar. The main reasons behind it are that FRP bars have higher tensile strength, but lower modulus of elasticity than steel, and demonstrate linear elastic behaviour in tension up to failure point (Fico et al., 2008). The lower modulus of elasticity of FRP causes a significant reduction in the stiffness of FRP reinforced concrete elements after cracking, and consequently higher levels of deflection under service conditions (El-Nemr et al., 2018). Therefore, the design of FRP reinforced concrete members is normally ruled by serviceability requirements.

The short-term deflections of a cracked concrete element reinforced with steel can be determined using an effective moment of inertia equation given by ACI 318 as shown in Table 2-9. It was observed that the equation leads to underestimated service level deflections in FRP RC beams. This is since the equation was only adjusted for steel-reinforced concrete beams.

Table 2-9: Deflection design equations for FRP reinforced concrete members

Author	Equation	No
ACI 318 (2000)	$I_e = \left(\frac{M_{cr}}{M_a}\right)^3 \times I_g + \left[1 - \left(\frac{M_{cr}}{M_a}\right)^3\right] \times I_{cr} \leq I_g$	Equation 2-8
ISIS Canada (2001)	$I_e = \frac{I_e \cdot I_{cr}}{I_{cr} + \left[1 - 0.5 \left(\frac{M_{cr}}{M_a}\right)^2\right] [I_g - I_{cr}]}$	Equation 2-9
CSA-02 (2002)	$I_e = \frac{I_{cr}}{1 - \left(1 + \frac{I_{cr}}{I_g}\right)^3 \left(\frac{M_{cr}}{M_a}\right)^3}$	Equation 2-10

**Note:**  $I_e$  is the effective moment of inertia ( $\text{mm}^4$ ),  $M_a$  is the applied moment (N.mm),  $M_{cr}$  is the cracking moment (N.mm),  $I_g$  is the moment of inertia of cross-section ( $\text{mm}^4$ ),  $I_{cr}$  is the moment of inertia of cracked section transformed to concrete ( $\text{mm}^4$ ).

Deflections of RC members reinforced with FRP found to be more sensitive to the variables affecting deflection than steel RC members of the same size and reinforcement layout because of the brittle-elastic nature, axial stiffness and particular bond features of FRP bars (ACI-440, 2002). However, in both steel and FRP RC beams the deflection is depending on the load magnitude and the number of loading cycles but the FRP reinforced beams deflection is 1.5 to 2.5 times that of identical steel-reinforced concrete beams (Ng et al., 2020).

### 2.12.2.1 Ultimate Load and Modes of Failure

The flexural design of concrete members reinforced with steel usually result in under reinforced sections to ensure that the steel reinforcement yield before the crush of concrete (Hosen et al., 2017). It is for this reason that the yielding of steel provides ductility and warning of the failure of the member. On the other hand, in the case of concrete members reinforced with FRP, there is no warning of failure due to the non-ductile behaviour of FRP reinforcement. In this case, failure would occur either due to rupturing (tension failure) of the FRP reinforcement or crushing (compression failure) of the concrete. If the flexural failure occurs due to FRP reinforcement rupture the failure will be sudden and catastrophic (Falade et al., 2014).

In the rupturing failure (tension failure) mode of FRP RC members, there would be a limited warning of impending failure in the form of large deflection and extensive cracking. However, the concrete crushing failure (compression failure) mode is slightly more desirable for flexural members reinforced with FRP bars, since the members exhibit some plastic behaviour before failure (ACI-440, 2002).

A study by Kara and Ashour (2012) adopted a numerical method for FRP concrete beams to predict the moment capacity. The study's results showed that the proposed numerical technique can estimate the moment capacity of FRP concrete beams. In addition, It was noticed that the (ACI-440, 2002) formulas could rationally predict FRP reinforced concrete beams moment capacity.

### 2.12.2.2 Cracking of FRP RC Members

Junaid et al., (2019) stated that the spacing and pattern of cracks in GFRP reinforced concrete beams is similar to those in steel-reinforced concrete beams at initial load level. However, as the load increased, more cracks appeared with increased width compared to steel reinforced concrete beams. This can be explained by the low modulus of elasticity of GFRP bars compare to steel rebar.

According to Hoffmann (2016), the maximum crack width in FRP concrete beams was observed to be 2-4 times that of identical beams reinforced with steel bars. The crack width in GFRP reinforced concrete beams directly proportional to the applied moment up until failure. Based on the formula developed by ACI-440 (2002) calculates the maximum crack width of concrete beams reinforced with FRP, taking into consideration the maximum distance from the centre of the bar to the concrete surface as shown in Equation 2-11.

$$w = \left( \frac{2.2}{E_f} \right) \cdot \beta \cdot f_f \cdot k_b \sqrt[3]{d_c x A} \quad \text{Equation 2-11}$$

Where

- $w$  Crack width measured at the extreme beam bottom level, mm
- $E_f$  Modulus of elasticity of FRP level, MPa
- $A$  Tension area per FRP bar level, mm<sup>2</sup>

- $d_c$  Concrete cover of an outermost bar measured from the centre of that bar level, mm
- $f_f$  Tensile stress in longitudinal FRP bar level, MPa
- $\beta$  Ratio of distances to the neutral axis from the extreme beam bottom level and the centroid of longitudinal bars
- $k_p$  1.0 for FRP bars with similar bond characteristics to that of steel

### 2.12.3 Shear Capacity in FRP RC Members

Studies by (Boulekbatche et al., 2012) and (Kim et al., 2015) on the shear capacity of flexural elements showed that the concrete shear strength is greatly influenced by the stiffness of the tensile (flexural) reinforcement. Failure of reinforced concrete elements due to shear usually occur under combined stresses resulting from the applied bending moment and shear force as shown in Figure 2-20.

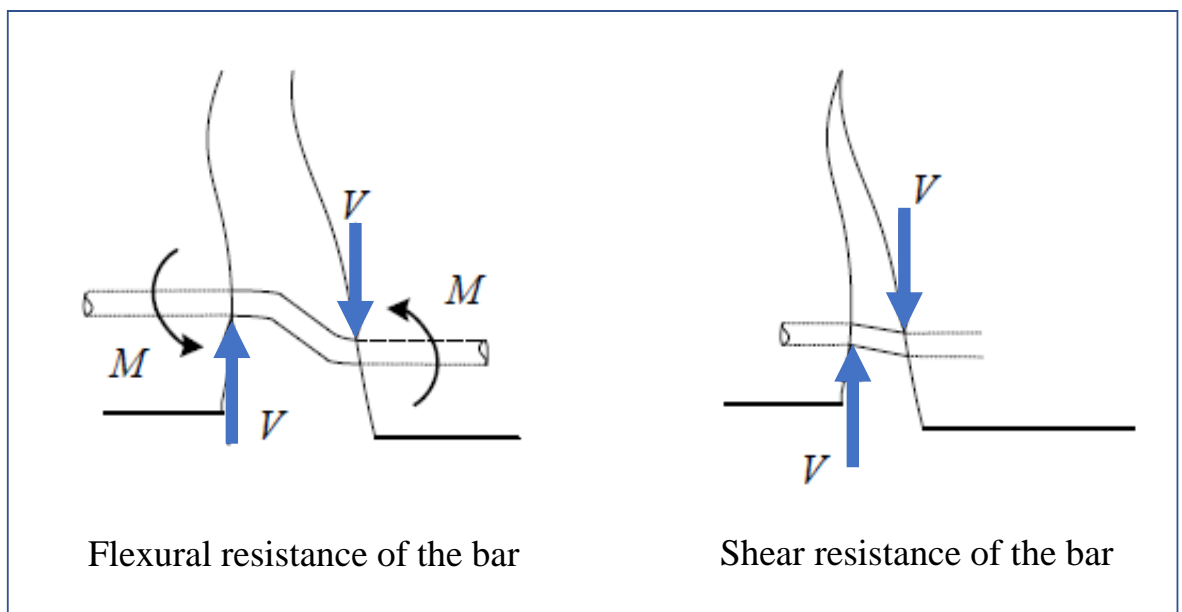


Figure 2-20: Mechanisms of flexural bars crossing a crack

In general, the shear strength of reinforced concrete beam without shear reinforcement is directly related to the axial stiffness of the longitudinal reinforcing bars. As the modulus of elasticity of GFRP is around 1/3 of it in steel, which results in a reduction of the axial stiffness of the longitudinal reinforcement, leading to a decrease of the overall beam shear strength (Ashour, 2006). The failure of the FRP reinforced beam without shear

reinforcement would be brittle and sudden. Consequently, a minimum amount of shear reinforcement is required when the factored shear force,  $V_f$  exceeds  $0.5V_c$  (Kim et al., 2015).

To evaluate the flexure and shear capacities of FRP reinforced concrete beams, Ashour (2006), conducted a comprehensive study on GFRP reinforced concrete beams, without transverse shear reinforcement. The main variables in the study were the depth of the beams and the amount of GFRP reinforcement. It was found that flexural failure take place in under reinforced beams due to the GFRP bar rupture, whereas shear failure occurred in over reinforced beams. Table 2-10 presents the shear design for FRP reinforced concrete elements without shear reinforcement.

Table 2-10: The shear design for FRP reinforced concrete elements without shear reinforcement

Model	Equation	Committee	No
ISIS Canada-01	$V_{c,f} = 0.2b_w \cdot d \sqrt{f'_c \frac{E_f}{E_s}}$	$d \leq 300 \text{ mm}$	Equation 2-12
CSA S806-02	$V_{c,f} = 0.035b_w \cdot d (f'_c \cdot \rho_f \cdot E_f \frac{V_f}{M_f})^{0.33}$	$\leq 300 \text{ mm}$	Equation 2-13
ACI 440-03	$V_{c,f} = \frac{\rho \cdot E_f}{90\beta \cdot f'_c} V_c$	$V_{c,f} \leq V_c$ $V_c = b_w \cdot d \sqrt{f'_c}$	Equation 2-14

**Note:**  $f'_c$  is the concrete compressive strength.  $d$  and  $b_w$  are beam's effective width and depth respectively.  $E_f$  and  $E_s$  are the modulus of elasticity of FRP and steel longitudinal bars.  $\rho_f$  is the longitudinal reinforcement ratio.  $V_f$  and  $M_f$  are shear force and moment respectively.

#### 2.12.4 Moment of Resistance of FRP RC Members

The existing guidelines for FRP design such as ACI-440.1R (2006), CSA- S806 (2002) and ISIS (2001), cover the two types of flexural failure of concrete reinforced with FRP elements (i.e. reinforcement rupture and concrete crushing). The flexural failure type is mostly based on the reinforcement ratio of the section. This ratio is principally influenced by the concrete and FRP mechanical properties, and it is calculated from expressions derived by considering internal-force equilibrium (Hoffmann, 2016).

For the flexural design of FRP RC sections compatibility of strains, perfect bond, the equilibrium of internal forces, and linear behaviour of FRP until failure are assumed. For calculations purposes and according to Pilakoutas et al., (2002) study the stress distribution for the concrete section is replaced by the Eurocode-2 equivalent rectangular stress block defined by parameters  $\lambda$  and  $\eta$  where the FRP bars contribution in the compression zone of the concrete is ignored.

The theoretical limit for the reinforcement ratio has to be determined at which the FRP RC section fails as a balanced section to be able to select the right mode of flexural failure. The balanced reinforcement ratio may be calculated by Equation 2-15.

$$\rho_{fb} = \eta \cdot \lambda \frac{f_{cd}}{f_{fd}} \left[ \frac{E_f \cdot \varepsilon_{cu}}{E_f \cdot \varepsilon_{cu} + f_{fd}} \right] \quad \text{Equation 2-15}$$

Where:

$f_{cd}$  Design compressive strength of concrete, MPa

$E_f$  Modulus of elasticity of FRP, MPa

$f_{fd}$  Design tensile strength of FRP rebar, MPa

$\varepsilon_{fd}$  FRP design tensile strain

$\varepsilon_{cu}$  Concrete ultimate compressive strain, MPa

When the ratio of longitudinal FRP reinforcement ( $\rho_f$ ), is higher than ( $\rho_{fb}$ ) the flexural failure is predicted to occur due to concrete crushing, therefore, the ultimate moment resistance ( $M_u$ ) may be calculated by Equation 2-16.

$$M_u = \eta f_{cd} \cdot b d^2 (\lambda \xi) \left(1 - \frac{\lambda \xi}{2}\right) \quad \text{Equation 2-16}$$

Where:

$$f_{cd} = \frac{\alpha_{cc} f_{ck}}{\gamma_c} \quad \text{Equation 2-17}$$

$$\alpha_{cc} = 1.0$$

$$\xi = \frac{x}{d} = \frac{\varepsilon_{cu}}{\varepsilon_f + \varepsilon_{cu}} \quad \text{Equation 2-18}$$

$$\lambda = 0.8 \text{ and } \eta = 1 \text{ for } f_{ck} \leq 50 \text{ MPa}$$

$$\lambda = 0.8 - \left(\frac{f_{ck}-50}{400}\right) \text{ for } 50 < f_{ck} \leq 90 \text{ MPa}$$

$$\eta = 1.0 - \left(\frac{f_{ck}-50}{200}\right) \text{ for } 50 < f_{ck} \leq 90 \text{ MPa}$$

$$\varepsilon_f = \frac{-\varepsilon_{cu} + \sqrt{\varepsilon_{cu}^2 + \frac{4 \eta \alpha_{cc} f_{ck} \lambda \varepsilon_{cu}}{\gamma_c \rho_f E_f}}}{2} \quad \text{Equation 2-19}$$

However, when the ratio of longitudinal FRP reinforcement ( $\rho_f$ ), is lower than ( $\rho_{fb}$ ) the flexural failure is predicted to occur due to reinforcement rupture, therefore, the ultimate moment resistance ( $M_u$ ) may be calculated by Equation 2-20.

$$M_u = \frac{A_f f_{fk}}{\gamma_f} \left(1 - \frac{\lambda \xi}{2}\right) \quad \text{Equation 2-20}$$

### 2.13 Summary

This chapter aims to provide the reader with a background of foamed concrete and GFRP reinforcement. In the past few decades, significant developments have been made to understand the GFRP reinforced structures behaviour. Based on the critical literature review and the results of previous research described in this chapter, the following summary can be drawn:

- Foamed Concrete is a type of lightweight concrete which is consisting of mortar or Portland cement paste with a homogeneous pore structure created by entrained air voids.
- FC can be produced by using foaming agents (physically aerated concrete) or by adding aluminium powder, calcium carbide and hydrogen peroxide (chemically aerated concrete).
- FC has been used in the construction industry in non/semi-structural applications such as void filling materials, thermal, sound insulation but not in structural applications when higher strength is required.
- FC mechanical properties could be influenced by its density, cement/sand ratio and additives that added to FC mixes.
- It was observed that the behaviour and structural performance of concrete members reinforced with FRP are different than those of steel-reinforced members.
- Unlike steel-reinforced beams, beams reinforced with FRP do not show any yield behaviour. For this reason, it is not recommended to use FRP reinforcement in members where moment redistribution is required, such as in moment frames.
- The bond strengths between concrete and FRP bars can be slightly lower than those provided by steel reinforcing bars.
- There are no full existing standards for FRP RC member's design. However, guidelines were published to estimate moment capacity, shear strength and deflection of FRP RC members.

## Chapter 3

# Foamed Concrete Development: Experimental Programme

### 3.1 Introduction

The purpose of this chapter is to clarify the methodological framework used to conduct this research. The methodology was chosen as relevant to the tasks. A quantitative study approach was adopted in this research to deal with the research problem. The data collection involves numeric information through experimental, theoretical and numerical programmes.

The experimental programme in this study is falling into two main phases: FC mechanical properties development phase and the structural behaviour phase. This chapter covers phase one, which is all about developing the mechanical properties of foamed concrete including; design mix trials, produce a range of foamed concretes of density between (800-1800)  $\text{kg/m}^3$  with and without additives, vary  $s/c$  and  $w/c$  ratios. Investigate the mechanical properties; compressive strength, tensile strength, flexural strength, direct tensile strength, shear strength, stress-strain relationship, and modulus of elasticity) and develop these properties to be suitable for structural use. Table 3-1 summarises the experimental research programme.

FC has been recognised as a multipurpose construction material that environmentally sustainable, lightweight, durable, simple to use with high thermal and sound insulation (Kong et al., 2018). However, the potential utilization of foamed concrete in structural applications has been inhibited by the challenge of achieving high strength (Falliano et al., 2020).

Phase two investigates the structural behaviour of foamed concrete by studying the bond behaviour of FC with steel and glass fibre reinforced polymer (GFRP) reinforcing bars using the pull-out test and beam test. Examine the flexural behaviour of full-scale simply supported normal/foamed concrete beams reinforced with steel/GFRP bars to study the load-displacement response, moment capacity, crack pattern and mode of failure with steel and GFRP bars reinforcement numerically and experimentally.

Table 3-1: Experimental research programme

	Purpose	Test programme	Expected Findings
<b>Phase 1</b>	Developing the mechanical properties of FC. Produce a range of FC with density (800-1800) kg/m <sup>3</sup> with/without Additives.	<b>Testing:</b> Compressive strength Tensile strength Flexural strength Shear strength Modulus of elasticity	Produce FC with a density of no more than 1800 kg/m <sup>3</sup> and compressive strength of 28 MPa or more
<b>Phase 2</b>	Study the Structural behaviour of FC experimentally and numerically.	<b>Testing:</b> The bond behaviour of FC with steel and GFRP reinforcing bars. Reinforced (Steel/GFRP) simply supported full-scale beam to examine the structural behaviour, crack pattern and mode of failure. Software modelling (simulating) studying the failure of the loaded beam and compare results.	Study the effect of additives on bond behaviour of FC with steel and GRP rebar. Examine the structural behaviour of foamed concrete

## 3.2 Materials

Tanveer *et al.*, (2017) stated that the key raw materials of foamed concrete are cement, sand, water and foam. However, additives or admixtures may be used to improve a specific property of the concrete. Consequently, in order to meet the aim of producing foamed concrete with enhanced strength certain additives, such as Metakaolin (MK), silica fume (SF) and Waste Toner were used in this study. A combination of the following constituent materials was used to produce foamed concrete in this research.

### 3.2.1 Cement

The Ordinary Portland cement (OPC) 32.5N and Portland cement CEM I 42.5 N conforming to BS EN 197: Part 1: 2000 were used in this study. The total cementitious material in this study was between (250- 560) kg/m<sup>3</sup>, as Ramamurthy and Nambiar (2009) stated that the improvement in strength obtained by increasing the cement content above 500 kg/m<sup>3</sup> is small. However, according to Mohammed and Hamad (2014) for structural foamed

concrete cement content may increase up to  $600 \text{ kg/m}^3$ . The chemical composition and main properties of cement used for the study were shown in Table 3-2.

### 3.2.2 Silica Fume (SF)

The silica fume (SF) used in this study is conforming to BS EN 13263-1 (2009). In order to improve the strength of FC, 10% and 15% of the total weight of the cement was replaced by SF. It was noticed that Silica fume might improve the compressive strength of FC if replaced up to 15% of cement content by weight only where the foam content is less than 30 per cent by size (Wang et al., 2020). However, for higher foam contents mixes, the increase in strength was minor. Lee *et al.*, (2014) stated that in foamed concrete silica fume was found to have little effect on shrinkage. Mohammed and Hamad (2014) mentioned that silica fume increased normal weight concrete compressive strength. However, it was found to generate much heat of hydration, which is not favourable for foamed concrete as it may lead to significant temperature increases which may have an adverse effect on foam bubbles. The chemical composition and main properties of silica fume are shown in Table 3-2.

### 3.2.3 Metakaolin (MK)

Chun *et al.*, (2007) noted that Metakaolin (MK) is a pozzolanic ultra-fine material, with a specific surface area in the range of  $4000 \text{ m}^2/\text{kg}$  to  $12000 \text{ m}^2/\text{kg}$ . MK is an extremely active and effective pozzolan for the partial replacement of cement in concrete (Mohammad, 2011). MK is normally produced by the calcination of kaolinitic clay at a high temperature reaching  $800^\circ\text{C}$ . Khan *et al.*, (2019) stated that the presence of MK in concrete improves several physical and mechanical properties of the produced concrete such as increases workability, compressive and tensile strengths, durability, resistance to chemical attack and reduces permeability, effects of alkali-silica reactivity (ASR), shrinkage. Despite the fact MK has the potential to improve the mechanical and durability properties of concrete, its use is still limited due to its high cost (Awang et al., 2014).

Table 3-2: Chemical composition and main properties of cement and fillers, percentage by mass compound (Othuman Mydin, 2010) and (Zhang et al., 2020).

Compounds/ properties	CEM I 42.5N	Silica fume	Metakaolin	Waste Toner
CaO	64.45	1.9	0.01	2.5
SiO <sub>2</sub>	22.25	96.95	56.7	10-20
Binder Resin	-	-	-	50-80
Al <sub>2</sub> O <sub>3</sub>	4.75	0.25	39.8	-
Fe <sub>2</sub> O <sub>3</sub>	3.35	0.15	0.51	10-20
Carbon black- C	-	-	-	0.1-5
SO <sub>3</sub>	1.95	0.00	0.00	0.05
Ground sand	-	-	-	1-5
MgO	1.45	0.25	0.25	-
K <sub>2</sub> O	0.9	0.15	1.82	-
TiO <sub>2</sub>	0.35	0.35	0.81	0.01
Na <sub>2</sub> O	0.35	-	0.09	-
MnO	0.20	-	0.01	-
Density (g/cm <sup>3</sup> )	3.15	2.25	2.60	1.7
Particle size distribution				
D90 (μm)	34.24	7.35	8.07	-
D50 (μm)	12.38	1.73	1.90	31.5
D10 (μm)	1.64	30.85	20.69	68.5

Khan *et al.*, (2019) mentioned that the incorporation of MK, up to 25 per cent by weight of cement, has shown pore refinement to 60 per cent of the original pore size. Up to date, very limited literature has been published on the use of MK in foamed concrete, and all of this literature is recommending more investigation on the Mk effect on FC properties. In the study of developing the mechanical properties and structural behaviour of foamed, MK was used as a replacement of cement of 20 per cent by weight.

### 3.2.4 Waste Toner

Toner is a dry ink powder with particles size of 5-50 micrometre, mainly made from a polyester resin/styrene acrylic copolymer which is brittle and has a low melting temperature of 110 °C. The waste toner used in this research is a mono-component type, it is magnetic and has a large proportion of binding resin and iron-oxides (Pirela et al., 2015). Shawnim, 2018 noted that Waste Toner could improve FC compressive strength by 20%. As shown in Table 3-2. Toner is composed of the following basic components.

- Polymer - commonly stiff to enable efficient particle manufacture and low melting point to allow quick thermal fusing.
- Colourant (pigments such as carbon black and Iron oxide) - to provide the desired toner colour.
- Charge control agent – to allow the charge features of the toner to be fine-tuned.
- Flow control additives (Amorphous silica / fumed silica) – to prevent the toner from caking.
- Wax – to prevent toner from sticking to the heated fuser rollers.

Toner is a waste material taken from used laser printers' cartridges. Toner could be considered as a sustainable and cost-effective additive material, where the material is from old printer cartridges. It might be collected of the expired and waste material which may come at no cost at all. In this research Toner is used as an additive to the mortar at 5 per cent of the binding cementitious material (cement) by weight. Figure 3-1 shows Portland cement and additives materials.



Figure 3-1: Portland cement and additives materials

### 3.2.5 Fine Aggregate

Natural siliceous sand conforming to ASTM C144 and BS EN 12620, (2009) sieved to remove particles greater than 2.36 mm in diameter was used to improve the stability and flow features of the final product (Jones et al., 2016). The Coarse aggregate is not used in foamed concrete production as the fine air voids structure cannot support bigger size (heavyweight) aggregate which may lead to segregation. Sands compliant with ASTM C144 and BS EN 12620, (2009) are suitable for foamed concrete production according to (Lesovik et al., 2020). Researchers such as Jones and McCarthy (2005), Ozlutas (2015) and Mehta, (2017) used fine aggregate conforming to BS EN 12620 to produce foamed concrete with a density between 800 and 1600 kg/m<sup>3</sup>.

Based on previous studies, Ikponmwosa *et al.*, (2017) noted that alternative fine aggregate materials such as chalk, Lime, incinerator bottom ash, crushed concrete, recycled glass and Lytag fines are possible to be used in foamed concrete as waste or sustainable materials to reduce the overall density.

### 3.2.6 Water

The significance of water in normal concrete is well-documented. However, a brief review would help understand the role of water in foamed concrete. Water is an essential element in the production of concrete; to wet the aggregate, precipitate chemical reaction with the

cement, and lubricate the mixture for easy workability (Lee et al., 2014). Water proportion is normally added to the mix by weight based on the water/cement ratio. The mix of water with cement should comply with BS: EN:1008:2002, (2002) Mixing Water for Concrete. This standard covers the utilization of potable water and establishes a guide to reuse the water that is reclaimed or recovered from processes in the concrete industry. Highways Agency (HG) and the future of Transport (TRL) (2001) stated that it is fundamental to use potable water in foamed concrete, especially when the foaming agent is protein-based for the reason that organic contamination may have an adverse effect on the quality of the foam, and hence the concrete produced (Ching, 2012).

Awang *et al.*, (2014) mentioned that the effect of water proportion on some foamed concrete properties is different to its effects on normal concrete. Ramamurthy and Nambiar (2009) stated that the w/c ratio plays fewer roles on the strength of foamed concrete than normal concrete. However, De Villiers (2015) noted found that the w/c ratio is an important factor in foamed concrete, where too much water may lead to segregation and too little water may lead to disintegration. (Meera and Gupta, 2020) stated that using a small proportion of water leads to water withdrawal from the foam and the foam degenerates quickly. However, they suggested that the w/c ratio required to achieve acceptable workability in foamed concrete is ranging from 0.35 to 1.25 dependent on; type of binder(s) used, the use of a plasticizing agent, wet density targeted, the strength required. The w/c ratio chosen for this study is 0.5 as it is the most recommended ratio by several researchers (Mohammed and Hamad, 2014).

### 3.2.7 Foaming Agents (surfactants)

There are several types of Surfactant available on the market. The surfactants used in this study have been proven to be effective in producing foamed concrete, which is protein - based surfactants. Ramamurthy and Nambiar (2009) mentioned that protein surfactants have more stable and closed cells, which result in higher foamed concrete strengths. Foamed concrete produced employing protein surfactant was found to have a strength/density ratio of about 50 - 100 per cent higher compared to those using synthetic

surfactants. Figure 3-2 illustrate Foam making products showing: foaming agent, foaming machine and foam.

Therefore, commercially available protein - based surfactant (ProPump, Protein 40) was employed to produce preformed foam aiming to achieve low density foamed concretes with higher strengths. The surfactant solution's concentration used in this study to produce foam is typically 50 g per one litre of water, which is used throughout this study to produce foam with a density of  $50 \pm 5 \text{ kg/m}^3$ . The preformed foam was prepared from a 5 per cent aqueous surfactant solution in a dry system generator. The foam density was found to be between 43 and 53  $\text{kg/m}^3$ .

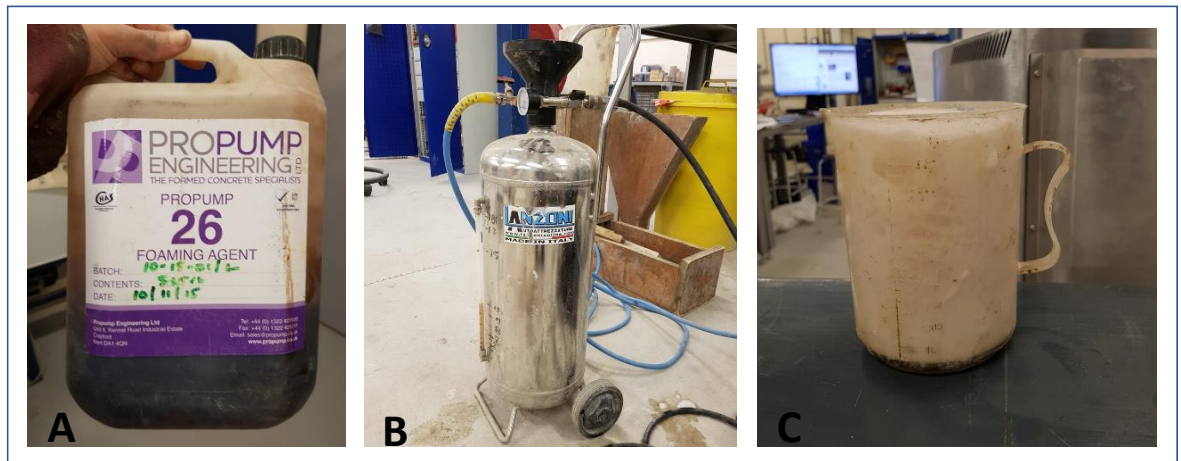


Figure 3-2: Foam making products showing (a) foaming agent (b) foaming machine and (c) foam

### 3.3 Mix Design

Gangatire and Suryawanshi (2016) stated that there is no standard specification for foamed concrete mix design. Therefore, in this study, the author used the method of absolute volumes. This method was used in a number of studies. The method began with the selection of  $w/c$  ratio, target plastic density and cement content were considered as essential factors while designing the foamed concrete mixes. The mix was then proportioned by the absolute method volumes (Ramamurthy and Nambiar, 2009).

Hashim (2014) mentioned that that mix proportions of foamed concrete should be chosen according to specific requirements such as strength, thermal conductivity, shrinkage, etc. Consequently, the constituent materials selected for this study have been chosen to produce foamed concrete with relatively high strength and low density. According to Lee

*et al.*, (2014), several studies have stated that in general, the optimum w/c ratio of foamed concrete lies between 0.4 and 0.6 but with superplasticizer, the w/c ratio might be reduced to as little as 0.25. As no superplasticizer used in this study, the w/c ratio chosen is 0.5, where it was provided sufficient consistency for the majority of mixes within the range of densities and constituent materials (Ramamurthy and Nambiar, 2009).

### 3.3.1 Examples of Mix Design

In the method of Absolute Volume, mix proportioning starts with the selection of the plastic concrete density, water/ binder (*w/b*) ratio and sand /cement (*s/c*) ratio or the cement content. The mix design steps are explained in the following example.

Plastic density of foamed concrete required =  $1600 \text{ kg/m}^3$

- Sand/ Cement ratio = 2
- Water/ Binder ratio (*w/b*) = 0.5
- Specific gravity of cement = 3.15
- Specific gravity of sand = 2.35
- Unit weight of water =  $1000 \text{ kg/m}^3$
- Unit weight of foam =  $45 \text{ kg/m}^3$

The total mass of raw materials =  $1\text{m}^3 \times 1600 \text{ kg/m}^3 = 1600 \text{ kg}$

Table 3-3: Absolute volume method for mix design

Material	Mass kg in $1\text{m}^3$	Calculation	Absolute Volume $\text{m}^3$
Cement	457.15	$457.15 \times \frac{1}{3.15 \times 1000}$	0.145
Sand	914.275	$914.275 \times \frac{1}{2.35 \times 1000}$	0.39
Water	228.571	$228.571 \times \frac{1}{1 \times 1000}$	0.228
<b>Total</b>			0.763
Air volume required		$1\text{m}^3 - 0.763$	0.236

The air content in foam produced by using ProPump, Protein 40 foaming agent is about 95%, therefore foam volume is:

$$\frac{0.236}{0.95} = 0.248 \text{ m}^3$$

The amount of foaming agent required to produce 248 litres of foam is:

$$\frac{0.8 \text{ ml} \times 248}{1\text{L}} = 198.4 \text{ ml} = 0.28 \text{ kg}$$

The amount of water required to produce (248) litre foam is:

$$\frac{45\text{g} \times 248\text{L}}{1\text{L}} = 11160\text{g} = 11.16 \text{ kg}$$

The excel sheet used for all mix designs is available in Appendix A.

### 3.4 Experimental Concrete Production

Foamed concrete production using the pre-formed foam method is a simple and not expensive process, apart from the foam generator, all equipment that already available for normal concrete production may be used for foamed concrete production (Krishna et al., 2021).

#### 3.4.1 Foam Production

Producing foam with a density of  $50 \pm 5 \text{ kg/m}^3$  required 50g of surfactant in a litre of water to prepare the aqueous surfactant solution. Foam is produced by foam generator shown in Figure 3-3 A. Foam densities were typically found to range between 43 and 53  $\text{kg/m}^3$ . The density of foam was found to be affected by the pressure applied in the foam generator (Jalal et al., 2017). Therefore, as recommended by Ramamurthy and Nambiar (2009), the pressure gauge of the foam generator was set to 345 KPa (50psi) in order to produce foam with the lowest possible density.

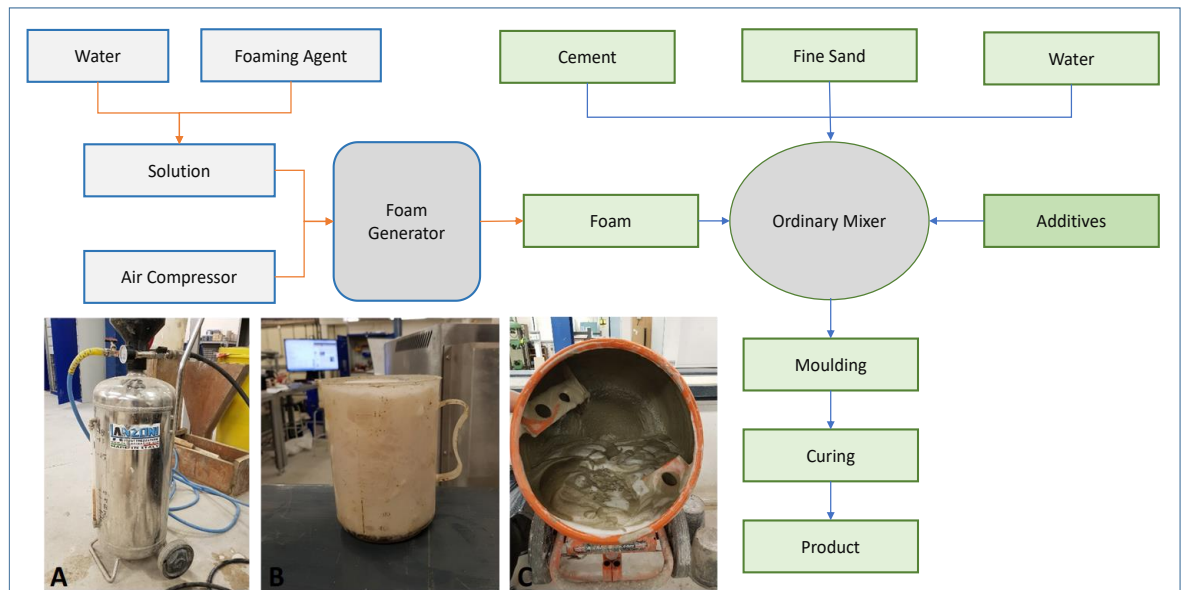


Figure 3-3: Foam production and use in foamed concrete showing (A) Foam generator (B) Foam (C) Foam mixed with raw concrete (Alkurdi et al., 2020)

### 3.4.2 Foamed Concrete Production

As no standard controls foamed concrete production, the procedure described by (Jones et al., 2005b) and followed by most researchers is applied in this study for the foamed concrete production see Figure 3-3. Therefore, the dry constituents (cement, fine aggregate and additives) were combined in the mixer for about one minute followed by the total amount of water to be mixed properly for about 2-4 minutes or up until a homogeneous mix with no lumps is obtained.

In the meantime, the pre-formed foam is produced by a foam generator, to be added to the base mix immediately. The mix then is combined for one minute or until the foam is evenly distributed throughout the mix. The plastic density of the mix is measured immediately once the mixing is completed in accordance with BS EN 12350-6, (2009) by weighing the foamed concrete sample in a known volume pre-weighed container. Check whether the plastic density of the mix is within the stated tolerance limit of  $\pm 50 \text{ kg/m}^3$ .

In case the measured plastic density found to be higher than the limit, additional foam is produced and added immediately to the mix until achieving the target density. However, mixes with lower plastic densities than the stated limits are excluded. Foamed concrete production in this study was mainly carried out in a rotary drum as shown in Figure 3-4.

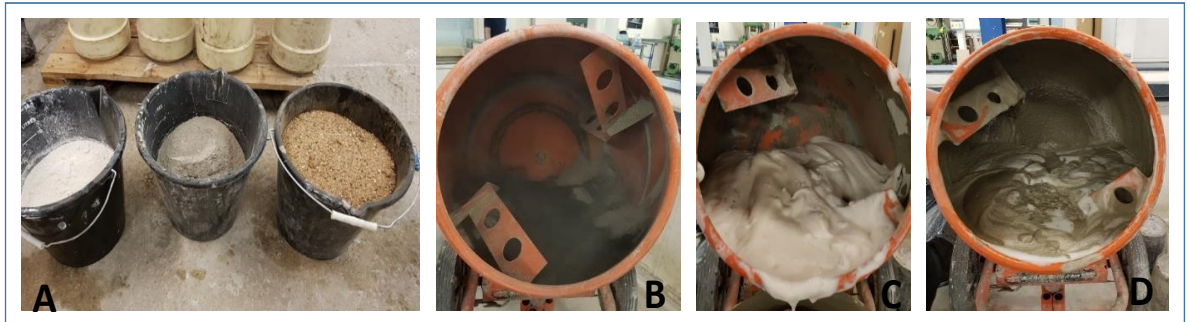


Figure 3-4: Foamed concrete production showing (A) dry materials (B) dry materials in rotary drum (belly mixer) (C) foam added to the wet mix (D) foamed concrete product.

### 3.4.3 Preparation of Forms and Sampling

Forms including cubes, cylinders and prisms are prepared before start mixing as described by Ramamurthy and Nambiar (2009). Mould release oil was applied by brush on all forms of internal surface to ease the deforming process. Then, carrying out the sampling and cover all samples with cling film as in Figure 3-5.



Figure 3-5: The form preparation and casting showing (A) Form preparation, (B) Foamed concrete in a cube form, (B) Foamed concrete is cast in cylinders, cube and prism form, (D) Demoulded foamed concrete cubes.

### 3.5 Curing

The definition of concrete curing by (BS 8110, 1985) is “the process of preventing the loss of moisture from the concrete whilst maintaining a satisfactory temperature regime”. The curing methods for conventional concretes are well-known. However, for foamed concrete, the curing regime is still being explored. Falade *at el.*, (2013) stated that for foamed concrete the highest strengths were obtained on specimens sealed in plastic bags and held at a constant temperature of 22 °C. Therefore, the curing method adopted in this research is sealed curing, where specimens are wrapped in cling film and stored at a constant temperature of 22 °C as this was the most common curing regime adopted by other researchers (Kearsley and Wainwright, 2001, Falade, *at el.*, 2013, Fouad, 2007, Tanveer *at*

*et al.*, 2017). Using cling film to wrap the specimens which had been de-moulded after 24 hours then the specimens are labelled and placed in a controlled dry room where the temperature was maintained at  $20 \pm 2$  °C until testing see Figure 3-6.

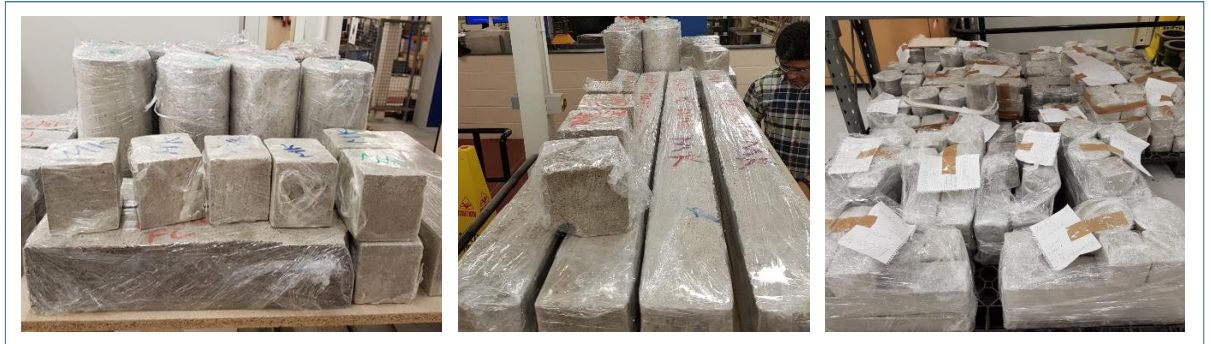


Figure 3-6: Foamed concrete beams, prism, cylinders and cubes are sealed for curing.

### 3.6 Test Programme

Foamed concrete will be tested in its fresh state to study its consistency and wet density, as well as in its hardened state to study the mechanical properties.

#### 3.6.1 Fresh State and Early Age Tests

##### 3.6.1.1 Consistency

Foamed concrete workability (flow behaviour) is assessed by modified Marsh cone method introduced in 1999 at Dundee University by Dhir, and used by (Brady *et al.*, 2001) (Ozlutas, 2015), (Hilal, 2015a), (Mohammad, 2011), (Hilal, 2015b) and (Mehta, 2017). Figure 3-7 illustrates the set-up and dimensions of the modified Marsh cone.

**The procedure is as follows:**

- I. A Marsh cone is attached to a stand. See Figure 3-7.
- II. Closing the nozzle, the cone then filled with 1.5 litres of foamed concrete.
- III. Measuring the time for 1 litre of foamed concrete to flow through the constricted orifice.

The flow time and behaviour are classified as in Table 3-4 (Jones *et al.*, 2003).

Table 3-4: Classification of foamed concrete flow ((Jones et al., 2003)

Main Class	Flow Rate	Sub Class	Description of flow
1	1 litre in < 1 minute	A	Constant flow
2	1 litre in > 1 minute	B	Interrupted flow
3	0.5 litres <efflux< 1 litre	C	Completing of flow after gentle tamping
4	Efflux < 0.5 litres	D	Low flow
5	No flow	E	No flow

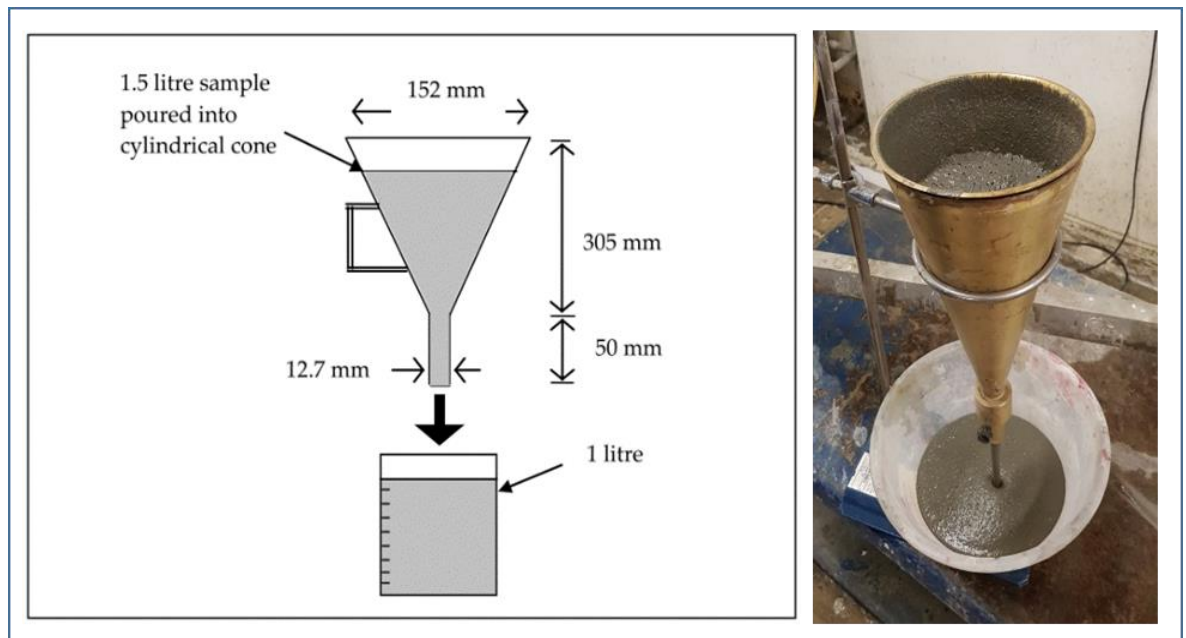


Figure 3-7: Dimensions of modified Marsh cone

### 3.6.1.2 Density

The plastic density of produced foamed concrete is measured in accordance with BS EN 12350-6 (2000) with values only of  $\pm 50 \text{ kg/m}^3$  of the target, density is accepted. This is done by filling a container of known volume and mass with foamed concrete Figure 3-5 b. Removing the excess amount from the top of the container and get it levelled without compaction. The container then is weighed to obtain the plastic density using the following equation:

$$\rho_m = \frac{(M_2 - M_1)}{V} \quad \text{Equation 3-1}$$

Where:

$\rho_m$  Target plastic density, kg/m<sup>3</sup>

$M_2$  Combined mass of container and samples, kg

$M_1$  Mass of empty container, kg

$V$  Volume of the container, m<sup>3</sup>

Jones, Ozlutas and Zheng (2016) established a linear equation that related foamed concrete plastic density with its dry density specially designed for a density range of 1200 kg/m<sup>3</sup> and 1800 kg/m<sup>3</sup>. Equation 3-2 suggested that in order to achieve the target dry density the plastic design density should at least be 105 kg/m<sup>3</sup> greater than the required dry density.

$$\rho_{dry} = \frac{\rho_{wet} - 105}{1.05} \quad \text{Equation 3-2}$$

Where:

$\rho_{dry}$  Target dry density, kg/m<sup>3</sup>

$\rho_{wet}$  Wet density, kg/m<sup>3</sup>

Table 3-5 shows the plastic (wet) and target dry density (oven-dry) after drying at 105°C until achieving a constant weight (No changes in weight), against the flow rate of the fresh mixes. For densities of the selected 1:1.5 c/s ratio mixes ranging from 800 to 1800 kg/m<sup>3</sup>. These values are adopted as the mean average value of three 100 mm cubes, Figure 3-8 summarises the designed wet, measured wet and fully dried densities.

Table 3-5: The plastic (wet) and target dry density

Mix	Design wet density (kg/m <sup>3</sup> )	Average measured wet density (kg/m <sup>3</sup> )	Average measured dry density (kg/m <sup>3</sup> )	Flow Rate Class
8Co	800	788	660	A
8Ton	800	761	646	A
8MK	800	841	712	B
8SF	800	810	686	A
10Co	1000	991	856	A
10Ton	1000	972	838	A
10MK	1000	1038	875	B
10SF	1000	1005	845	A
12Co	1200	1189	1049	A
*12Ton	1200	1195	1060	A
12MK	1200	1234	1077	B
12SF	1200	1211	1070	A
14Co	1400	1362	1235	A
14Ton	1400	1373	1240	A
*14MK	1400	1440	1268	B
*16Co	1600	1569	1433	A
16Ton	1600	1601	1450	A
16SF	1600	1623	1462	B
18Co	1800	1807	1647	B
18Ton	1800	1796	1640	B
*18SF	1800	1841	1670	C

**Note:** \*12Ton is waste toner FC with a target plastic density of 1200 kg/m<sup>3</sup>.

\*14MK is Metakaolin FC with a target plastic density of 1400 kg/m<sup>3</sup>.

\*16Co is the control (No additives) FC with a target plastic density of 1600 kg/m<sup>3</sup>.

\*18FS is silica fume FC with a target plastic density of 1800 kg/m<sup>3</sup>.

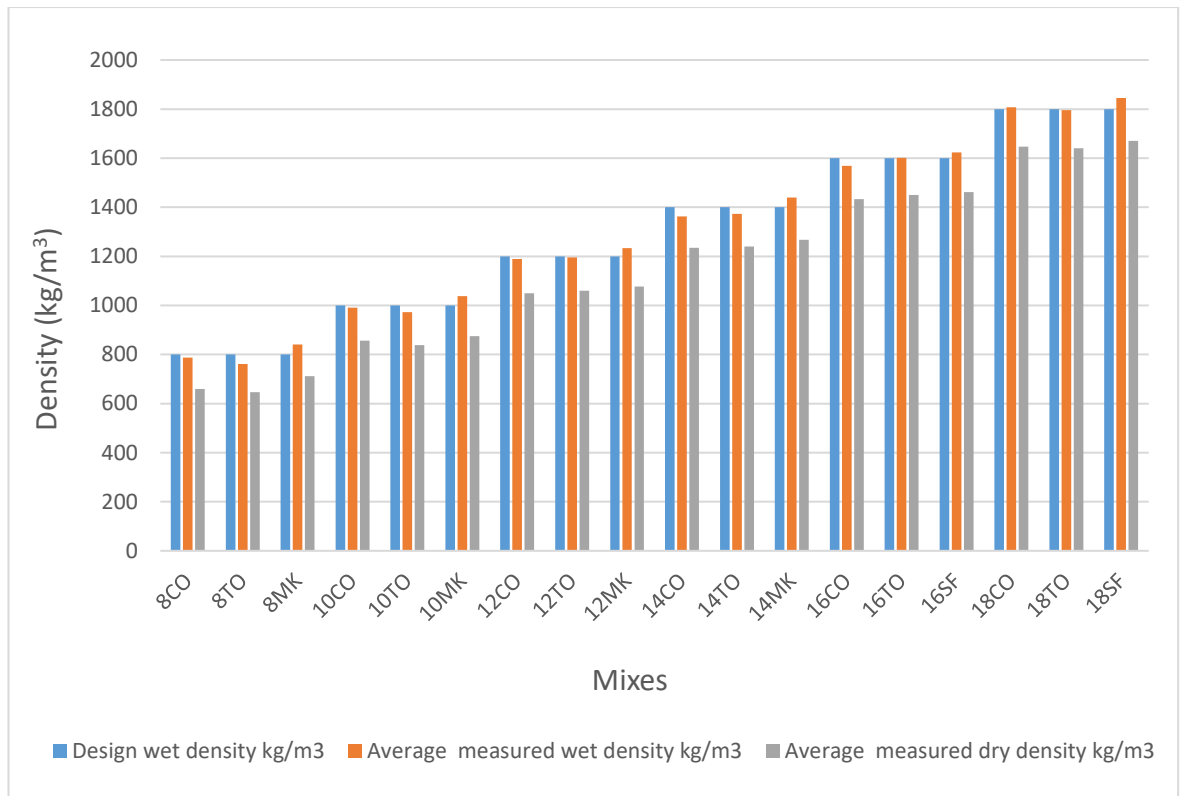


Figure 3-8: Designed wet, measured wet and fully dried densities of foamed concrete.

### 3.6.2 Hardened Concrete Tests

#### 3.6.2.1 Compression Test

Unlike normal concrete, foamed concrete designed for specific density rather than compressive strength as in standard concrete. The compressive strength of foamed concrete is affected greatly by the density, sand/cement ratio and less by water/cement ratio. Sealed cured cylinders and cubes of size 150 X 300 mm and 100 X 100 X 100 mm respectively were tested for compressive strength 28 days in accordance with BS EN 12390-3, (2009). The specimens were located and centred under the loading plate and positioned to have even surfaces in contact with the loading plates see Figure 3-9. The equipment calibrated to apply low load values ranging from 10 to 50 N/Sec. The failure loads are recorded, and concrete compressive strengths are calculated using Equation 3-3. The compressive strength of the specimens is calculated to the nearest  $0.1 \text{ N/mm}^2$ . In the case of cylinders, a dial gauge is used to measure the displacement while loading in progress to draw the stress-strain relations, thus find the modulus of elasticity.



Figure 3-9: Compression test for cubes and cylinders.

Compressive strength for cubes and cylinders calculated as follows:

$$f'c = \frac{F}{A_c} \quad \text{Equation 3-3}$$

Where:

$f'c$  Compressive strength, N/mm<sup>2</sup>

$F$  Maximum load at the time of failure, N

$A_c$  Cross-sectional area on which the load is applied, mm<sup>2</sup>

### 3.6.2.2 Modulus of Elasticity

The modulus of elasticity ( $E$ ) of foamed concrete mixes with and without additives was determined using 150 × 300 mm cylinder specimens. Following BS 1881-121 (1983) three specimens were tested for each mix at an age of 28 days. Each specimen was fitted with two potentiometers and strain gauge to measure the axial displacement as shown in Figure 3-10. Throughout the testing, every specimen was loaded with cyclic loading up to 1/3 of the ultimate load capacity as follows:

- The specimens placed in the machine, then 0.5 MPa as basic stress ( $\sigma_b$ ) was applied and the strain gauge reading at each potentiometer was recorded.
- The stress was increased gradually at a constant rate of 0.5 MPa/s up to 1/3 of the ultimate compressive strength ( $\sigma_a$ ) (estimated from the 100 mm cube strength

assuming that the cylinder strength is about 80% the cube strength (Tanveer *et al.*, 2017).

- Then, the stress was kept for one minute before start reducing the stress at the same rate up to the level of the basic stress ( $\sigma_b$ ) to finish the first cycle.
- After completion of the second cycle and a waiting period of 60 seconds under stress ( $\sigma_b$ ), the strain readings ( $\epsilon_b$ ) were recorded at the four potentiometers.
- The specimen then reloaded to stress ( $\sigma_a$ ), and record the strain reading ( $\epsilon_a$ ) and take the average from the four readings.
- Finally, to determine the compressive strength, the stress was increased at the same rate up to the failure point. This loading process is illustrated in Figure 3-10. The modulus of elasticity ( $E$ ) might be calculated by Equation 3-4:

$$E = \frac{\sigma_a - \sigma_b}{\epsilon_a - \epsilon_b} \qquad \text{Equation 3-4}$$

Where:

$\sigma_a$  Upper loading stress (MPa), where ( $\sigma_a = f'c/3$ )

$\sigma_b$  Basic stress (i.e. 0.5 MPa)

$\epsilon_a$  Strain under ( $\sigma_a$ )

$\epsilon_b$  Strain under ( $\sigma_b$ )

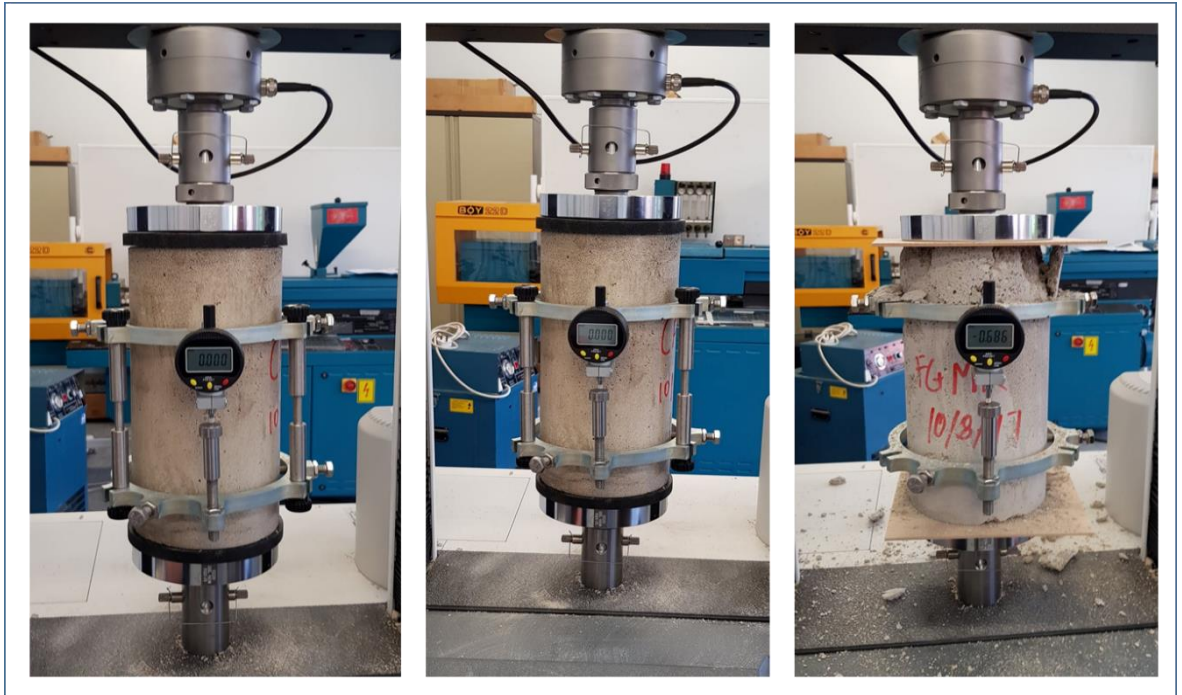


Figure 3-10: Static Modulus of Elasticity test

### 3.6.2.3 Four Points Flexural Test

The modulus of rupture ( $f_r$ ) value is measured at 28 days and calculated based on the location of the observed fracture in accordance with BS EN 12390-5, (2009). The tests were carried out with a digital log keeping and digitally controlled automatic loading machine. The prisms were placed centrally on the supports under the four-point loading machine and positioned to have even surfaces in contact with the loading plates, Figure 3-11. The rate of loading was kept constant at 500 N/min for low-density specimens, and 1000 N/min for high-density specimens during testing until prism failure. The failure load and flexure extension (deflection) were recorded by the digital software of the machine.

Wahyuni (2012) stated that the values of tensile strength measured using a flexural test is higher than those obtained by the cylinder splitting test, and the value obtained by the cylinder splitting test still higher than those obtained by direct uniaxial tension test.

A total of 36 prisms (100 x 100 x 400) mm samples and 12 beams (90 x 120 x 1200) mm samples were tested, and the experimental average flexure strength test results are presented in Figure 3-11. The flexure test results conducted for all mixes, each of which contained six prisms and two beams. Modulus of rupture could be calculated by Equation 3-5 in accordance with BS EN-12390-5 (2000).

$$f_r = \frac{F x L}{b x d^2}$$

Equation 3-5

Where:

$f_r$  Flexural strength, N/mm<sup>2</sup>

$F$  Maximum load, N

$L$  Beam span, mm

$b$  Average width of the specimen, mm

$d$  Average depth of the specimen, as oriented for testing, mm



Figure 3-11: Four points load flexural test

#### 3.6.2.4 Splitting Tensile Test

Tensile strength ( $f_{sp}$ ) is not one of the performance criteria in the design of concrete. However, it is an essential property of the foamed concrete that should be determined on the hardened concrete and it can be used to estimate the time and place of cracks that occur in the concrete under a given load. The splitting tensile strength is rather well established and included for instance in ASTM C496-96, (1996) and Eurocode 2 (BS EN1992-1-1:2004).

The preparation for testing in accordance with ASTM C496-96, (1996) starts with cleaning the bearing surfaces of the testing machine, removing any loose material from the surfaces of the test specimen. Placing the test specimen in the centring jig, with packing loading pieces carefully positioned along the top and bottom of the plane of loading of the specimen. Then place the jig in the machine so that the specimen is located centrally. Ensuring that the upper platen is parallel with the lower platen with cylindrical specimens.

Apply and increase the load continuously at a nominal rate within the range of 500-1000 N/min. Maintain the rate and record the maximum load applied to the specimen. The tensile splitting strength ( $f_{sp}$ ) in N/mm<sup>2</sup> is given by the formula:

$$f_{sp} = \frac{2F}{\pi \times d \times l} \quad \text{Equation 3-6}$$

Where:

$f_{sp}$      Splitting tensile strength, N/mm<sup>2</sup>

$F$         Measured peak load, N

$d$         Diameter of the specimen, mm

$l$         Length of the specimen, mm



Figure 3-12: Splitting tensile (Brazilian) test

### 3.6.2.5 Direct Tensile Test

The direct tensile strength is calculated based on the test results obtained from splitting flexural strength or tensile strength using conversion factors. Nevertheless, (ACI Committee, 2003) stated that these conversion factors might not be applicable for foamed concrete. Understanding the direct tensile stress-strain behaviour of the foamed concrete is significantly important, as it affects the cracking, deflections, shear and bonding behaviours of reinforced concrete elements constructed with foamed concrete. This study proposes a new test setup to determine the uniaxial direct tensile strength of the foamed concrete as shown in Figure 3-13a.

Wooden mould dimension of 100 x 100 x 500 mm to create samples for direct tensile strength. The width of the mould was narrowed by two pieces of the triangular-shaped timber with the base of 40 mm and height of 20 mm were taped in the centre of the specimen inside the wooden box as shown in Figure 3-13B, to control the failure place to be in the middle of the specimen. The Framework was embedded with two gripping claws assembled from bolts, nuts and washers with the gripping claws as shown in Figure 3-13a all were specifically designed for this study in the workshop. Recent research (Alhussainy et al., 2016) used a similar technique to cast samples for direct tensile tests. Nevertheless, the method used in this study is easier, faster, and cost-effective.



Figure 3-13: Direct tensile test shown (A) Test setup, (B) prism casting, (C) Direct tension applied on the prism and (D) Failed prisms.

As there is no standard of practice for direct tensile strength tests for foamed concrete, the test was established according to a study conducted in the school of Civil and Environmental Engineering at the University of Wollongong Australia (Alhussainy et al., 2016).

With a loading capacity of 30 kN, the INSTRON automated testing machine is used to apply an axial tensile load on the specimen as shown in Figure 3-14 with a stress rate of 1 kN/min. Two threaded jaw attachments with a diameter of 14 mm holes were designed. One side of the nut will fit in the bolt embedded in the specimen and the other side will go into the jaw of the INSTRON machine to create a grip to allow axial tension in the specimen. The direct tensile splitting strength ( $f_t$ ) in (N/mm<sup>2</sup>) is given by Equation 3-7:

$$f_t = \frac{F}{b \times d}$$

Equation 3-7

Where:

$f_t$  Direct tensile strength, N/mm<sup>2</sup>

$F$  Measured peak load, N

$d$  Depth of specimen, mm

$b$  Width of the specimen, mm

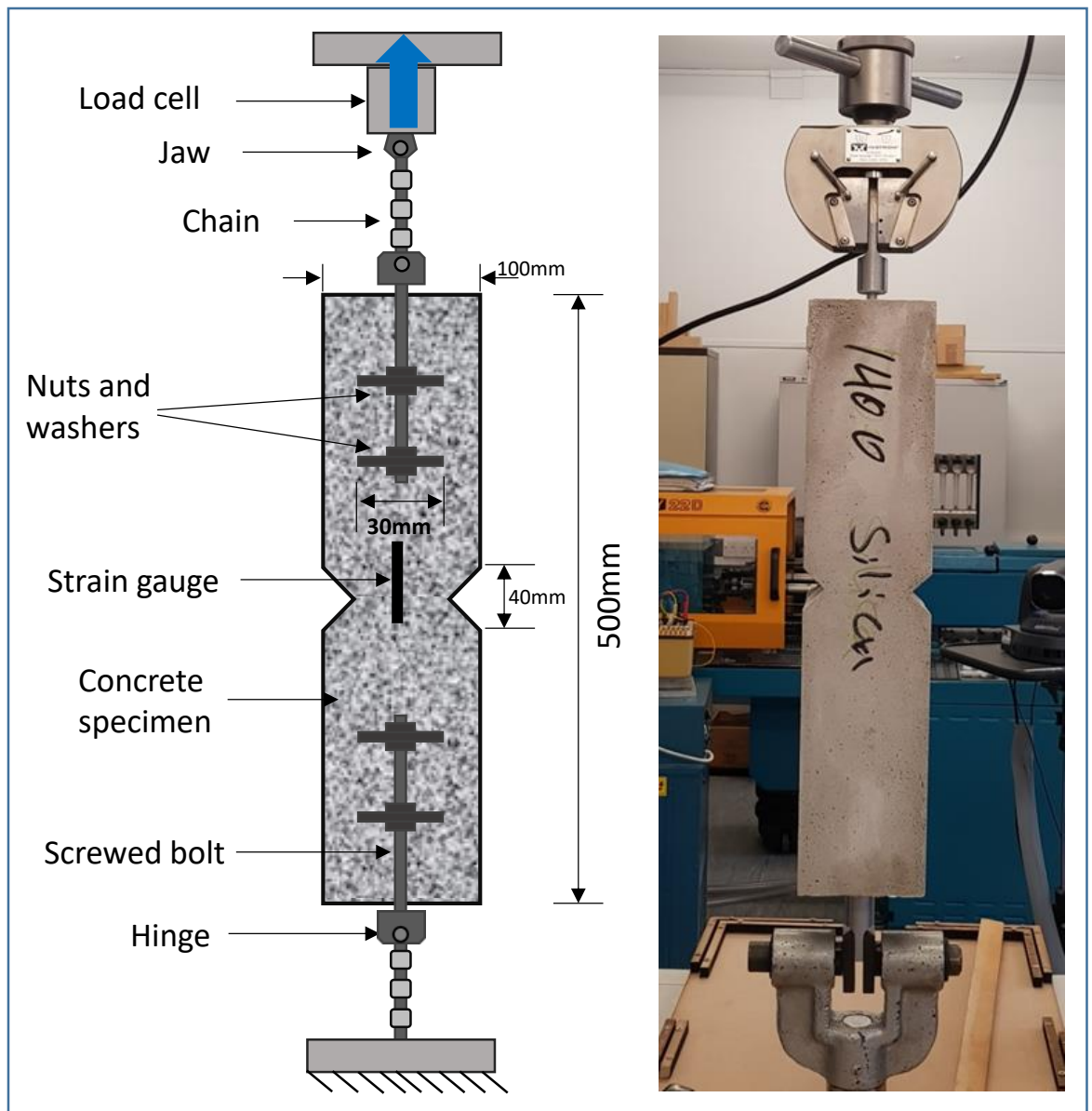


Figure 3-14: Direct tensile test for foamed concrete

### 3.6.2.6 Direct Shear Test

Investigating the shear strength using a modified push-off specimens test method as there is no standard of practice for direct shear behaviour for foamed concrete. A total of 18 push-off specimens 100 x 100 x 500 mm were tested.

The specimen is supported on two rigid steel blocks 250 mm apart. A 10 mm deep notch was sawed all around the specimens in between the loading and the supporting edges, to ensure the shear failure plane, as shown in Figure 3-15. To simulate the foamed concrete specimen real behaviour in direct shear test, the end parts of the specimen were secured against any rotation using two adjustable yokes on each side as shown in Figure 3-15 and Figure 3-16.

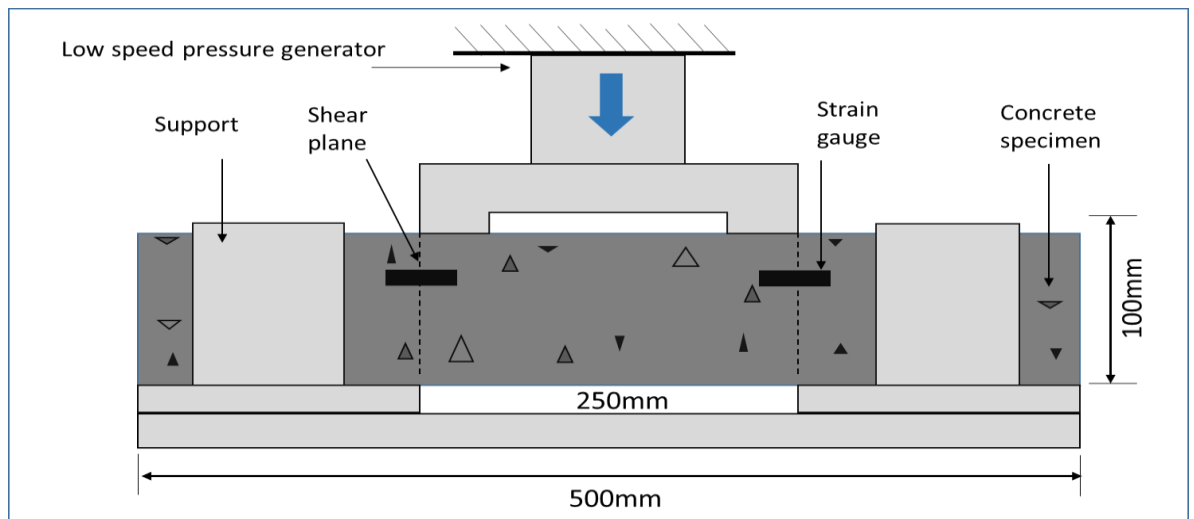


Figure 3-15: Modified direct shear test setup for foamed concrete

A static load was applied at a rate of about 50 N/sec. The applied load data were electronically recorded every second. All measurements were made on three specimens for each mix. The ultimate shear strength ( $\tau_{max}$ ) of the specimen was calculated using the following Equation 3-8.

$$\tau_{max} = \frac{F}{2(b \times d)} \quad \text{Equation 3-8}$$

Where:

$\tau_{max}$  Ultimate shear strength, N/mm<sup>2</sup>

- $F$  Measured peak load, N
- $d$  Depth of specimen, mm
- $b$  Width of the specimen, mm



Figure 3-16: Shear test shows (A) test setup (B) shear test and (C) shear cracks under loading.

### 3.7 GFRP Mechanical Properties Testing

GFRP rebar, as an alternative material to steel, is used to reinforce structural elements. In this study, six samples, three of each bar size 8 mm and 16 mm of GFRP bars were tested under uniaxial tensile test to investigate the ultimate tensile strength ( $f_u$ ), tensile strain ( $\epsilon_{fu}$ ) and the modulus of elasticity ( $E_f$ ) of the material. Figure 3-17 show the direct tensile test setup for the GFRP bars.

The ultimate tensile strength of GFRP bars may be calculated by dividing the measured maximum load over the cross-sectional area of the GFRP bar as shown in Equation 3-9.

$$f_u = \frac{F_u}{A} \quad \text{Equation 3-9}$$

Where:

- $f_u$  Ultimate tensile strength, N/mm<sup>2</sup>
- $F_u$  Maximum load at the time of failure, N
- $A$  Cross-sectional area on which the load is applied, mm<sup>2</sup>

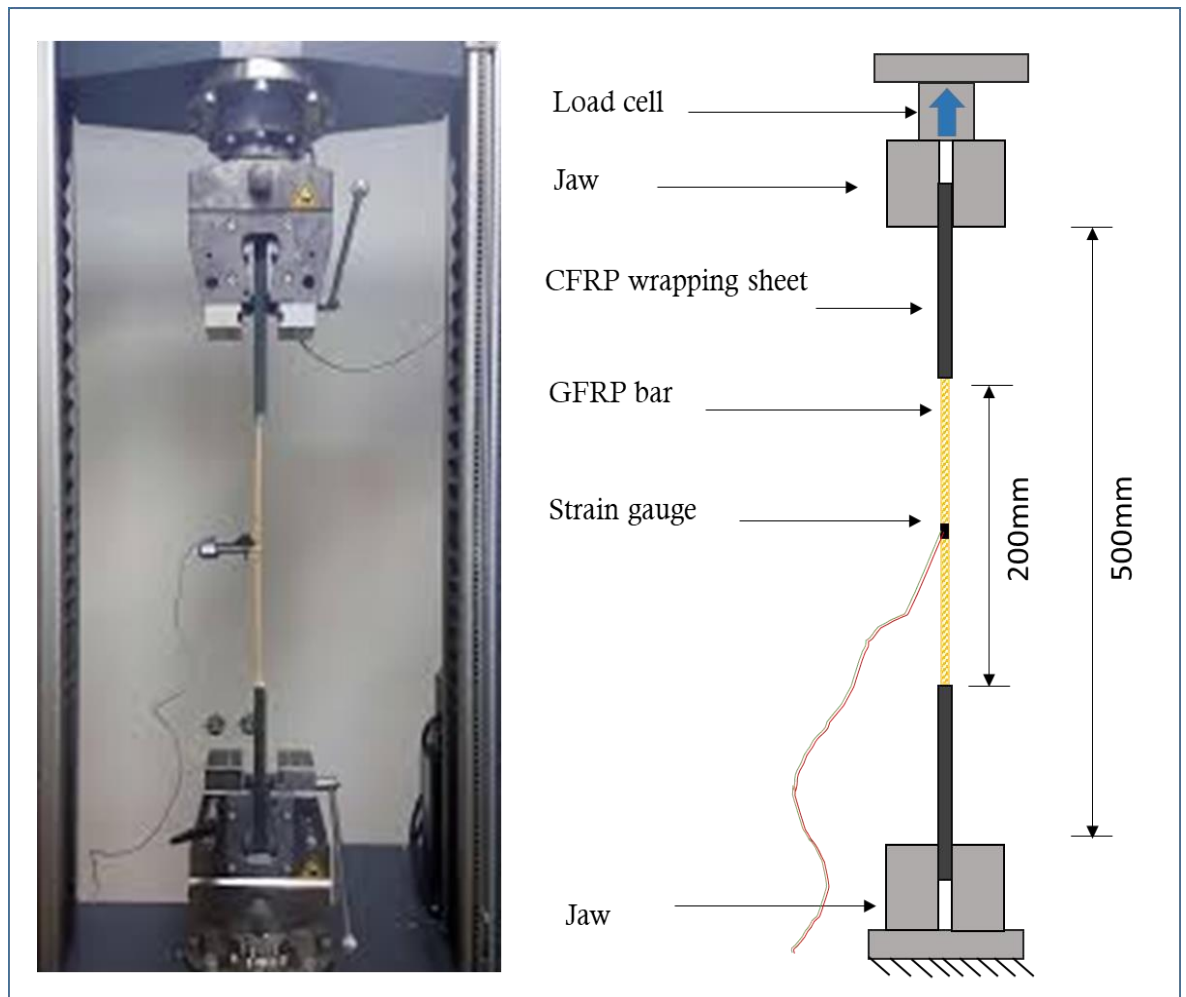


Figure 3-17: Direct tensile test setup for GFRP bar

The modulus of elasticity of GFRP bars can be given by the following Equation 3-10.

$$E = \frac{(F_1 - F_2)}{(\varepsilon_1 - \varepsilon_2) \cdot A} \quad \text{Equation 3-10}$$

Where:

$F_1, F_2$  Applied loads corresponding to 50% and 25% of the ultimate load respectively, N

$\varepsilon_1, \varepsilon_2$  Corresponding strain to forces  $F_1$  and  $F_2$

$A$  Cross-sectional area of GFRP bar,  $\text{mm}^2$

### 3.7.1 Bond Behaviour

#### 3.7.1.1 Pull-out Test

The pull-out test is normally used in the assessment of the bond performance of steel bars in concrete. However, in this study steel and glass fibre reinforced polymer GFRP bars are tested. Two different bar sizes used in this study 8 mm and 16 mm. Following RILEM/TC9-RC (1983) cube sizes of 200 x 200 x 200 mm or ( $10 \times d_b$ ) were used with 16 mm and 8 mm bars. The moulds were fabricated using 6 mm MDF. According to BS EN12390-3 (2002), the bonded length of samples is  $5d_b$  and the un-bonded length of the bar achieved by wrapping the bar section with parcel tape before pouring the concrete as shown in Figure 3-18. The bars were inserted through the base of the moulds and secured in place externally and the gap was sealed to reduce seepage and retain pore water during the initial 24 hours of curing. After 24 hours of curing at  $20 \pm 5 \text{ }^\circ\text{C}$  the samples were removed from their moulds cured using cling film and placed in a control room at  $20 \pm 5 \text{ }^\circ\text{C}$  for 28 days.

A total of 48 specimens prepared in accordance with BS EN12390-3 (2002) and cast with two different sizes based on the rebar sizes. Concrete samples were cast as controls to monitor the concrete properties of each mix including three cylinders for compressive strength test and another three for splitting tensile test.

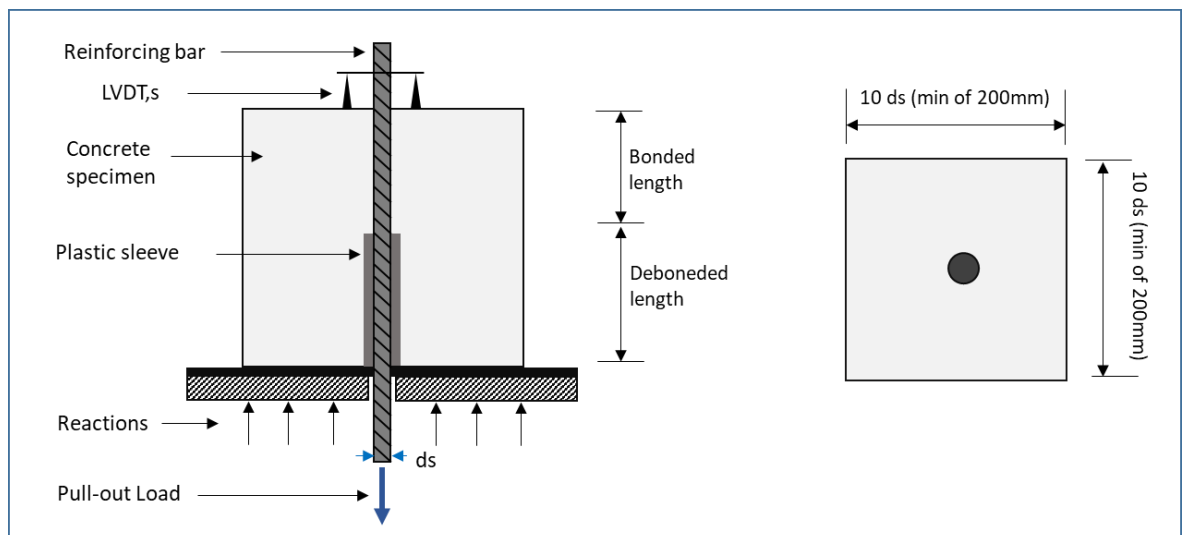


Figure 3-18: Pull-out test specimen

The tests were carried out following the test method and specification in RILEM TC9-RC, (1983). Figure 3-19 shows the setup of the test. The specimens were tested using a universal testing machine with a maximum capacity of 100 kN. The specimens were placed on a 250 x 250 mm steel plate supported by the stationary head. A rubber sheet was placed between the plate and the cube, in order to ensure that a uniform stress distribution was applied to the face of the cube. The tension force  $F$  was applied to the longer end of the reinforcing bar gripped by a moving head of the test machine through the 50mm diameter central hole in the plate as shown in Figure 3-19.



Figure 3-19: Pull-out test shows (A) specimens casting, (B) specimens curing, (C) pull-out test, (D) failed specimens

The maximum bond stress could be calculated based on pull-out force using Equation 3-11.

$$\tau_{b.max} = \frac{F_{max}}{(\pi \cdot d_b \cdot L_b)} \quad \text{Equation 3-11}$$

Where:

$\tau_{b.max}$  Maximum bond strength, N/mm<sup>2</sup>

$F_{max}$  Maximum pull-out force, kN

$d_b$  Bar diameter, mm

$L_b$  Embedment length, mm

### 3.7.1.2 Bond Beam Tests

The bond beam specimens were prepared according to the specifications in RILEM TC5-RC, (1982). The ribbed bar has a bonded length of  $10 \times$  bar diameter embedded in  $100 \times 180 \times 800$  mm. One-millimetre thick plastic sleeves were used to ensure that the bar was deboned elsewhere, see Figure 3-20. A total of 12 beams were tested, six with steel bars and six with GFRP bars. Two bar sizes 8 mm and 16 mm were used in both steel and GFRP bars.

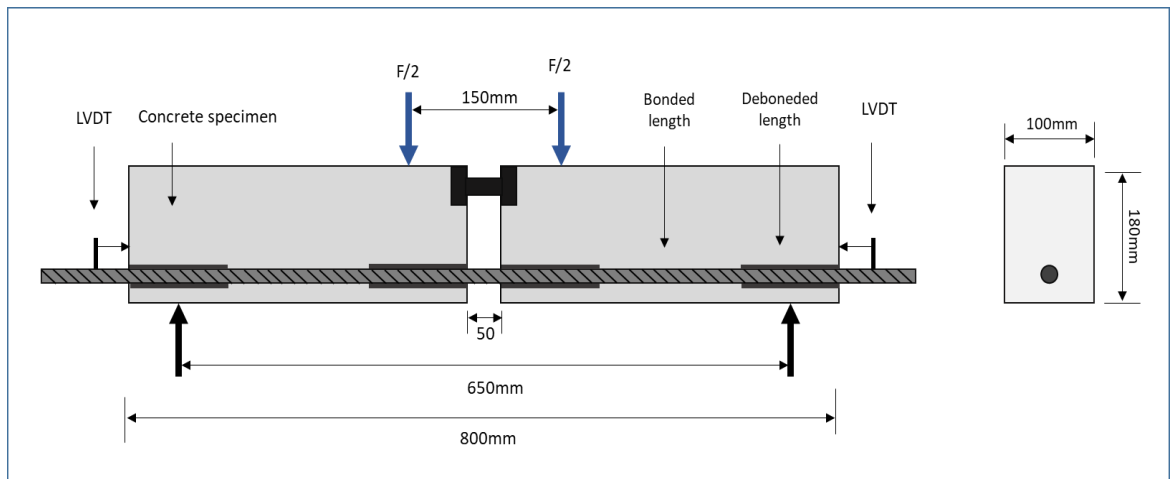


Figure 3-20: Beam bond test specifications and dimensions

The specimens were tested in a two-column hydraulic universal testing machine with a maximum capacity of 300 kN. Supported by two rollers supports in both ends on top of the stationary head to avoid any arching effect. A 100 mm wide steel hinge made from two pieces in a T shape was placed at mid-span in the compression zone of the beams, as shown in Figure 3-21.

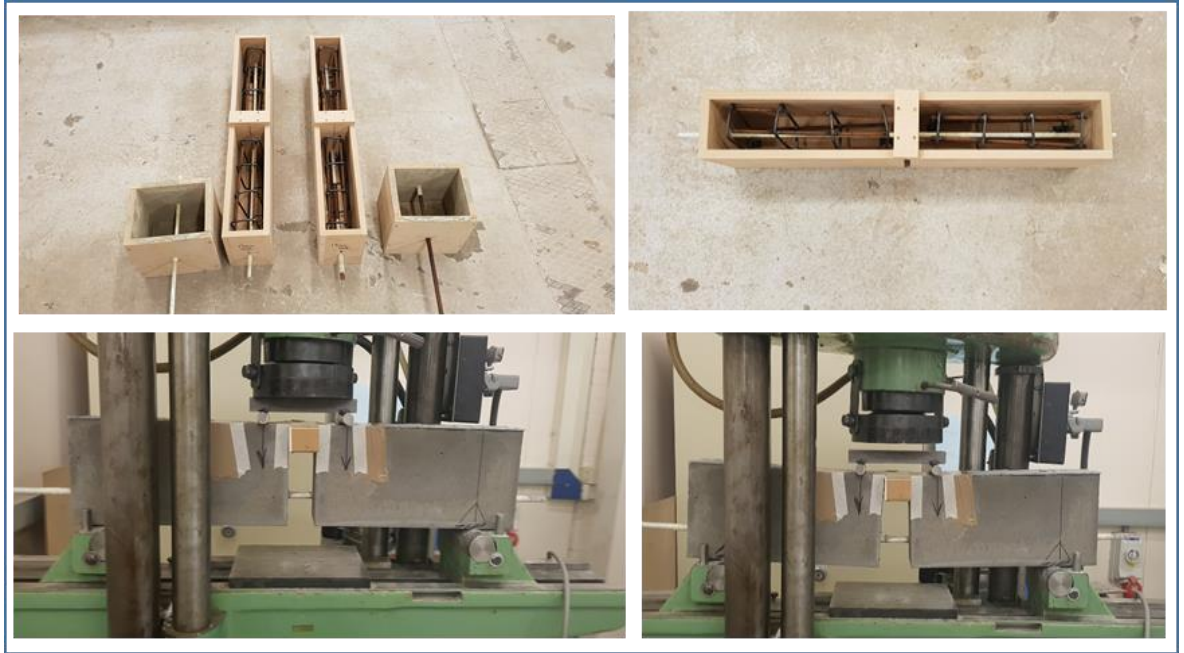


Figure 3-21: Beam bond test preparing and testing

The load was applied on the top of the beam continuously throughout the test, with a loading rate of 10 N/sec until bond failure occurred. Two LVDT transducers with an accuracy of 50 $\mu$ m were to measure the slip displacements. The LVDT transducers were mounted on each side on a cross yoke attached to the reinforcing bar. Clamps were introduced on both sides to stop the bars from slipping any further when the bond failed on one side only. However, the test continued until bond failure occurred on the other side.

The maximum bond stress could be calculated based on pull-out force using Equation 3-12.

$$\tau_{b.max} = \frac{F_{max}}{(\pi \cdot d_b \cdot L_b)} \quad \text{Equation 3-12}$$

Where:

$\tau_{b.max}$  Maximum bond strength, N/mm<sup>2</sup>

$F_{max}$  Maximum applied force, kN

$d_b$  Bar diameter, mm

$L_b$  Embedment length, mm

### 3.8 Summary

Due to the unique properties of foamed concrete including high flowability and self-compacting, low density, high thermal and sound insulation, ease of production and relative cost-effectiveness. For those reasons, FC has found applications in many civil and structural engineering areas such as cavity filling and thermal insulation, building blocks, void filling and non/semi-structural walls. However, FC has not been used in structural applications yet, due to its low compressive strength.

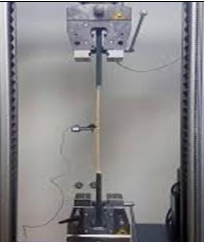
To investigate and develop the mechanical properties of foamed concrete and bond behaviour, the following procedure was conducted: see Table 3-6.

- An experimental programme was conducted, including testing and developing the density, workability, compressive strength, tensile and flexural strengths, shear strength, the stress-strain relationship. More than 875 specimens classified into six different densities (800, 1000, 1200, 1400, 1600 and 1800 kg/m<sup>3</sup>) were tested. For each concrete density, four mixes were designed including the control mix and three different additives: silica fume, metakaolin and waste toner. The experimental programme was considered to introduce a modified shear and direct tensile test, where splitting and flexural tests were conducted to confirm its reliability.
- Two tests (Pull-out test and beam-test) were conducted to study the bond behaviour between foamed and reinforcement steel and GFRP bars.

Table 3-6: Summary of the experimental procedure to test and develop FC mechanical properties.

Test code (designation)	Test purpose	Code of practice	Number of groups	Number of samples	Sample size	Image
<b>Concrete Compression test</b>	To determine the compressive strength of concrete	BS EN 12390-3, (2009)	144	432	100 x 100 x 100 mm 150 x 300 mm	
<b>Four points flexural test</b>	To determine the flexural strength of concrete	BS EN 12390-5, (2009)	16	48	100 x 100 x 400 mm	
<b>Concrete Compression test</b>	To determine the Modulus of Elasticity of concrete	BS 1881-121 (1983)	72	216	150 x 300 mm	

Chapter 3

<b>Splitting tensile test</b>	To determine the splitting tensile strength of concrete	BS EN1992-1-1:2004)	16	48	150 x 300 mm	
<b>Direct Tensile Test</b>	To determine the tensile strength of concrete	New approach	16	48	100 x 100 x 500 mm	
<b>Direct shear test</b>	To determine the shear strength of concrete	Modified push-off specimens' approach	16	48	100 x 100 x 500 mm	
<b>Direct Tensile Test</b>	To determine the tensile strength of GFRP bars	BS EN ISO 6892-1:2016	2	6	8 /16 mm $\varnothing$ x 200 mm	

### Chapter 3

---

<b>Pull-out test</b>	To determine the bond behaviour between concrete and reinforcing bars	RILEM/TC9-RC (1983)	16	16	200 x 200 x 200 mm or ( $10 \times d_b$ )	
<b>Bond Beam Tests</b>	To determine the bond behaviour between concrete and reinforcing bars	RILEM TC5-RC, (1982)	16	16	100 x 180 x 800 mm	

## Chapter 4

# Foamed Concrete Development: Results and Analysis

### 4.1 Introduction

Foamed concrete FC is a type of lightweight concrete, mainly consist of cement, sand and water with a homogeneous pore structure which is created by introducing air (foaming agent) in the concrete (Bing et al., 2014). Due to its lower density compared to normal concrete, foamed concrete achieves lower compressive, flexure and tensile strengths.

This chapter provides background information relevant to the mechanical properties of foamed concrete FC. This information includes a description of the mechanical properties of FC and the development of these properties to be suitable for structural applications.

### 4.2 Mechanical Properties

#### 4.2.1 Compressive Strength

The 28th-day compressive strength of foamed concrete mix at different densities from 800 to 1200 kg/m<sup>3</sup> prepared with and without additives. To test and develop the mechanical properties of foamed concrete mixes, different cement/sand ratios, different additives include Metakaolin, Toner and Silica fume were added at specified ratios as a replacement of cement. To identify the effect of cement/sand ratio and additives, together or individually on the compressive strength of the concrete, an experimental programme was carried out at different concrete densities (800 - 1800 kg/m<sup>3</sup>), with an increment of 200 kg/m<sup>3</sup>, see Table 4-1. It may be seen that the increase of c/s ratio and adding Toner, Mk and Silica fume have improved the 28-day compressive strength of the foamed concrete.

Table 4-1: compressive strength for concrete mixes with different densities and different cement /sand ratios with 0.5 as w/s ratio for all mixes.

Density (kg/m <sup>3</sup> )	Mix	Compressive strength based on cylinder (MPa)			
		Cement/ Sand ratio	1:2	1:1.5	1:1
800	Control		1.13	1.51	1.59
	Toner		1.15	1.83	1.92
	Mk		1.45	1.67	1.76
	SF		1.47	1.65	1.73
1000	Control		2.95	3.45	3.63
	Toner		3.25	4.95	5.20
	Mk		3.00	3.93	4.13
	SF		3.30	4.10	4.31
1200	Control		5.76	8.54	8.98
	Toner		8.25	13.00	13.66
	Mk		6.35	10.48	11.01
	SF		6.5	11.40	11.98
1400	Control		12.65	15.75	16.55
	Toner		18.05	21.24	22.32
	Mk		13.00	17.65	18.55
	SF		14.58	18.35	19.29
1600	Control		20.86	23.12	24.30
	Toner		26.12	30.45	32.00
	Mk		24.24	26.25	27.59
	SF		24.36	26.37	27.71
1800	Control		24.79	27.88	29.30
	Toner		32.85	36.02	36.86
	Mk		28.24	32.25	30.89
	SF		29.07	34.15	31.11

- **Effect of Cement Content on Compressive Strength**

With reference to Figure 4-1, it is clear that samples with higher cement content possessed higher compressive strength. For instance, mixes with a 1:1.5 c/s and 1:1 ratio have higher

28-days compressive strength than mixes with a 1: 2 c/s ratio by an average increase of 26.2% and 31.8% respectively. Therefore, it is clear that the compressive strength improved by only 5.5% comparing mixes with 1:1.5 c/s ratio to mixes with 1:1 c/s ratio. This means that it is not cost-effective to have a c/s ratio higher than 1:1.5 in the foamed concrete mix as the improvement of compressive strength is slight as shown in Figure 4-1. This indicates that higher cement content creates stronger bonding between the particles of FC, which subsequently increases its compressive strength. However, the relation between compressive strength and cement content is a direct nonlinear relationship.

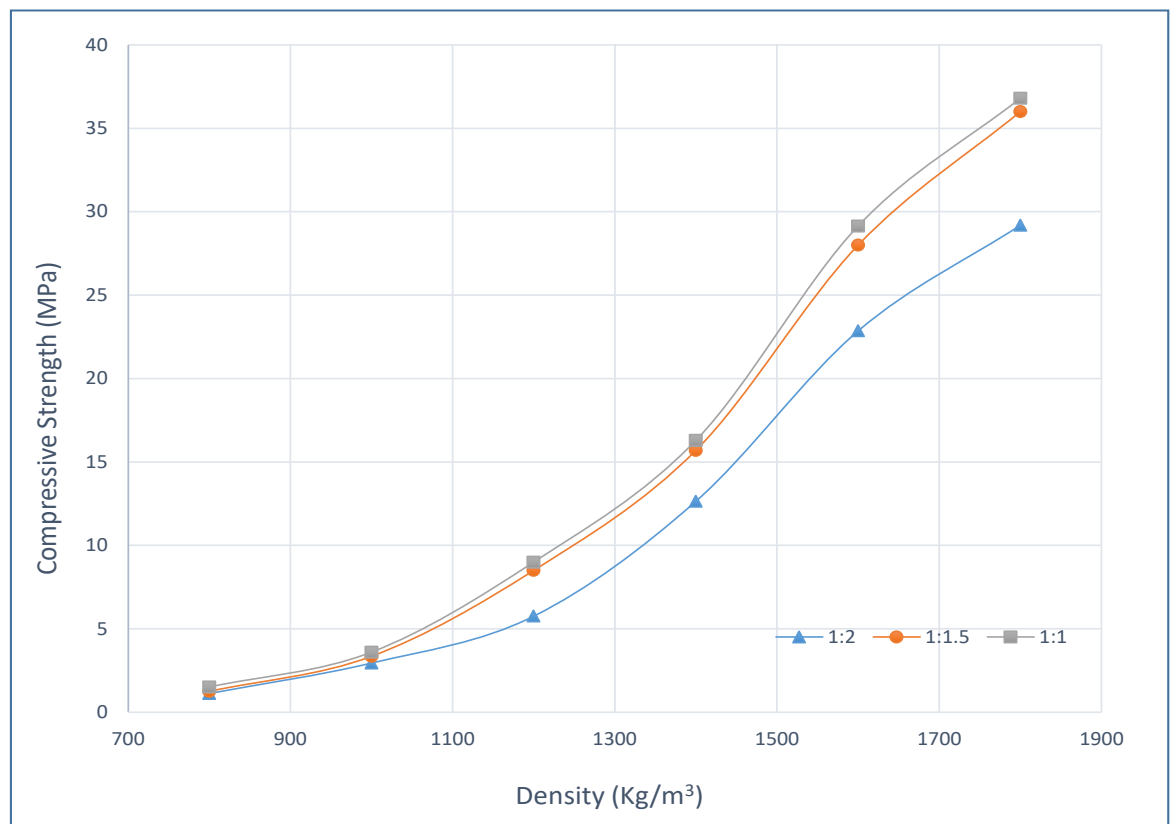


Figure 4-1: Effect of cement content on compressive strength

- **Effect of Density on Compressive Strength**

Compressive strength testing was carried out on 150 x 300 mm cylinders and 100 X 100 X 100 mm cubes in accordance with BS EN 12390-3, (2009) and in each case, the results quoted are the average of three specimens. As expected by Gangatire and Suryawanshi, (2016) and Othuman Mydin (2010), the compressive strength of foamed concrete decreases dramatically with a reduction in density, as shown in Figure 4-2.

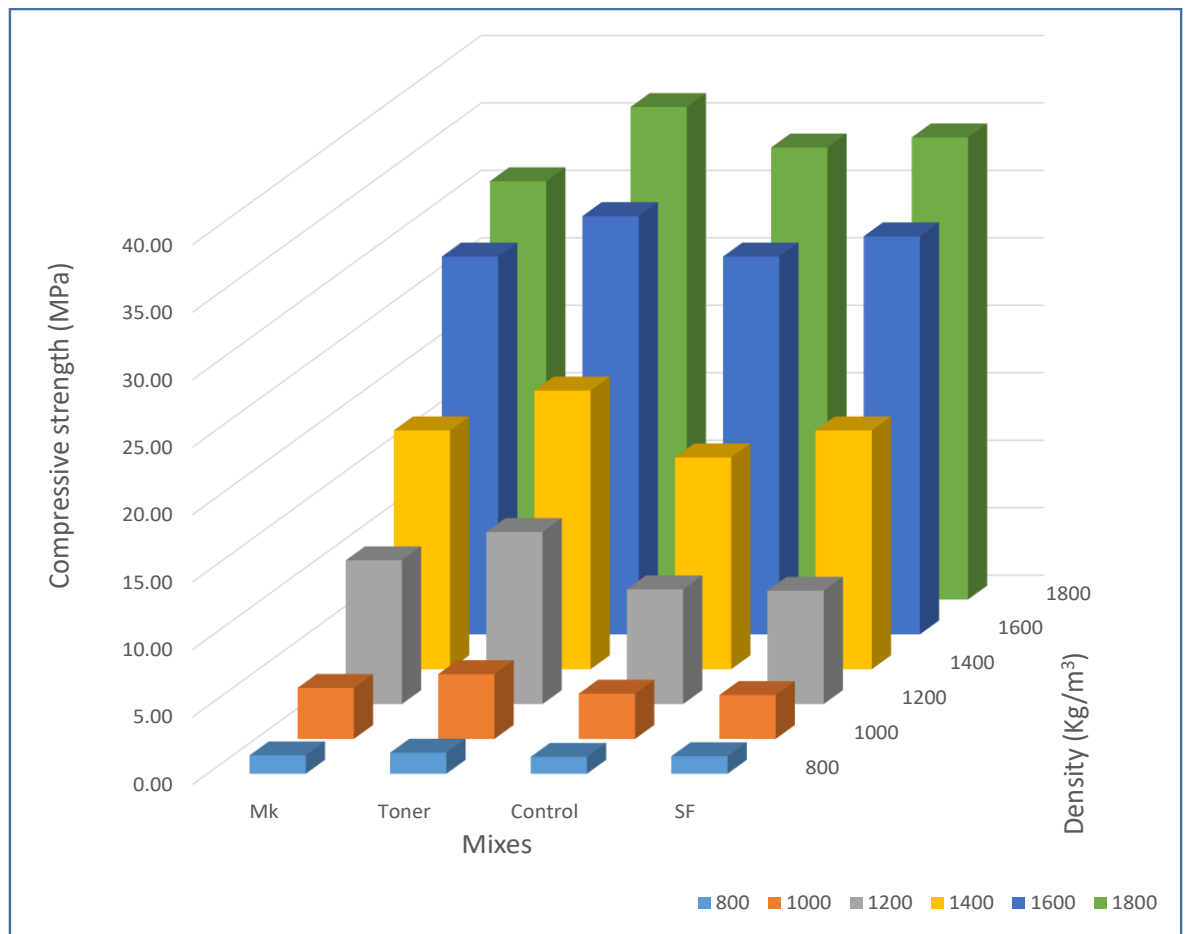


Figure 4-2: The effect of density on the compressive strength

By referring to Figure 4-2, it was found that the compressive strength was positively proportional to the density of FC mixes. The higher the density, the greater the compressive strength. For instance, in control mixes with 1:1.5 *c/s* ratio, in densities of 800, 1000, 1200, 1400, 1600, and 1800 kg/m<sup>3</sup>, the compressive strengths were 1.51, 3.45, 8.54, 15.75, 23.12, and 27.88 MPa respectively. It shows that increasing the mix density 200 kg/m<sup>3</sup> increases the compressive strength by an average of 300%. The compressive strength of the FC mix increased by about 15 times by only doubling its density, where the compressive strength of 1600 kg/m<sup>3</sup> mix is 23.88 MPa and the mix with a density of 800 kg/m<sup>3</sup> has a compressive strength of only 1.51 MPa, as shown in Figure 4-2.

Compressive strength to density ratio results of the present study is highly agreed with a research study by Pan *et al.*, (2007) and reasonably higher than the reported study by Jones

and McCathy (2005), Nambiar and Ramamurthy (2006), and in Ameer (2015), as shown in Figure 4-3.

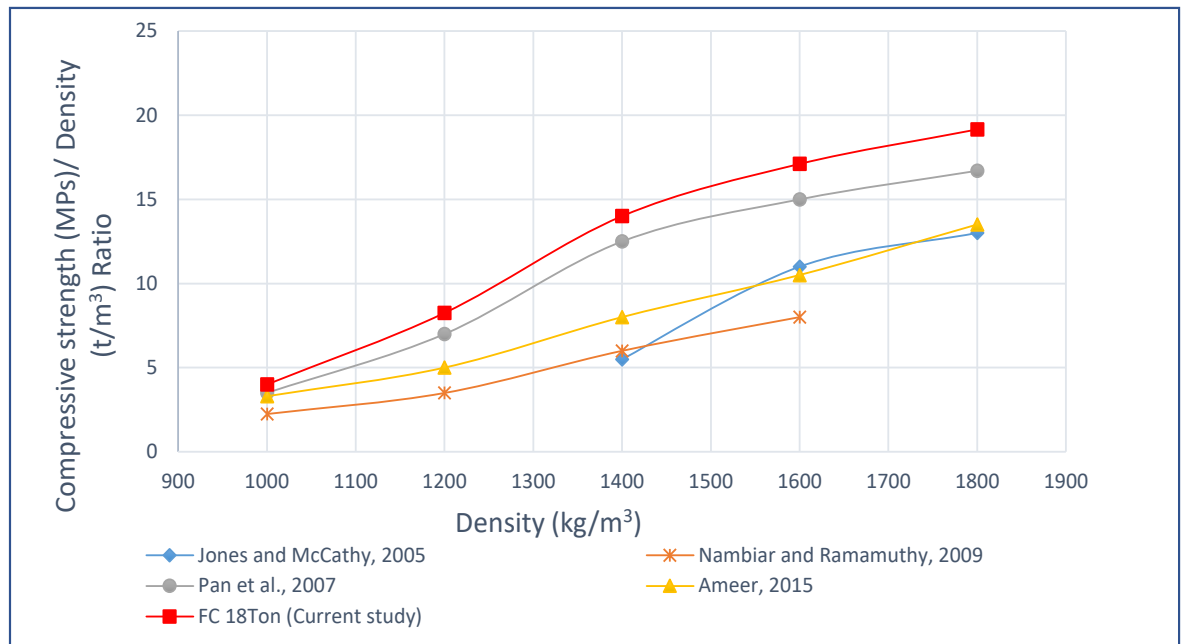


Figure 4-3: Compressive strength/ density ratio with Density

- **Effect of Additives on Compressive Strength**

Based on previous studies, introducing silica fume in the mix proportion of the material is one of the most common strategies to increase the mechanical performance of foamed concrete. The utilization of additives (Toner, Metakaolin MK and silica fume SF) improves the compressive strength of the FC at all densities. It was found that adding Mk by 20% as a replacement of cement by wright improves compressive strength by an average of 18.22%. However, Mk in foamed concrete mixes found to have a chemical reaction leads to killing the foam bobble more rapidly, and this process increases the density of mixes by (6-10%). Moreover, the use of MK in foamed concrete generates extra heat for hydration, where after 24hrs the MK mixes were 6-8 °C hotter than the other mixes.

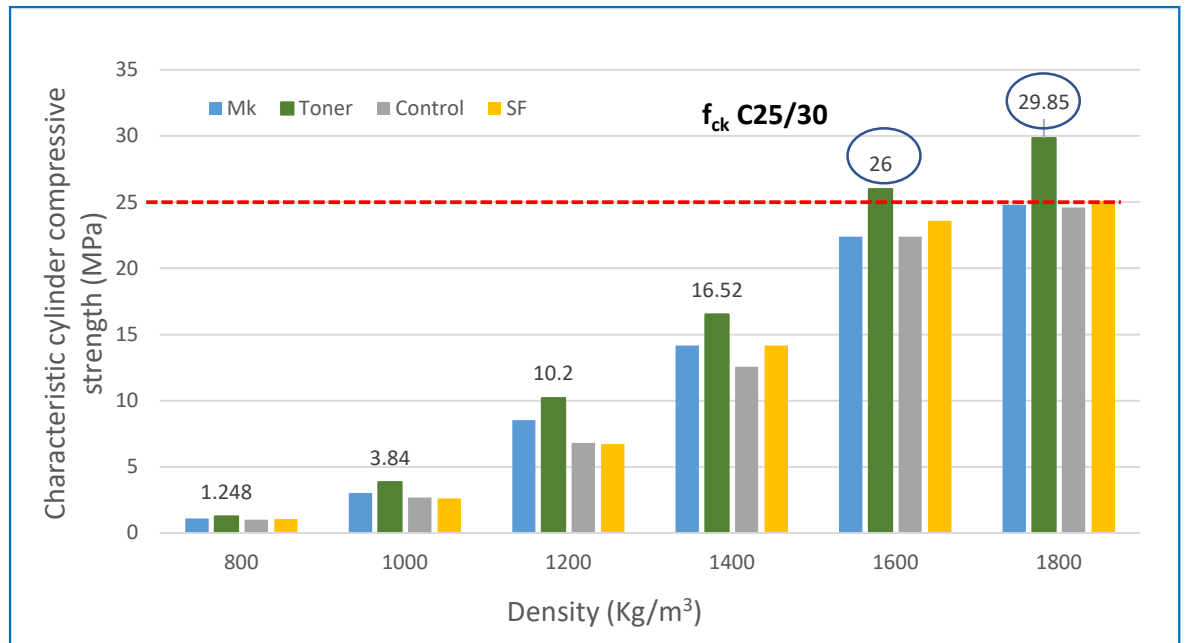


Figure 4-4: The effect of additives on compressive strength (in 1:1.5 c/s ratio mix)

Silica fume (SF) was added as a replacement of 15% by weight of cement for all densities, it was found that SF increases the compressive strength by an average of 9%. There is an upsurge in compressive strength by the addition of waste toner in foamed concrete with reference. Toner as an additive has a higher impact on compressive, where it increases the strength by an average of 30.51%. Results suggest that the mixes with density 1600 – 1800 kg/m<sup>3</sup> with Toner as an additive have a compressive strength that suitable for structural purposes, where their 28-day compressive strengths are higher than 25 MPa (Habsya et al., 2018), see Figure 4-4.

By comparing foamed concrete mixes from literature (Jones and McCarthy, 2005, Nambiar and Ramamurthy, 2006, Pan *et al.*, 2007 and Ameer, 2015) with FC Ton mix in different densities at 28 days, it showed that FC Ton mix has greater strength to density ratio than all other mixes in all densities (1000-1800 kg/m<sup>3</sup>).

To conclude with the fact that, the increase of mix density improved the compressive strength significantly, where increasing the density from 800 kg/m<sup>3</sup> to 1800 kg/m<sup>3</sup> increases the compressive strength by about 2500%, from 1.5 MPa in 800 kg/m<sup>3</sup> mix to 35 MPa in 1800 kg/m<sup>3</sup> mix as shown in Figure 4-5.

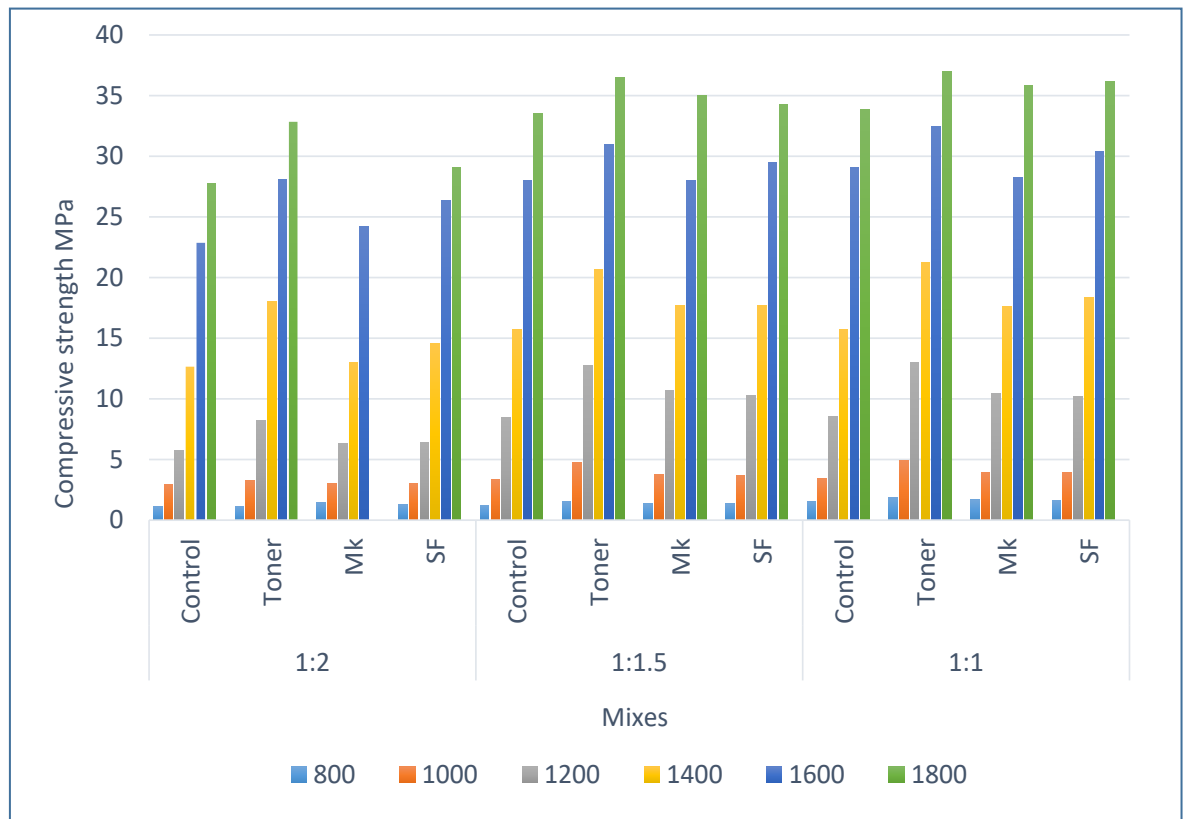


Figure 4-5: Compressive strength of different design mix

#### 4.2.2 Flexural Strength (Modulus of Rupture)

Different mix densities were used with different additives added at specified ratios as a replacement of cement in order to develop the selected foamed concrete mixes. To identify the effect of mix densities, cement/sand ratio and additives, together or individually, on the flexural strength of the concrete, an experimental programme was carried out to test prisms 100 x 100 x 500 mm and beams 90 x 120 x 800 mm made of plain foamed concrete with different densities (800 - 1800 kg/m<sup>3</sup>), with an increment of 200 kg/m<sup>3</sup>, see Table 4-2. Flexural strength testing (Four-point loading) was conducted at the age of 28 days to determine the modulus of rupture ( $f_r$ ) in accordance with BS EN 12390-5, (2009). Table 4-2 shows the flexural strength for each mix.

Table 4-2: Flexural strength for different FC mixes with densities (800-1800) kg/m<sup>3</sup>

Mix Density (kg/m <sup>3</sup> )	Co (MPa)	MK (MPa)	Ton (MPa)	SF (MPa)
800	0.480	0.455	0.493	0.485
1000	0.768	0.897	0.914	0.88
1200	1.719	1.786	1.818	1.75
1400	2.585	2.80	2.922	2.853
1600	3.163	3.081	3.293	3.250
1800	3.836	3.91	4.157	3.895

- **Effect of Density on Flexural Strength**

It was found that the flexural strength was positively proportional to the density of FC mixes. This means that the higher the density, the greater the flexural strength. For instance, in control mixes with densities of 800, 1000, 1200, 1400, 1600, and 1800 kg/m<sup>3</sup> the flexural strengths were 0.48, 0.76, 1.71, 2.58, 3.16 and 3.83 MPa respectively. Increasing the mix density from 1000-1200 kg/m<sup>3</sup> increases the flexural strength by more than 123%. The flexural strength of the FC mix increased by 560% by only doubling its density, where the flexural strength of 1600 kg/m<sup>3</sup> is 3.16 MPa compared to 0.48 MPa in the mix with a density of 800 kg/m<sup>3</sup>, as shown in Figure 4-6.

- **Effect of Additives on Flexural Strength**

The use of additives (Toner, Metakaolin MK and silica fume SF) improves the flexural strength of the FC at all densities. It was found that adding Mk by 20% as a percentage of cement by weight improves flexural strength by an average of 5%. Silica fume SF were added as 15% by weight of cement for 1400, 1600 and 1800 kg/m<sup>3</sup> densities, it was found that SF increases the flexural strength by only 3%. Toner as an additive has a higher impact on flexural strength, where it increases the strength by an average of about 10% Figure 4-6.

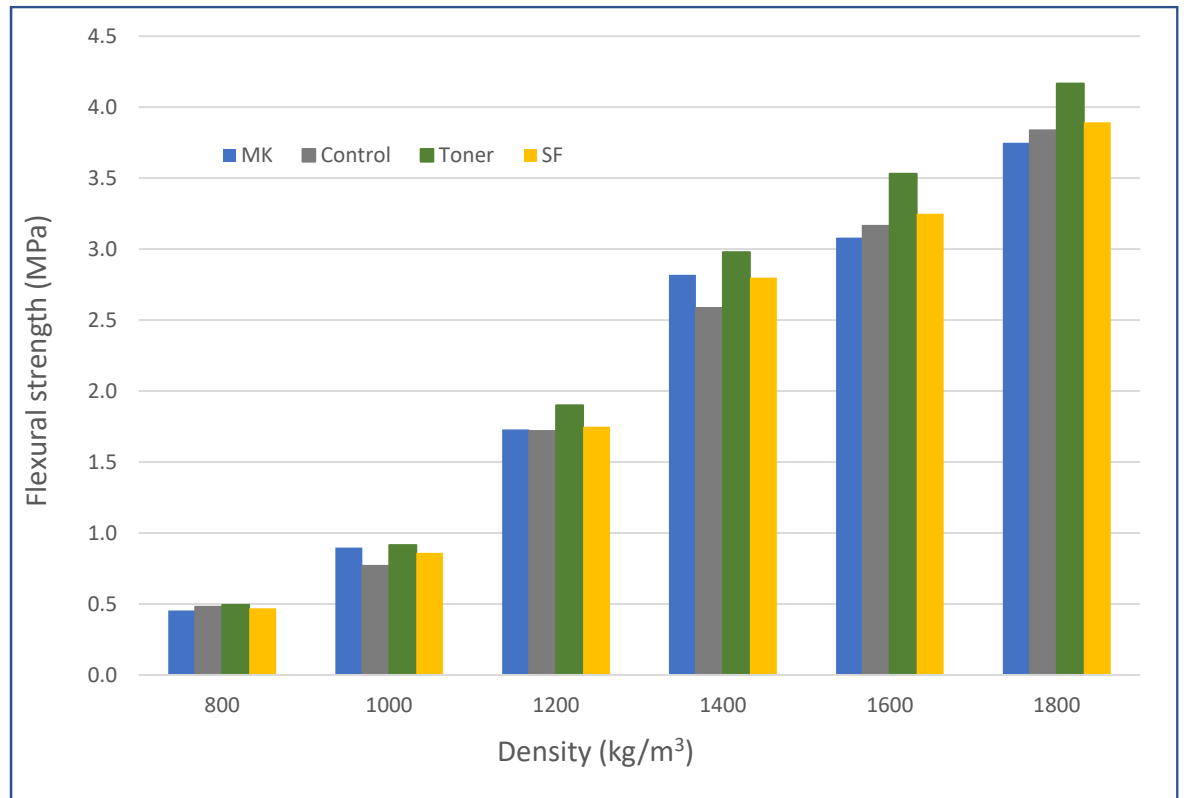


Figure 4-6: Effect of density and additives on flexural Strength

Flexural strengths obtained in this experimental programme were compared with BABU (2008), Fédération Internationale de la précontrainte, (1983), Sldozian *et al.*, (2021) flexural strength, corresponding 28- day compressive strengths. Note that in Figure 4-7, the NWC, FC, and LWC graphs were plotted from the equations below.

$$f_r = 0.31(f'c)^{0.83} \quad \text{Equation 4-1}$$

$$f_r = 0.46 (f'c)^{0.67} \quad \text{Equation 4-2}$$

$$f_r = 0.438 (f'c)^{2/3} \quad \text{Equation 4-3}$$

Where:

$f_r$  Flexural tensile strength, MPa

$f'c$  Compressive strength, MPa

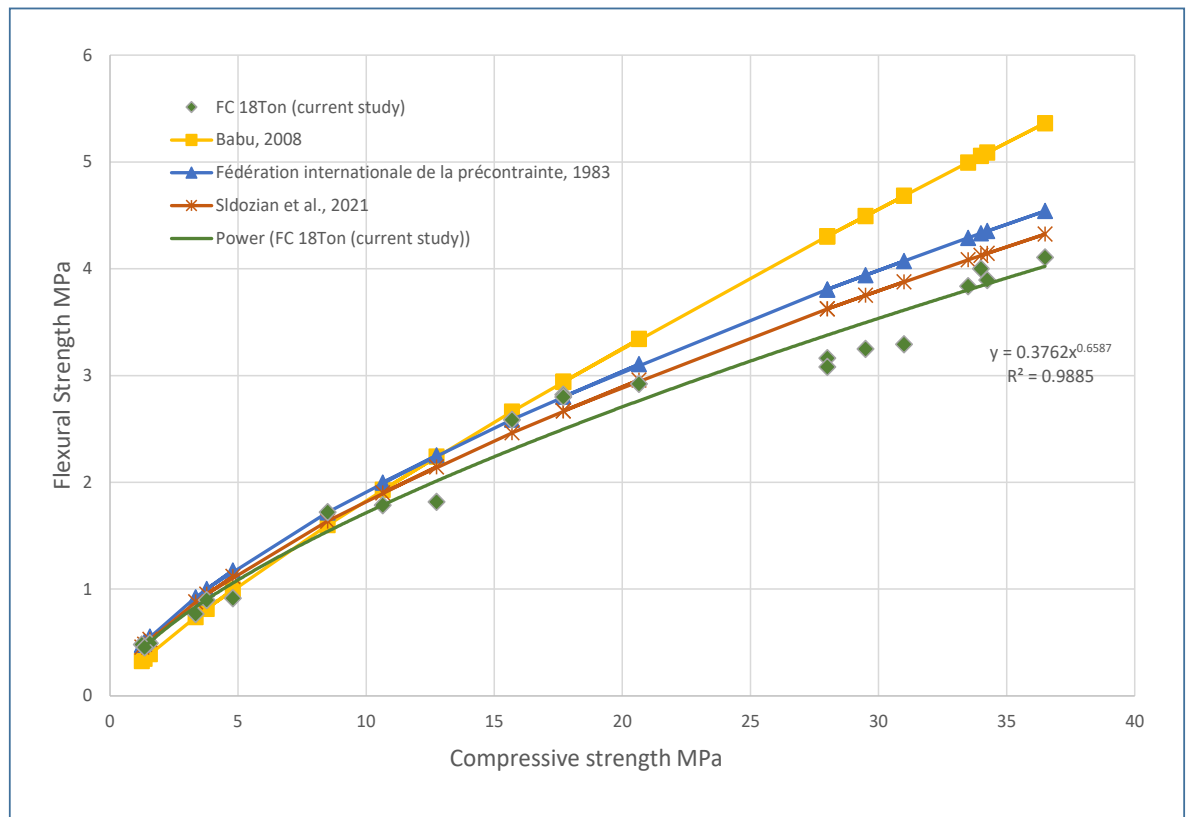


Figure 4-7: Relationship between flexural strength and 28-day compressive strength of FC18Ton, NWC, LWC and FC

### 4.2.3 Splitting Tensile Strength

To develop the selected foamed concrete mixes, different mix densities were used with different additives added at specified ratios as a replacement of cement. To identify the effect of mix densities, cement/sand ratio and additives on the splitting strength of foamed concrete, an experimental programme was carried out to test and develop the tensile strength of different foamed concrete mix designs and densities ( $800 - 1800 \text{ kg/m}^3$ ), see Table 4-3. The splitting tensile testing (Brazilian test) was conducted on three  $300 \times 150$  mm cylinders for each mix at age of 28 days to determine the splitting tensile strength ( $f_{sp}$ ) in accordance with BS EN 12390-6, (2009).

Table 4-3 shows the splitting strength for each mix.

Table 4-3: Splitting tensile strength for different FC mixes with densities (800-1800) kg/m<sup>3</sup>

Mix Density (kg/m <sup>3</sup> )	Co (MPa)	Ton (MPa)	MK (MPa)	SF (MPa)
800	0.24	0.30	0.26	0.27
1000	0.97	1.18	1.09	1.10
1200	1.96	2.31	1.96	1.90
1400	3.00	3.40	3.18	3.23
1600	3.70	4.20	3.88	3.90
1800	4.10	4.60	4.00	4.12

- **Effect of Density on Splitting Tensile Strength**

It was found that the splitting tensile strength is positively proportional to the density of FC mixes. This means that the higher the density, the greater the splitting tensile strength. For instance, as shown in Figure 4-8, in the control mixes with densities of 800 to 1800 kg/m<sup>3</sup> the splitting tensile strengths were increasing affectedly by more than 1600%. The tensile strength of foamed concrete increased by an average of 320% by increasing its density only by 15%. The splitting tensile strength of the FC mix increased by 15 times by only doubling its density, where the splitting tensile strength of 1600 kg/m<sup>3</sup> mix is 3.7 MPa and the mix with a density of 800 kg/m<sup>3</sup> has a splitting tensile strength of only 0.24 MPa, as shown in Figure 4-8.

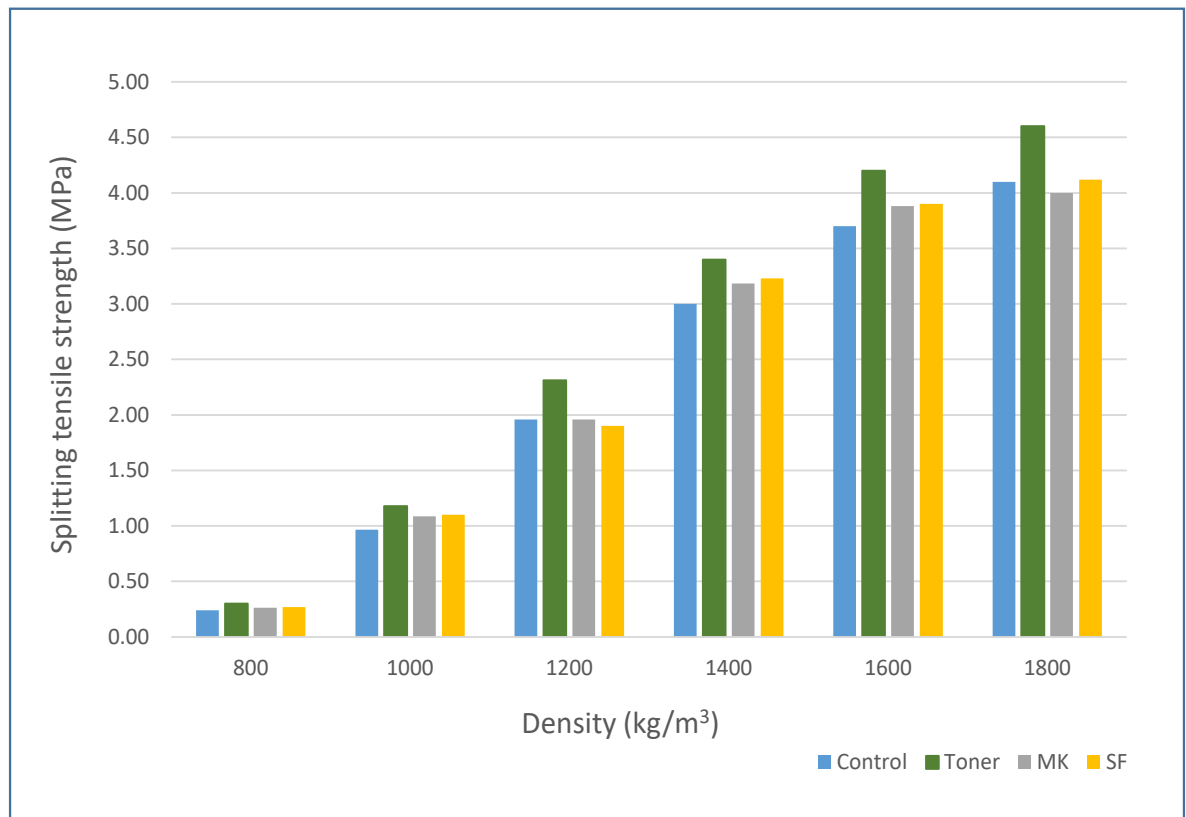


Figure 4-8: Effect of density and additives on FC splitting tensile strength

- **Effect of Additives on Splitting Tensile Strength**

It was found that the use of additives (Toner, Metakaolin and silica fume) improves the splitting tensile strength of the FC especially for mixes with densities higher than 1000 kg/m<sup>3</sup>. It was found that adding Mk by 20% as a replacement of cement by wright improves splitting tensile strength by an average of 5%. Silica fume was added as 15% by weight of cement and it was found that SF increases the splitting tensile strength by only 2.5%. Toner as an additive was found to have a higher impact on splitting tensile strength, where 10% of Toner as replacement of cement increases the strength by an average of 15%, see Figure 4-8.

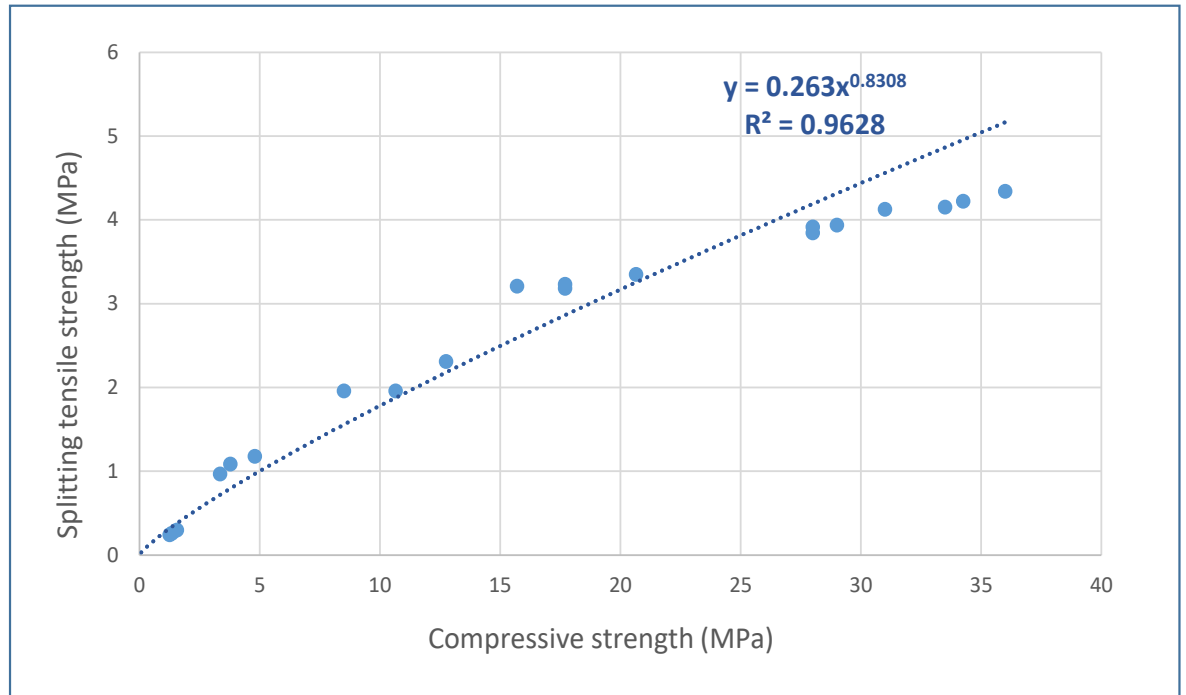


Figure 4-9: Compressive and splitting tensile strength relationship.

Figure 4-9 shows, a relationship between splitting tensile strength with compressive strength  $f'c$  and  $f_{sp}$  in this study. Figure 4-10 compare the tensile-compressive strength relationship in the current study with previous studies (Babu, 2008b) for lightweight concrete, (Jones and McCarthy, 2005) for foamed concrete and (Falade et al., 2013) for foamed concrete, respectively are shown below:

$$f_{sp} = 0.263 (f'c)^{0.8308} \quad \text{Equation 4-4}$$

$$f_{sp} = 0.28 (f'c)^{0.69} \quad \text{Equation 4-5}$$

$$f_{sp} = 0.2 (f'c)^{0.7} \quad \text{Equation 4-6}$$

$$f_{sp} = 0.4 (f'c)^{0.66} \quad \text{Equation 4-7}$$

Where:

$f_{sp}$      Splitting tensile strength, MPa

$f'c$      Compressive strength, MPa

It can be seen in Figure 4-10, for a given 28-day 18Ton foamed concrete in the current study has higher splitting tensile strengths, than those with LW aggregate and foamed concrete in previous studies. However, the splitting tensile strength of FC 18Ton mix in the current study strongly conforms with the results of the splitting tensile of FC in Falade, Ikponmwsa and Fapohunda, (2013) study. Falade, Ikponmwsa and Fapohunda, (2013) used Pulverized Bone as an additive to FC, which contains around 10% of silicon dioxide ( $\text{SiO}_2$ ) which almost the same amount that waste toner does. According to Zhuang and Chen, (2019), silicon dioxide improves the mechanical properties of concrete including bending and tensile strength.

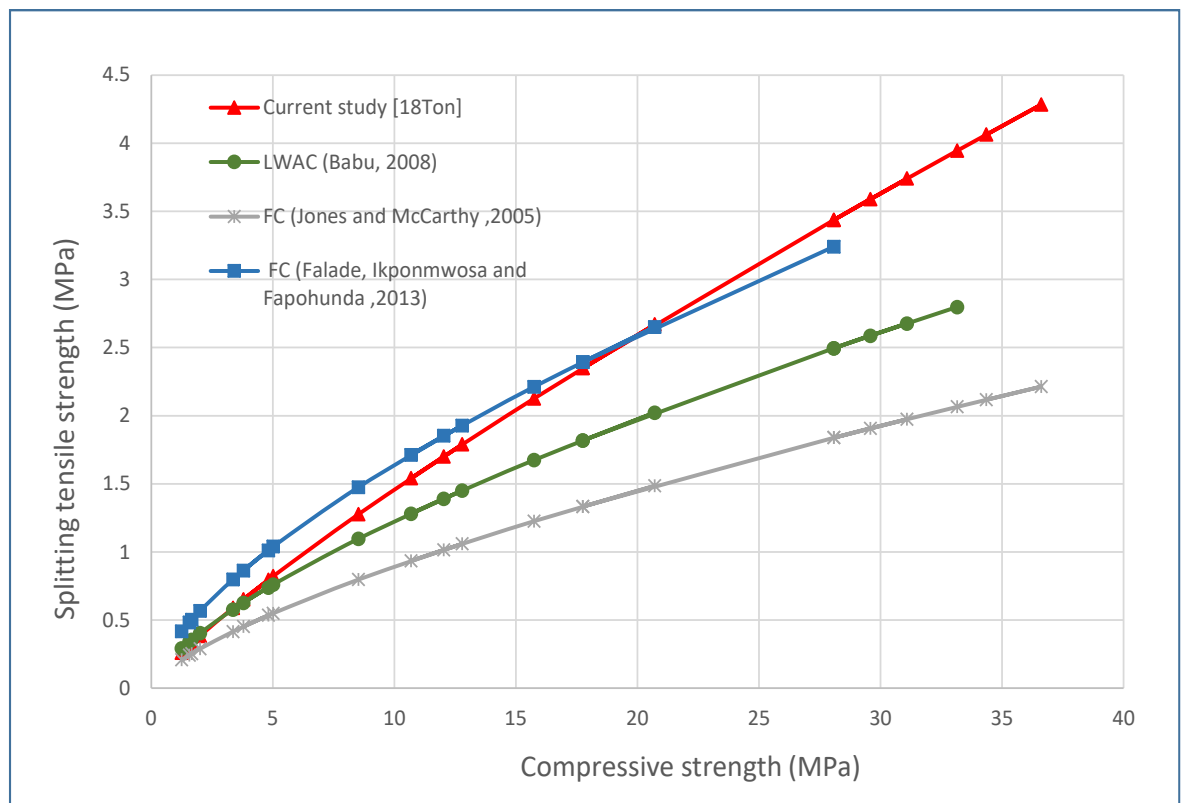


Figure 4-10: Relationship between splitting tensile strength and 28 days compressive strength of LWCA and FC

#### 4.2.4 Direct Tensile Strength

A direct tensile strength test under uniaxial tensile was developed and carried out using the 100 x 100 x 500 mm foamed concrete specimen as illustrated in Figure 4-11. New special steel claws were designed, built and installed for direct tensile tests of FC concrete. The claws make it possible to use prismatic specimens without inducing stress

concentrations of too high a magnitude and this significantly simplifies the manufacturing of specimens and the performance of direct tensile tests.

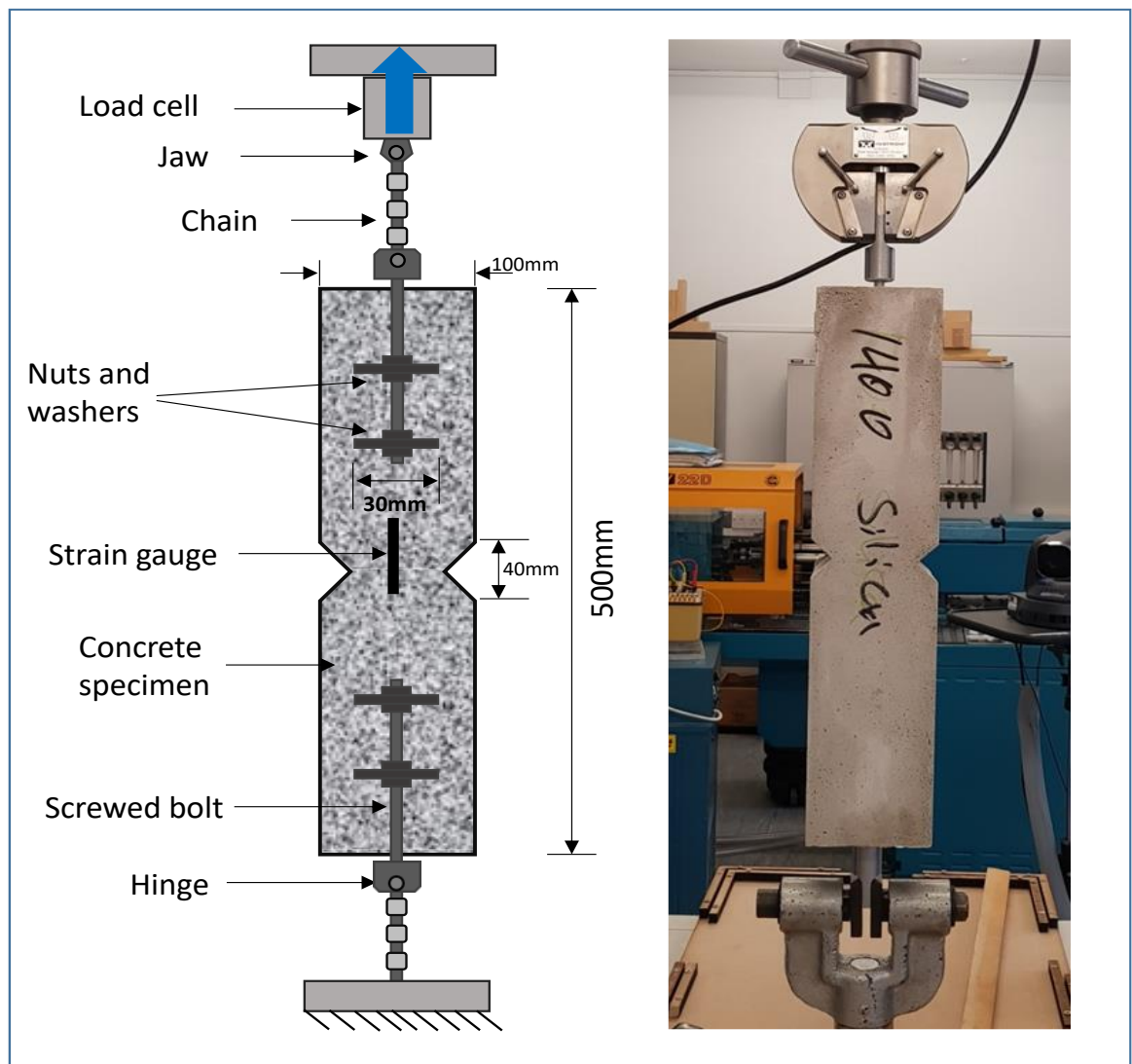


Figure 4-11: Direct tensile testing for foamed concrete

As predicted, failure of all specimens occurred in the middle where the cross-section was reduced by 40%, as shown in Figure 4-11. Reduction of the cross-sectional area of the specimens resulted in increasing the stress at the middle of the specimens, which induced a consistent failure in the middle. It is also prevented the failure to occur at undesirable locations along the length of the specimen. No concrete cracking occurred at either end of the specimens, as the designed claws created a strong and evenly distributed bond between the claws and the concrete.

To develop the selected FC mixes, three mix densities were used with different additives added at specified ratios as a replacement of cement. To identify the effect of mix densities, cement/sand ratio and additives, on the direct tensile strength of the concrete, an experimental programme was carried out at different concrete densities (1400, 1600 and 1800 kg/m<sup>3</sup>). Direct tensile testing was conducted on three 100 x 100 x 500 mm prisms for each mix at age of 28 days to determine the direct tensile strength ( $f_t$ ). The difference between the maximum and minimum values of the direct tensile strength of each mix of the FC specimens was less than 4%. Figure 4-12 shows load vs displacement for each mix design.

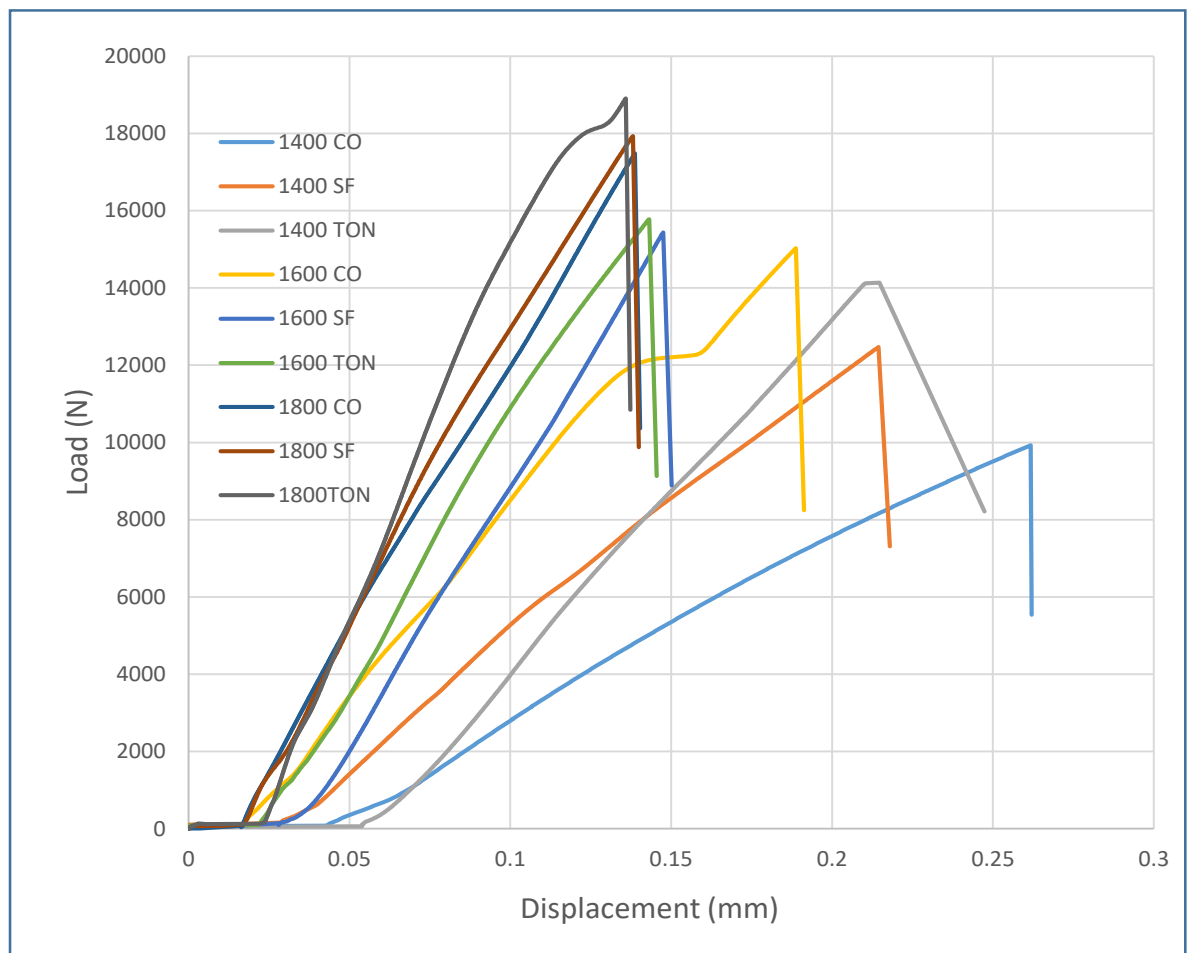


Figure 4-12: Load - displacement for FC specimens under direct tension

- **Effect of Density on Direct Tensile Strength**

It was found that the direct tensile strength is positively proportional to the density of FC mixes. This means that the higher the density, the greater the direct tensile strength. For

instance, as shown in Figure 4-13, in control mixes with densities of 1400, 1600 and 1800 kg/m<sup>3</sup> the direct tensile strengths were increasing from 2.085, 3.068 and 3.461 MPa respectively. For instance, increasing the mix density from 1400 to 1800 kg/m<sup>3</sup> increases the direct tensile strength by more than 65%.

- **Effect of Additives on Direct Tensile Strength**

The utilization of additives (Toner and silica fume) improves the direct tensile strength of the FC at all densities. Where it was found that adding SF by 15% as replacement of cement by weight improves direct tensile strength by an average of 8%. Toner as an additive was found to have a higher impact on direct tensile strength, where 5% of Toner as replacement of cement increases the direct tensile strength by an average of about 18%, see Figure 4-13.

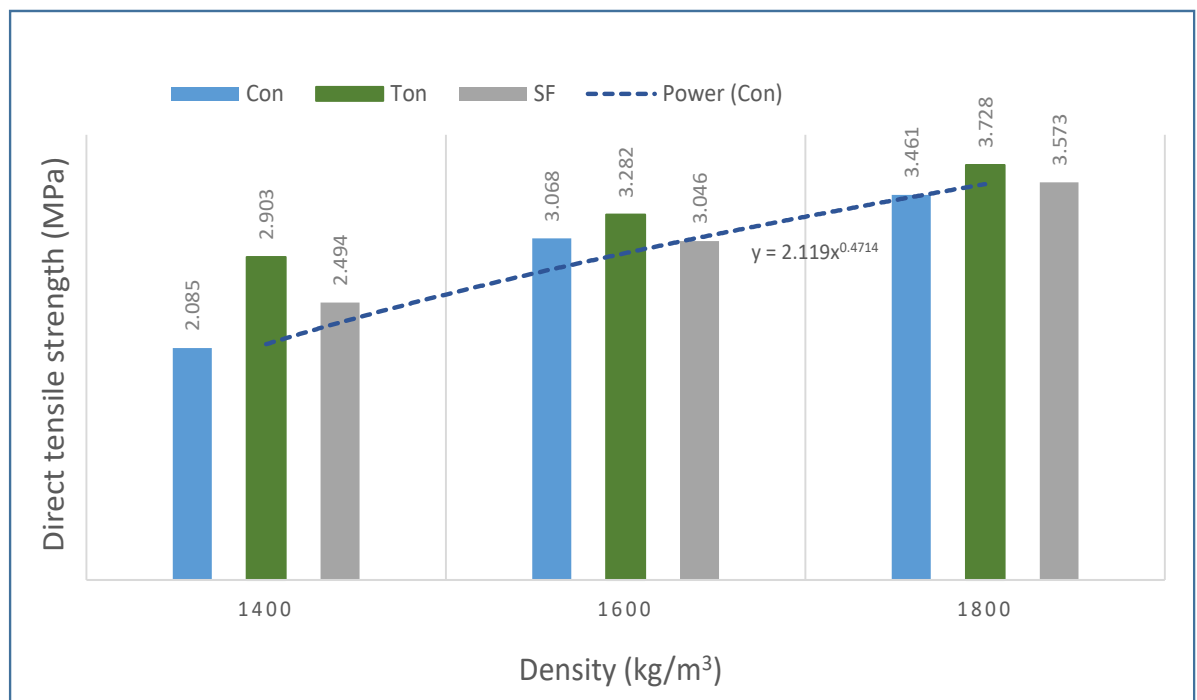


Figure 4-13: Effect of density and additives on direct tensile strength

It was observed that the tensile strength of the FC from the direct test is less than the indirect testing includes the splitting and flexural strength (modulus of rupture). The average direct tensile strength of the FC was found to be only 5% less than the average flexural strength. However, the average splitting tensile strength of the FC was found to be about 20% higher than the average direct tensile strength for all mixes.

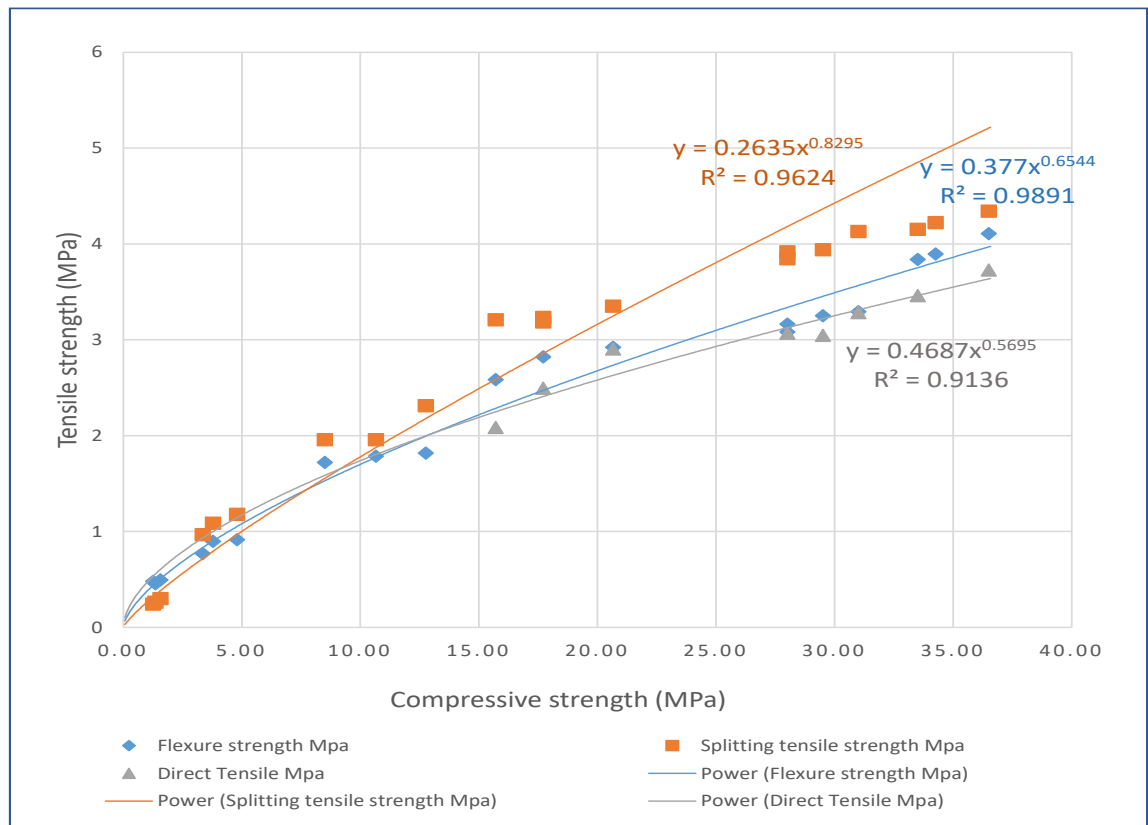


Figure 4-14: Tensile strength from direct and indirect tension testes

Previous studies (Alhussainy et al., 2016), (Choi et al., 2014) and (Falade et al., 2013) suggested that the direct tensile strength of concrete is lower than the indirect tensile strength. This can be explained by the fact that during the direct tensile test, the failure surface has less resistance to the applied force as it is perpendicular to the direction of the applied force. However, in the indirect tensile test such as the Brazilian test, the cylindrical sample is subjected to diametrical compression stresses. These stresses applied over a small width throughout the sample's length and with a controlled load area to avoid the concentration of stresses and compensate small irregularities on the surface of the sample. In the flexural test, the rupture plan is under tension at the bottom of the beam section and compression stress at the top of the section and concrete is strong in compression which leads to higher tensile strength (Slag Cement Association, 2013).

#### 4.2.5 Shear Strength

Wang, Kou and Xing, (2013) stated that the increase in concrete strength has always been associated with compressive and tensile strengths. Nevertheless, concretes with higher strength are known to be more brittle than normal strength concrete. Concrete with low

toughness characteristics may result in sudden and catastrophic shear failure even with high compressive strength. Therefore, it was necessary to study the shear behaviour for developed foamed concrete.

To develop the selected foamed concrete mixes, three mix densities were used with different additives added at specified ratios as a replacement of cement. To identify the effect of mix densities, cement/sand ratio and additives, on the shear strength of the foamed concrete, an experimental programme was carried out at different concrete densities (1200, 1400, 1600 and 1800 kg/m<sup>3</sup>). A modified push-off specimens test was conducted on three 100 × 100 × 500 mm prisms at ages of 28 days to determine the shear strength ( $v_c$ ). Table 4-4 shows the shear strength for each mix.

*Table 4-4: Shear strength for different Foamed Concrete mixes*

<b>Density (kg/m<sup>3</sup>)</b>	<b>Mix</b>	<b>Shear strength (MPa)</b>
1200	Co	1.96
	Ton	2.31
	SF	1.96
	MK	1.91
1400	Co	2.482
	Ton	2.825
	SF	2.454
	MK	2.134
1600	Co	3.093
	Ton	3.795
	SF	3.224
	MK	3.092
1800	Co	3.884
	Ton	4.055
	SF	3.890
	MK	3.85

- **Effect of Density on Shear Strength**

It was found that the shear strength is positively proportional to the density of FC mixes. This means that the higher the density, the greater the shear strength. For instance, in control mixes with densities of 1200, 1400, 1600 and 1800 kg/m<sup>3</sup>. The shear strengths were 1.93, 2.482, 3.093 and 3.884 MPa respectively. Increasing the mix density from 1400-1800 kg/m<sup>3</sup> increases the shear strength by more than 57%.

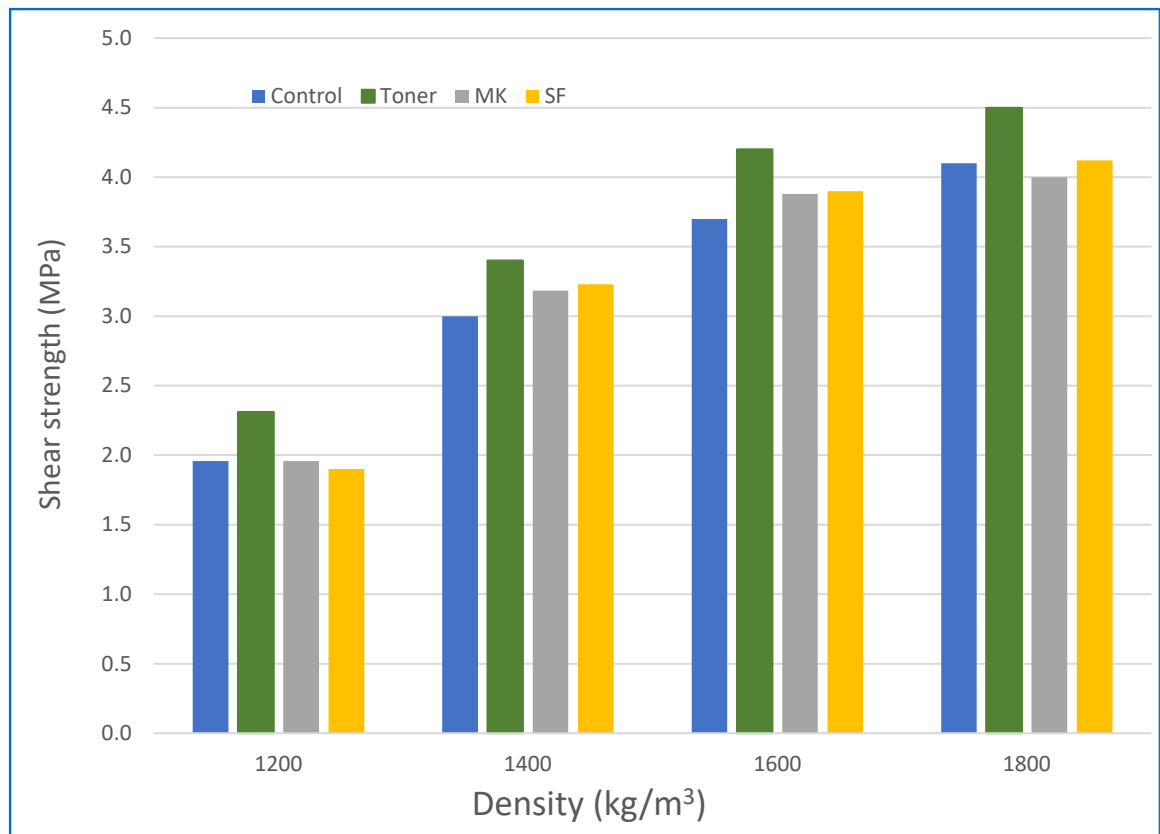


Figure 4-15: Effect of density and additives on FC shear strength

- **Effect of Additives on Shear Strength**

Additives (Toner Ton, Metakaolin MK and silica fume SF) added to FC mixes to study their effect on the shear strength of foamed concrete. Toner and silica fume illustrate an improvement in shear strength. However, MK shows a slight reduction in the shear strength of FC. In FC mix 1400, 1600 and 1800 kg/m<sup>3</sup> MK was added by 20% as a percentage of cement by weight shows a reduction in shear strength by an average of 5%. Silica fume replaced 15% of cement by weight improved the shear strength by an average

of only 6%. However, Toner as an additive by 5% as replacement of cement by wright improved shear strength by an average of 13.65% as shown in Figure 4-15.

Figure 4-16, illustrates a relationship between shear strength with compressive strength and  $v_c$  and  $f'_c$  obtained from the current study.

$$v_c = 0.371 (f'_c)^{0.654} \quad \text{Equation 4-8}$$

Where:

$v_c$  Shear strength in, MPa

$f'_c$  Compressive strength, MPa

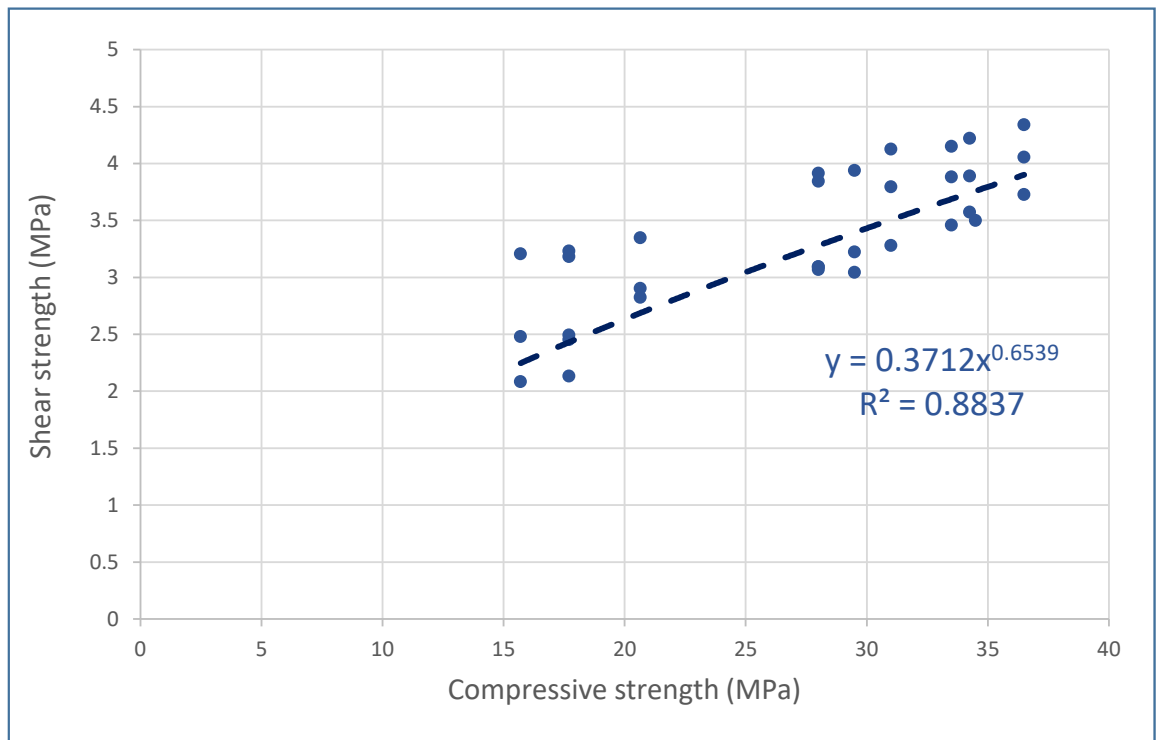


Figure 4-16: Shear and compressive strength relationship in foamed concrete

#### 4.2.6 Stress-Strain Relationship and Modulus of Elasticity

The modulus of elasticity of concrete is a key factor to estimate the deformation of members and structures. The static modulus of elasticity (E) of the conventional mixes of FC and mixes with additives was determined using 150 × 300 mm cylinder specimens. The stress-strain relationships of normal and foamed concrete obtained from the static

modulus of elasticity test are presented in Figure 4-17. It was observed that FC has greater strain at maximum stress than normal-weight concrete, which means FC is a more flexible material than normal concrete. However, the increase of FC compressive strength decreases its flexibility and become more brittle. The reduction of foamed concrete density leads to a decrease of its compressive strength and an increase in the strain at the maximum stress, which greatly reduces the modulus of elasticity.

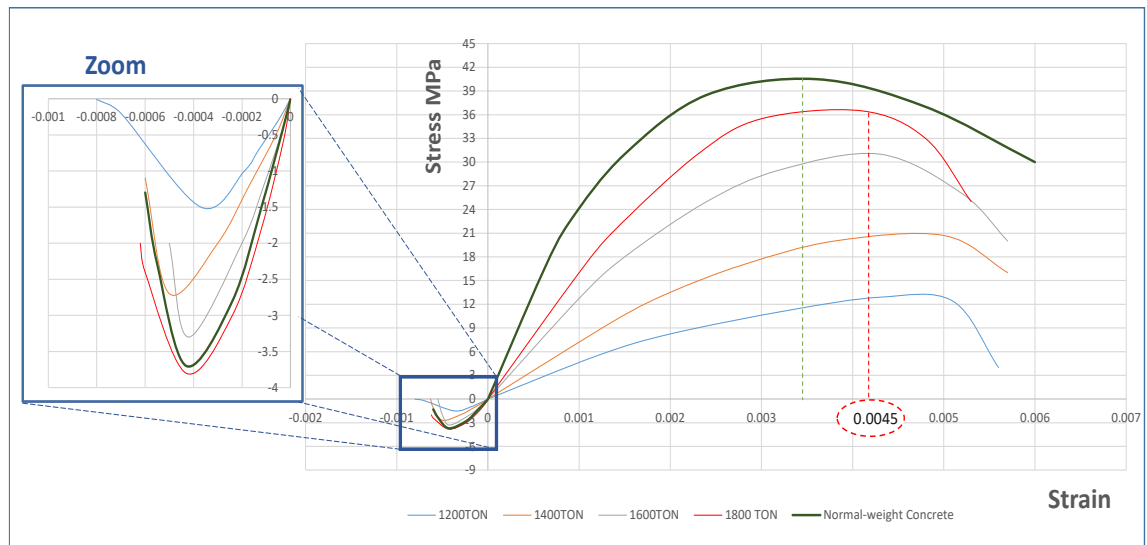


Figure 4-17: The stress-strain relationships of normal and foamed concrete

To develop the FC mechanical properties, different mix densities were tested with different additives added at specified ratios as a replacement of cement. To identify the effect of mix densities,  $c/s$  ratio and additives, on the modulus of elasticity of foamed concrete, an experimental programme was carried out at different concrete densities (800 – 1800)  $\text{kg/m}^3$  with an increment of 200  $\text{kg/m}^3$  see Table 4-5. Compression testing was conducted on three 300 x 150 mm cylinders for each mix at age of 28 days to determine the modulus of elasticity ( $E$ ) in accordance with BS 1881-121, (1983).

Table 4-5: Modulus of elasticity for different FC mixes

Modulus of elasticity (MPa)				
Density (kg/m <sup>3</sup> )	Co	Ton	Mk	SF
800	394	477	437	413
1000	1172	1500	1400	1388
1200	2591	3438	2857	3000
1400	4444	6161	5000	4650
1600	8250	9566	8288	8250
1800	9900	11990	10575	10875

- **Effect of Density on the Modulus of Elasticity**

The Modulus of Elasticity is positively proportional to the density of FC mixes. This means that the higher the density, the greater the Modulus of Elasticity. An average improvement of 450% in the modulus of elasticity in FC mixes by increasing the density of foamed concrete mix by only 200 kg/m<sup>3</sup>. However, as shown in Table 4-5, in control mixes with densities of 800 kg/m<sup>3</sup> the modulus of elasticity is 394 MPa and the mix with a density of 1600 kg/m<sup>3</sup> has Modulus of elasticity of 8250 MPa, which, means that by doubling the density from 800 to 1600 kg/m<sup>3</sup> the modulus of elasticity was increased by about 2000%, as shown in Figure 4-18.

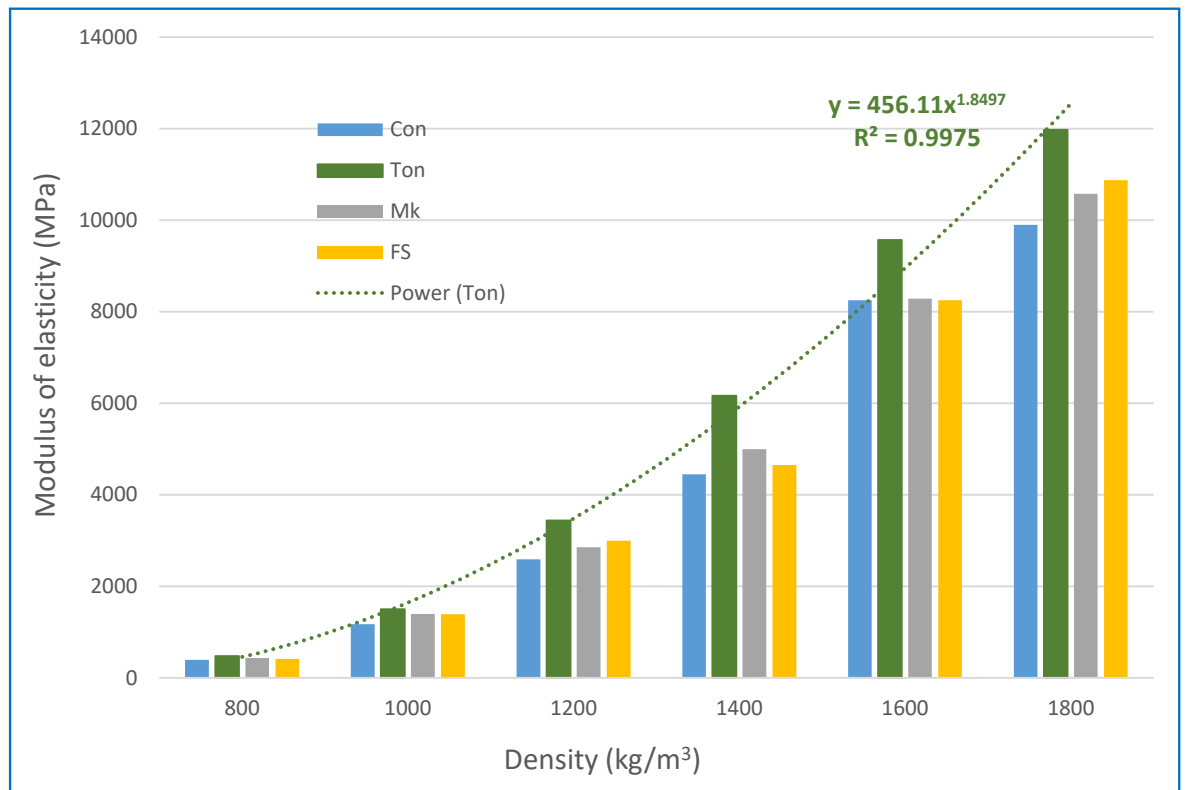


Figure 4-18: Effect of density and additives on FC modulus of elasticity from direct compression

- **Effect of Additives on Modulus of Elasticity**

It was found that additives (Toner, Metakaolin and silica fume) improve the modulus of elasticity of the FC at all densities (800 - 1800 kg/m<sup>3</sup>). Replacing 20% cement by Mk improves FC modulus of elasticity by an average of 11%. Silica fume SF replaced 15% by weight of cement, it was found that SF increases the modulus of elasticity by about 7% compared to control (Con) mix. However, Toner as an additive was found to have a greater effect on the modulus of elasticity, where 5% of Toner as replacement of cement increases FC modulus of elasticity by an average of 22%, see Figure 4-18.

The literature review values of the modulus of elasticity relationship with corresponding 28 days compressive strength of NWC, SSC and FC are based on the expressions below:

$$\text{The current study (18Ton)} \quad E = 0.0046(f'c)^2 + 0.25f'c + 0.84 \quad \text{Equation 4-9}$$

Jones and McCarthy (2005)  $E = 0.42 (f'c)^{1.08}$  Equation 4-10  
 for FC with coarse FA

Neville (2011) for NWC  $E = 2.1 \times 10^5 (\gamma/2.3)^{1.5} (f'c/200)^{0.5}$  Equation 4-11

Craeye *et al.*, (2014) for SCC  $E = 0.872 (f'c)^{0.8112}$  Equation 4-12

Where:

- $E$  Modulus of elasticity, MPa
- $\gamma$  Unit weight of concrete, t/m<sup>3</sup>
- $f'c$  Specified compressive strength of the concrete, MPa

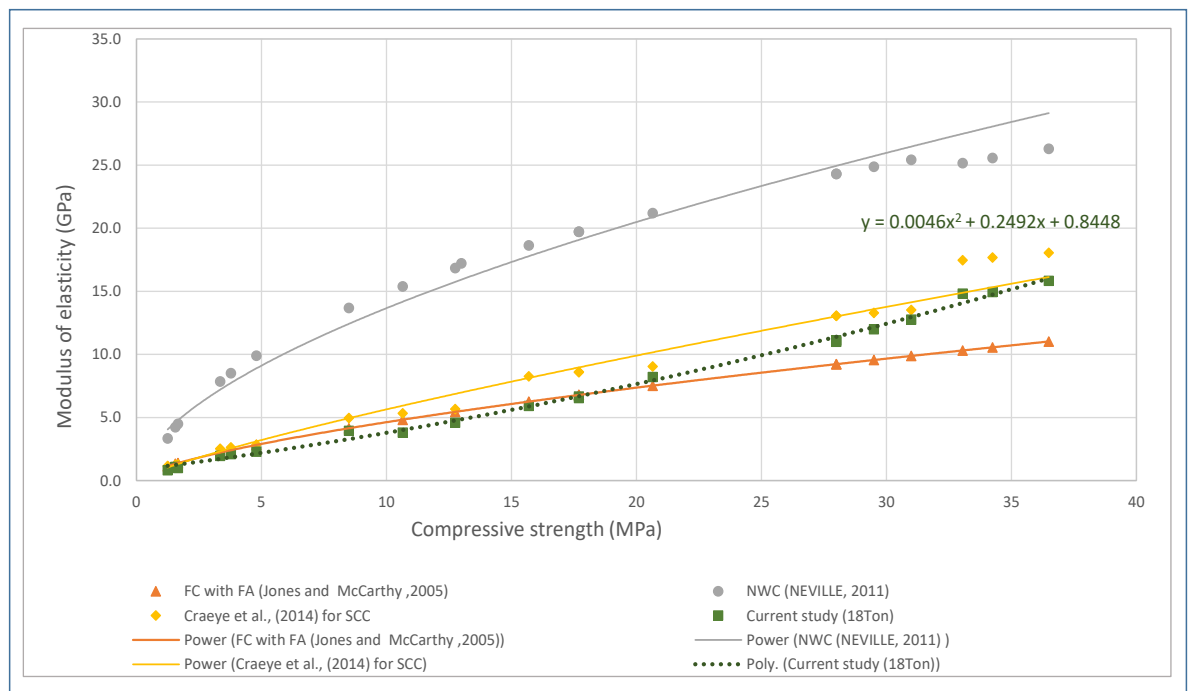


Figure 4-19: Relationship between compressive strength and modulus of elasticity of NWC, SCC and FC.

It can be seen that for a given compressive strength, the 18Ton mix in the current study exhibited lower  $E$  values than those obtained from NWC and SCC mixes. However, 18Ton mix exhibited higher  $E$  values than foamed concrete in Jones and McCarthy, (2005) mixes as shown in Figure 4-19.

### 4.3 Bond Behaviour from Pull-out and Beam Tests

The pull-out test is used commonly in the assessment of the bond performance of reinforcing bars in the concrete. The bond mechanism in concrete consists of three components: chemical adhesion, friction, and mechanical interlocking. Adhesion depends on the chemical reaction between the concrete and the reinforcing steel bars, friction is determined by the surface roughness, and mechanical interlock is subjected to the surface deformation and reinforcement geometry (Marco, 2015).

Chemical adhesion and friction play the main and primary role in the bond of plain bars, even though some mechanical interlocking takes place due to the bar surface's roughness. The three bond components are not independent, they interact with each other and cannot be analysed as separated issues. The combined effect of these components leads to different behaviours. Mainly there are four types of bond failure, which are bar pull-out, concrete pull-out, bar failure and concrete splitting.

From the experimental test result, bond stress can be defined as the change of stresses in the reinforcing bar with bar length as illustrated in Figure 4-20. Bond resistance can be determined by dividing the tensile force with the reinforcing bar area embedded in concrete see Figure 4-20.

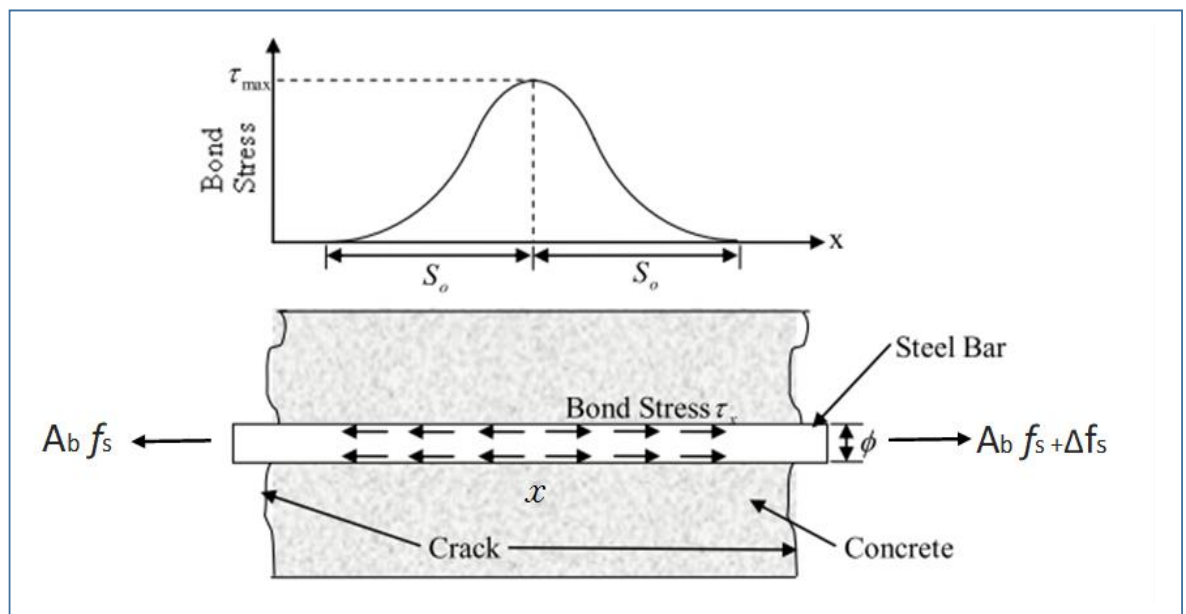


Figure 4-20: Distribution of bond stress between cracks

$$\tau = \frac{A_b \cdot \Delta f_s}{\pi \cdot d_b \cdot x} = \frac{d_b \cdot \Delta f_s}{4x} \quad \text{Equation 4-13}$$

Where:

- $\tau$  Bond stress, MPa
- $A_b$  Reinforcement bar area, mm<sup>2</sup>
- $d_b$  Reinforcement bar diameter, mm
- $f_s$  Stress in the reinforcement bar, MPa

The bond strength expression can be simplified as follows:

$$\tau = \frac{P_{max}}{\pi \cdot d \cdot L} \quad \text{Equation 4-14}$$

Where:

- $P_{max}$  Maximum pull-out load, N
- $d$  Diameter of the reinforcement bar, mm
- $L$  Embedded reinforcement length, mm

To study the structural behaviour of foamed concrete, two mix densities 1600 and 1800 kg/m<sup>3</sup> with and without additives are tested as they met the structural requirement of 25 MPa. To identify the effect of densities, and additives, on the bond strength between reinforcement rebar (steel/GFRP) and concrete, an experimental programme was carried out applying two methods: pull-out and beam method. Pull-out testing was conducted on three specimens for each type of reinforcement (steel and GFRP) for each mix at age of 28 days to determine the bond stress ( $\tau$ ) and mode of failure as shown in Figure 4-21.

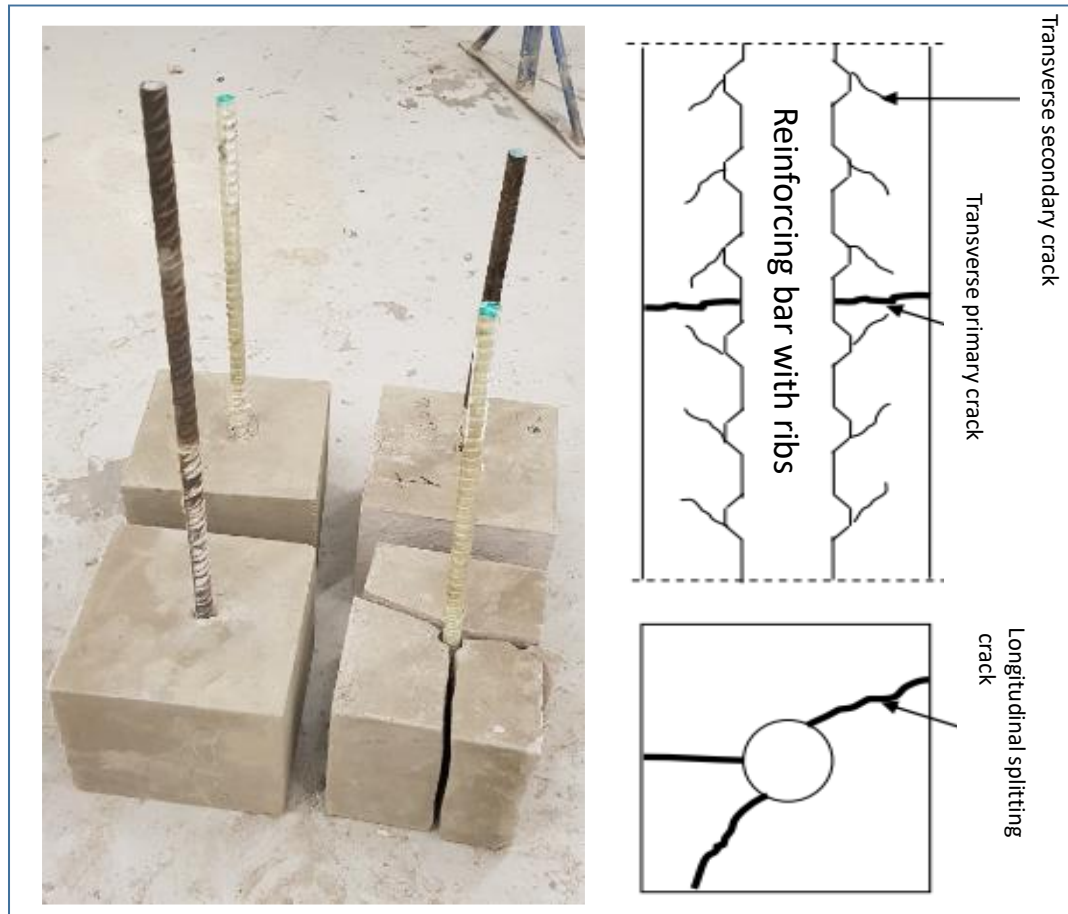


Figure 4-21: Typical modes of failures that occurred experimentally

- **Effect of Density on Bond Strength**

From the pull-out and beam tests, it was found that the bond strength is positively proportional to the density of FC mixes. This means that the higher the density, the greater the bond strength. As shown in Figure 4-22, in control mixes with densities of 1600 and 1800 kg/m<sup>3</sup> the bond strength was increased by 16%. However, in Toner mixes the bond strength increased by 21% by increasing the density from 1600 to 1800 kg/m<sup>3</sup>. It is observed that the chance of splitting failure increases with increasing density, where, double the number of splitting failures accrued in mixes with 1800 kg/m<sup>3</sup> density compare to 1600 kg/m<sup>3</sup> mixes.

**Note:** for example, Con16St mix refers to control mix reinforced with 16mm steel bar

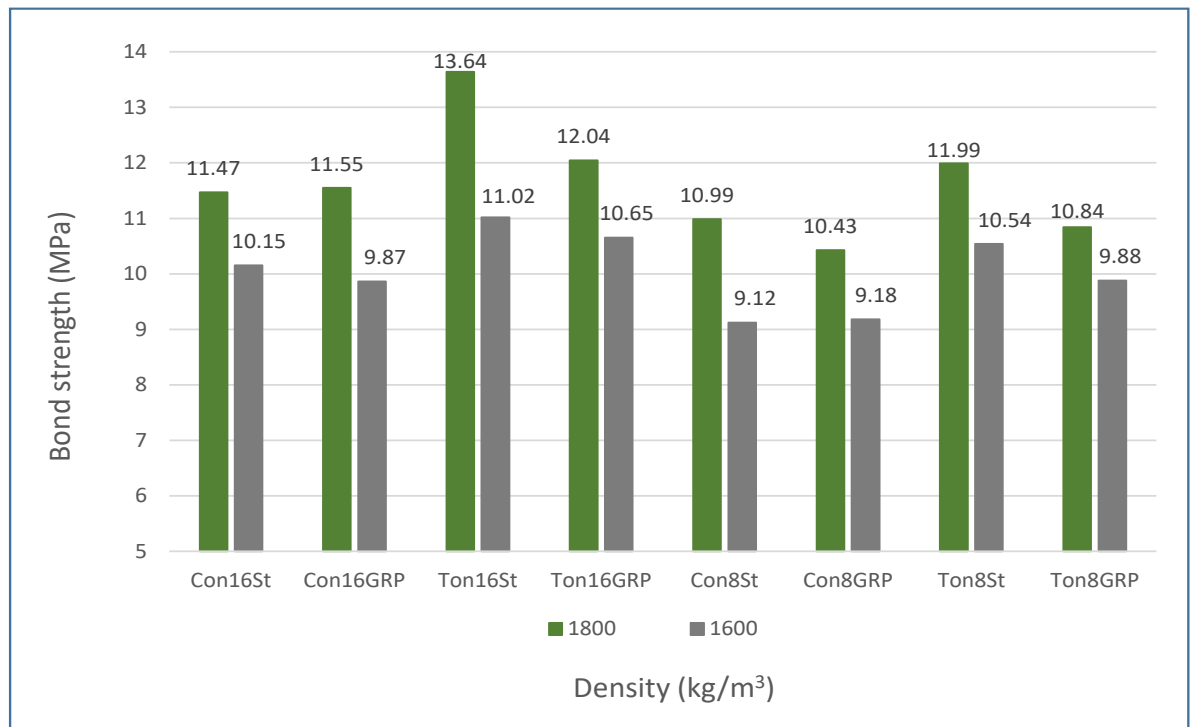


Figure 4-22: Effect of density on the bond strength

- **Effect of Additives on Bond Strength**

The use of Toner as an additive improves the bond strength of the FC at both densities. It was found that adding Toner by 5% as a percentage of cement by weight improves bond strength by an average of about 10%, see Figure 4-23. All mixes containing Toner failed in the pull-through mode of failure, which might be explained by the fact that Toner improved the tensile strength of foamed concrete. However, 50% of the control mixes that did not contain Toner failed in the splitting mode of failure, see Figure 4-21.

**Note:** for example, 16-16St mix refers to 1600 kg/m<sup>3</sup> mix reinforced with 16 mm steel bar

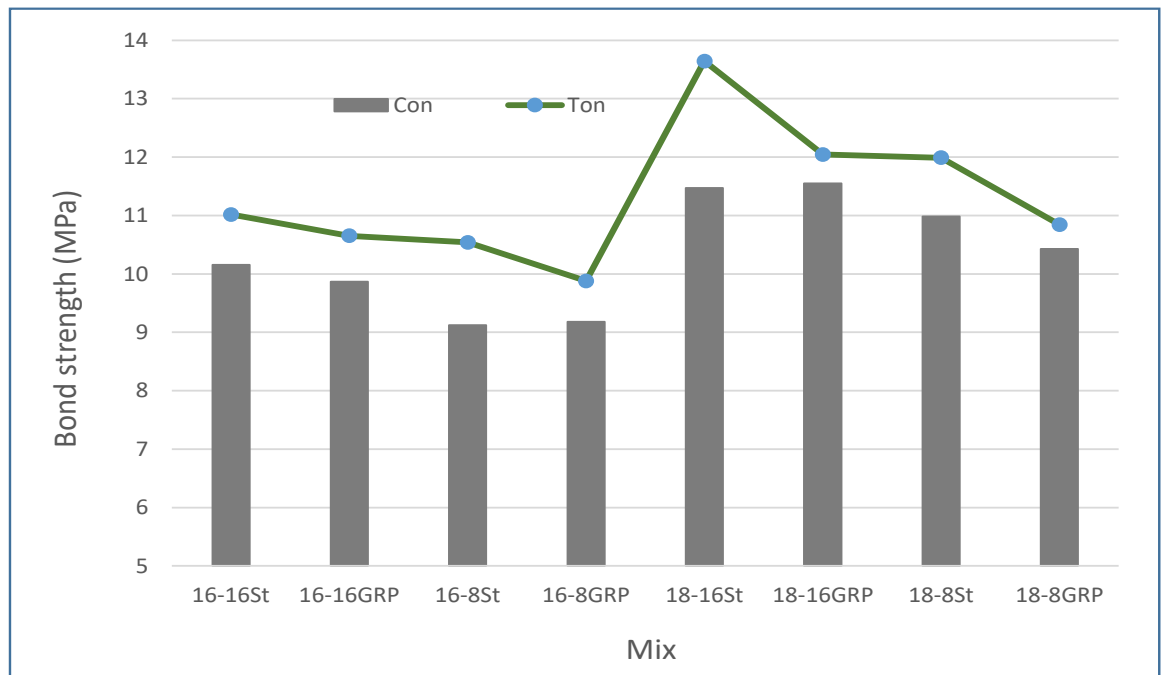


Figure 4-23: Effect of additives on bond strength

- **Effect of Bar size on Bond Strength**

The pull-out and beam tests showed that the bond load is positively proportional to the bar diameter. This means that the greater the bar size, the higher the bond load. However, bond stress for example in a bigger bar size is not much higher than bond stress in a smaller bar size. Where, in 8 mm bar size the average bond stress is 10.37 MPa, but in 16 mm bar size the average bond stress is 11.30 MPa with an increase of 8.7%. Diameter appears to have little influence on bond strength as shown in Figure 4-24. Therefore, further investigations covering different GFRP bars size effects on bond strength with FC are needed in future work.

**Note:** for example, 18Ton-GRP mix refers to Waste toner mix reinforced with GFRP bar

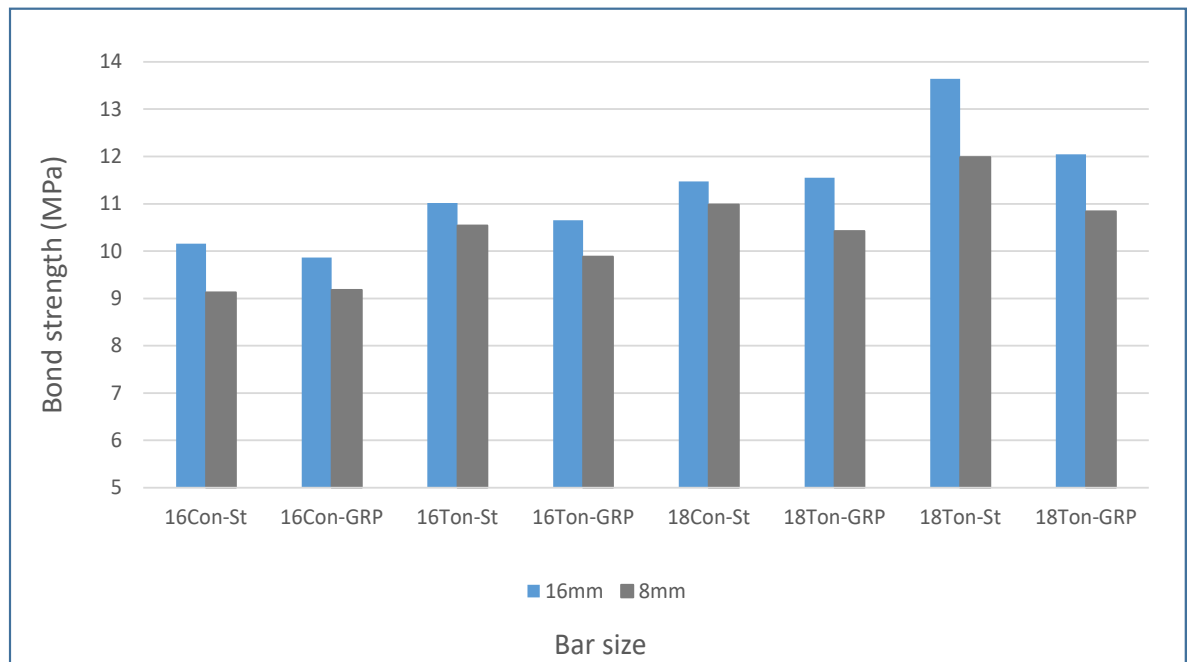


Figure 4-24: Effect of bar size on bond strength

- **Effect of the Bar Material on Bond Strength**

Two types of reinforcement bars used in the pull-out and beam tests (Steel and Glass Fibre Reinforced Polymer GFRP). It was found that in all bar sizes the average bond strength in steel bars is 11.12 MPa and the average bond strength in GFRP Bars is 10.56 MPa. GFRP bond performance with foamed concrete was found to be 95% of steel bond strength with FC. Poisson's ratio of GFRP is smaller than that in steel, which might result in a better bond performance at high tensile stress, in other words, Poisson's ratio measures the deformation in the material in a direction perpendicular to the direction of the applied force, under tension force, steel bar deforms and becomes slimmer which leads to slipping bond failure. Figure 4-25 illustrates the effect of bar material on bond strength.

**Note:** for example, 16Ton8 mix refers to 1800 kg/m<sup>3</sup> Waste Toner mix reinforced with 8 mm bar.

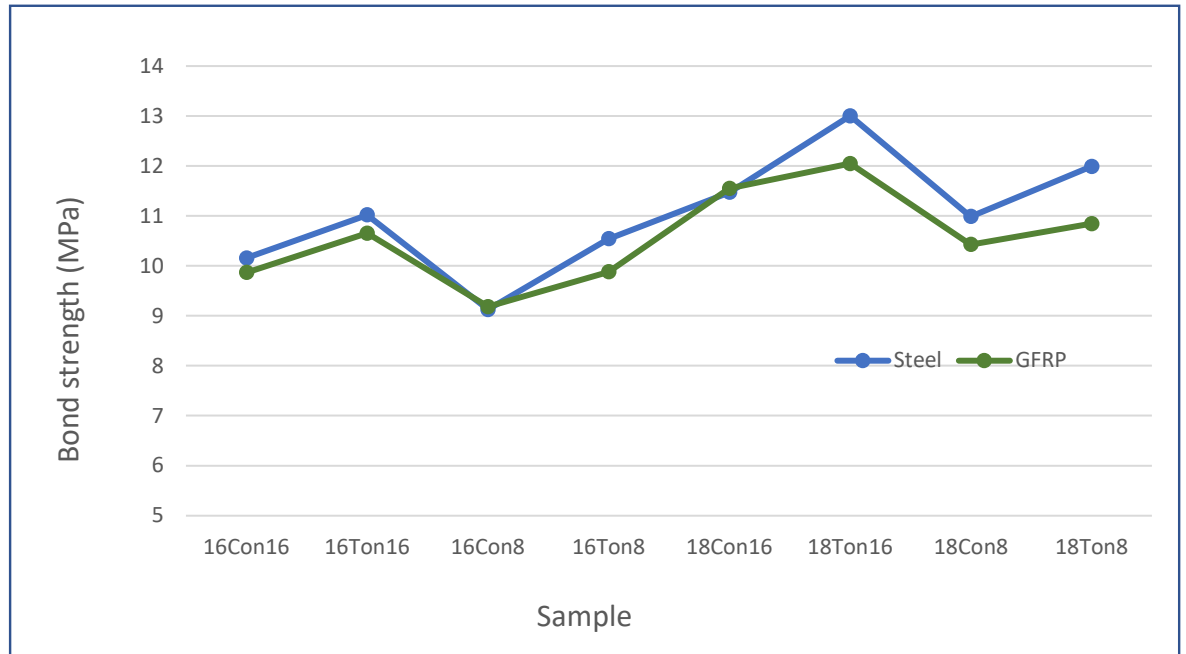


Figure 4-25: Effect of bar material on bond strength

There is more than one developed theory of concrete embedded reinforcing bar bond strength. The theoretical bond strengths of the embedded reinforcing bar in concrete are produced based on comparison with experimental test results and make it aspects for bond behaviour properties for bond strength predictions. The existing theoretical bond strength expressions have developed theoretical bond strength based on regression analysis. The developed theories of embedded reinforcing bar bond strength are:

ACI Committee,  
(2002) for steel rebar

$$\tau = 20.23 \frac{\sqrt{f'c}}{d_b}$$

Equation 4-15

Pour *et al.*, (2016) for  
FRP rebar

$$\tau = 14.7 \frac{\sqrt{f'c}}{d_b}$$

Equation 4-16

Yalciner *et al.*, (2012)  
for steel rebar

$$\tau = -2.7143 + 0.3621f'c + 2.3296 \frac{c}{d_b}$$

Equation 4-17

Quayyum and Rteil, (2012) for FRP rebar

$$\tau = 0.083 (f'c)^{0.5} \left( 1.2 + \frac{c_{min}}{d_b} \left( 0.92 + 0.08 \frac{c_{max}}{c_{min}} \right) + 75 \frac{c_{min}}{d_b} \right)$$

*Equation 4-18*

Bilek *et al.*, (2017) for steel rebar

$$\tau = 0.083 \sqrt{f'c} \left( 1.2 + 3 \frac{c_{min}}{d_b} + 50 \frac{d_b}{l_d} \right)$$

*Equation 4-19*

Where:

$f'c$  Concrete compressive strength, MPa

$d_b$  Bar diameter, mm

$l_d$  Embedded length of the reinforcing bar, mm

$c_{max}, c_{min}$  Maximum and minimum concrete cover, mm

ACI Committee (2002), expressed that the bond strength is influenced by the effects of concrete strength, bar diameter, embedded length. However, Quayyum and Rteil, (2012) added the ratio between the maximum and minimum concrete cover as shown in Equation 4-18. From the experimental programme results, bond strength can be defined as the change of stresses in the reinforcing bar with bar length and can be determined by dividing the pull-out force with the reinforcing bar area embedded in concrete as illustrated in Figure 4-20.

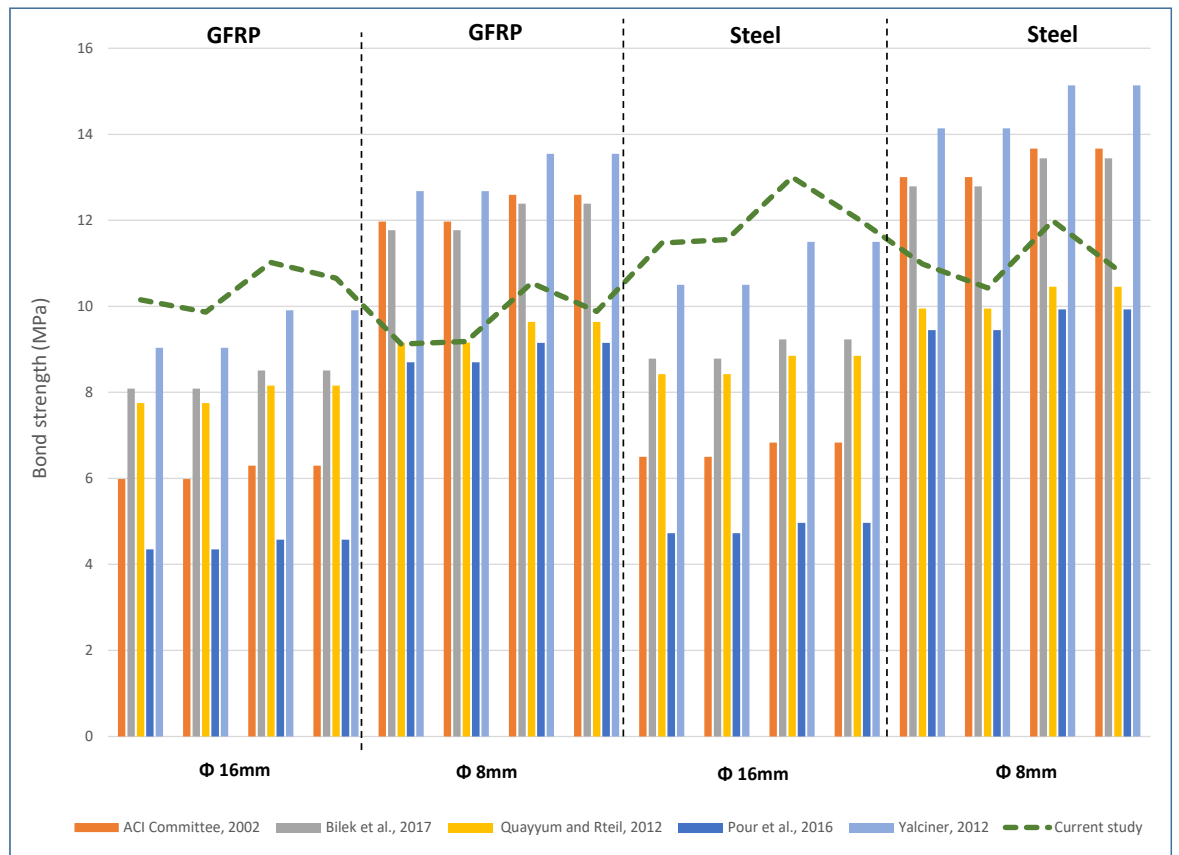


Figure 4-26: Experimental and theoretical bond strength for steel and GFRP bars

The theoretical equation adopted by ACI and previous researchers produced varying results, as illustrated in Figure 4-26. It can be seen that the equation provide underestimation for the larger diameter bars. The ACI Committee (2002), Pour *et al.*, (2016) and Yalciner *et al.*, (2012) adopted equations that consider only the concrete strength and bar diameter but no account for concrete cover thickness. Three of the equations consider concrete cover thickness: Quayyum and Rteil, (2012), Bilek *et al.*, (2017) and Yalciner *et al.*, (2012). Yalciner *et al.*, (2012) formula highly agreed with the current study in 16 mm bars bond strength but provides overestimation bond strength, especially with 8 mm bars size. Table 4-6 summarize the foamed concrete- steel/GFRP bond behaviour testing results.

Table 4-6: Bond behaviour from Pull-out test

Bar diameter $d_s$ mm	Specimen	Embedment length mm	Pull-out load (KN)	Experimental bond strength (MPa)	Compressive strength (MPa)	Mode of failure
16	16Con16St	80	40.81	10.15	27.56	Pull-through
16	16Con16GRP	80	39.66	9.87	29.03	Pull-through
16	16Ton16St	80	44.28	11.02	33.54	Splitting
16	16Ton16GRP	80	42.81	10.65	31.96	Pull-through
8	16Con8St	40	9.17	9.12	29.09	Pull-through
8	16Con8GRP	40	9.23	9.18	29.26	Pull-through
8	16Ton8St	40	10.59	10.54	32.02	Pull-through
8	16Ton8GRP	40	9.93	9.88	33.86	Pull-through
16	18Con16St	80	46.10	11.47	34.66	Splitting
16	18Con16GRP	80	46.42	11.55	33.96	Splitting
16	18Ton16St	80	54.86	13.64	36.25	Pull-through
16	18Ton16GRP	80	48.41	12.04	36.01	Pull-through
8	18Con8St	40	11.04	10.99	34.75	Splitting
8	18Con8GRP	40	10.48	10.43	35.07	Pull-through
8	18Ton8St	40	12.05	11.99	36.75	Pull-through
8	18Ton8GRP	40	10.89	10.84	35.89	Pull-through

#### 4.4 Summary

The FC properties are more independently follow its density, the type of additives they consist of. Subsequently, the stress-strain relationship is different for FC mixes based on either the density or the additive materials used. The 18Ton mix showed a strain in the maximum stress of 0.0045. The utilisation of additives Waste Toner, Metakaolin and silica fume improve the compressive strength of the FC at all densities. Waste Toner improved the concrete mechanical properties where the compressive strength exceeds the minimum strength of  $25 \text{ N/mm}^2$  required for structural applications. Waste Toner contains 15% of silicon dioxide ( $\text{SiO}_2$ ) which might be the main reason behind enhancing the FC mechanical properties. According to Zhuang and Chen, (2019), silicon dioxide improves the mechanical properties of concrete including bending and tensile strength.

The bond performance between foamed concrete and steel and GFRP reinforcing bar depends on the manufacturing process, design, and environmental conditions as well as the mechanical properties of the concrete and the bar itself. A number of experimental investigations have been done for the bond behaviour of GFRP reinforcing bars.

To investigate the bond behaviour of steel/GFRP with foamed concrete two tests were carried out: Pull-out test and beam test. The investigations covered the effect of concrete density, additive, bar size and bar material on the bond strength between steel/GFRP bars and foamed concrete.

- It was found that GFRP bars have 95% of the steel bond with FC and bond failure occurred partly on the surface between concrete and resin and partly near the surface between resin and glass fibres.
- The bond strength of steel/GFRP bars tended to increase when the compressive strength of concrete increased.

Table 4-7 shows a summary of the main FC mechanical properties testing outcomes.

Table 4-7: Summary of the main FC mechanical properties testing outcomes.

Foamed concrete testing	Main outcomes
Compressive strength	FC with Toner with density between 1600-1800 kg/m <sup>3</sup> can reach 28 MPa, which is suitable to be used in Structural applications.
Flexural Strength (Modulus of Rupture)	Toner increases the flexural strength by an average of about 10% but Mk and SF increase the strength by 5 and 3% only.
Splitting Tensile Strength	Splitting tensile strength is positively proportional to the density of FC mixes. It reached 4.6 MPa
Direct Tensile Strength	Direct tensile strength of concrete is lower than the indirect tensile strength of FC.
Stress-Strain Relationship and Modulus of Elasticity	The reduction of foamed concrete density leads to a decrease of its compressive strength and an increase in the strain at the maximum stress, which greatly reduces the modulus of elasticity.
Bond Behaviour from Pull-out and Beam Tests	the bond strength is positively proportional to the density of FC mixes.  GFRP bond performance with foamed concrete was found to be 95% of steel bond strength with FC

## Chapter 5

# Flexural Behaviour of GFRP Reinforced Foamed Concrete Beams

### 5.1 Introduction

This chapter covers an experimental programme and numerical analysis which were developed to investigate the flexural behaviour of steel/GFRP reinforced concrete beams. Four reinforced beam models include: normal concrete beam reinforced with steel bars, foamed concrete beam reinforced with steel bars, a normal concrete beam reinforced with GFRP bars and foamed concrete beam reinforced with GFRP bars. The beams are being examined experimentally and numerally regarding flexural behaviour.

In the past years, there have been many different methods developed to study the structural response of concrete members reinforced with FRP bars. Experiments have been widely used to study and analyse different members of concrete structures and their response under loading. This part is built up by introducing a full-scale beam flexure test followed by theoretical derivations for concrete beam sections under flexural loading. The geometrical and strength parameters needed for the analysis are included, and afterwards, the assumptions that needed to be considered in order to perform the analytical calculation are presented as well as the steps of the analysis leading to the expected results.

### 5.2 Full-scale Beam Flexural Testing

#### 5.2.1 Materials Properties

Four beams were constructed using cast in situ, normal weight concrete and foamed concrete with a target compressive strength of 35 MPa at 28 days. Three 100 x 100 x 100 mm cubes and three 150 mm diameter 300 mm high cylinders were made to determine the average values of compressive strength and tensile strength. After concrete casting, all specimens were covered with polyethene sheets to keep down moisture loss at all times during the period of curing and stored in the laboratory under the same condition for 28 days, see Figure 5-1 and Figure 5-2.

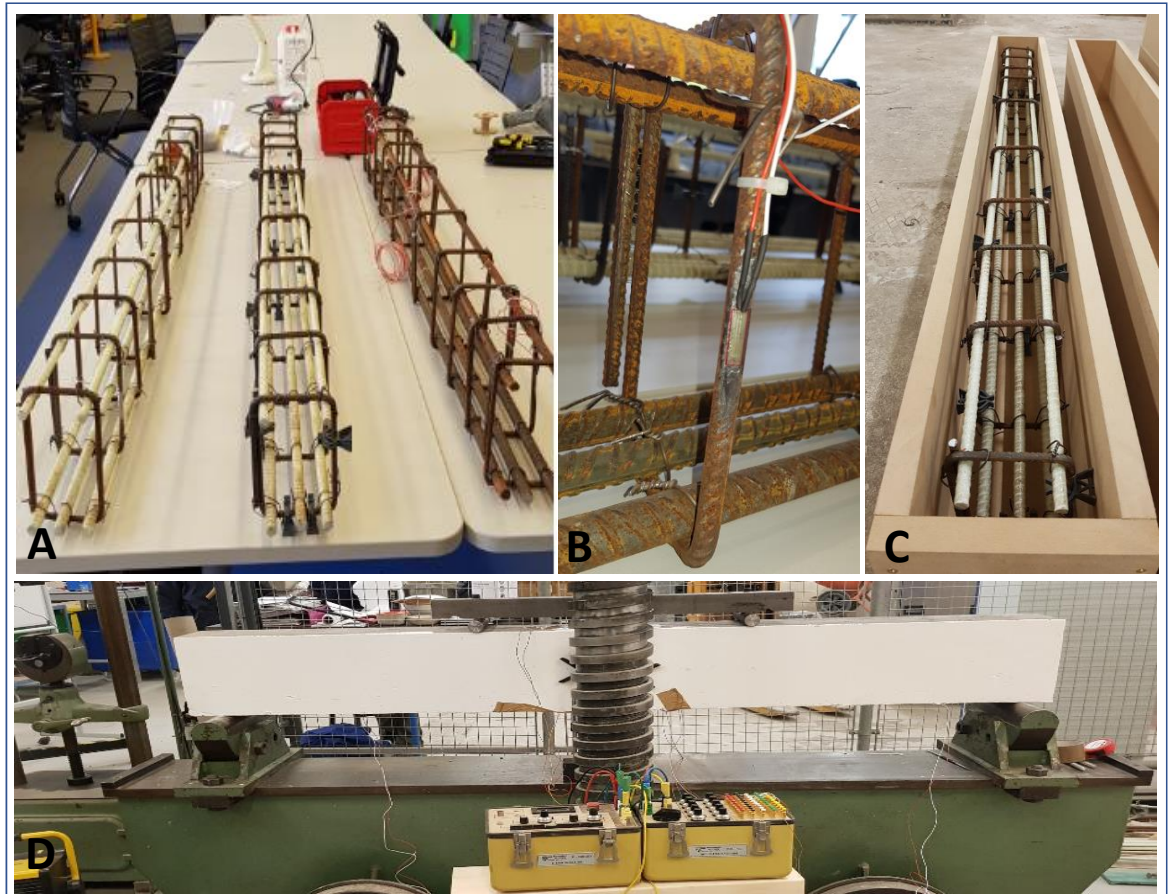


Figure 5-1: Full scale beams flexure test preparations (A) GFRP and steel reinforcement (B) Strain gage on reinforcement (C) Beams ready for casting (D) Concrete beam testing

The GFRP bars used in this investigation are manufactured in the UK by ENGINEERED COMPOSITES LTD, the technical data of the bars are available in Appendix B. Table 5-1 illustrates the mechanical properties of GFRP and steel reinforcing bar.

Table 5-1: The mechanical properties of GFRP and Steel reinforcing bar (Abbood et al., 2021)

Type of bars	Bar diameter: (mm)	Modulus of elasticity (GPa)	Ultimate tensile strength (MPa)	Ultimate strain	Yield strength (MPa)
Steel	10-16	210	645	0.005	500
GFRP	10	60	1200	0.02	N/A
GFRP	16	60	1200	0.02	N/A

### 5.2.2 Test Specimens and Preparations

Four simply supported beams were tested in flexure. All beams tested were 220 mm in depth and 150 mm in width and span of 2000 mm as shown in Figure 5-3. The beams are: Normal concrete reinforced with steel (NC+S), foamed concrete reinforced with steel (FC+S), normal concrete reinforced with GFRP (NC+GFRP) and foamed concrete reinforced with GFRP (FC+GFRP). Plywood forms were made with dimensions of 2000 x 220 x 150 mm to accommodate the required reinforcement cages. After cleaning and brushing all internal sides with oil, the reinforcement cages were placed inside the forms.

The reinforcement cage rested on transverse rods to maintain a 20 mm concrete cover. Each of the four beams was cast together with 3 cubes and 3 cylinders each to determine the concrete characteristics. In the laboratory environmental conditions, the beams were stored and covered with a plastic sheet for 28 days. Before testing, the beams were painted white to trace the crack patterns during testing as shown in Figure 5-2.

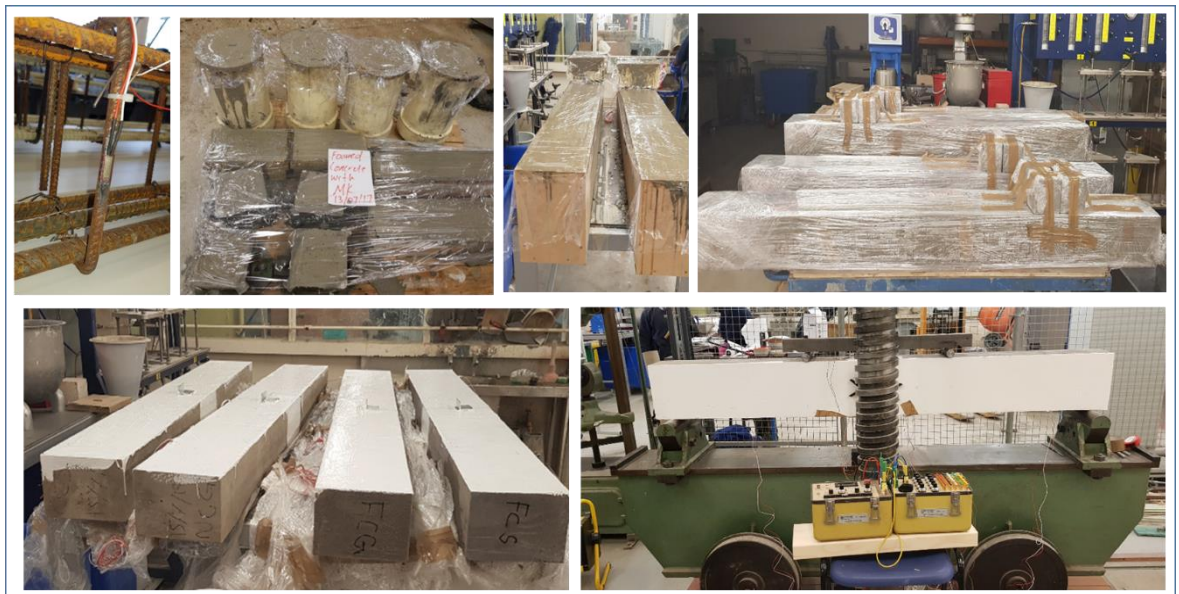


Figure 5-2: Full-scale beams casting, curing and testing

### 5.2.3 Beam Properties and Assumptions

All beams have the same dimensions 150 x 200 x 2000 mm length, depth and width respectively. The beams materials strength, geometry and stiffness parameters are presented in Table 5-2. The materials properties including normal/foamed concrete and

the steel/GFRP reinforcement of the beam are selected by taking into account the EC2 requirements and limitations.

Table 5-2: Beam materials properties

Property	Normal concrete	Foamed concrete	Steel	GFRP
Ultimate strength (MPa)	37	37	600	1200
Modulus of elasticity (MPa)	28000	16000	200000	60000
Ultimate compressive strain	0.0035	0.0045	0.005	0.02
Concrete cover (mm)	25	20	-	-

The beam model is shown in Figure 5-3. It is a simply supported beam subjected to four points loading. Two LVDT gauges fitted on both sides to measure the mid-span deflections of each beam, also six strain gauges of 10 mm-long ESGs were placed on the extreme concrete compression and tension fibre and the tension and shear reinforcements as shown in Figure 5-3.

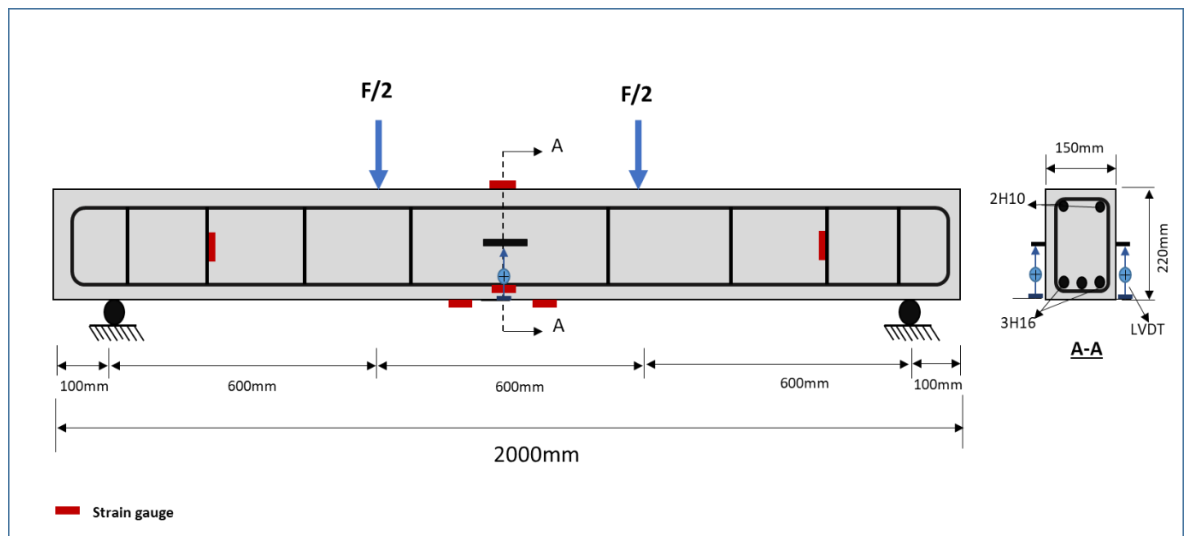


Figure 5-3: Full-scale beam model under four-point load test

### 5.3 Theoretical Derivations of Reinforced Concrete Beam

In all of the failure theories that have been presented as yet, a typical stress-strain diagram has been assumed for concrete in compression. There is no single curve is typical of all concrete even up to the maximum stress developed. It is worthwhile mentioning that, up

to the maximum developed stress, the higher strength concretes show a more nearly linear stress-strain relationship. However, concrete with lower strength shows a relationship that looks like a second-degree parabola.

For the theoretical derivations, the parabolic rectangular stress block in the EC2 for the ultimate strength design calculations is adopted in this study.

The analysis of a cross-section at the ultimate limit state is based on the following assumptions:

- 1- The plane section before deformation remains plane after deformation. This implies that the strain in concrete and reinforcement are linearly proportional to the perpendicular distance from the neutral axis.
- 2- The compression stress in the concrete is derived from the idealized parabolic-rectangular design stress block shown in Figure 5-8.
- 3- The ultimate limit state of collapse is reached when the concrete strain at the extreme compression fibre reached a value of 0.0035 for normal weight concrete and 0.0045 for foamed concrete.
- 4- The tensile strength of concrete is neglected.
- 5- The stress in the reinforcement is derived from the idealized stress-strain curve shown in Figure 5-6, with maximum stress of  $f_{yk} / 1.15$ .
- 6- Good bond exists between concrete and steel/GFRP.
- 7- Buckling does not occur before the ultimate load is attained.
- 8- The areas of concrete displaced by steel in compressions is small that it has not been taken into account.

### 5.3.1 Material Characteristics

The behaviour of reinforced concrete elements subject to axial force or bending moment is closely related to the stress-strain curve of the concrete and the reinforcement bars.

### 5.3.1.1 Concrete

The exact shape of a concrete stress-strain curve is dependent on the concrete strength. Figure 5-4 shows a typical stress-strain curve for short term loading of concrete. Up to one-third of the maximum stress, the curve is approximately straight, from that up to the maximum stress it is curved ascending, and beyond that, it is curved descending. The modulus of elasticity  $E_c$  of both NWC and FC increase with an increase in the compressive strength of concrete.

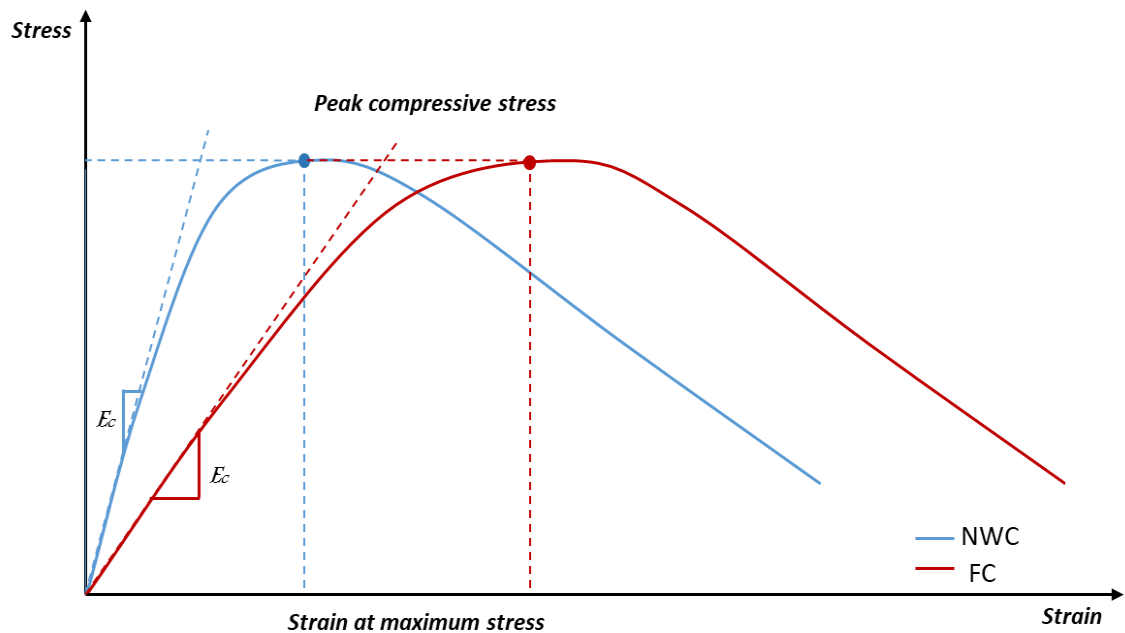


Figure 5-4: Typical short-term stress-strain curve for concrete

For design purposes, EC2 prefers the utilization of an idealized stress-strain curve of parabolic-rectangular shape given in Figure 5-5. As shown in Figure 5-5 the maximum ultimate concrete compressive strain  $\epsilon_{cu}$  is 0.0035 for normal weight concrete and 0.0045 for foamed concrete. However, the EC2 suggested other idealized stress-strain diagrams (bi-linear and simplified diagrams), they are effectively equivalent to the parabolic-rectangular diagram, with regards to the shape of the compression zone in the cross-section.

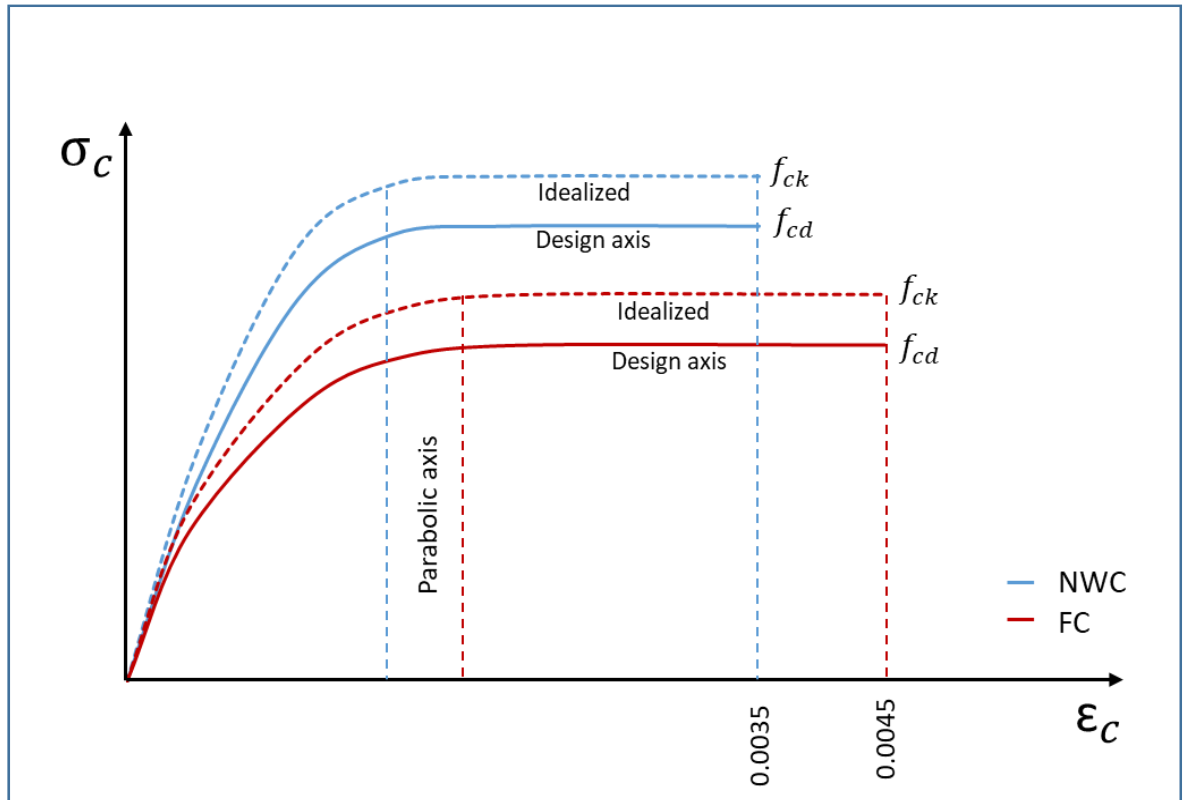


Figure 5-5 Parabolic –rectangular stress-strain diagram for concrete in compression as per EC2.

According to EC2, the compressive strength of concrete is denoted by concrete strength classes which relate to the characteristic (5%) cylinder strength  $f_{ck}$  or cube strength  $f_{ck\ cube}$  in accordance with BS EN 206-1. The strength classes for concrete are presented in the table below.

Table 5-3: The concrete characteristic strength classes (Eurocode 2, 2004)

$f_{ck}$ (N/mm <sup>2</sup> )	12	16	20	25	30	35	40	45	50
$f_{ck\ cube}$ (N/mm <sup>2</sup> )	15	20	25	30	37	45	50	55	60

Where:

- $f_{ck}$  Characteristic compressive cylinder strength of concrete at 28 days.
- $f_{ck\ cube}$  Corresponding characteristic cube strength. The value of the design compressive strength is defined as:

$$f_{cd} = \alpha_{cc} \frac{f_{ck}}{\gamma_c}$$

Where:

$\gamma_c$  Safety factor for concrete at the Ultimate Limit State, for persistent and transient design situations,  $\gamma_c = 1.5$  irrespective of the action whether it is an axial force, shear, bending or bearing as stated in EC2.

$\alpha_{cc}$  Coefficient taking into account the long-term effects on compressive strength and of unfavourable effects resulting from the way the load is applied. The value of  $\alpha_{cc}$  should lie between 0.8 and 1.0.

It should be noted that higher concrete strength shows more brittle behaviour, reflected by shorter horizontal branches, as will be shown in the stress-strain relationships, later.

### 5.3.1.2 Reinforcing Steel

The behaviour of the steel is identical in tension and compression, being linear in the elastic range up to the design yield stress of  $f_{yd}$  for design purposes, EC2 recommends the use of an idealized bi-linear diagram shown in Figure 5-6. This diagram is valid for temperatures no more than 200°C. The EC2 assumes a mean value of 200 kN/mm<sup>2</sup> for the modulus of elasticity of the reinforcing steel  $E_s$  to be used in the design. The design strength of the reinforcing steel is derived from the idealized characteristic strength by dividing it by the partial safety factor  $\gamma_s$  which is equal to 1.15.

The present study assumes that the reinforcing steel will be applied to the BS EN 1993, EC2 and that the grades is be 500 N/mm<sup>2</sup> for high yield steel (hot rolled or cold worked).

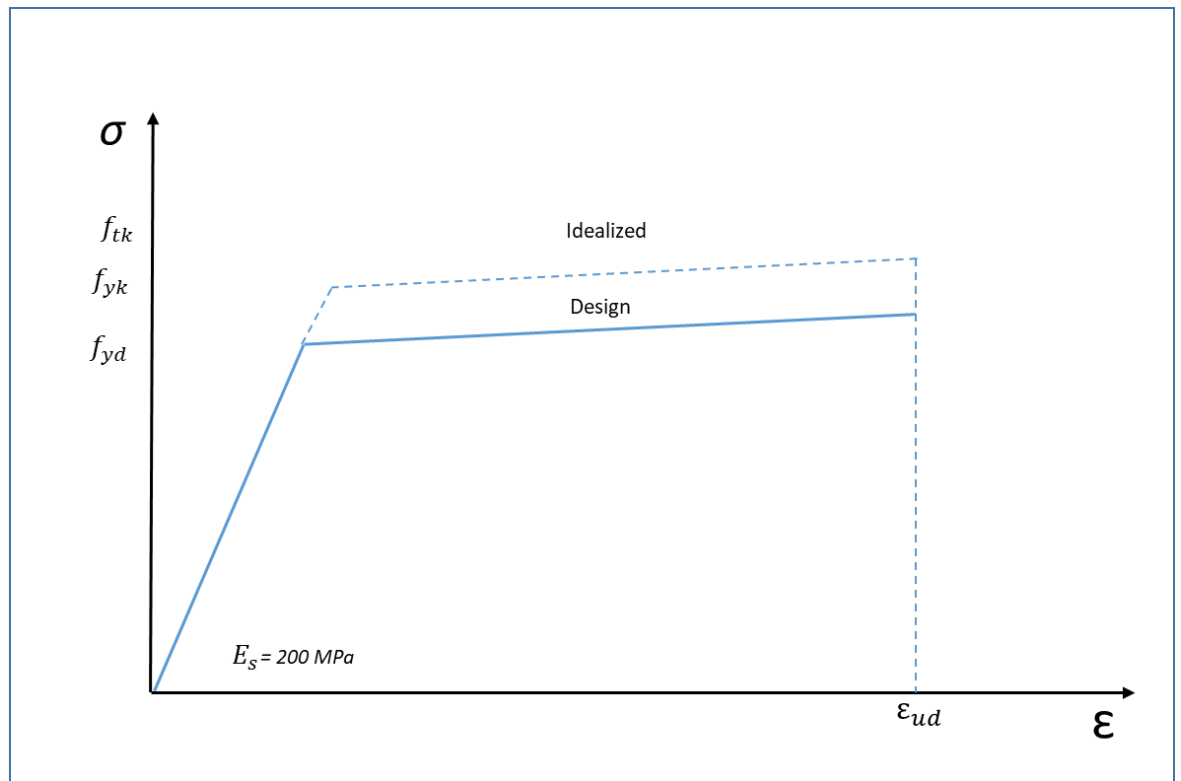


Figure 5-6 Design stress-strain diagram for reinforcing steel

### 5.3.1.3 Reinforcing GFRP

It is generally accepted that the basic principles of section analysis could be applied in GFRP reinforced RC elements. Plane sections are expected to remain plane and no significant bond-slip occur. According to Junaid et al., (2019) for flexural resistance, the amount of GFRP reinforcement required depends on the stiffness and strength of the composite material. The GFRP strength to stiffness ratio is greater than that of steel and this has a significant impact on the distribution of stresses along the section. Figure 5-7 illustrates the design stress-strain diagram for reinforcing steel and GFRP.

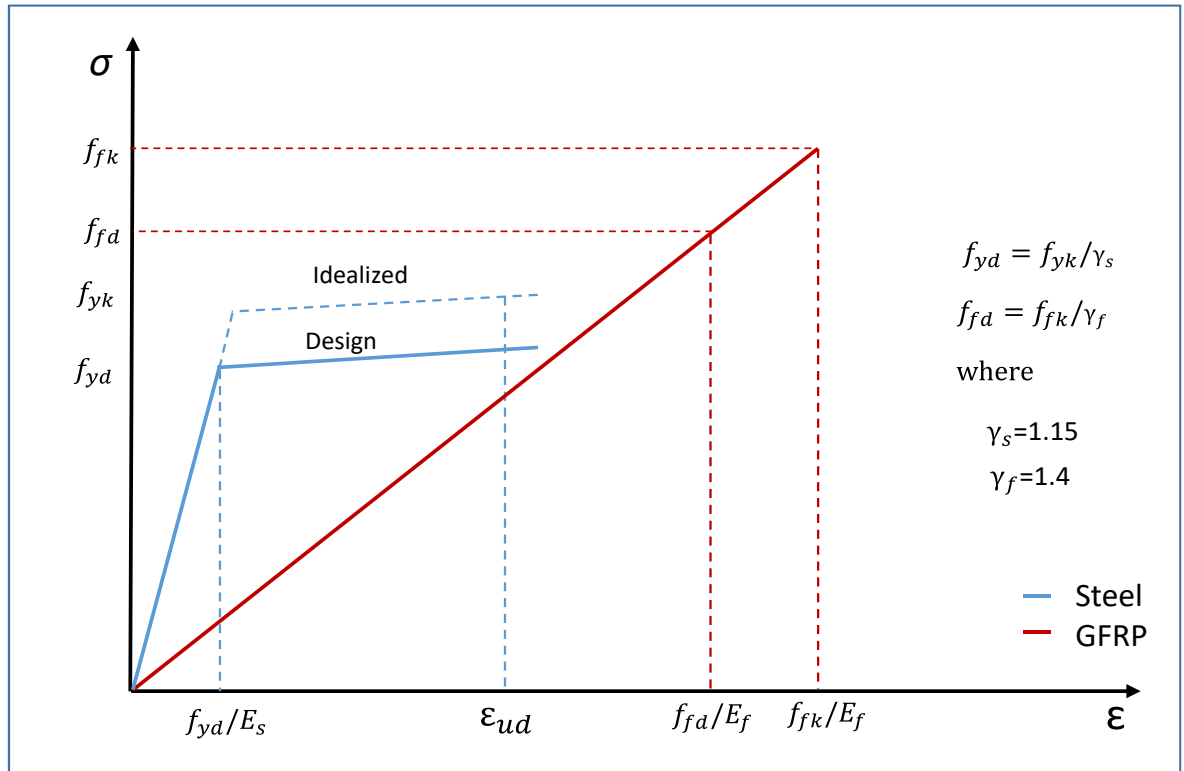


Figure 5-7 Design stress-strain diagram for reinforcing steel and GFRP

Once concrete cracked under loading, the position of the neutral axis in a cross-section of a reinforced concrete beam gradually moves upwards with the increase of loading, which is attributed to the nonlinear material properties of concrete and reinforcing bars. The parabolic- rectangular stress blocks for rectangular beam sections for the ultimate strength design for the four beams are presented below.

### 5.3.2 Normal Concrete Beam Reinforced with Steel (NC+S)

The parabolic-rectangular stress block adopted by EC2 for the ultimate strength of normal weight concrete design calculations is presented in Figure 5-8.

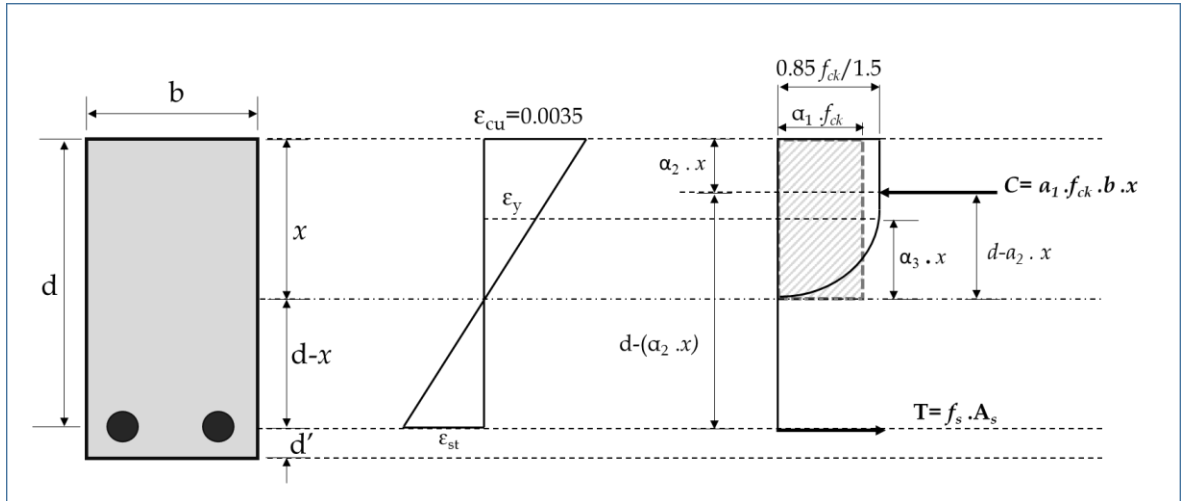


Figure 5-8 Parabolic-rectangular design stress block for the ultimate limit state- EC2 (Normal concrete reinforced with steel)

The strain at the interface between the parabolic and linear partitions of the curve  $\varepsilon_0$  are 0.002 and the maximum stress is  $\alpha \cdot f_{cd}$ .

Where:

$\alpha$  Coefficient taking into account long term effects on the compressive strength and of unfavourable effects resulting from the way the load is applied.

$f_{cd}$  Concrete design compression strength based on the cylinder test.

$f_{ck}$  Concrete characteristic compressive strength based on the cylinder test.

$\alpha_3$  Ratio of the distance between  $\varepsilon_0 = 0.002$  and the neutral axis to the depth of the neutral axis. Therefore, it might be obtained from the strain diagram as follows:

$$\alpha_3 = \frac{x_0}{x} = \frac{\varepsilon_0}{\varepsilon_{cu}} \quad \text{Equation 5-1}$$

$$\alpha_3 = \frac{0.002}{0.0035} = 0.5714$$

$\alpha_2$  Ratio of the depth of the neutral axis to the centroid of the stress block from the compression face depth.

$\alpha_1$  Ratio of the average of characteristic compressive strength of concrete  $f_{ck}$  to the average compressive stress.

Then the  $\alpha_1$  ratio can be obtained by considering the volume of the concrete stress block of uniform width  $b$ .

Where the volume of parabolic rectangular stress block is:

$$V \text{ of parabolic rectangular} = \frac{0.85 f_{ck} \cdot b \cdot x}{1.5} - \frac{0.334 \cdot 0.85 f_{ck} \cdot b \cdot (0.5714 x)}{1.5}$$

$$V \text{ of parabolic rectangular} = 0.4587 \cdot f_{ck} \cdot b \cdot x \quad \text{Equation 5-2}$$

The volume of an equivalent rectangular stress block is:

$$V \text{ of equivalent rectangular} = \alpha_1 \cdot f_{ck} \cdot b \cdot x$$

Since the two volumes are equal then

$$\alpha_1 = 0.4587$$

The  $\alpha_2$  ratio is determined by finding the centroid of resultant force by taking a moment of the area about the extreme compression fibre.

$$\alpha_2 \cdot x = \frac{V \cdot x}{V} \quad \text{Equation 5-3}$$

Where

$$V \cdot x = \frac{0.5667 f_{ck} \cdot b \cdot x \cdot x}{2} - 1.079 f_{ck} \cdot b \cdot x \cdot \frac{x - 0.5714 x}{4}$$

$$V \cdot x = 0.1908 \cdot f_{ck} \cdot b \cdot x^2$$

Therefore

$$\alpha_2 \cdot x = \frac{0.1908 f_{ck} \cdot b \cdot x^2}{0.4587 f_{ck} \cdot b \cdot x}$$

$$\alpha_2 = 0.416$$

It seems that these dimensionless factors  $\alpha_1$  and  $\alpha_2$  are independent of concrete compressive strength  $f_{ck}$ .

To calculate the distance from the natural axis to the extreme compression fibre ( $x$ ).

From the strain block of the beam section.

$$\frac{\epsilon_{cu}}{x} = \frac{\epsilon_s}{(d - x)} \quad \text{Equation 5-4}$$

$$\varepsilon_s = \varepsilon_{cu} \frac{(d - x)}{x}$$

$$f_s = E_s \cdot \varepsilon_s = \frac{(d-x)}{x} \cdot \varepsilon_{cu} \cdot E_s \leq f_y \quad \text{Equation 5-5}$$

As the section is in equilibrium, then:

$$C_C = T$$

or

$$\alpha_1 \cdot f_{ck} \cdot b \cdot x = f_s \cdot A_s$$

Then

$$\alpha_1 \cdot f_{ck} \cdot b \cdot x = \frac{(d - x)}{x} \cdot \varepsilon_{cu} \cdot E_s \cdot A_s$$

$$\alpha_1 \cdot f_{ck} \cdot b \cdot x^2 + \varepsilon_{cu} \cdot E_s \cdot A_s \cdot x - \varepsilon_{cu} \cdot E_s \cdot A_s \cdot d = 0 \quad \text{Equation 5-6}$$

The equation is quadratic and can be solved using the quadratic formula for the roots of the general quadratic equation as below:

$$x = \frac{-b \pm \sqrt{b^2 - 4ac}}{2a} \quad \text{Equation 5-7}$$

Using fundamental principles of compatibility of strain, material stress-strain relationship and equilibrium equations a relationship between ultimate moment resistance and the moment of reinforcement can be constructed.

A balance section is defined as one in which the strain at the extreme concrete compression fibre reached the maximum (0.0035 for normal concrete) simultaneously with the tension steel reaching a strain of  $\varepsilon_y$ . Therefore, the amount of steel ratio  $\rho$  is:

$$\rho_{bal} = \frac{A_{s\ bal}}{b \cdot d}$$

Which can be determined as follows:

From the strain diagram at balance,

$$\frac{x}{d} = \varepsilon_{cu} / (\varepsilon_{cu} + \varepsilon_y) \quad \text{Equation 5-8}$$

From stress-strain of the reinforcement,

$$\varepsilon_y = \frac{f_{yk}}{1.15} \cdot E_s \quad \text{Equation 5-9}$$

Substitute Equation 5-9 into Equation 5-8, gives:

$$\frac{x}{d} = \varepsilon_{cu} \cdot E_s / (\varepsilon_{cu} \cdot E_s) + 0.87 f_{yk} \quad \text{Equation 5-10}$$

The compression force in concrete  $C_C$  above the neutral axis is given by:

$$C_C = \text{stress} \times \text{area}$$

$$C_C = \alpha_1 \cdot f_{ck} \cdot b \cdot x$$

$$C_C = 0.4587 f_{ck} \cdot b \cdot x$$

The tension force in the reinforcing bar at balance T is:

$$T = \text{stress} \times \text{area}$$

$$T = \frac{A_{s \text{ bal}} \cdot f_{yk}}{1.15}$$

As the section is in equilibrium, then:

$$C_C = T$$

or

$$0.4587 f_{ck} \cdot b \cdot x = \frac{A_{s \text{ bal}} \cdot f_{yk}}{1.15}$$

$$A_{s \text{ bal}} = \frac{0.5275 f_{ck} \cdot b \cdot x}{f_{yk}} \quad \text{Equation 5-11}$$

Substituting Equation 5-10 into Equation 5-11 and rearranging the terms results in:

$$A_{s \text{ bal}} = \frac{0.5275 f_{ck} \cdot b \cdot \varepsilon_{cu} \cdot E_s \cdot d}{f_{yk} (\varepsilon_{cu} \cdot E_s + 0.87 f_{yk})} \quad \text{Equation 5-12}$$

Then  $\rho_{bal}$  will be:

$$\rho_{bal} = \frac{0.5275 f_{ck} \cdot \varepsilon_{cu} \cdot E_s}{f_{yk} (\varepsilon_{cu} \cdot E_s + 0.87 f_{yk})} \quad \text{Equation 5-13}$$

If the reinforcement ratio  $\rho$  is below  $\rho_{bal}$ , the steel will yield before concrete crushes in compression. Such a beam is known to be under-reinforced, and the ultimate moment of resistance can be expressed as:

Ultimate moment = T. lever arm

or

$$M = 0.87 f_{yk} \cdot A_s (d - \alpha_2 \cdot x) \quad \text{Equation 5-14}$$

For equilibrium equation.

$$\frac{x}{d} = \frac{0.87 f_{yk} \cdot \rho}{\alpha_2 \cdot f_{yk}} \quad \text{Equation 5-15}$$

For  $\rho$  greater than  $\rho_{bal}$ , the concrete fails by compression before steel reaches the yield point. The beam is known as an over-reinforced beam.

From strain compatibility.

$$\frac{x}{d} = \varepsilon_{cu} / (\varepsilon_{cu} + \varepsilon_s)$$

And from the stress-strain relationship of reinforcing bar,

$$f_s = \varepsilon_s \cdot E_s$$

Replace  $0.87 f_{yk}$  by  $f_s$  in Equation 5-15 and substitute Equation 5-13 and Equation 5-14 into Equation 5-15 results in:

$$\frac{x}{d} = \frac{\varepsilon_{cu} \cdot f_{yk}}{(\varepsilon_{cu} \cdot f_{yk} + \alpha_1 \left(\frac{x}{d}\right) \cdot f_{ck} / \rho)}$$

Or

$$\alpha_1 \left(\frac{f_{ck}}{\rho}\right) \cdot \left(\frac{x}{d}\right)^2 + \varepsilon_{cu} \cdot f_{yk} \cdot \left(\frac{x}{d}\right) - (\varepsilon_{cu} \cdot f_{yk}) = 0$$

The ultimate moment of resistance can then be obtained by taking moment of tension steel.

$$M = \alpha_1 \cdot f_{ck} \cdot b \cdot x \cdot (d - \alpha_2 \cdot x) \quad \text{Equation 5-16}$$

### 5.3.3 Foamed concrete beam reinforced with steel (FC+S)

The parabolic-rectangular stress block adopted by EC2 for the ultimate strength design calculations is presented in Figure 5-9.

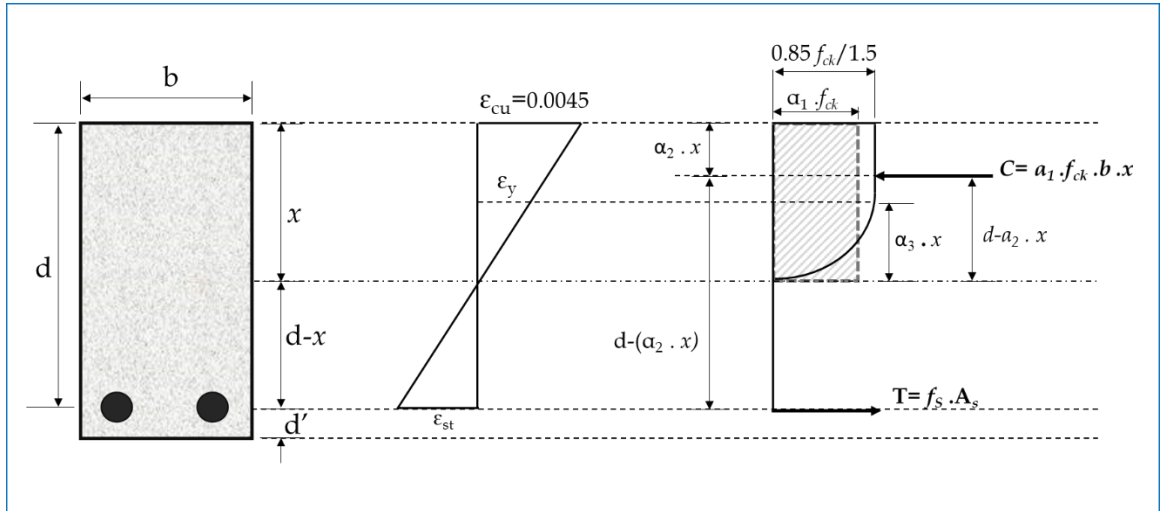


Figure 5-9: Parabolic-rectangular design stress block for the ultimate limit state- EC2 (Foamed concrete reinforced with steel)

$$\alpha_3 = \frac{0.002}{0.0045} = 0.444$$

Where the volume of parabolic rectangular stress block is:

$$V \text{ of parabolic rectangular} = \frac{0.85 f_{ck} \cdot b \cdot x}{1.5} - \frac{0.334 \cdot 0.85 f_{ck} \cdot b \cdot (0.444 x)}{1.5}$$

$$V \text{ of parabolic rectangular} = 0.4827 \cdot f_{ck} \cdot b \cdot x \quad \text{Equation 5-17}$$

The volume of an equivalent rectangular stress block is:

$$V \text{ of equivalent rectangular} = \alpha_1 \cdot f_{ck} \cdot b \cdot x$$

Since the two volumes are equal then

$$\alpha_1 = 0.4827$$

The  $\alpha_2$  the ratio is determined by finding the centroid of resultant force by taking a moment of the area about the extreme compression fibre.

$$\alpha_2 \cdot x = \frac{V \cdot x}{V} \quad \text{Equation 5-18}$$

Where

$$V \cdot x = \frac{0.5667 f_{ck} \cdot b \cdot x \cdot x}{2} - 1.079 f_{ck} \cdot b \cdot x \cdot \frac{x - 0.4444 x}{4}$$

$$V \cdot x = 0.2087 \cdot f_{ck} \cdot b \cdot x^2$$

Therefore

$$\alpha_2 \cdot x = \frac{0.2087 f_{ck} \cdot b \cdot x^2}{0.4827 f_{ck} \cdot b \cdot x}$$

$$\alpha_2 = 0.4324$$

It seems that these dimensionless factors  $\alpha_1$  and  $\alpha_2$  are independent of concrete compressive strength  $f_{ck}$ .

To calculate the distance from the natural axis to the extreme compression fibre ( $x$ ).

From the strain block of the beam section.

$$\frac{\epsilon_{cu}}{x} = \frac{\epsilon_s}{(d - x)} \quad \text{Equation 5-19}$$

$$\epsilon_s = \epsilon_{cu} \frac{(d - x)}{x}$$

$$f_s = E_s \cdot \epsilon_s = \frac{(d-x)}{x} \cdot \epsilon_{cu} \cdot E_s \leq f_y \quad \text{Equation 5-20}$$

As the section is in equilibrium, then:

$$C_C = T$$

or

$$\alpha_1 \cdot f_{ck} \cdot b \cdot x = f_s \cdot A_s$$

Then

$$\alpha_1 \cdot f_{ck} \cdot b \cdot x = \frac{(d - x)}{x} \cdot \epsilon_{cu} \cdot E_s \cdot A_s$$

$$\alpha_1 \cdot f_{ck} \cdot b \cdot x^2 + \epsilon_{cu} \cdot E_s \cdot A_s \cdot x - \epsilon_{cu} \cdot E_s \cdot A_s \cdot d = 0 \quad \text{Equation 5-21}$$

The equation is quadratic and can be solved using the quadratic formula for the roots of the general quadratic equation as below:

$$x = \frac{-b \pm \sqrt{b^2 - 4ac}}{2a} \quad \text{Equation 5-22}$$

Using fundamental principles of compatibility of strain, material stress-strain relationship and equilibrium equations a relationship between ultimate moment resistance and the moment of reinforcement can be constructed.

A balance section is defined as one in which the strain at the extreme concrete compression fibre reached the maximum (0.0045 for Foamed concrete) simultaneously with the tension steel reaching a strain of  $\epsilon_y$ . Therefore, the amount of steel ratio  $\rho$  is:

$$\rho_{bal} = \frac{A_{s\ bal}}{b \cdot d}$$

Which can be determined as follows:

From the strain diagram at balance,

$$\frac{x}{d} = \epsilon_{cu} / (\epsilon_{cu} + \epsilon_y) \quad \text{Equation 5-23}$$

From stress-strain of the reinforcement,

$$\epsilon_y = \frac{f_{yk}}{1.15} \cdot E_s \quad \text{Equation 5-24}$$

Substitute Equation 5-24 into Equation 5-23, gives:

$$\frac{x}{d} = \epsilon_{cu} \cdot E_s / (\epsilon_{cu} \cdot E_s) + 0.87 f_{yk}) \quad \text{Equation 5-25}$$

The compression force in concrete  $C_C$  above the neutral axis is given by:

$$C_C = \text{stress} \times \text{area}$$

$$C_C = \alpha_1 \cdot f_{ck} \cdot b \cdot x$$

$$C_C = 0.4827 f_{ck} \cdot b \cdot x$$

The tension force in the reinforcement bar at balance T is:

$$T = \text{stress} \times \text{area}$$

$$T = \frac{A_{s\ bal} \cdot f_{yk}}{1.15}$$

As the section is in equilibrium, then:

$$C_C = T$$

or

$$0.4827 f_{ck} \cdot b \cdot x = \frac{A_{s\ bal} \cdot f_{yk}}{1.15}$$

$$A_{s\ bal} = \frac{0.555 f_{ck} \cdot b \cdot x}{f_{yk}} \quad \text{Equation 5-26}$$

Substituting Equation 5-25 into Equation 5-26 and rearranging the terms results in:

$$A_{s\ bal} = \frac{0.555 f_{ck} \cdot b \cdot \epsilon_{cu} \cdot E_s \cdot d}{f_{yk} (\epsilon_{cu} \cdot E_s + 0.87 f_{yk})} \quad \text{Equation 5-27}$$

Then  $\rho_{bal}$  will be:

$$\rho_{bal} = \frac{0.555 f_{ck} \cdot \epsilon_{cu} \cdot E_s}{f_{yk} (\epsilon_{cu} \cdot E_s + 0.87 f_{yk})} \quad \text{Equation 5-28}$$

If the reinforcement ratio  $\rho$  is below  $\rho_{bal}$ , the steel will yield before concrete crushes in compression. Such a beam is known to be under-reinforced, and the ultimate moment of resistance can be expressed as:

Ultimate moment = T. lever arm

Or

$$M = 0.87 f_{yk} \cdot A_s (d - \alpha_2 \cdot x) \quad \text{Equation 5-29}$$

For equilibrium equation,

$$\frac{x}{d} = \frac{0.87 f_{yk} \cdot \rho}{\alpha_2 \cdot f_{yk}}$$

Equation 5-30

For  $\rho$  greater than  $\rho_{bal}$ , the concrete fails by compression before steel reaches the yield point. The beam is known as an over-reinforced beam.

From strain compatibility.

$$\frac{x}{d} = \varepsilon_{cu} / (\varepsilon_{cu} + \varepsilon_s)$$

From the stress-strain relationship of reinforcing bar:

$$f_s = \varepsilon_s \cdot E_s$$

Replace  $0.87 f_{yk}$  by  $f_s$  in Equation 5-30 and substitute Equation 5-28 and Equation 5-29 into Equation 5-30 results in:

$$\frac{x}{d} = \frac{\varepsilon_{cu} \cdot f_{yk}}{(\varepsilon_{cu} \cdot f_{yk} + \alpha_1 \left(\frac{x}{d}\right) \cdot f_{ck} / \rho)}$$

Or

$$\alpha_1 \left(\frac{f_{ck}}{\rho}\right) \cdot \left(\frac{x}{d}\right)^2 + \varepsilon_{cu} \cdot f_{yk} \cdot \left(\frac{x}{d}\right) - (\varepsilon_{cu} \cdot f_{yk}) = 0$$

The ultimate moment of resistance can then be obtained by taking moment about tension steel.

$$M = \alpha_1 \cdot f_{ck} \cdot b \cdot x \cdot (d - \alpha_2 \cdot x)$$

Equation 5-31

### 5.3.4 Normal Concrete Beam Reinforced with GFRP (NC+GFRP)

The parabolic-rectangular stress block adopted by EC2 for the ultimate strength design calculations is presented in Figure 5-10.

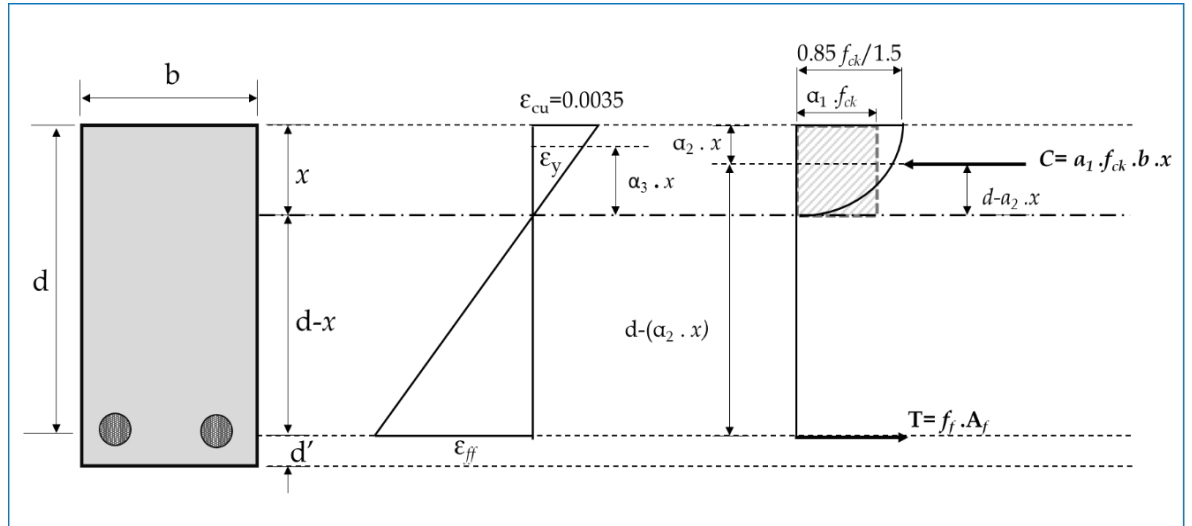


Figure 5-10: Parabolic-rectangular design stress block for the ultimate limit state- EC2 (Normal concrete reinforced with GFRP)

Values of  $\alpha_1$ ,  $\alpha_2$  and  $\alpha_3$  are the same for the case of normal concrete with steel reinforcement.

$$\alpha_3 = 0.5714$$

$$\alpha_1 = 0.4587$$

$$\alpha_2 = 0.416$$

It seems that these dimensionless factors  $\alpha_1$  and  $\alpha_2$  are independent of concrete compressive strength  $f_{ck}$ .

To calculate the distance from the natural axis to the extreme compression fibre ( $x$ ).

From the strain block of the beam section.

$$\frac{\epsilon_{cu}}{x} = \frac{\epsilon_f}{(d-x)}$$

Equation 5-32

$$\epsilon_f = \epsilon_{cu} \frac{(d-x)}{x}$$

$$f_f = E_f \cdot \epsilon_f = \frac{(d-x)}{x} \cdot \epsilon_{cu} \cdot E_f \leq f_{fk}$$

Equation 5-33

As the section is in equilibrium, then:

$$C_C = T$$

or

$$\alpha_1 \cdot f_{ck} \cdot b \cdot x = f_f \cdot A_f$$

Then

$$\alpha_1 \cdot f_{ck} \cdot b \cdot x = \frac{(d - x)}{x} \cdot \varepsilon_{cu} \cdot E_f \cdot A_f$$

$$\alpha_1 \cdot f_{ck} \cdot b \cdot x^2 + \varepsilon_{cu} \cdot E_f \cdot A_f \cdot x - \varepsilon_{cu} \cdot E_f \cdot A_f \cdot d = 0 \quad \text{Equation 5-34}$$

The equation is quadratic and can be solved using the quadratic formula for the roots of the general quadratic equation as below:

$$x = \frac{-b \pm \sqrt{b^2 - 4ac}}{2a} \quad \text{Equation 5-35}$$

Using fundamental principles of compatibility of strain, material stress-strain relationship and equilibrium equations a relationship between ultimate moment resistance and the moment of reinforcement can be constructed.

A balance section is defined as one in which the strain at the extreme concrete compression fibre reached the maximum 0.0035 (for normal concrete) simultaneously with the tension GFRP reaching a strain of  $\varepsilon_{fu}$ . Therefore, the amount of GFRP ratio  $\rho$  is:

$$\rho_{bal} = \frac{A_{f\ bal}}{b \cdot d}$$

Which can be determined as follows:

From the strain at balance:

$$\frac{x}{d} = \varepsilon_{cu} / (\varepsilon_{cu} + \varepsilon_y) \quad \text{Equation 5-36}$$

From stress-strain of the reinforcement:

$$\varepsilon_y = \frac{f_{fk}}{1.3} \cdot E_f$$

Equation 5-37

Substitute the above equation into the one before, gives:

$$\frac{x}{d} = \varepsilon_{cu} \cdot E_f / ((\varepsilon_{cu} \cdot E_f) + 0.77 f_{fk})$$

The compression force in concrete  $C_C$  above the neutral axis is given by:

$$C_C = \text{stress} \times \text{area}$$

$$C_C = \alpha_1 \cdot f_{ck} \cdot b \cdot x$$

$$C_C = 0.4587 f_{ck} \cdot b \cdot x$$

The tension force in the reinforcement bar at balance T is:

$$T = \text{stress} \times \text{area}$$

$$T = \frac{A_{f \text{ bal}} \cdot f_{fk}}{1.3}$$

As the section is in equilibrium, then:

$$C_C = T$$

or

$$0.4587 f_{ck} \cdot b \cdot x = \frac{A_{f \text{ bal}} \cdot f_{fk}}{1.3}$$

$$A_{f \text{ bal}} = \frac{0.5963 f_{ck} \cdot b \cdot x}{f_{fk}}$$

Equation 5-38

Substituting Equation 5-37 into Equation 5-38 and rearranging the terms results in:

$$A_{f \text{ bal}} = \frac{0.5963 f_{ck} \cdot b \cdot \varepsilon_{cu} \cdot E_f \cdot d}{f_{fk} (\varepsilon_{cu} \cdot E_f + 0.77 f_{fk})}$$

Equation 5-39

Then  $\rho_{\text{bal}}$  will be:

$$\rho_{\text{bal}} = \frac{0.5963 f_{ck} \cdot \varepsilon_{cu} \cdot E_f}{f_{fk} (\varepsilon_{cu} \cdot E_f + 0.77 f_{fk})}$$

If the reinforcement ratio  $\rho$  is below  $\rho_{bal}$ , the GFRP bars will yield before concrete crushes in compression. Such a beam is known to be under-reinforced and the ultimate moment of resistance can be expressed as:

Ultimate moment = T. leaver arm

Or

$$M = 0.77 f_{fk} \cdot A_f (d - \alpha_2 \cdot x) \quad \text{Equation 5-40}$$

For equilibrium equation,

$$\frac{x}{d} = \frac{0.77 f_{fk} \cdot \rho}{\alpha_2 \cdot f_{fk}} \quad \text{Equation 5-41}$$

For  $\rho$  greater than  $\rho_{bal}$ , the concrete fails by compression before steel reaches the yield point. The beam is known as an over-reinforced beam.

The flexural capacity is limited either by rupture of the GFRP reinforcement in tension or crushing the concrete in compression. Even though both modes are brittle and undesirable, the GFRP design approach currently adopted is to accept that GFRP RC sections will be over-reinforced and that the ultimate failure will be by concrete crushing rather than by reinforcement failure.

From strain compatibility,

$$\frac{x}{d} = \varepsilon_{cu} / (\varepsilon_{cu} + \varepsilon_f)$$

And from the stress-strain relationship of reinforcing bar,

$$f_f = \varepsilon_f \cdot E_f$$

Replace  $0.77 f_{fk}$  by  $f_f$  in Equation 5-41 and substitute Equation 5-39 and Equation 5-40 into Equation 5-41 results in:

$$\frac{x}{d} = \frac{\varepsilon_{cu} \cdot f_{fk}}{(\varepsilon_{cu} \cdot f_{fk} + \alpha_1 \left(\frac{x}{d}\right) \cdot f_{ck} / \rho)}$$

Or

$$\alpha_1 \left(\frac{f_{ck}}{\rho}\right) \cdot \left(\frac{x}{d}\right)^2 + \varepsilon_{cu} \cdot f_{fk} \cdot \left(\frac{x}{d}\right) - (\varepsilon_{cu} \cdot f_{fk}) = 0$$

The ultimate moment of resistance can then be obtained by taking moment about tension reinforcement

$$M = \alpha_1 \cdot f_{ck} \cdot b \cdot x \cdot (d - \alpha_2 \cdot x) \quad \text{Equation 5-42}$$

### 5.3.5 Foamed Concrete Reinforced with GFRP (FC+GFRP)

The parabolic-rectangular stress block adopted by EC2 for the ultimate strength design calculations is presented in Figure 5-11.

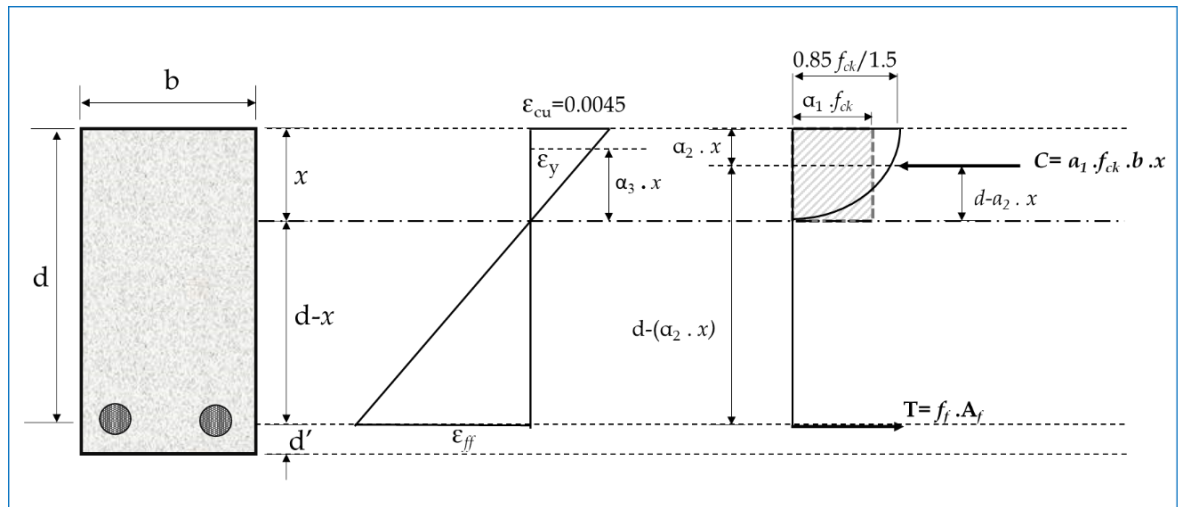


Figure 5-11: Parabolic-rectangular design stress block for the ultimate limit state- EC2 (Foamed concrete reinforced with GFRP)

Values of  $\alpha_1$ ,  $\alpha_2$  and  $\alpha_3$  are the same for the case of foamed concrete with steel reinforcement.

$$\alpha_3 = \frac{0.002}{0.0045} = 0.444$$

$$\alpha_1 = 0.4827$$

$$\alpha_2 = 0.4324$$

To calculate the distance from the natural axis to the extreme compression fibre ( $x$ ).

From the strain block of the beam section.

$$\frac{\epsilon_{cu}}{x} = \frac{\epsilon_f}{(d - x)} \quad \text{Equation 5-43}$$

$$\varepsilon_f = \varepsilon_{cu} \frac{(d - x)}{x}$$

$$f_f = E_f \cdot \varepsilon_f = \frac{(d-x)}{x} \cdot \varepsilon_{cu} \cdot E_f \leq f_{fk} \quad \text{Equation 5-44}$$

As the section is in equilibrium, then:

$$C_C = T$$

or

$$\alpha_1 \cdot f_{ck} \cdot b \cdot x = f_f \cdot A_f$$

Then

$$\alpha_1 \cdot f_{ck} \cdot b \cdot x = \frac{(d - x)}{x} \cdot \varepsilon_{cu} \cdot E_f \cdot A_f$$

$$\alpha_1 \cdot f_{ck} \cdot b \cdot x^2 + \varepsilon_{cu} \cdot E_f \cdot A_f \cdot x - \varepsilon_{cu} \cdot E_f \cdot A_f \cdot d = 0 \quad \text{Equation 5-45}$$

The equation is quadratic and can be solved using the quadratic formula for the roots of the general quadratic equation as below:

$$x = \frac{-b \pm \sqrt{b^2 - 4ac}}{2a} \quad \text{Equation 5-46}$$

Using fundamental principles of compatibility of strain, material stress-strain relationship and equilibrium equations a relationship between ultimate moment resistance and the moment of reinforcement can be constructed.

A balance section is defined as one in which the strain at the extreme concrete compression fibre reached the maximum of 0.0045 (for foamed concrete) simultaneously with the tension GFRP reaching a strain of  $\varepsilon_{fu}$ . Therefore, the amount of GFRP ratio  $\rho$  is:

$$\rho_{bal} = \frac{A_{f\ bal}}{b \cdot d}$$

Which can be determined as follows:

From the strain at balance,

$$\frac{x}{d} = \varepsilon_{cu} / (\varepsilon_{cu} + \varepsilon_y) \quad \text{Equation 5-47}$$

From stress-strain of the reinforcement,

$$\varepsilon_y = \frac{f_{fk}}{1.3} \cdot E_f \quad \text{Equation 5-48}$$

Substitute Equation 5-48 into Equation 5-47, gives:

$$\frac{x}{d} = \varepsilon_{cu} \cdot E_f / ((\varepsilon_{cu} \cdot E_f) + 0.77 f_{fk})$$

The compression force in concrete  $C_C$  above the neutral axis is given by:

$$C_C = \text{stress} \times \text{area}$$

$$C_C = \alpha_1 \cdot f_{ck} \cdot b \cdot x$$

$$C_C = 0.4827 f_{ck} \cdot b \cdot x$$

The tension force in the reinforcement bar at balance T is:

$$T = \text{stress} \times \text{area}$$

$$T = \frac{A_{f \text{ bal}} \cdot f_{fk}}{1.3}$$

As the section is in equilibrium, then:

$$C_C = T$$

or

$$0.4827 f_{ck} \cdot b \cdot x = \frac{A_{f \text{ bal}} \cdot f_{fk}}{1.3}$$

$$A_{f \text{ bal}} = \frac{0.6275 f_{ck} \cdot b \cdot x}{f_{fk}} \quad \text{Equation 5-49}$$

Substituting Equation 5-48 into Equation 5-49 and rearranging the terms results in:

$$A_{f \text{ bal}} = \frac{0.6275 f_{ck} \cdot b \cdot \varepsilon_{cu} \cdot E_f \cdot d}{f_{fk} (\varepsilon_{cu} \cdot E_f + 0.77 f_{fk})} \quad \text{Equation 5-50}$$

Then  $\rho_{\text{bal}}$  will be:

$$\rho_{\text{bal}} = \frac{0.6275 f_{ck} \cdot \varepsilon_{cu} \cdot E_f}{f_{fk} (\varepsilon_{cu} \cdot E_f + 0.77 f_{fk})}$$

If the reinforcement ratio  $\rho$  is below  $\rho_{bal}$ , the GFRP bars will yield before concrete crushes in compression. Such a beam is known to be under-reinforced, and the ultimate moment of resistance can be expressed as:

Ultimate moment = T. leaver arm

Or

$$M = 0.77 f_{fk} \cdot A_f (d - \alpha_2 \cdot x) \quad \text{Equation 5-51}$$

For equilibrium equation,

$$\frac{x}{d} = \frac{0.77 f_{fk} \cdot \rho}{\alpha_2 \cdot f_{fk}} \quad \text{Equation 5-52}$$

For  $\rho$  greater than  $\rho_{bal}$ , the concrete fails by compression before steel reaches the yield point. The beam is known as an over-reinforced beam.

As mentioned earlier, it is accepted that GFRP RC sections will be over-reinforced, and that the ultimate failure will be by concrete crushing rather than by reinforcement failure. From strain compatibility,

$$\frac{x}{d} = \varepsilon_{cu} / (\varepsilon_{cu} + \varepsilon_f)$$

And from the stress-strain relationship of reinforcing bar,

$$f_f = \varepsilon_f \cdot E_f$$

Replace  $0.77 f_{fk}$  by  $f_f$  in Equation 5-52 and substitute Equation 5-50 and Equation 5-51 into Equation 5-52 results in:

$$\frac{x}{d} = \frac{\varepsilon_{cu} \cdot f_{fk}}{(\varepsilon_{cu} \cdot f_{fk} + \alpha_1 \left(\frac{x}{d}\right) \cdot f_{ck} / \rho)}$$

Or

$$\alpha_1 \left(\frac{f_{ck}}{\rho}\right) \cdot \left(\frac{x}{d}\right)^2 + \varepsilon_{cu} \cdot f_{fk} \cdot \left(\frac{x}{d}\right) - (\varepsilon_{cu} \cdot f_{fk}) = 0$$

The ultimate moment of resistance can then be obtained by taking moment about tension reinforcement

$$M = \alpha_1 \cdot f_{ck} \cdot b \cdot x \cdot (d - \alpha_2 \cdot x)$$

Equation 5-53

## 5.4 Summary of the Ultimate Moments of Resistance

Table 5-4 shown below summarizes the ultimate moment of resistance of all beams.

Table 5-4: Summary of all beam's ultimate moment of resistance

Beam	$\rho_{bal}$	$M$ when $\rho \leq \rho_{bal}$	$M$ when $\rho > \rho_{bal}$
NC+S	$\frac{369.25 f_{ck}}{f_{yk} (700 + 0.87 f_{yk})}$	$0.87 f_{yk} \cdot A_s (d - 0.416 x)$	$0.459 f_{ck} \cdot b \cdot x \cdot (d - 0.416 x)$
FC+S	$\frac{499.5 f_{ck}}{f_{yk} (900 + 0.87 f_{yk})}$	$0.87 f_{yk} \cdot A_s (d - 0.432x)$	$0.483 f_{ck} \cdot b \cdot x \cdot (d - 0.432x)$
NC+GFRP	$\frac{125.223 f_{ck}}{f_{fk} (210 + 0.77 f_{fk})}$	$0.77 f_{fk} \cdot A_f (d - 0.416 x)$	$0.459 f_{ck} \cdot b \cdot x \cdot (d - 0.416x)$
FC+GFRP	$\frac{169.425 f_{ck}}{f_{fk} (270 + 0.77 f_{fk})}$	$0.77 f_{fk} \cdot A_f (d - 0.432x)$	$0.483 f_{ck} \cdot b \cdot x \cdot (d - 0.432x)$

The theoretical ultimate moment of resistance values in the current study for all beams compared to EC2 and ACI-440 guides are presented in Table 5-5. Appendix C shows an excel sheet example of stress block analysis.

Table 5-5: The theoretical ultimate moment of resistance

	<b>NC with Steel</b>	<b>FC with Steel</b>	<b>NC with GFRP</b>	<b>FC with GFRP</b>
<i>M</i> in current study	38.03 kN. m	37.67 kN. m	31.60 kN. m	32.48 kN. m
<i>M</i> in EC2 guide	39.71 kN. m	39.71 kN. m	44.76 kN. m	44.77 kN. m
<i>M</i> in ACI-440 guide	42.23 kN. m	42.23 kN. m	51.79 kN. m	51.79 kN. m

## 5.5 Result and Analysis

### 5.5.1 Load-Deflection Response

The load-deflection relationship is a critical part of reinforced concrete beam analysis especially from the serviceability point of view. As discussed in the literature review chapter that GFRP bars have a lower modulus of elasticity compared to conventional steel. Consequently, the deflection limit is a principal parameter in GFRP reinforced concrete design. The Load-deflection analysis of a beam is an effective method to predict the second moment of area of the section after the section has cracked in the tension zone. Once the concrete in the tension zone is cracked, a noticeable reduction of the effectiveness of the second moment of area results in a reduction in the overall stiffness of the section.

The applied load versus the recorded mid-span deflections of all beams tested are shown in Figure 5-12. At the early stages of loading, all beams were uncracked, thus, demonstrated linear-elastic load-deflection behaviour. After the section is cracked, the reduction in the flexural stiffness was observed. With the increase of the applied load, the stiffness of beams is further reduced due to more crack's occurrence. In general, the amount of steel/GFRP reinforcement is a crucial factor in improving the beams flexural stiffness.

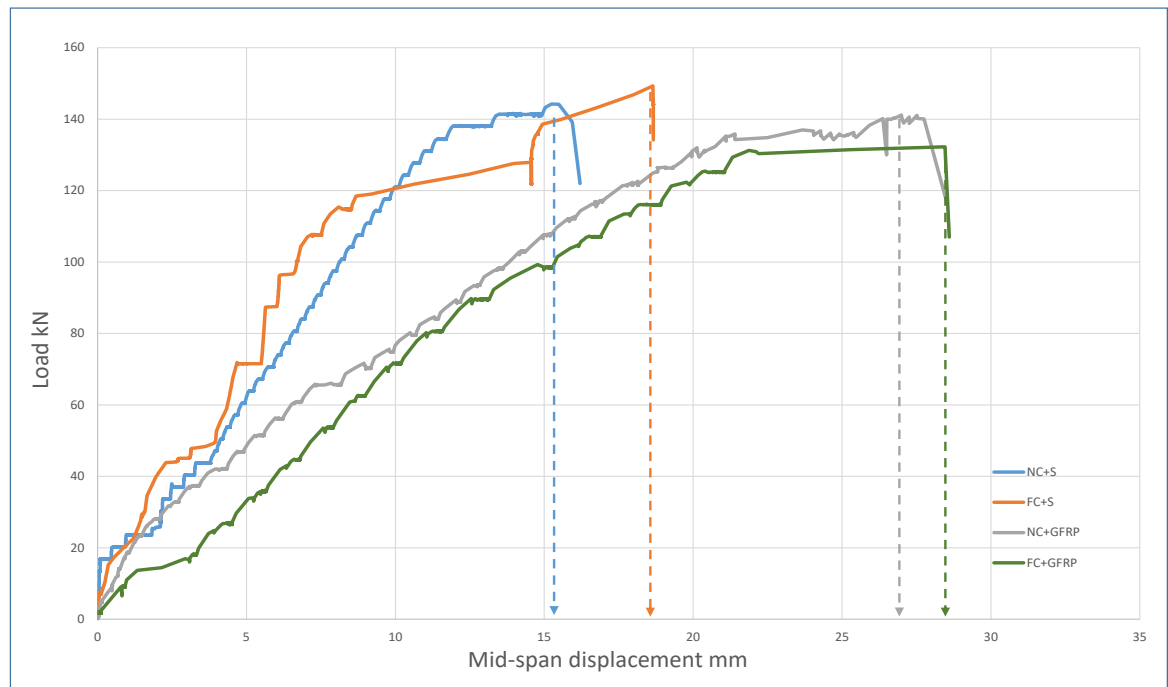


Figure 5-12: Midspan Load-deflection response

With the direct effect of the modulus of elasticity on beam flexural stiffness. As expected, due to the relatively low modulus of elasticity of GFRP, the NC+GFRP and FC+GFRP beams experienced larger deformation compared to the beams reinforced with steel. Normal weight concrete beams demonstrated less mid-span deflection compared to foamed concrete beams due to the larger strains at maximum stress in foamed concrete (0.0045) than that in normal concrete (0.0035).

Since the glass fibre reinforced plastic bars have no yield point, the load-deflection relationship in beams reinforced with GFRP demonstrated a more even and linear load-displacement relationship than that in beams reinforced with steel. Moreover, it was observed that the beams reinforced with steel failed at a higher load than those with GFRP as reinforcement. However, even though the modulus of elasticity of GFRP material is less than  $1/3$  of that in steel, the FC+GFRP beam showed reasonably good flexural response compare to steel reinforced beams.

### 5.5.2 Concrete and Reinforcement Load - Strain Response

Strain gauges of 10 mm-long ESGs mounted on the concrete service, longitudinal bars and shear links as shown in Figure 5-13. The measured strains from the gauges were plotted with the corresponding applied loads to produce the load-strain plots for each of the

normal/foamed concrete and steel/GFRP bars. Six strain gages, one on the extreme concrete compression fibre, two on the extreme tension concrete fibre, two on shear links and one on the longitudinal bars.

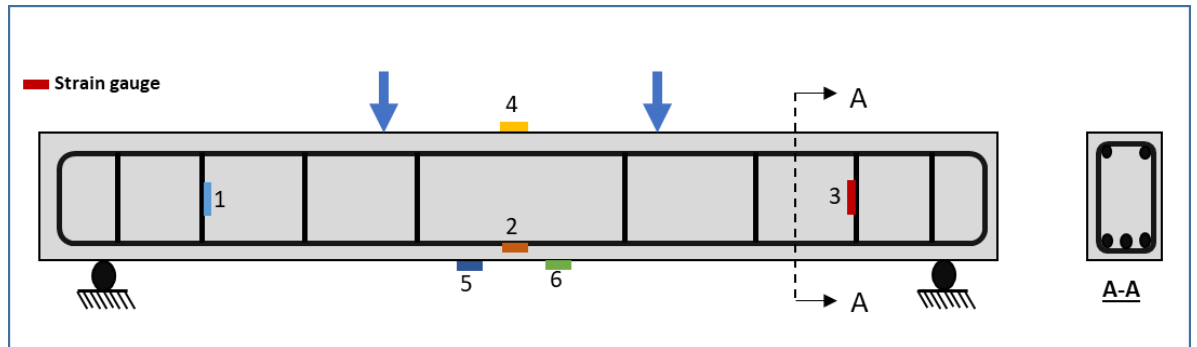


Figure 5-13: The load-strain relationship for concrete and reinforcement for all beams

It was noticed that the strains in all shear links were very low especially in GFRP reinforced beams. Main reinforcement, GFRP bars experienced larger strains compare to steel bars which are expected due to their low modulus of elasticity as shown in Figure 5-14. As modulus of elasticity of both normal weight and foamed concrete, as well as the steel and GFRP reinforcement, are known, the stresses could be calculated.

The two beams (NC+GFRP and FC+GFRP) both showed similar strain behaviour, especially in the bottom main reinforcement. That indicates that GFRP bars behave in the same manner with normal weight concrete and foamed concrete under the same loading condition.

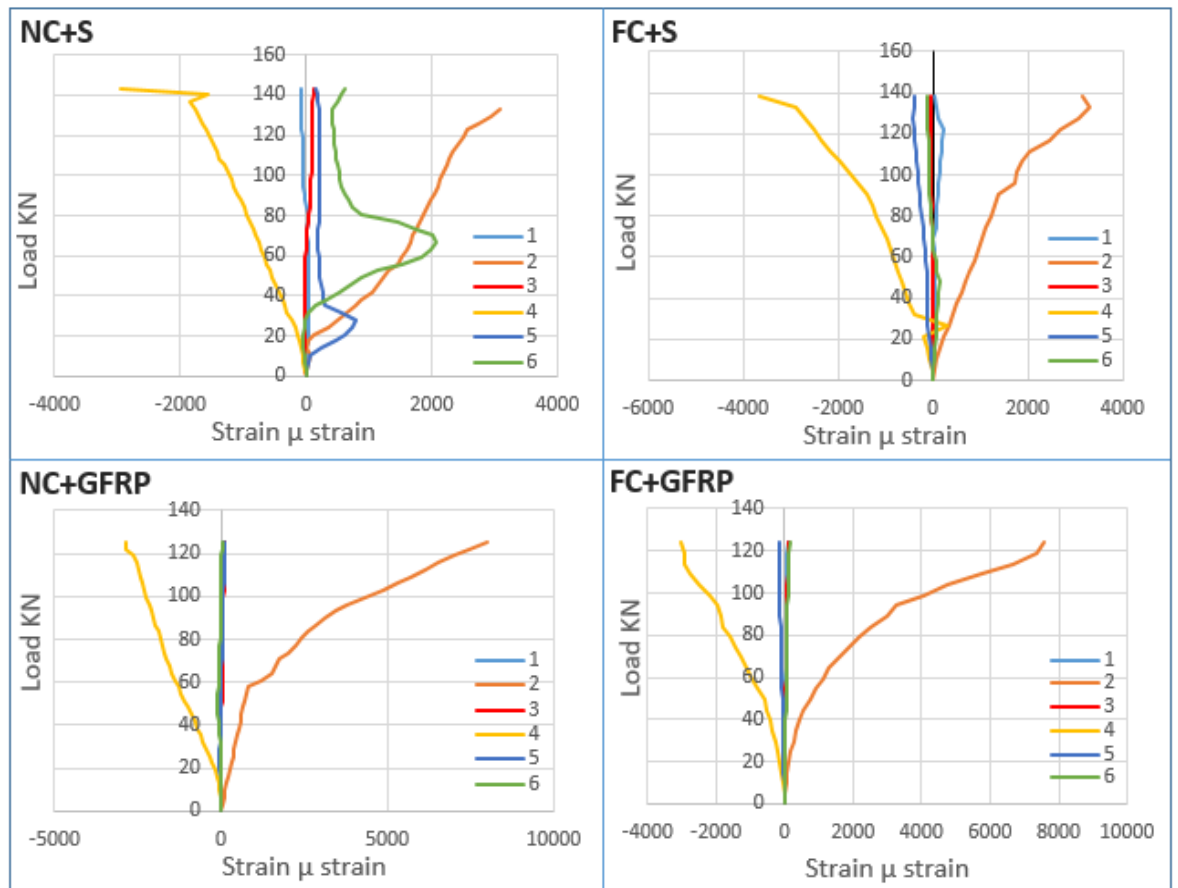


Figure 5-14: Concrete and reinforcement Load-strain relationships

### 5.5.3 Bending Moment

Data collected from LVDTs placed at mid-span of all beams plotted against the corresponding bending moments, as illustrated in Figure 5-15. The experimental ultimate moment compared with the theoretical ultimate bending capacity in the current study, the ultimate bending moment in the EC2 and ACI-440 guides.

In the case of a normal concrete beam reinforced with steel (NC+S), large flexural cracks developed immediately after the mid-span bending moment reached 6kN.m results in a sudden change in bending stiffness. It was observed primarily due to cracks forming. However, the foamed concrete beam reinforced with steel (FC+S) has a higher cracking moment NC+S and the cracks developed gradually and more evenly. The experimental ultimate bending moment in both NC+S and FC+S beams were very similar to that from the ACI-440 guide and slightly higher than the theoretical ultimate moment in the current study and the ultimate moment in the EC2 guide as shown in Figure 5-16.

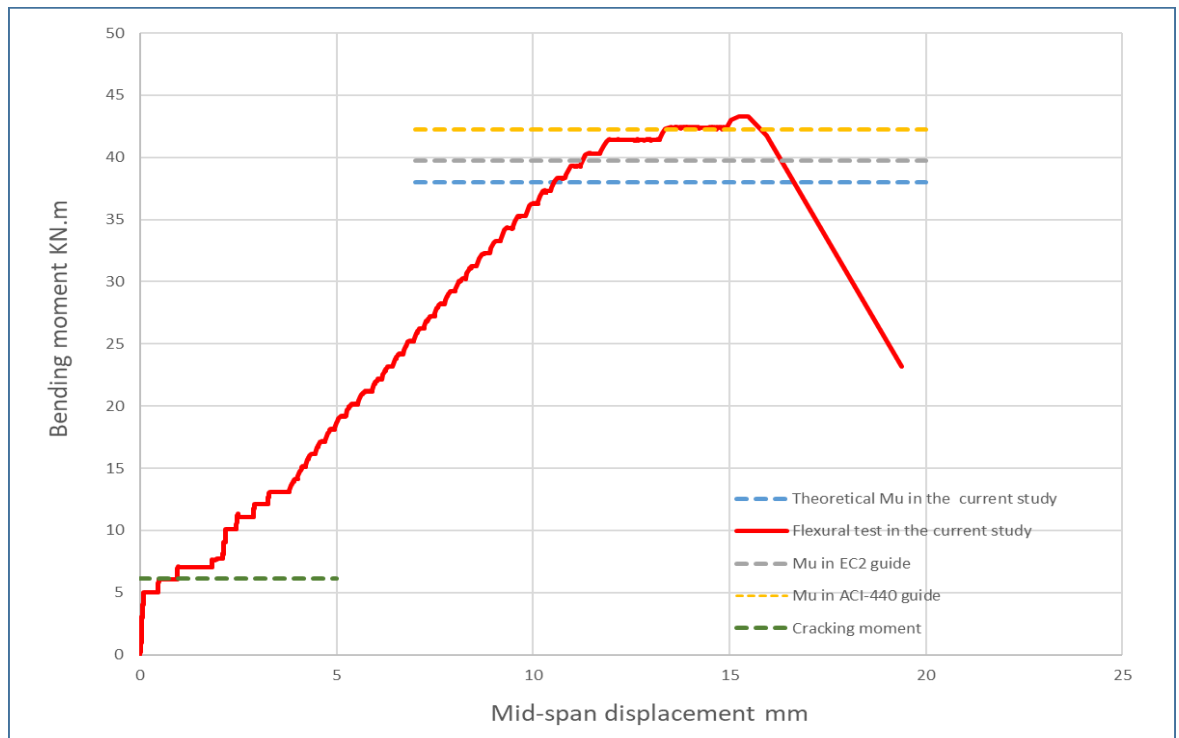


Figure 5-15: Bending moment-deflection for normal concrete reinforced with steel

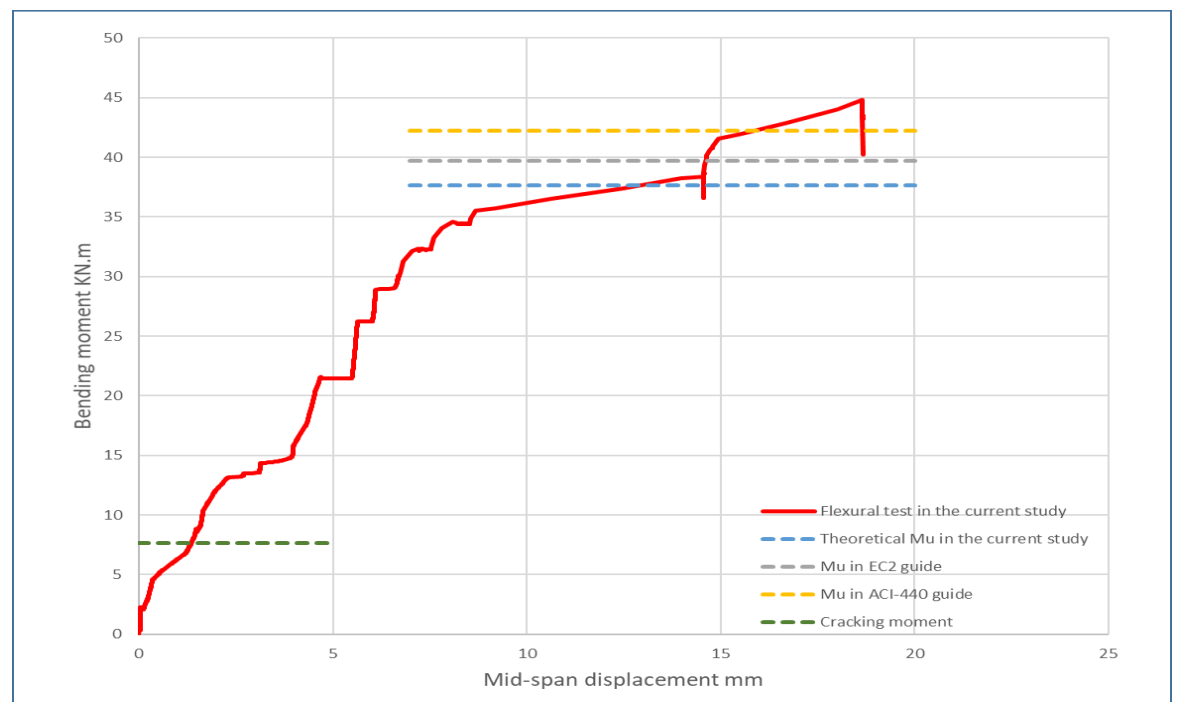


Figure 5-16: Bending moment-deflection for foamed concrete reinforced with steel

Despite the fact that GFRP has less than 1/3 of modulus of elasticity than in steel, both normal and foamed concrete beams reinforced with GFRP bars performed higher ductility, with flexural capacity only 7% less than that in steel-reinforced beams. Foamed concrete

beams showed a higher cracking moment than normal-weight concrete because the enhanced foamed concrete has higher ultimate compressive strain (0.0045) at ultimate stress than normal-weight concrete (0.0035).

For GFRP reinforced beams the prediction of the ultimate moment in EC2 and ACI-440 guides are found to be higher than the ultimate moment from the experiential testing. However, the theoretical ultimate moment in the current study is lower than the experimental ultimate moment as shown in Figure 5-17 and Figure 5-18. These differences between the obtained moment capacity from experimental flexural testing and those obtained from the EC2, ACI-440 design guides and theoretical calculations, could be basically from the fact that EC2 and ACI recommendations do not consider the “actual” concrete non-linear behaviour, nor considering concrete-GFRP bars bond.

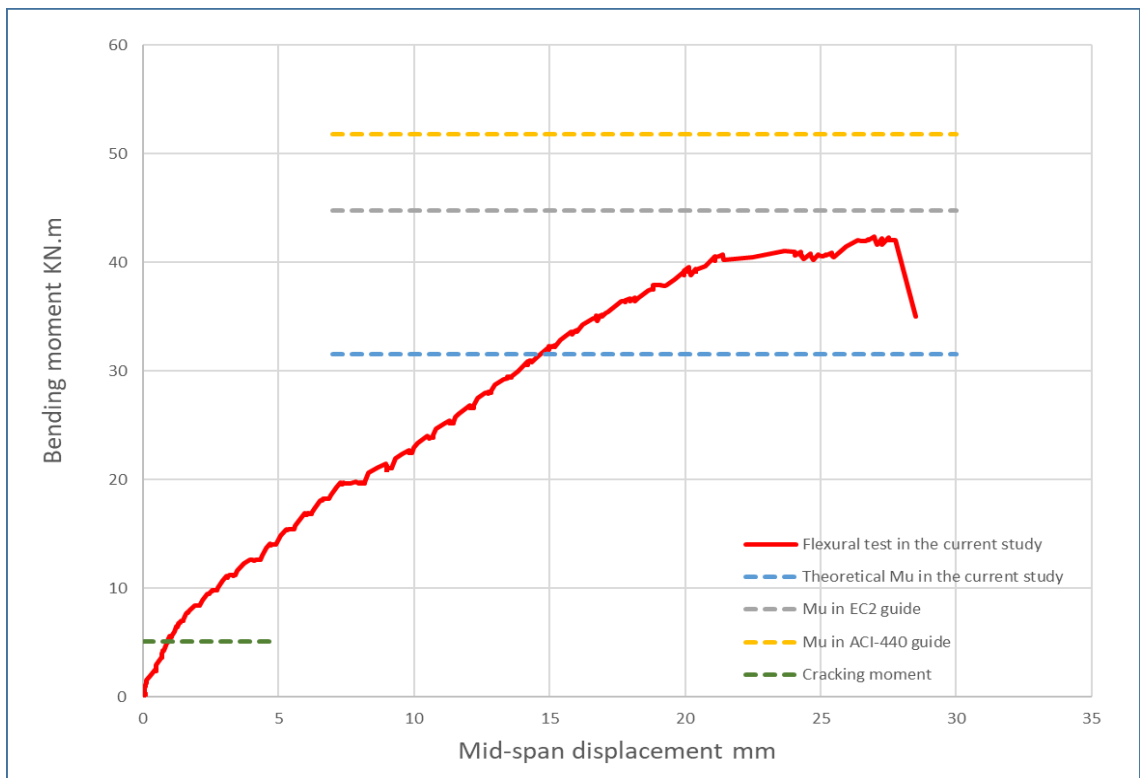


Figure 5-17: Bending moment-deflection for normal concrete reinforced with GFRP

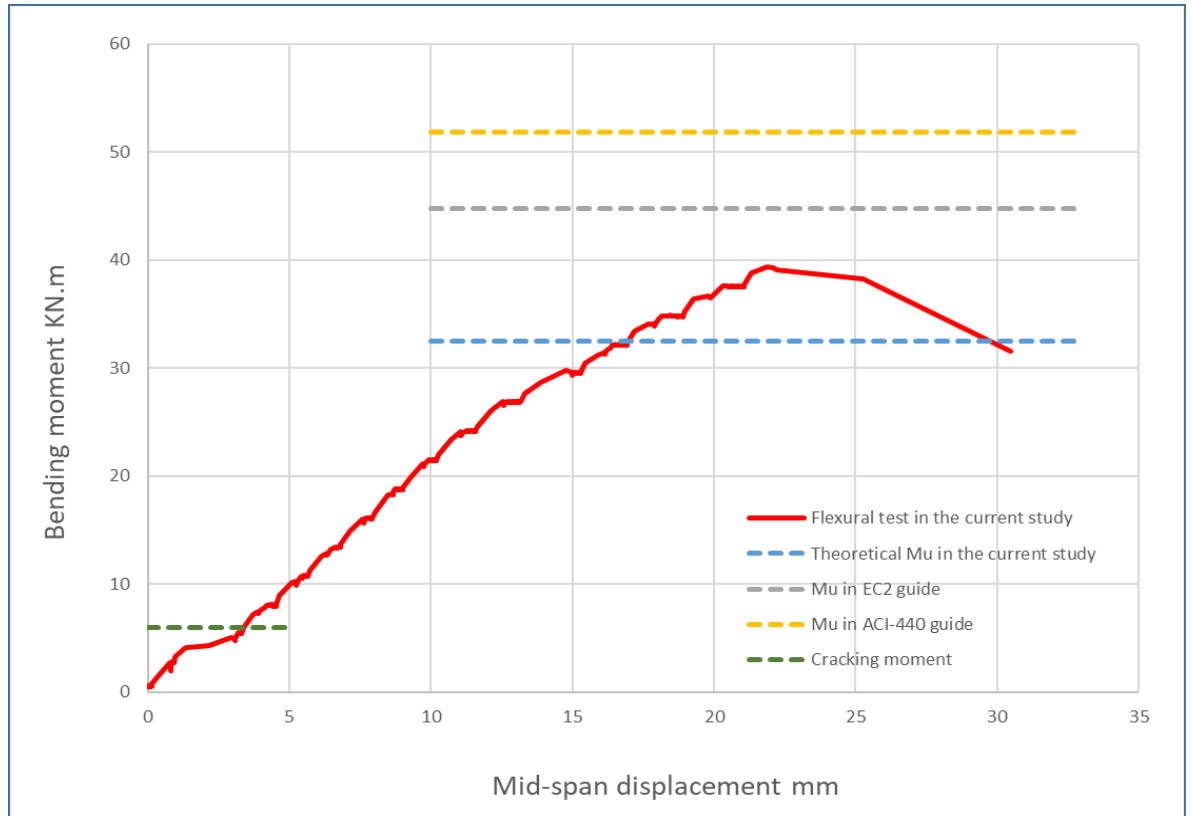


Figure 5-18: Bending moment-deflection for foamed concrete reinforced with GFRP

#### 5.5.4 Crack Propagation and Failure Modes

The crack propagation for the tested beams was recorded and sketched manually during the loading process. All beams started to develop vertical flexural cracks at the middle region of the tension zone which propagates diagonally towards flexural failure. Visible cracks developed in beam NC+GFRP when the applied load accessed 16.9 kN. However, in the FC+S beam, the cracking load was found to be 50% higher than that in NC+GFRP. Beams reinforced with steel required a higher load to cause section crack than beams reinforced with GFRP. Moreover, the enhanced foamed concrete was found to have a higher cracking load than normal concrete and that since the enhanced foamed concrete was found to be less brittle than normal-weight concrete. The experimental results concerning cracking load, ultimate load, mid-span deflection and failure mode are summarized in Table 5-6.

Table 5-6: Structural performance and failure mode of the concrete beams

Beam	Cracking load (kN)	Ultimate load (kN)	Ultimate moment strength (kN. m)	Mid-span deflection (mm)	Failure mode
NC+S	20.154	142.5	43.65	15.75	Compression
FC+S	25.394	144.8	44.95	18.3	Shear- Compression
NC+GFRP	16.964	140.5	42.25	27.1	Compression
FC+GFRP	19.972	138.25	39.85	21.7	Shear- Compression

Foamed concrete beams found to have fewer cracks in number but wider cracks than those in normal-weight concrete. Crack patterns and failure mode are sketched for each beam and presented in the figures below. Regarding the failure mode in both NC+S and NC+GFRP beams the failure was compression failure caused by concrete crushing with the yield of the hanger bars. However, in foamed concrete beams FC+S and FC+GFRP the failure was a shear-compression failure as shown in Figure 5-19 to Figure 5-22.

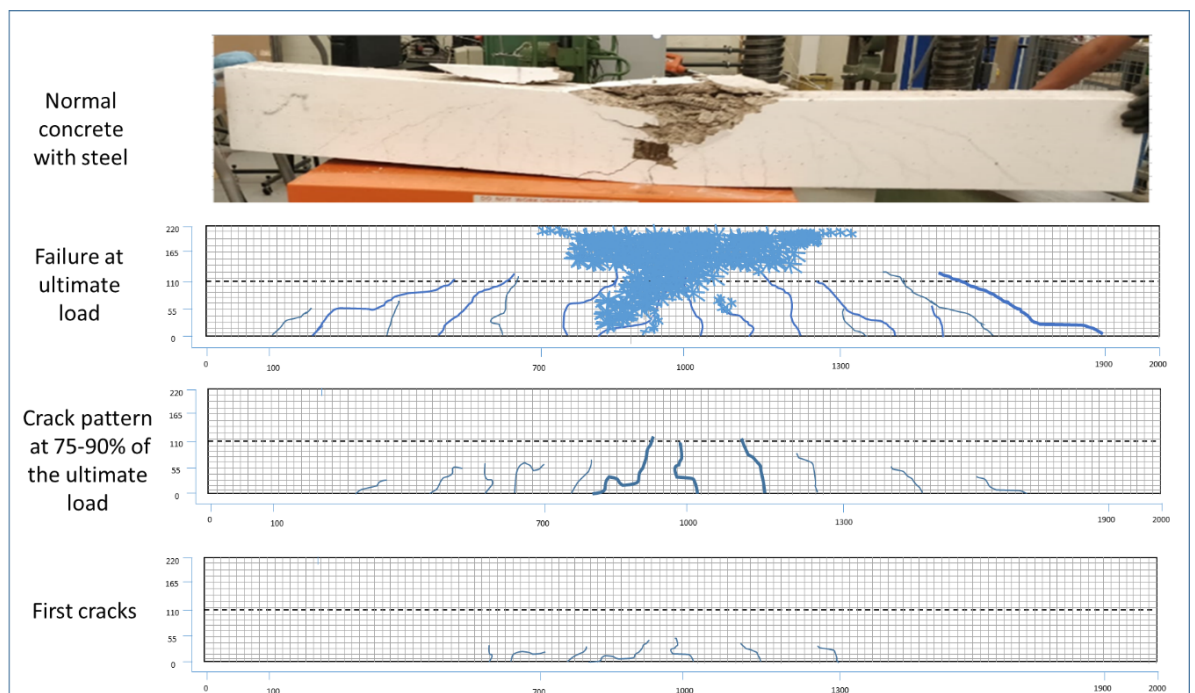


Figure 5-19: Crack pattern and failure mode of NC+S beam

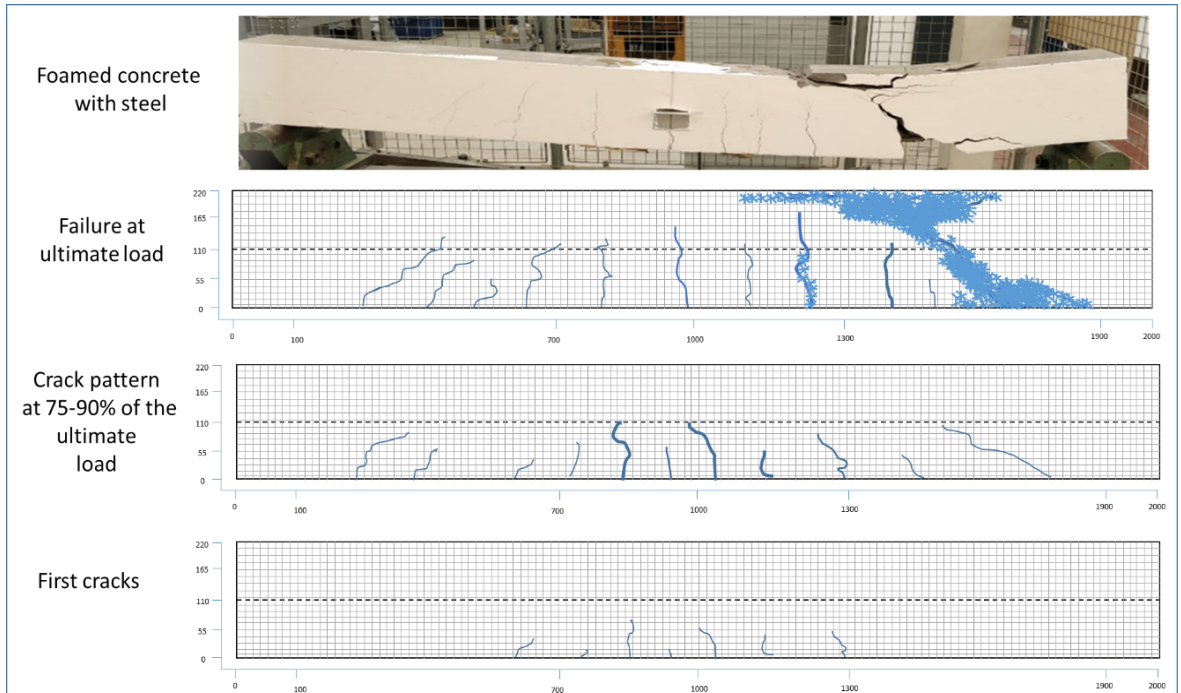


Figure 5-20: Crack pattern and failure mode of FC+S beam

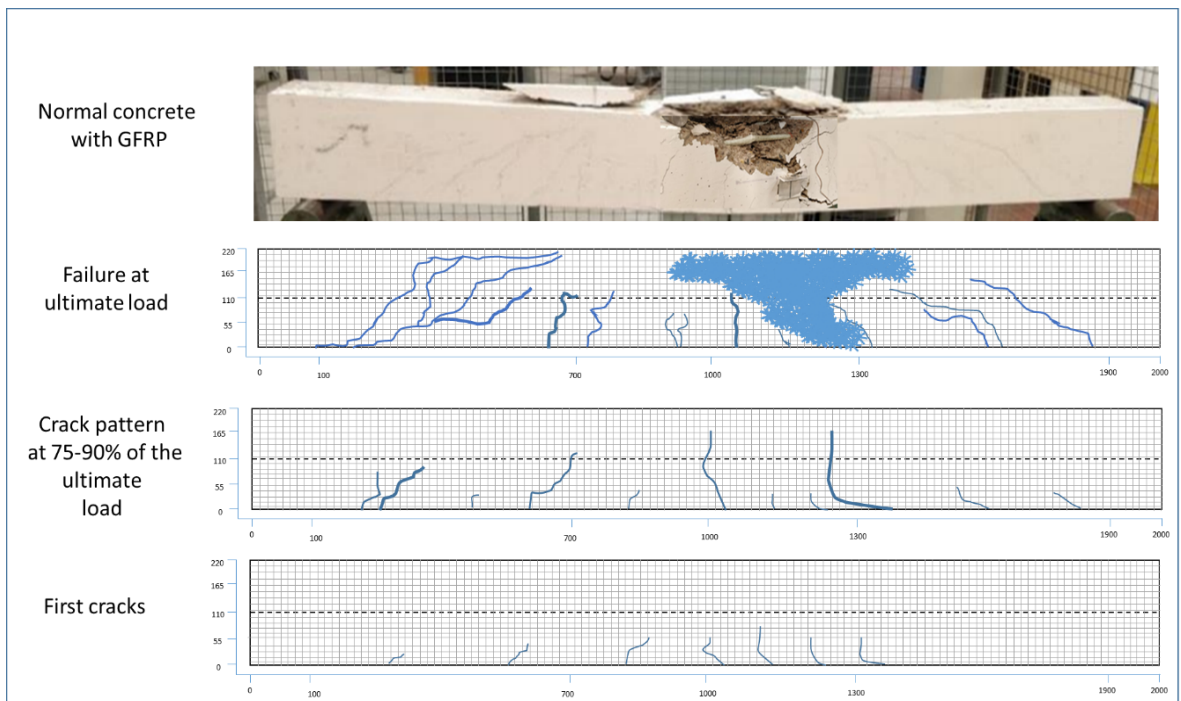


Figure 5-21: Crack pattern and failure mode of NC+GFRP beam

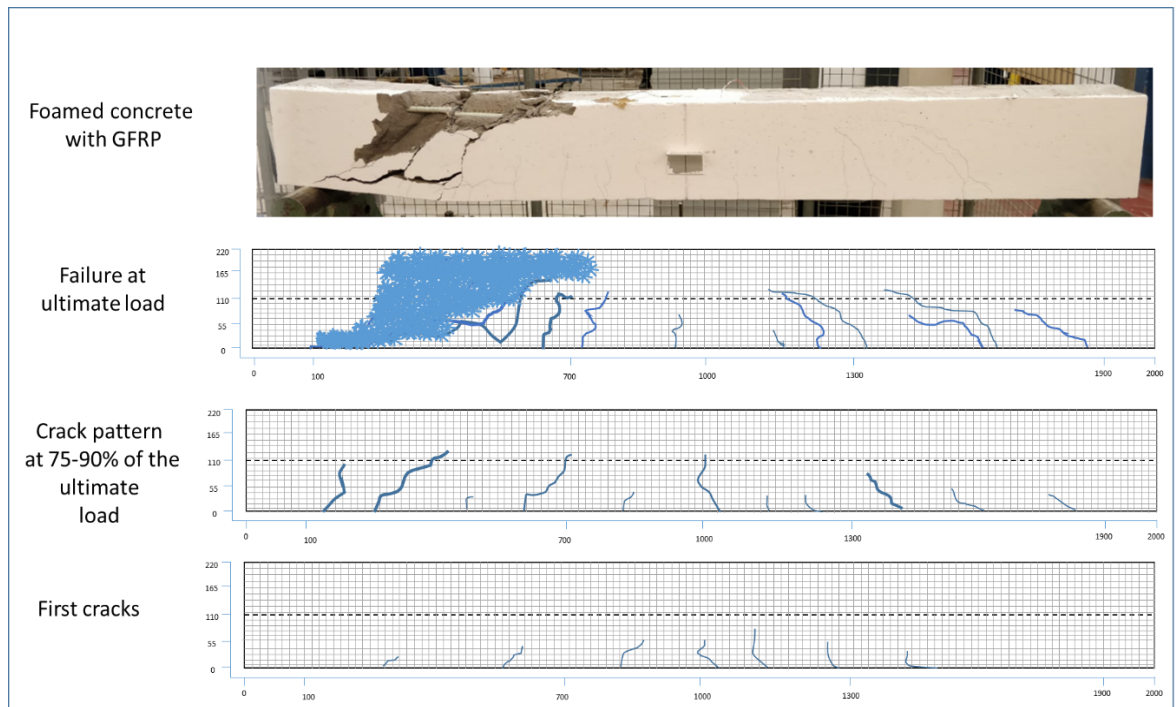


Figure 5-22: Crack pattern and failure mode of FC+GFRP beam

## 5.6 Summary

This chapter covers an experimental programme and numerical analysis to investigate the flexural behaviour of steel/GFRP reinforced normal/foamed concrete beams. Four reinforced beam models were considered, including a normal concrete beam reinforced with steel bars, foamed concrete beam reinforced with steel bars, a normal concrete beam reinforced with GFRP bars and foamed concrete beam reinforced with GFRP bars.

The principal findings drawn from the present investigation are presented below:

- The equations obtained from the theoretical derivations of the reinforced concrete beams in the current study to determine the ultimate moment showed slightly under-estimation compare to experimental results.
- The ACI-440 equations showed similarity with the experimental ultimate moment in both normal and foamed concrete beams reinforced with steel. However, in beams reinforced with GFRP, the ACI-440 equations overestimated the experimental ultimate moment.

- Foamed concrete beams have a higher cracking moment and few cracks compared to normal weight concrete beams. However, the cracks are bigger, which may be attributed to the shear effect combined with flexure at failure.
- GFRP reinforced beams illustrated higher deflection than the steel-reinforced beams, owing to the lower elastic modulus of GFRP bars compared with steel.
- Normal concrete beams (NC+S and NC+GFRP) failed in compression. Nevertheless, foamed concrete beams (FC+S and FC+ GFRP) have combined shear and flexural failure.
- Unlike steel, GFRP was found to behave in a similar way with both normal and foamed concrete. Dispit the fact that the foamed concrete beam that reinforced with GFRP has overall mdulus of elasticity of  $1/4$  that in normal weight concrete reinforced with steel. It perform better than expected with flexural capacity of 87% of normal concrete beam.

## Chapter 6

# Finite Element Modelling of GFRP Reinforced Foamed Concrete Beams

### 6.1 Introduction

In recent decades, the finite element method has been immensely considered as an effective method in the analysis of simple structures, such as reinforced concrete beams, columns, and slabs. As well as complex concrete structures, such as a shear wall, deep beam, FRP reinforced concrete structures. Finite Element Modelling FEM is known as a robust numerical technique to find approximate solutions to practical engineering problems, particularly those with complex geometries, loading and boundary conditions. There are many different methods to study the structural behaviour of concrete elements. Experiments have always been used to study and analyse different concrete structures and their behaviour under loading. In general, it is an accurate method. However, it is costly and time-consuming (Warner, 1997). Therefore, the finite element method (FEM) was developed and used in the 1950s to study structures behaviour. Many finite element analysis packages such as ABAQUS have been developed in recent years. FEM is an accurate and cost-effective method and has become the choice method for structural analysis. For this thesis, ABAQUS from the Dassault systems suite is chosen as the FE software for beams simulating. ABAQUS has widely used FE software in the aerospace composites industries due to its versatile and reliable simulation capabilities.

### 6.2 Finite Element Method

FEM method is based on the mechanic's laws and depending on the problem nature, it can be associated with structural mechanics, thermo mechanics or fluid mechanics. The finite element analysis modelling procedure may be described as a loop. The first step involves physical problem numerical modelling by using the appropriate differential equations, which is known as shape functions. The second step involves applying loads to the model and quantifying displacements at the nodes, followed by stress-strain analyses of the system.

The obtained results are validated against real data. The numerical model might need additional improvement and refinement based on the analysis results review, and the system is reanalysed for the same applied loads. Additional result's review may be performed, with extra refinement might be required until the results reflect the system experimental results under similar loading conditions.

The finite element method includes the choice of elements such as 2D or 3D beam or truss, meshing, and boundary conditions. The method is typically utilized to analyse various material properties and structures with complex features. FEM offers an effective analytical technique to study the structural behaviour of reinforced concrete members. Nonlinearity in geometry or material properties, cracking, tension stiffening, interface behaviour, and other mechanisms that are passed over or treated approximately can be modelled rationally using the finite element method (Xingyu et al., 2020).

For a structural finite element analysis, the stiffness matrix comprises the material and geometric behaviour information that defines the resistance to deformation of the element when subjected to external loading. These deformations may include shear, axial bending, and torsional effects. In the early applications of FEM and without the advantage of modern computers, the flexibility method was used when force analysis is used to develop the matrix. In this technique, the knowns are displacements, and the unknowns are the forces. Nevertheless, the FEM corresponds to the displacement method, where the unknowns are system displacements in response to applied loads. The structural stiffness matrix typically takes the form:

$$[K] \{U\} = \{F\} \qquad \text{Equation 6-1}$$

Where:

[K]     Assembled global stiffness matrix

{U}     Vector of global displacement

{F}     Vector of applied nodal forces

### 6.3 Nonlinear Finite Element Analysis

The majority of problems in engineering applications are nonlinear. Overall, nonlinearities in structural mechanics arise in two different ways: From geometric nonlinearity or/and from physical or material nonlinearity (Sataloff et al., 2019). In the case of geometric nonlinearity, this form of nonlinearity is based on elastic body deformations. In geometric nonlinearity, the relationships between strains such as the extensional and shear strains with the displacement components are taken to be nonlinear, leading to nonlinear strain–displacement relationships. However, in the material nonlinearity, the generalised Hooke’s law is not valid as long as the stress-strain behaviour of a material is nonlinear. The material nonlinearity has a great effect on the behaviour of structural in finite element analysis. Figure 6-1 shows nonlinear finite element solution procedures for reinforced concrete beams.

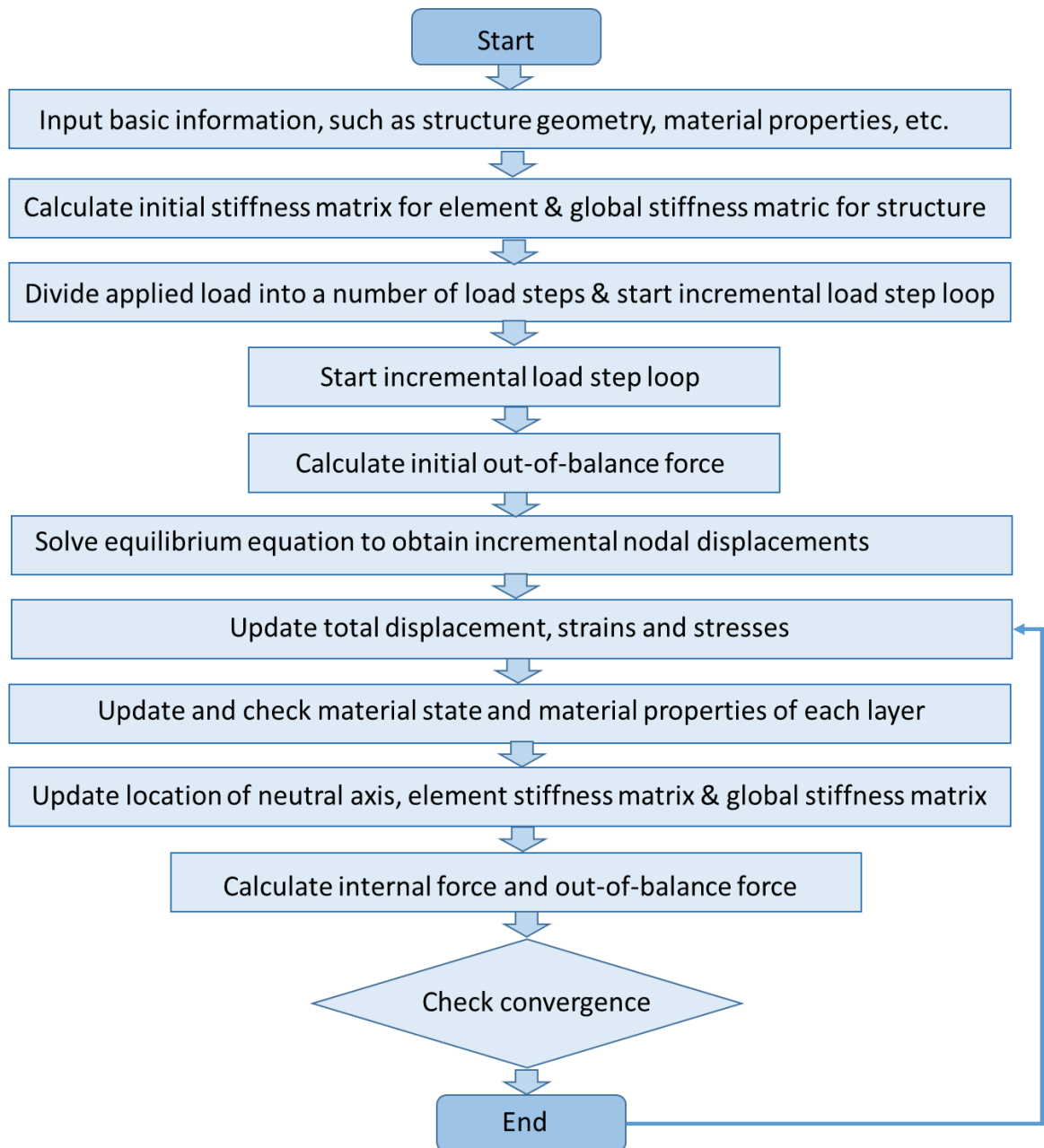


Figure 6-1: Nonlinear finite element solution procedures for reinforced concrete beams

## 6.4 ABAQUS Overview

Many finite element analysis (FEA) software packages are available for concrete structural analysis. Examples include Automatic Dynamic Incremental Nonlinear Analysis ADINA developed by ADINA R&D Inc, Analysis Systems Inc ANSYS and ABAQUS by Dassault Systemes Simulia Corp. ABAQUS was developed and designed primarily for the nonlinear static and dynamic analysis of structures. ABAQUS product suite includes three core products ABAQUS/CAE, ABAQUS/Standard, and ABAQUS/Explicit (Dassault Systèmes,

2014). ABAQUS/CAE was used for the beam's simulations performed in this study for its capability of nonlinear analysis for concrete structures. ABAQUS/CAE or Complete ABAQUS Environment allows users to create, analyse and visualize model output all in one environment using a customizable graphical user interface (GUI). ABAQUS/CAE allows users to create geometries using the GUI or by importing CAD models for meshing. Users can then analyse models and use the comprehensive visualization options to interpret and communicate the analysis results.

## 6.5 FE Modelling of Concrete in ABAQUS

For modelling reinforced concrete using the finite element method in ABAQUS, there are different models that ABAQUS offers and their application depends on the type of structural loading and cracking analysis. These models include:

- 1- Smearred Crack Model (SCM)
- 2- Brittle Cracking Model (BCM)
- 3- Concrete Damaged Plasticity Model (CDPM)

All three models have a general capability for modelling typical concrete structures such as columns, beams, trusses and shells. The models could be used for quasi-brittle materials, plain concrete. However, they are mainly intended for reinforced concrete structures analysis.

- **The Smearred Crack Model**

This model can be implemented in ABAQUS/Standard for applications in which the material is subjected to predominantly monotonic low loading. Concrete cracking is the most important aspect of the concrete behaviour in this model; therefore, the modelling is dominated by the cracking and post-cracking behaviour. Apply the crack detection surface to determine the failure point of the integration point by tensile cracking. The SCM approach is utilized to characterise the discontinuous brittle behaviour of cracked concrete under loading. However, this approach is not designed to track the formation of macro cracks, but instead, it modifies the stiffness material and stresses according to the presence of cracks (Ng et al., 2020).

- **The Brittle Cracking Model**

The BCM is implemented in ABAQUS/Explicit for applications in which the tensile cracking is dominating the behaviour of the material. This model is adequate if brittle tensile behaviour dominates the material behaviour such as plain concrete, ceramics and brittle rock. The compressive behaviour of the material is assumed to be linear-elastic, with simplification of the actual compressive behaviour. The BCM is considering mainly the brittle aspects of material behaviour and utilizes the smeared crack approach to represent the discontinuous brittle behaviour.

- **The Concrete Damaged Plasticity Model**

The Concrete Damaged Plasticity Model CDPM can be implemented in ABAQUS/Explicit and ABAQUS/Standard and can be used to analyse concrete and other quasi-brittle materials and to represent the inelastic behaviour of concrete. It uses the concept of isotropic tensile and compressive plasticity in combination with isotropic damaged elasticity to represent the inelastic behaviour of concrete. The development of the yield surface in the CDPM is controlled by two hardening variables, the compression equivalent plastic strain and the tensile equivalent plastic strain, which are related to the failure mechanisms under compression and tension loading (Stoner and Polak, 2020).

The stress-strain response under uniaxial tension loading follows a linear elastic relationship until it reaches the failure stress, then the micro-cracks occur which is categorised by the softening stress-strain response as shown in Figure 6-2b. In the case of uniaxial compression, the stress-strain relationship is linear up to the initial yield point, which is followed by stress hardening up until the ultimate stress point as shown in Figure 6-2a.

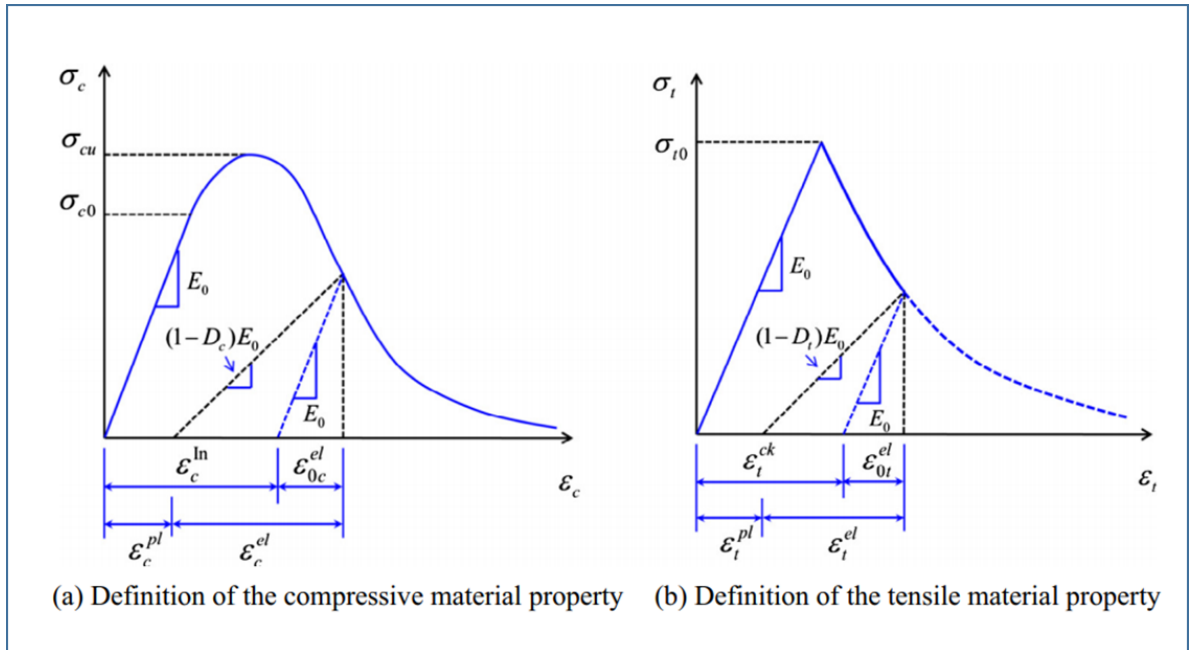


Figure 6-2: Definitions of the stress-strain curves of the concrete damage model in ABAQUS (Bitusca and Clausen, 2016)

The CDPM is defined by using the concrete compression hardening and concrete tension stiffening option and the concrete compression damage and tension damage options. Previous research by Sabău and Oneţ, (2011) cited that the Smearred Crack Model has a drawback since it may lead to the strain localization phenomenon which leads to zero energy consumption during crack development when the element size approaches zero. However, the Concrete Damaged Plasticity Model is highly versatile in modelling concrete under various loading conditions. Therefore, the CDPM was used for the beam nonlinear analysis performed in this study. The concrete damage plasticity parameters are shown in Table 6-1.

Table 6-1: The concrete damage plasticity parameters

	Modulus of elasticity (GPa)	Poisson ratio	Dilation angle, $\psi$	Eccentricity, $\epsilon$	$f_{b0}/f_{c0}$	$K_c$	Viscosity Parameter, $\mu$
NWC	28	0.2	36	0.1	1.16	0.667	0.0
FC	16	0.25	40	0.1	1.16	0.67	0.0

## 6.6 FE Modelling of Reinforcement in ABAQUS

For reinforced concrete modelling using the FEM, there are three approaches available for modelling reinforcement bars. They are the smeared model, the discrete model and the embedded model.

### 6.6.1 Smeared Model

In this model, it is assumed that the reinforcement is distributed uniformly in the concrete elements in a defined region of the FE mesh. Therefore, the material model properties in the element are constructed as share properties from individual properties of both reinforcement and concrete using composite theory. This method is suitable for a large scale model in which the reinforcement does not significantly contribute to the overall response of the structure, see Figure 6-3.

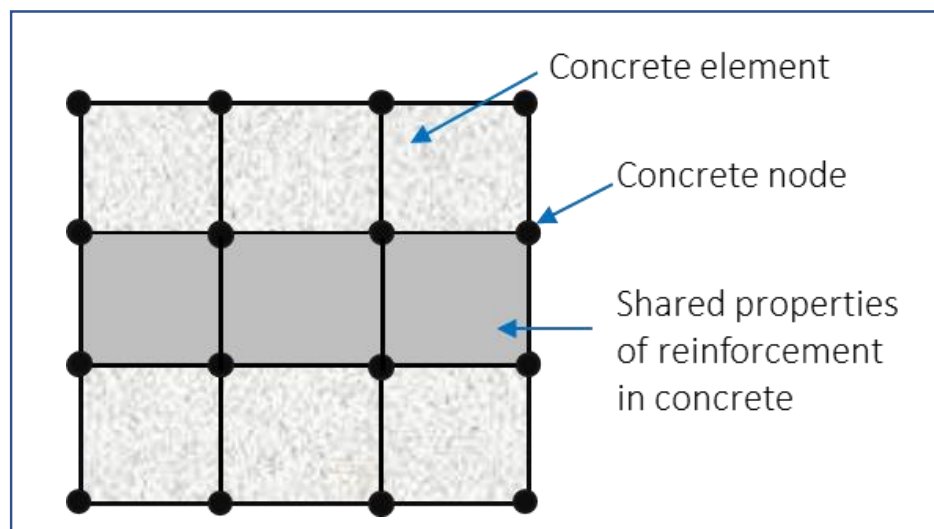


Figure 6-3: Smeared formulations for reinforced concrete

### 6.6.2 Discrete Model

In this model, the reinforcement is modelled by either using a beam or bar element which is connected to the concrete mesh nodes, creating shared nodes between reinforcement and concrete elements. In the DM technique, the reinforcement is superimposed in the concrete mesh. Therefore, the concrete occurs in the same regions occupied by the reinforcement, as shown in Figure 6-4. The discrete model technique drawback is that the concrete mesh is restricted by the location of the reinforcement.

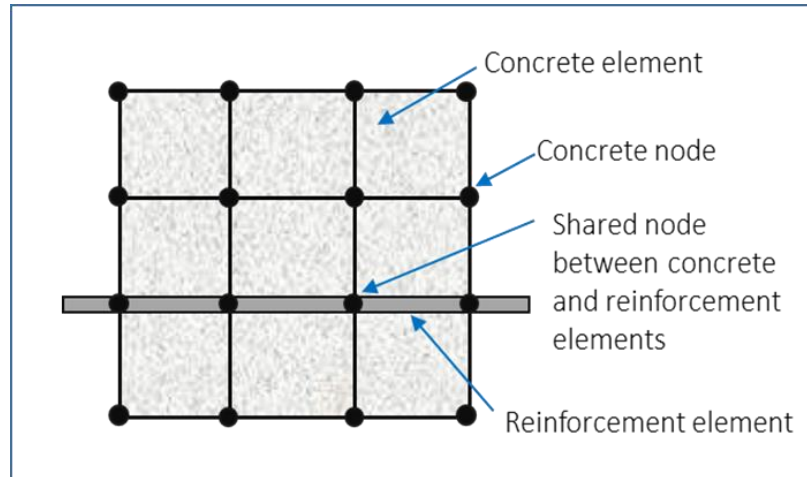


Figure 6-4: Shared nodes between concrete elements and reinforcement elements

### 6.6.3 Embedded Model

The embedded method was adopted in this study to model the reinforcement in the reinforced concrete beams. This method overcomes the drawback of mesh restrictions in the smeared and the discrete methods, as the stiffness evaluation in reinforcement elements is carried out separately from the concrete elements. In addition, in the embedded method the reinforcement elements displacement is compatible with the displacement of surrounding concrete elements. This method is adequate with complex models. Nevertheless, it increases the nodes and the degrees of freedom number in the model. Therefore, it requires more run time and increases the computational cost, as illustrated in Figure 6-5.

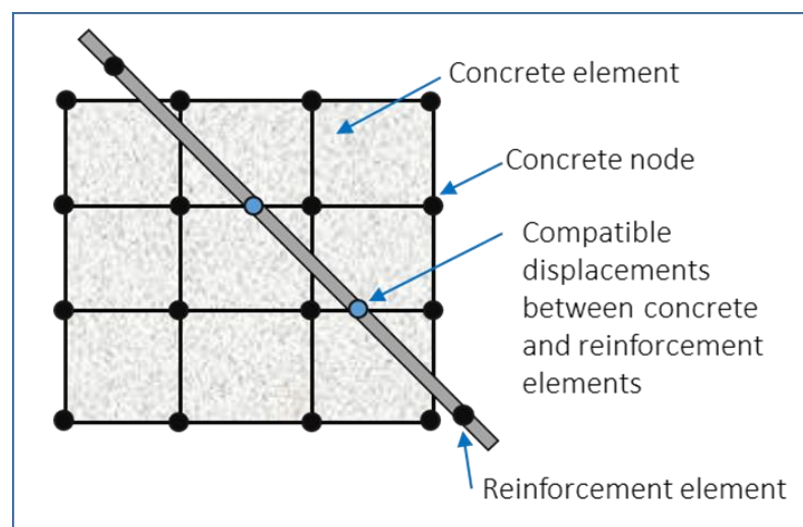


Figure 6-5: Embedded formulations for reinforced concrete

The embedded element technique is used to identify that an element or set of elements is embedded in “host” elements. For instance, the embedded element technique may be used to model rebar reinforcement as shown in Figure 6-6.

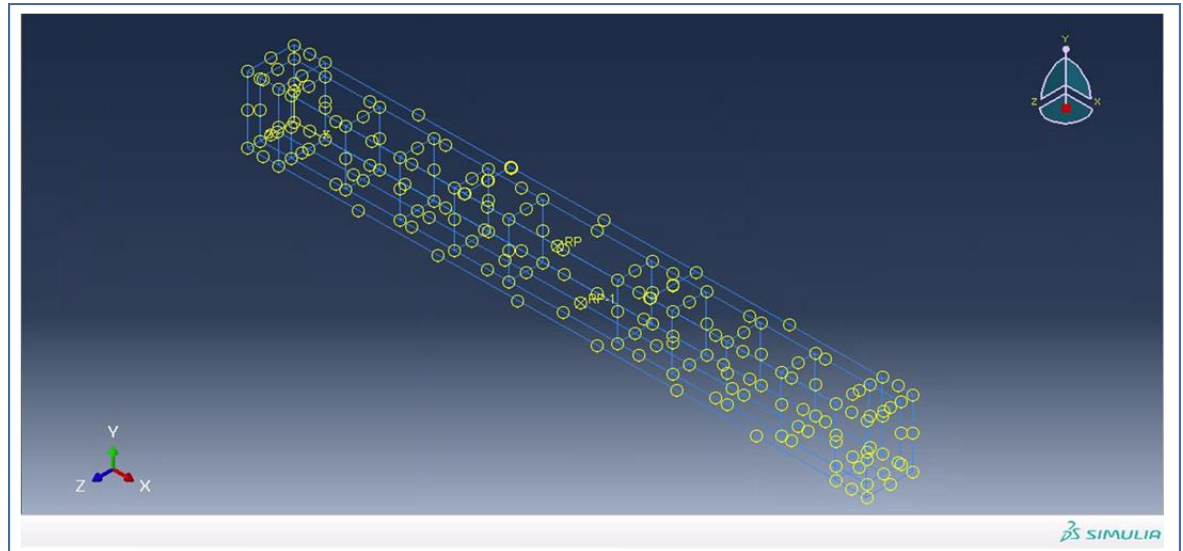


Figure 6-6: Embedded element technique applied for the reinforced concrete beams

## 6.7 Element Types

ABAQUS has a wide element library providing a comprehensive set of tools to solve various problems. In ABAQUS each element has a unique name, such as C3D8R, S4R, T2D2 or C3D8I.

### 6.7.1 Concrete

The 3D model was used for modelling the steel-reinforced and GFRP reinforced normal and foamed concrete beams. In the 2D models, the element has four nodes with two degrees of freedom at each node, translation in the x and y directions. This type of element is capable to calculate plastic deformation, cracking and crushing. The node locations and geometry for this element type are illustrated in Figure 6-7a. However, in the 3D models, eight-node linear brick was applied. This model has eight nodes with three degrees of freedom at each, translation in the x, y and z directions. They are able to predict plastic deformation, cracking, and crushing. The node locations and geometry for this element type are illustrated in Figure 6-7b.

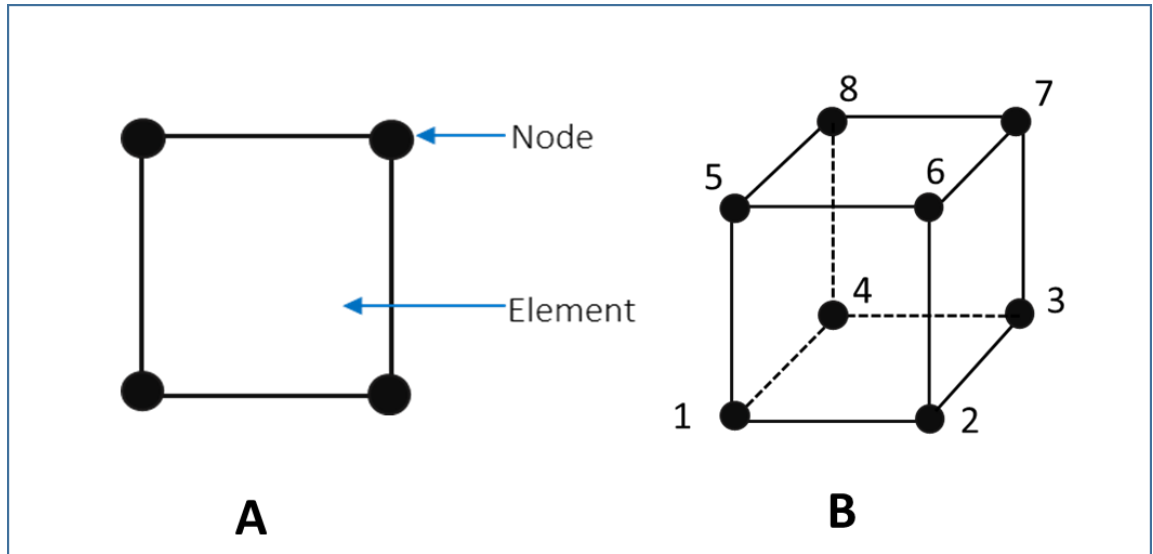


Figure 6-7: (A) Typical plane stress quadrilateral 4 node element (B) Typical 8 nodes linear brick element

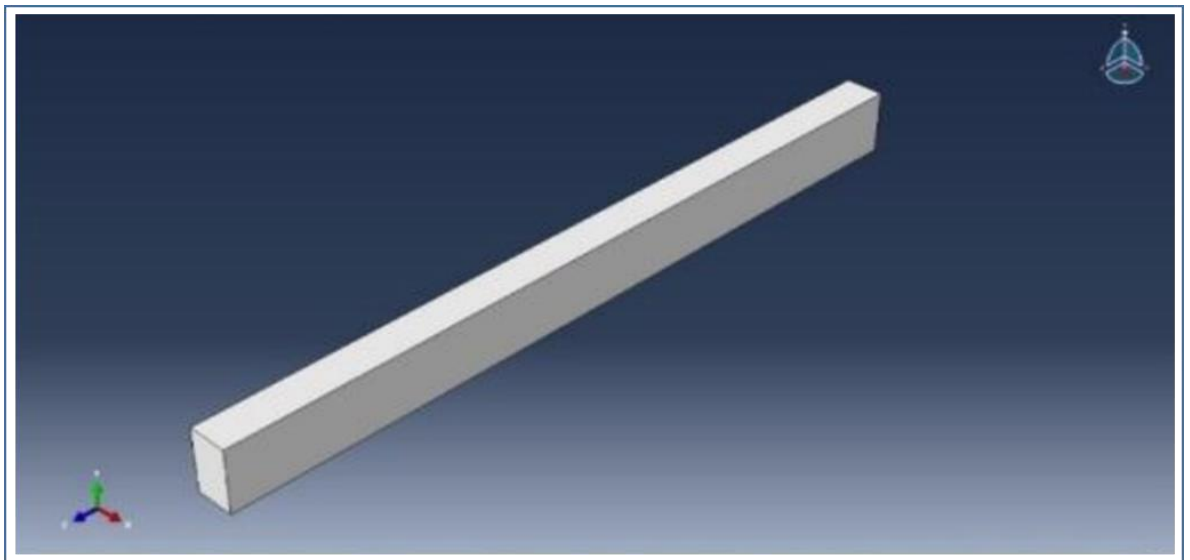


Figure 6-8: ABAQUS mode of the concrete beams

### 6.7.2 Reinforcement

Reinforcement bars (steel/GFRP) were modelled using 3D truss elements. In this model, a two-node linear T3D2 truss element was used. In ABAQUS the truss element is a slender long structural member that can transmit only axial force, as shown in Figure 6-9. Both steel rebars were embedded into the concrete element; henceforth no interface element

was needed and a perfect bond between concrete and steel reinforcement was applied. However, it was 95% between concrete and GFRP bars.

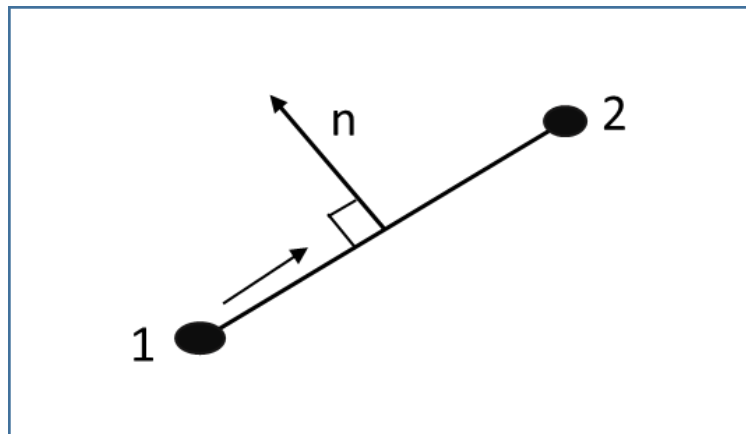


Figure 6-9: Typical 2 nodes truss element

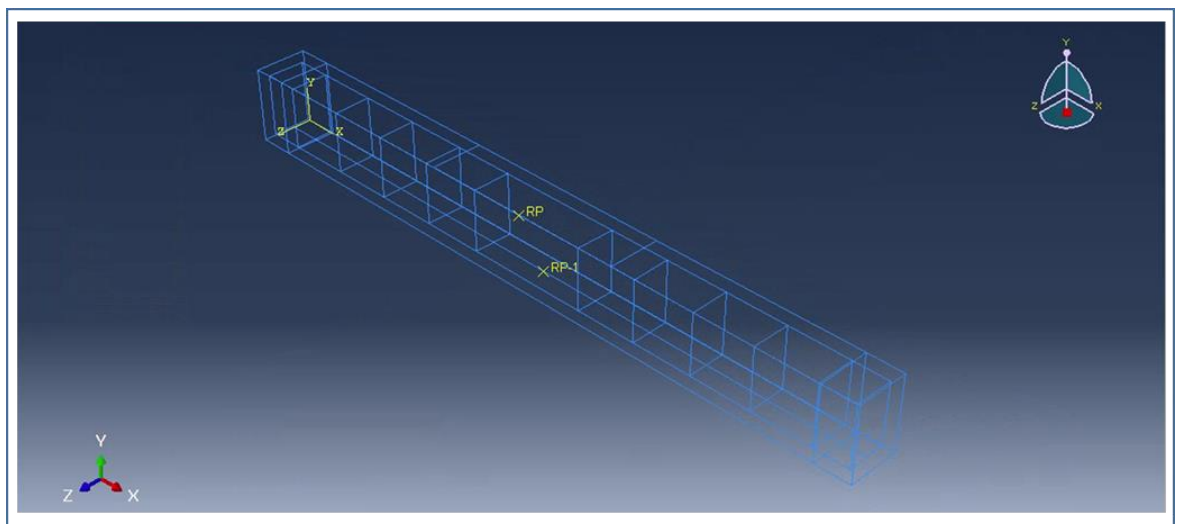


Figure 6-10: ABAQUS model of reinforcement

## 6.8 Materials Proprieties

Idealized elastic-perfectly plastic stress-strain behaviour is adopted in this study for every analysis, this approach built on the assumption that plastic yielding only occurs when the stress in the material reaches the value of the yielding stress up until failure.

### 6.8.1 Concrete

The concrete elastic behaviour was modelled considering a linear elasticity with a Poisson ratio and modulus of elasticity as constant. The values for both parameters are presented in Table 6-2. The modulus of elasticity is defined as the ratios of the stress over strain and represents the stiffness parameter of the concrete. Concrete is a quasi-brittle material and it behaves differently in compression and tension. C3D8 element type was used for concrete. Thus, the development of a model to study the behaviour of concrete could be a challenging task. Figure 6-11 illustrated a typical stress-strain curve for normal-weight concrete.

Table 6-2: Elastic parameters of concrete

Property	Normal concrete	Foamed concrete
Modulus of elasticity MPa	28000	16000
Poisson ratio	0.2	0.25

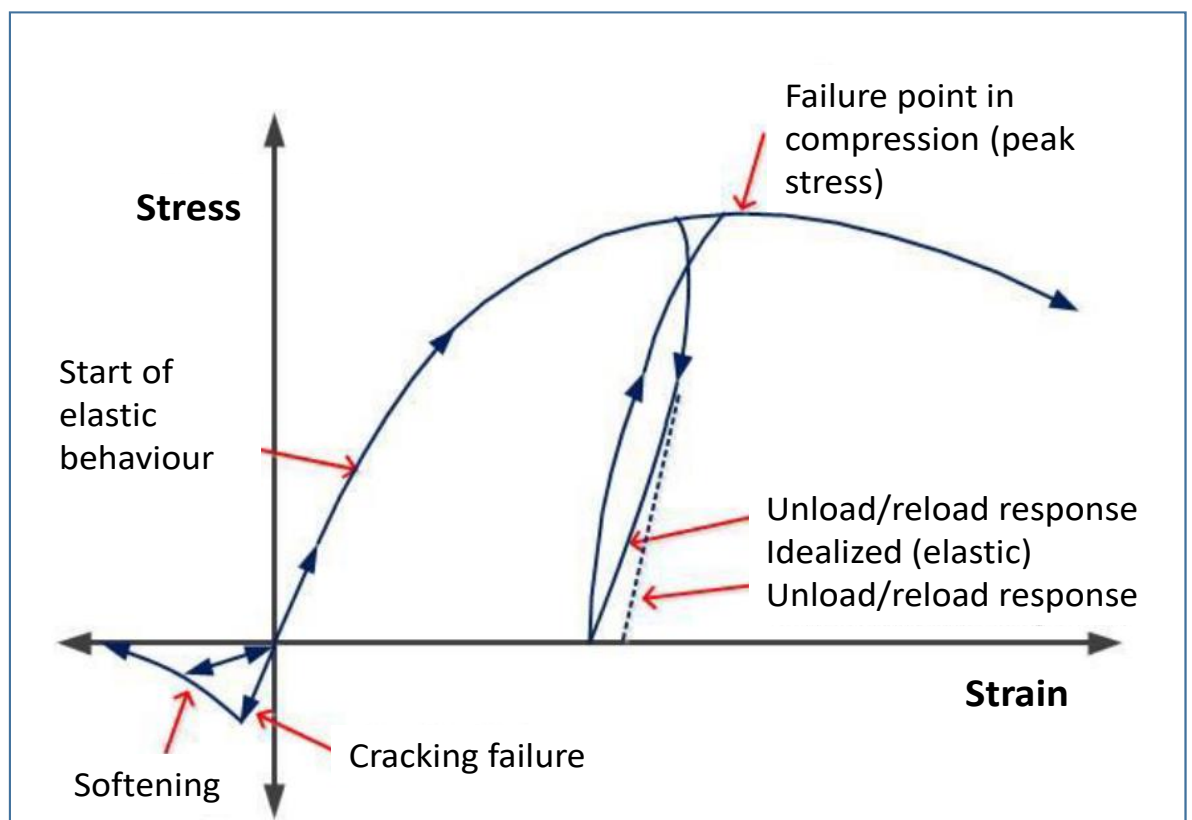


Figure 6-11: Typical uniaxial behaviour of plain concrete

### 6.8.2 Reinforcement Rebar

In modelling steel reinforcement in ABAQUS, it was assumed to be elastic-perfectly-plastic material. All steel properties including Poisson's ratio, the modulus of elasticity and the yield stress are presented in Table 6-3.

The two main aspects of GFRP that are important to consider when modelling the material are GFRP bars are: The rebar behaviour is perfectly elastic up to the ultimate stress of the material. It has a linear behaviour up to failure and its physical properties are directionally dependent. The GFRP rebar properties are presented in Table 6-3.

*Table 6-3: Steel and GFRP rebar main properties*

<b>Property</b>	<b>Steel</b>	<b>GFRP</b>
Young's Modulus MPa	200000	60000
Poisson ratio	0.3	0.2
Yield stress MPa	460	-
ultimate stress MPa	530	1000
Plastic strain	0.2%	2%
ultimate strain	0.5%	2%

### 6.9 Geometry

The beams dimensions are 150 x 220 x 2000 mm. The clear span between supports is 1800 mm. Tension reinforcement is 3H16 and 2H10 as hanger bars as shown in Figure 6-12. The bond strength between the steel/GFRP bars and the surrounding concrete was considered a perfect bond and 95% bond respectively. Hence the embedded region option was adopted in defining the reinforcement inside the host concrete element.

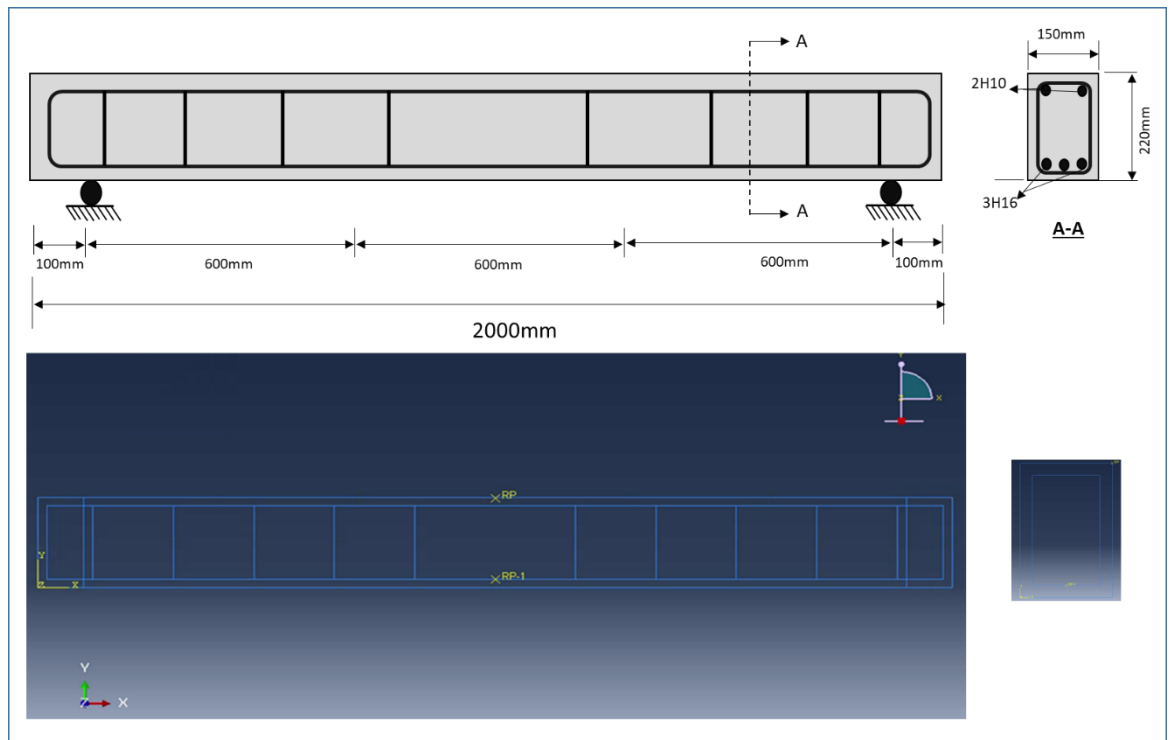


Figure 6-12: Beam geometry and diminutions

## 6.10 Meshing

The FEA requires the meshing of the model as an initial step. Therefore, the concrete beams (meshed) divided into a number of small elements. The stress and strain generated from the loading are calculated at the integration points of these elements. The selection of mesh density is an important step in finite element modelling. A results convergence was obtained in a reasonable analysis timeline when an adequate number of elements are used in a model. The meshed elements size was 24 mm in each direction as shown in Figure 6-13. This was achieved when an increase in mesh density has a negligible effect on the result. The initial mesh density study was achieved using a concrete beam in non-linear analysis, in which the model worked well and showed the beam deflection curve and failure.

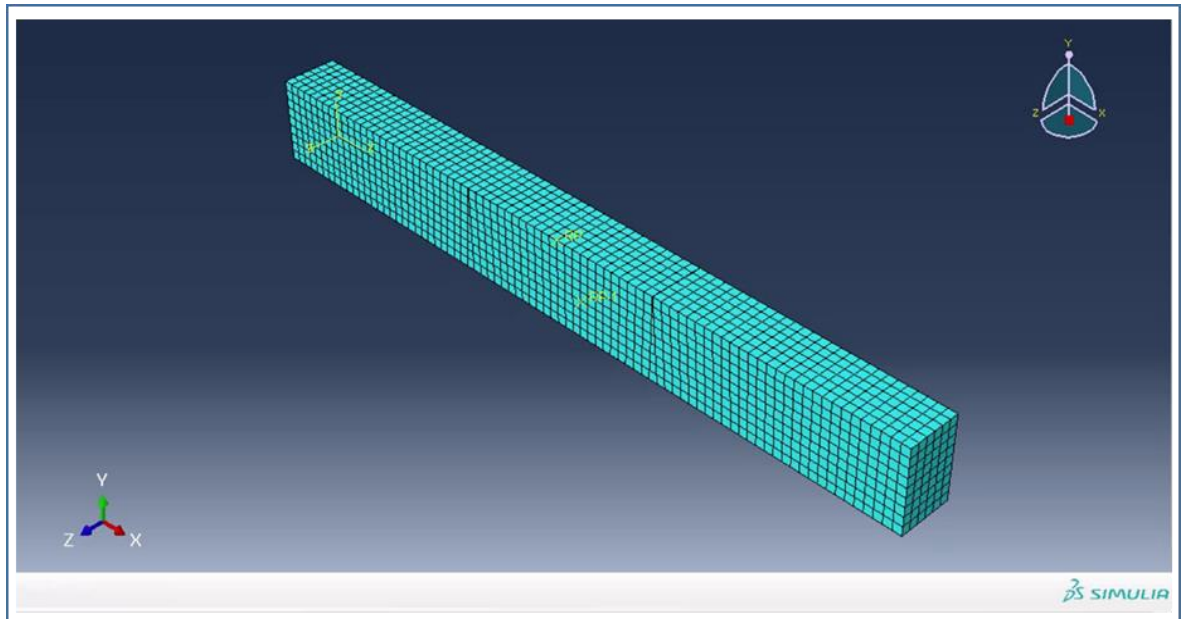


Figure 6-13: Concrete beam meshing

### 6.11 Loading and Boundary Conditions

The beams were tested under the four-point bending test. The beams FEM were set up according to the experimental beam testing. Two supports pinned and roller support applied at 100 mm from both ends of the beam. The boundary conditions and constraints type applied to the geometry are presented in Figure 6-14. The loads applied on 1/3 of the span length from both supports as shown in Figure 6-15. The loading rate that simulates the experimental test applied, with a load rate of 300 N/Sec.

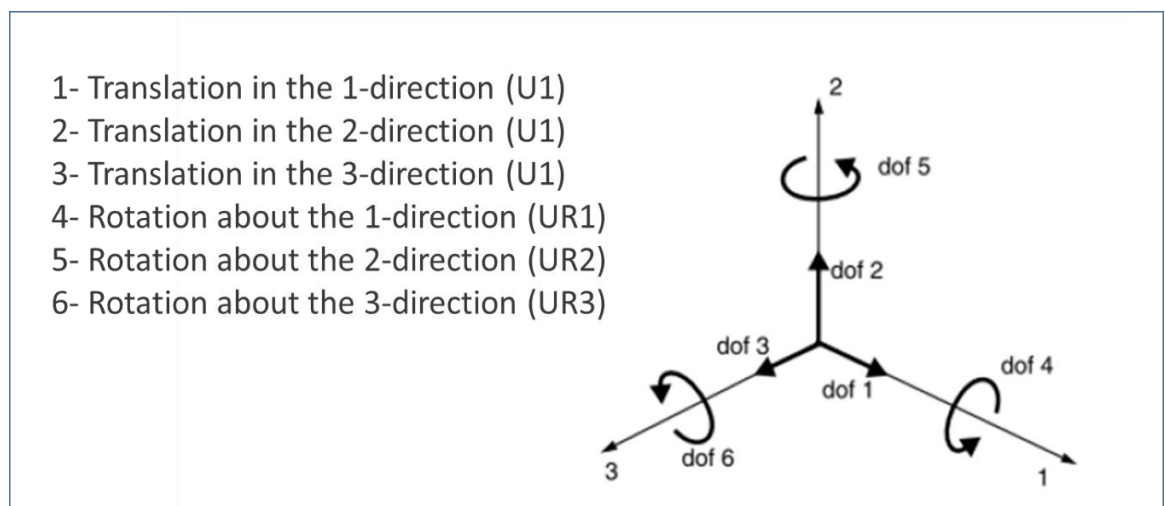


Figure 6-14: Boundary condition notation in ABAQUS

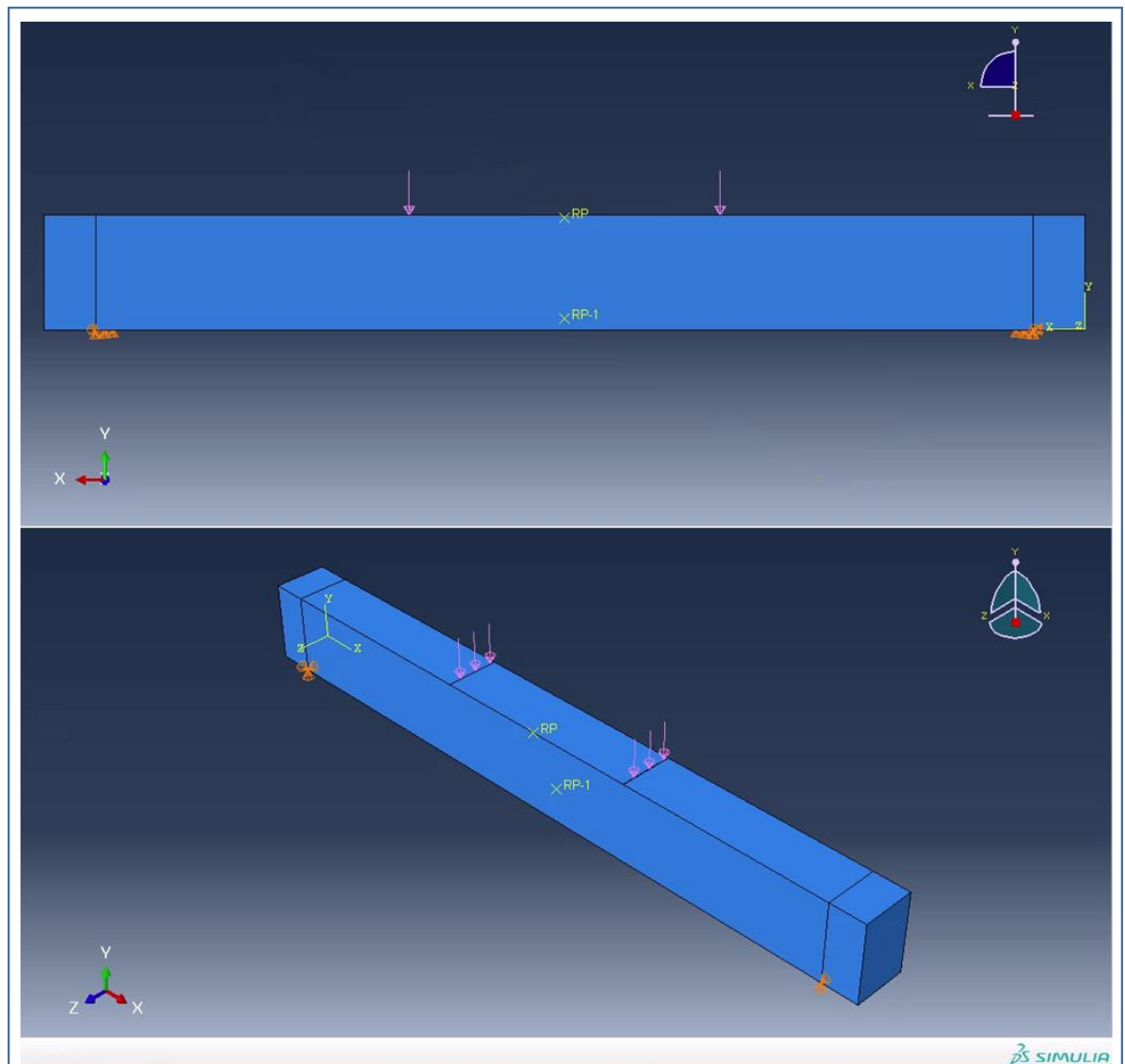


Figure 6-15: Supports and applied loads on concrete beams

## 6.12 Load Stepping and Failure Definition for FE Model

In ABAQUS automatic time stepping controls and predicts load step size for nonlinear analysis. After each step and based on the physics of the models and the previous solution history, when the convergence behaviour is smooth, the automatic time stepping increases the load increment up to a selected maximum load step size. However, if the convergence behaviour is abrupt, then the time-stepping bisects the load increment up until it is equal to a selected minimum load step size. Maximum and minimum load step sizes are required for the automatic time stepping. In the current study, the minimum increment size is  $1E-015$ , the increment initial size is 0.001 and the maximum increment size is 0.01. The time period set to be 0.1 and the maximum number of increments was 100000.

### 6.13 Methods for Non-Linear Solution

In ABAQUS there are several methods available for non-linear analysis such as the plastic method, the Newton Raphson method, and the modified Newton Raphson method. Modified Newton Raphson approach was adopted in this study to solving the simultaneous equations and finding incremental equilibrium, which is an iterative process of solving the non-linear equations.

In the non-linear approach, the load was broken down into a series of load increments. The load increments applied over several load steps within a load step. At the completion of each incremental solution, ABAQUS amends the stiffness matrix to reflect the non-linear changes in structural stiffness in advance proceeding to the next load increment. The flowchart shown in Figure 6-16 summarises the nonlinear finite element analysis procedures for steel/GFRP-reinforced concrete beams.

Furthermore, the concrete damage plasticity parameters for concrete are given in Table 6-1. Therefore, the degradation of concrete under both compression and tension is captured in the FE model. Simply supported boundary conditions were simulated for all the beams. The typical assembly of different parts and FE model is shown in Figure 6-12, Figure 6-13 and Figure 6-15. Nonlinear FE analysis by using Newton- Raphson method was performed for the normal and foamed concrete beams reinforced with steel or GFRP bars.

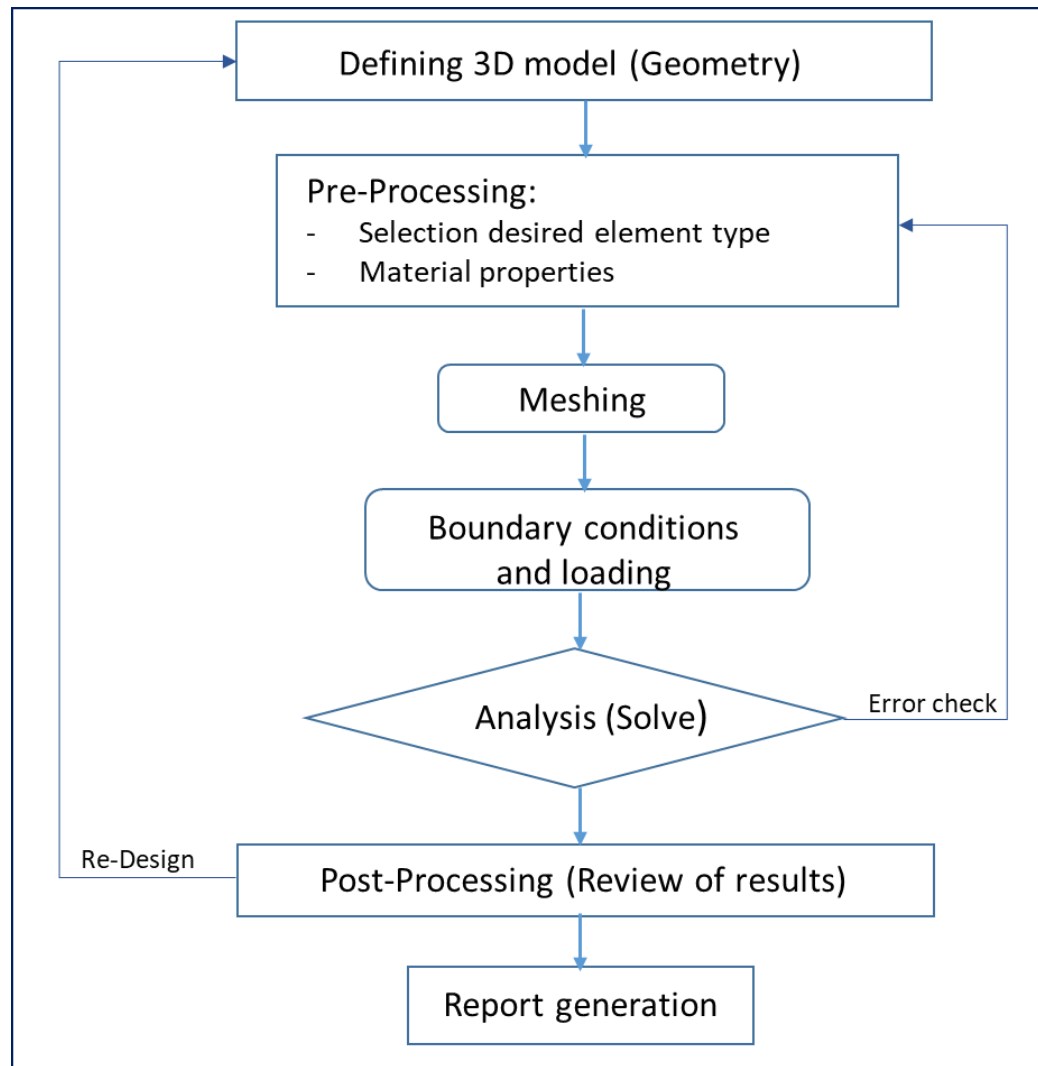


Figure 6-16: Steps in ABAQUS simulation

### 6.14 Numerical Modelling Results

One of the key objectives of this study is to investigate the flexural behaviour of normal/foamed concrete beams reinforced with steel/GFRP. The chapter investigates the moment capacity, crack pattern, mode of failure of foamed concrete beam reinforced with GFRP. Additionally, a comparison is carried out of different methods to determine the ultimate moment capacity and load-deflection relationship of foamed reinforced concrete with GFRP. The four beams tested under static loading were analysed using the ABAQUS/CAE.

#### 6.14.1 Load-Deflection Analysis

The load-deflection relationship for reinforced concrete beams analysis is a very essential aspect especially from the serviceability point of view. It was discussed in the literature review chapter that GFRP bars have a lower modulus of elasticity compared to conventional steel. Consequently, the deflection limit is a principal parameter in GFRP reinforced concrete design. The beams were tested under a four-point load test and analysed by using ABAQUS non-linear finite element analysis. The nonlinear load-deformation response of the concrete beams at different load levels are presented in Figure 6-17. The beams NC+S, FC+S, NC+GFRP and FC+GFRP exhibit ultimate loads of 140 kN, 134 kN, 121 kN and 125 kN respectively, and the corresponding mid-span deflections obtained were 15 mm, 21 mm, 26 mm and 29 mm respectively. It was found that GFRP reinforced beams experienced larger deflections than steel-reinforced beams by an average of 38%. However, It is noticed that the FC+GFRP beam has only 10% less ultimate load than the NC+S beam even though the modulus of elasticity of GFRP is less than 1/3 of that in steel and foamed concrete has less than 50% modulus of elasticity of that in normal-weight concrete.

The load–Midspan deflection curves for all steel/GFRP reinforced beams are presented in Figure 6-18. The first part of the curve up to the crack point (0-20 kN) represents the behaviour of the un-cracked beams. The second part (higher than 20 kN) represents the behaviour of the cracked beams with reduced stiffness. It noticed that, as the modulus of elasticity of the GFRP bars reduced, the reinforcement’s axial stiffness declined, leading to an increase in mid-span deflections.

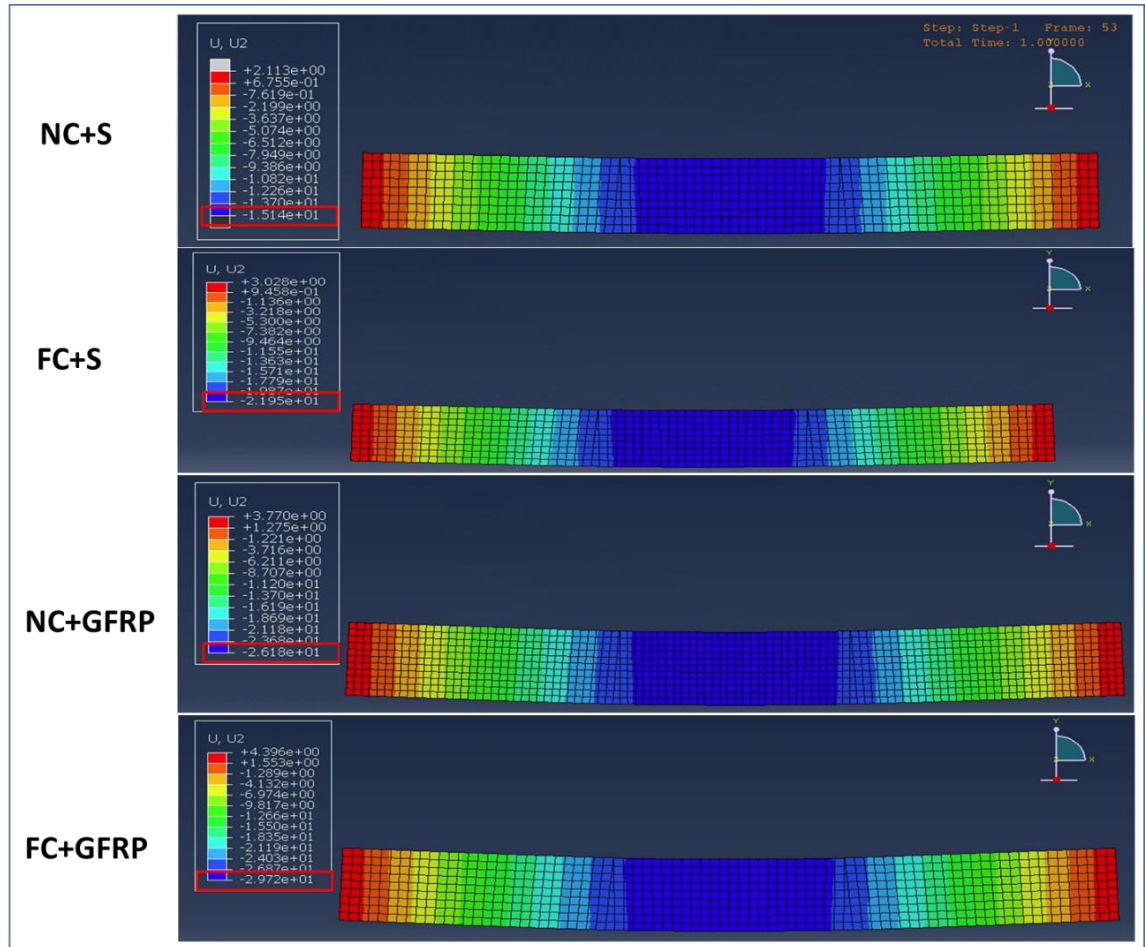


Figure 6-17: FEA ABAQUS mid-span deflection of GFRP and steel-reinforced beams

The test results obtained experimentally and those obtained through non-linear finite element analysis were compared in Figure 6-18. The entire load-deformation response of the model produced in ABAQUS compares well with the response from the experimental testing, which gave confidence in the use of ABAQUS and the model developed. Figure 6-18 shows the numerical and experimental mid-span load-deflection relationship of GFRP and steel-reinforced foamed and normal concrete beams.

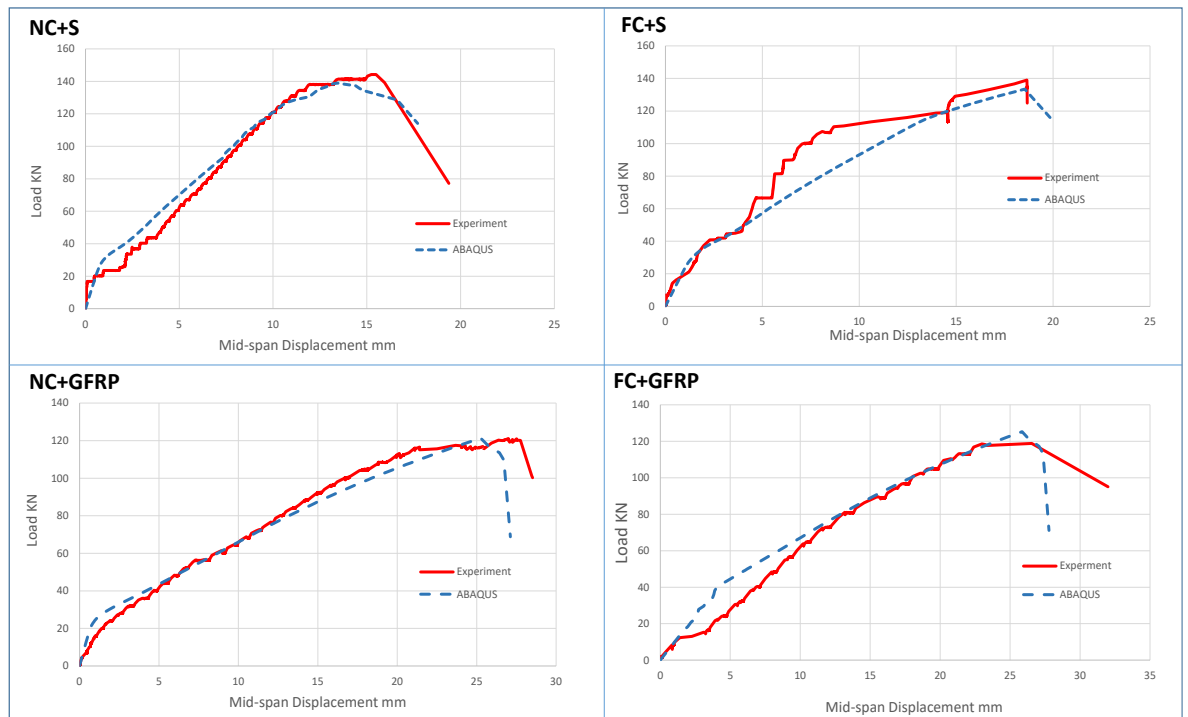


Figure 6-18: Load-deflection values (ABAQUS Vs Experiment)

#### 6.14.2 Strain Distribution of Beam Section.

The development of strains distributions in both the extreme compression fibre of the concrete and in the tension reinforcement bars are illustrated in Figure 6-19. ABAQUS calculated and recalculated strains in each node of the beam with the increase of the applied loads. Figure 6-19 shows nonlinear strain distribution at the mid-span in the beam's section every 25 kN increment.

Strains developed in concrete and reinforcement bars were plotted for steel and GFRP reinforced beams. It was noticed that the strains developed linearly across the section up to the cracking point with an applied load around 20 kN, as shown in Figure 6-19. It was found that the strains developed in GFRP reinforcement in NC+GFRP and FC+GFRP beams have significantly higher values than the strain in steel bars in steel-reinforced beams. The ultimate strains in compression normal concrete recorded in NC+S and NC+GFRP beams reached values of 0.00325 and 0.0032 respectively. However, foamed concrete beams FC+S and FC+GFRP recorded higher compression strain values of 0.0039 and 0.00385 respectively.

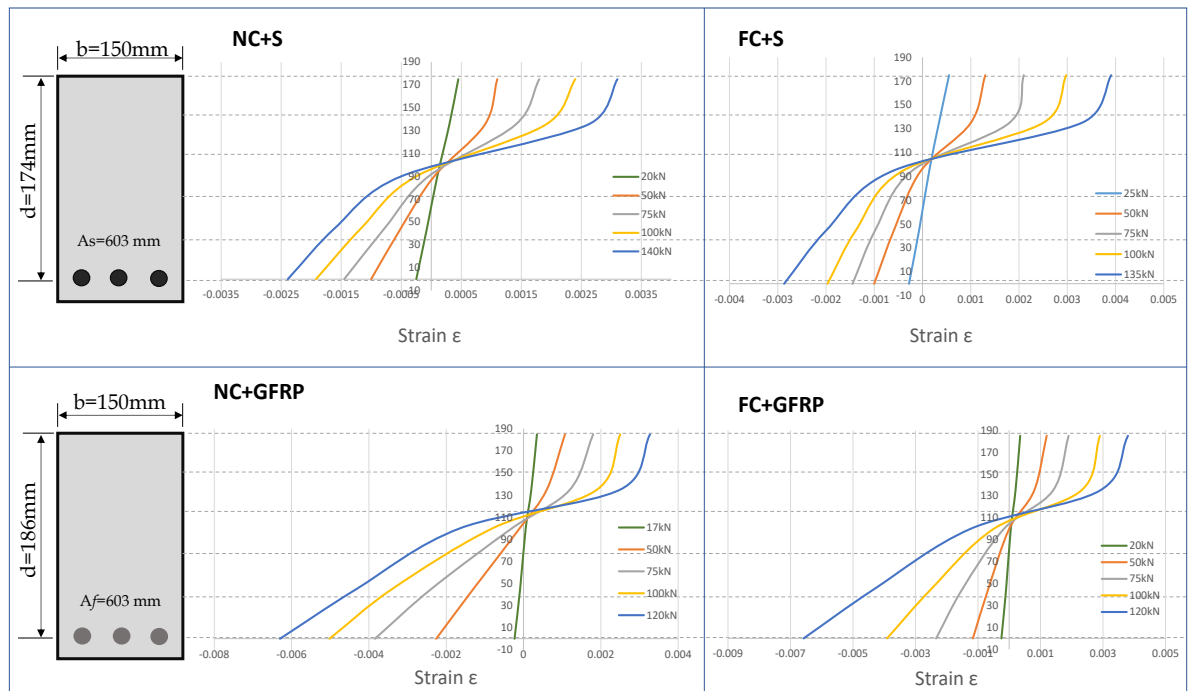


Figure 6-19: Non-linear strain distribution along the depth of the beams

Due to its low modulus of elasticity, GFRP reinforcing bars experienced higher strain values than steel reinforcing bars by more than 100%, where GFRP bars in beams NC+GFRP and FC+GFRP reached strain of 0.00615 and 0.0064 respectively as illustrated in Figure 6-19.

Figure 6-20 presents FEA measured stresses of the reinforcement under the ultimate applied load. Steel reinforcement bars in beam NC+S and FC+S reached tensile stress values of 480 MPa and 446 MPa respectively. However, the tensile stress in GFRP bars at ultimate load reached 355 MPa and 382 MPa for beam NC+GFRP and FC+GFRP respectively. Tensile stresses developed in GFRP reinforcement bars under ultimate load are 25% less than tensile stresses developed in steel reinforcement and that mainly due to the low modulus of elasticity of GFRP bars compared to steel.

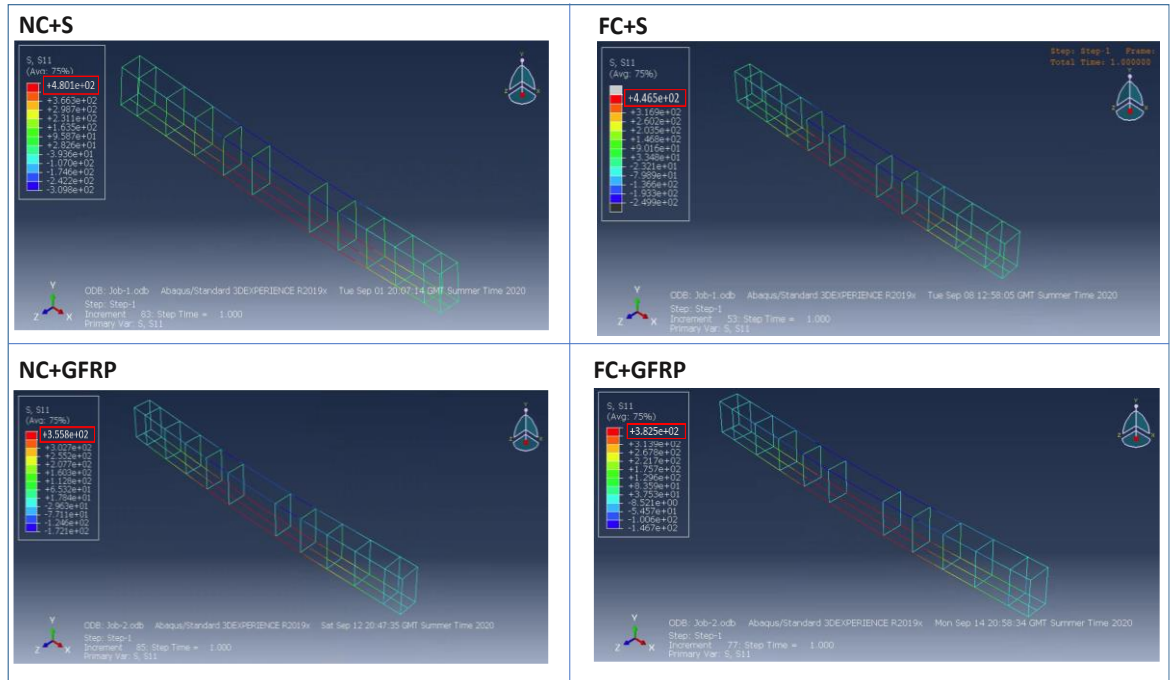


Figure 6-20: The stress in reinforcement at the ultimate applied load

### 6.14.3 Moment Resistance of RC Beam

At the initial stage of ABAQUS beam loading, the beams behaved in a linear elastic manner until cracks appeared at a moment of 20-35% of the ultimate moment at failure and a mid-span deflection of 9–15% of the ultimate deflection. Figure 6-21 compares the moment capacity predictions obtained from the theoretical derivations of the reinforced concrete beam in the current study against the experimental and FEA moment capacity of steel and GFRP reinforced beams. It is indicated that there is a great agreement between the experimental and FEA moments capacity. The theoretical equations reasonably predicted the failure moments of the steel-reinforced beams and underestimated the moment capacity for beams reinforced with GFRP.

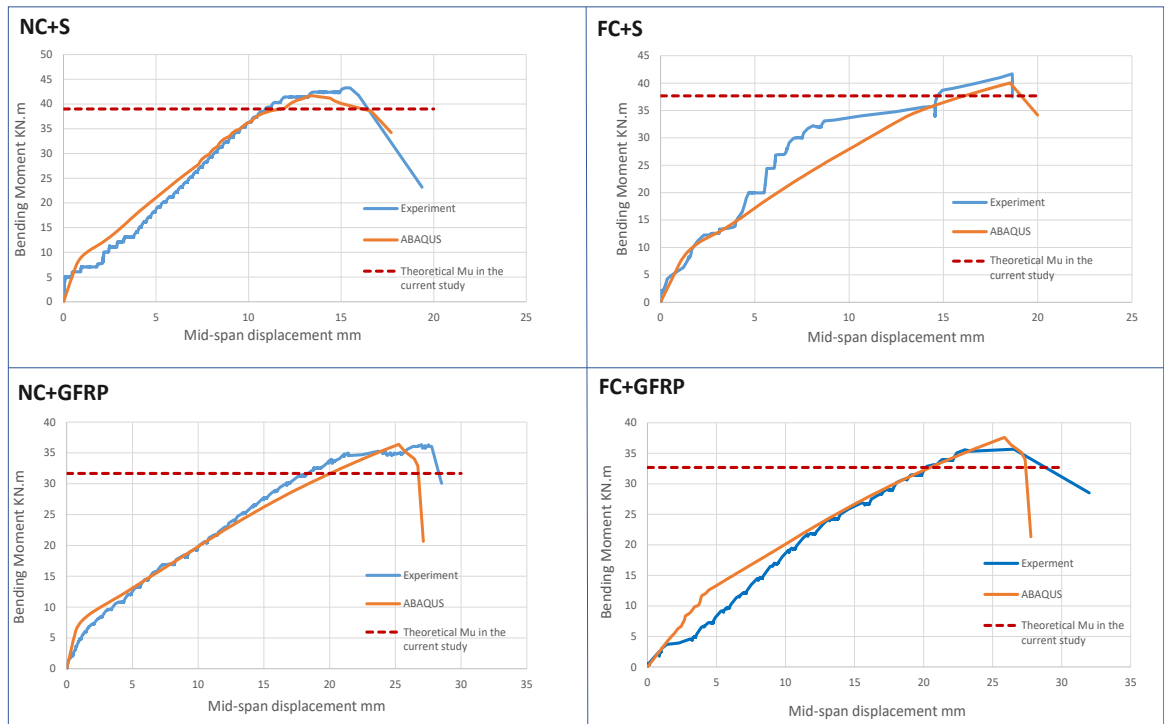


Figure 6-21: The theoretical, experimental and ABAQUS moment capacity of the beams

#### 6.14.4 Cracking Pattern and Failure Mode

The failure modes for all beams were observed and examined in the FEA and experiment. The increasing applied load was set in constant increments until failure. The figures below show the cracking behaviour and failure mode of the beams. The load applied on the beams in the increment of 300 N/Sec, all beams show relatively low deflection until the beams reached the cracking point. It was observed that foamed concrete beams FC+S and FC+GFRP illustrated higher cracking loads compared to normal weight concrete beams by 22%.

When the applied loads accessed the cracking loads, 20.15 kN, 25.39 kN, 16.96 kN and 19.97 kN respectively for beams NC+S, FC+S, NC+GFRP and FC+GFRP the vertical cracks started to develop from the extreme tension fibre zone of the concrete section. The formation of further cracks increased, and the former cracks propagated and widened as the applied load increases.

When the applied loads reached 70-90% of the ultimate load, the concrete started to fail in the tension zone, and the stiffness of the beam started to decline dramatically, and large deformations started to be observed. Additionally, diagonal shear cracks developed at each

support. When the applied load reached as high as 120 kN -140 kN the beams start to fail. Figure 6-22 to Figure 6-25 illustrated the ABAQUS crack pattern and failure mode of all beams. In both beams, NC+S and NC+GFRP, the extreme compression fibre zone of the concrete section was yielded and some disconnected diagonal shear lines yielding as well. However, beams FC+S and FC+GFRP experienced less yielding in the concrete compression fibre zone and more yielding of the shear diagonal lines. The failure modes of all beams in FEA concrete have great much with the failure mode of the beams in the experimental programme as shown in the figures below.

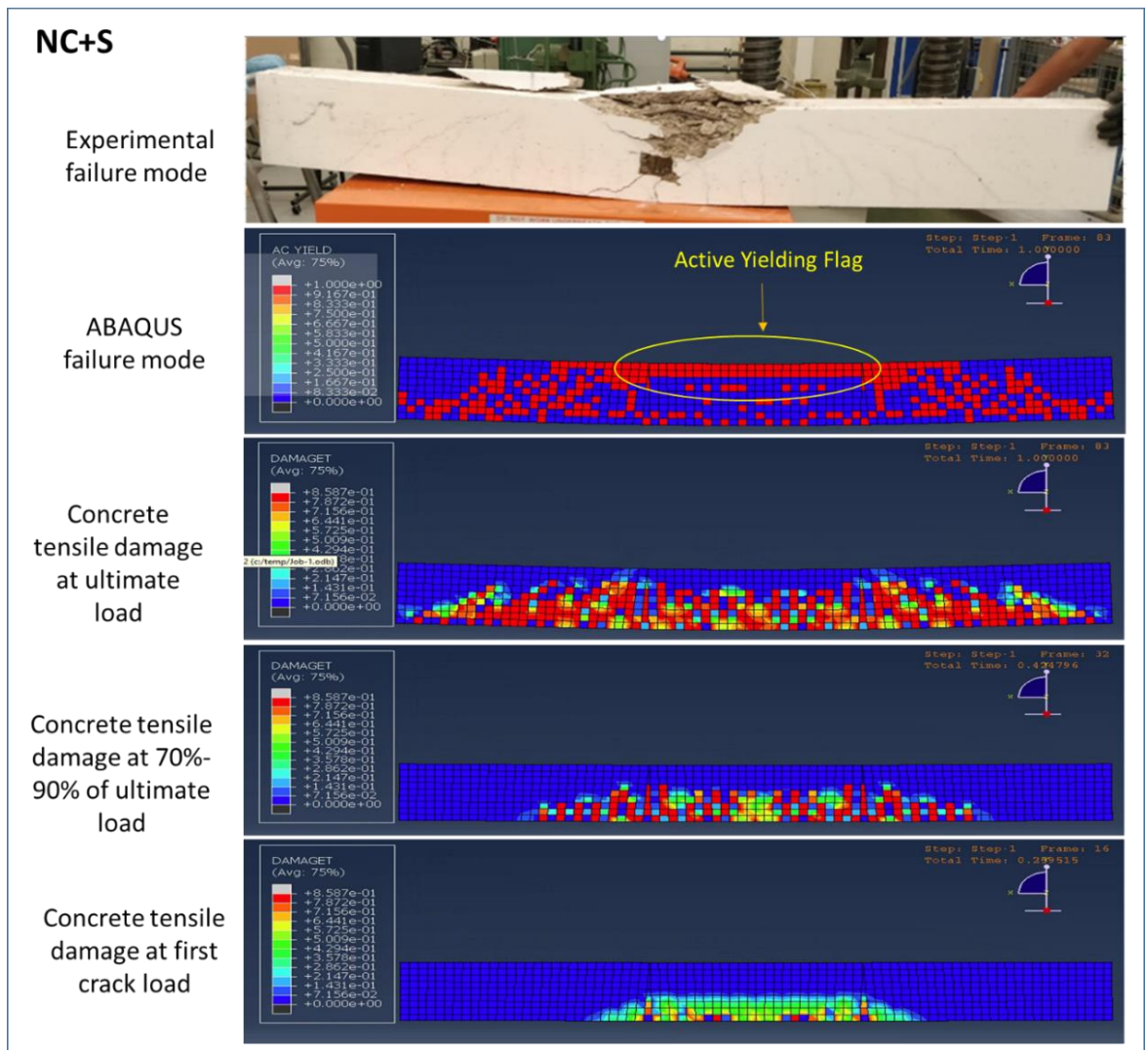


Figure 6-22: Normal concrete reinforced with steel crack pattern and failure mode in ABAQUS

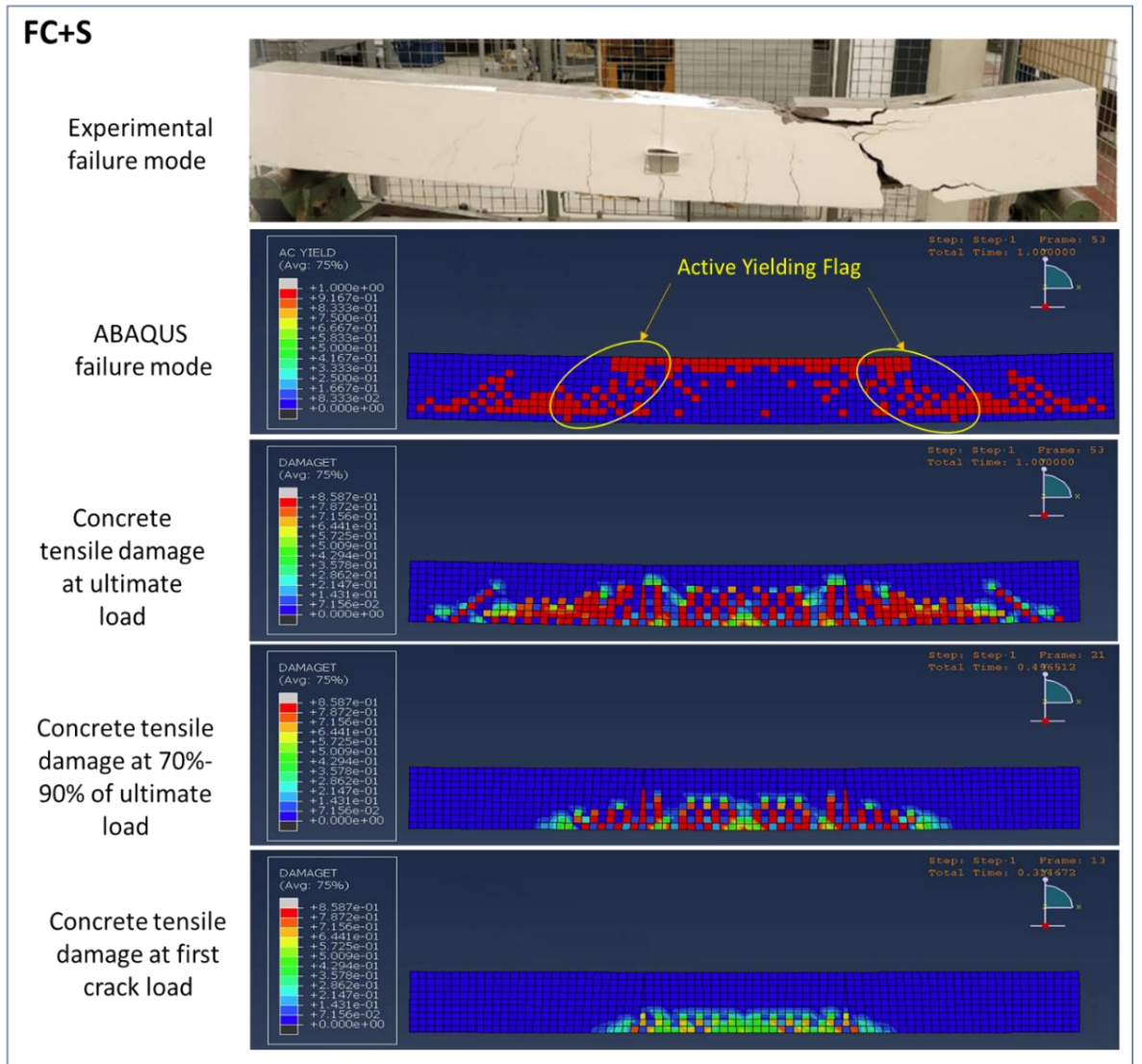


Figure 6-23: Foamed concrete reinforced with steel crack pattern and failure mode in ABAQUS

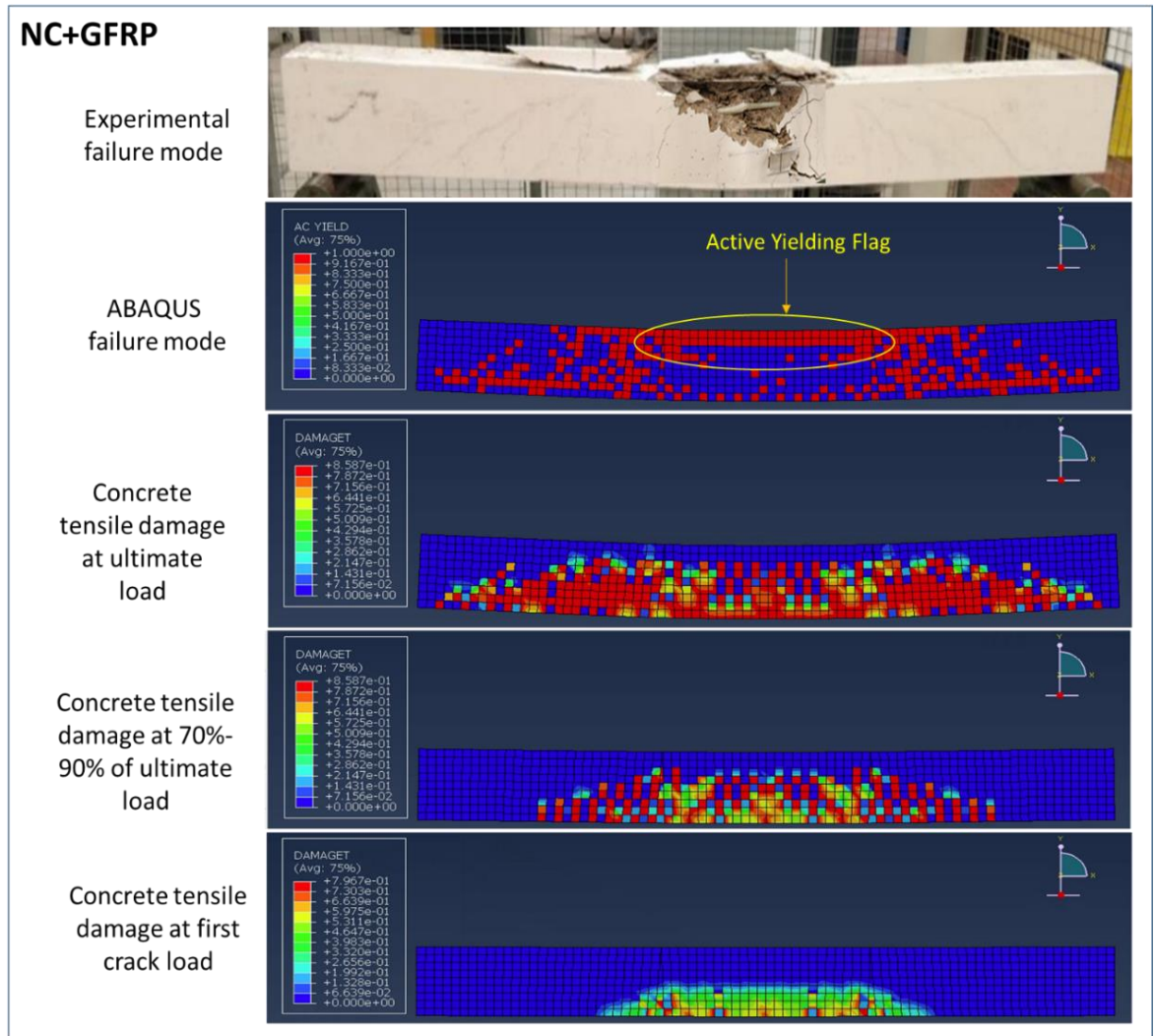


Figure 6-24: Normal concrete reinforced with GFRP crack pattern and failure mode in ABAQUS

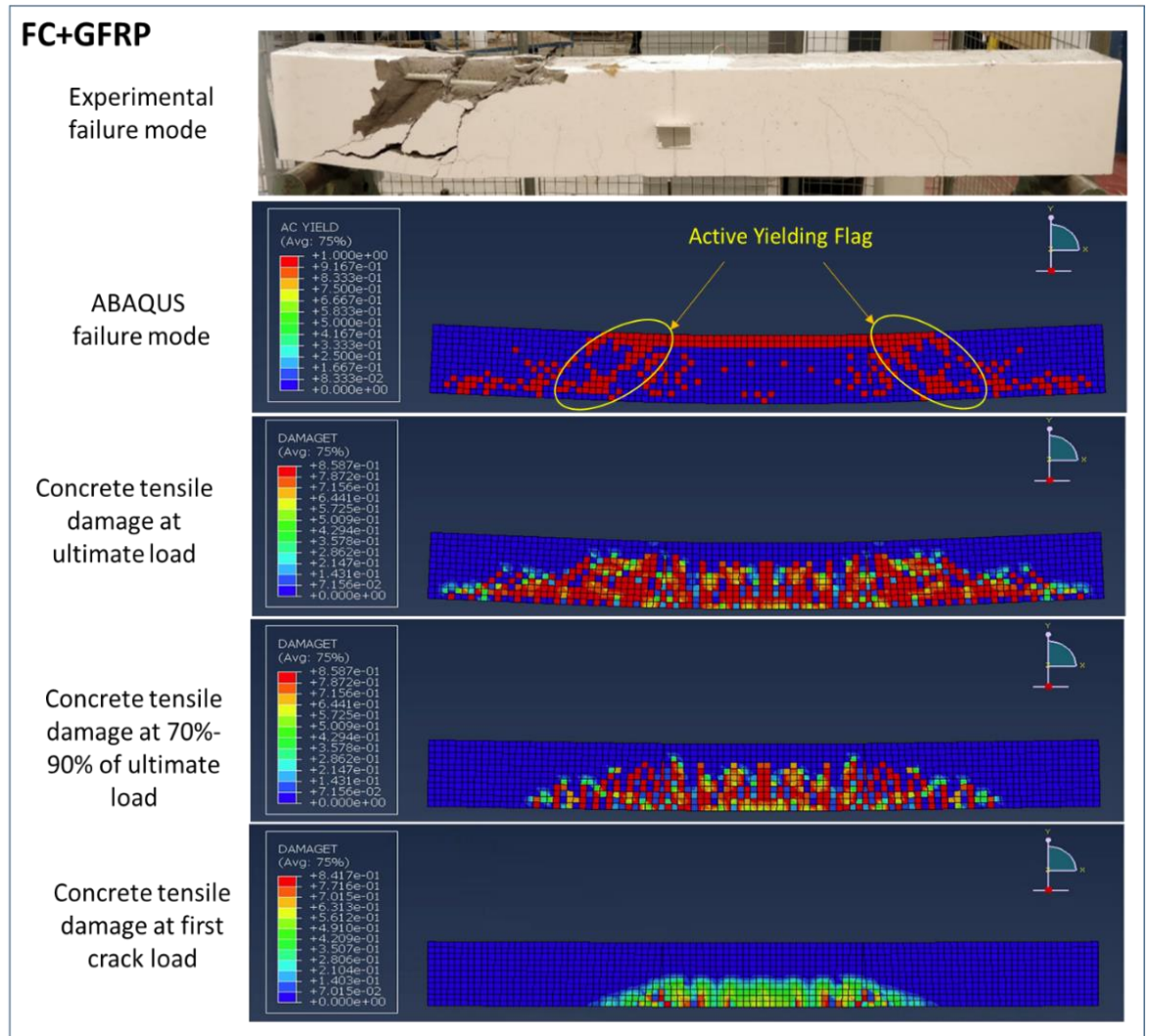


Figure 6-25: Foamed concrete reinforced with GFRP crack pattern and failure mode in ABAQUS

Both experimental beam testing and ABAQUS simulations have agreed on the general crack pattern failure mode. Nevertheless, the ABAQUS simulation was unable to show hair cracking propagation surrounds the beam model compared with beams in the experimental testing. This suggests that tensile and compressive behaviour data in the concrete damage plasticity beam model is highly beneficial but limited to predict the flexural strength, main crack pattern and failure mode, this limitation can be overcome by the addition of pre-cracking displacement and fracture energy in the input manager as suggested by the previous researcher.

### 6.15 Summary

This chapter presents a finite element analysis for normal weight and foamed concrete beams reinforced with steel and GFRP bars. Foamed concrete is an alternative material to normal weight concrete, and GFRP is an available alternative material to replace steel reinforcements in concrete structures. Four-point bending tests conducted on the steel and GFRP reinforced beams. The main finding might be summarised as follows:

- The results from FEA, which are presented in the load-displacement plot show good agreement with the experiment results.
- GFRP reinforced beams experienced larger deflections than steel-reinforced beams by an average of 38%. However, GFRP reinforced beams experienced only 10% less ultimate load than steel-reinforced beams despite the fact that the modulus of elasticity of GFRP is less than 1/3 of that in steel.
- Due to its low modulus of elasticity, GFRP reinforcement bars show higher strain values than steel-reinforced bars by more than 100% at the ultimate load.
- The theoretical equations developed in this study reasonably predicted the failure moments of the steel/ GFRP reinforced.
- Foamed concrete beams have higher cracking moments than normal-weight concrete by 20% and less ultimate moment capacity by 10%.
- The failure modes of all concrete beams in FEA match the failure mode of the beams in the experimental programme well. However, the FEA simulation was unable to show hair cracking propagation surrounding the beam model compared with beams in the experimental testing.

## Chapter 7

### Conclusions and Recommendations

#### 7.1 Overview

The use of normal weight concrete reinforced with steel in the future construction industry is facing a number of obstacles due to its relatively heavy weight with a density of 2500 kg/m<sup>3</sup>. Reinforcement corrosion has been one of the main durability problems in reinforced concrete and it is the chief factor in limiting the life expectancy of RC structures.

Foamed concrete is known as a lightweight with low-grade strength, high porosity and permeability which can only be used for non- or semi-structural applications. However, adding a waste material namely toner to the mix improved the concrete mechanical properties where the compressive strength exceeds the minimum strength of 25 N/mm<sup>2</sup> required for structural applications.

#### 7.2 Conclusions

From the results and discussions of the experimental, theoretical and numerical analysis of this research on developing mechanical properties and structural behaviour of foamed concrete, the following conclusions can be drawn:

- The FC properties more independently follow its density and the type of additives they consist of. Subsequently, the stress-strain relationship is different for FC mixes based on either the density or on the additive materials used.
- The use of additives Waste Toner, Metakaolin and silica fume improve the compressive strength of the FC at all densities. Waste Toner improved the concrete mechanical properties where the compressive strength exceeds the minimum strength of 25 N/mm<sup>2</sup> required for structural applications.
- Waste Toner as an additive has the highest effect on FC mechanical properties compared to MK and SF. It increases the compressive strength by an average of 30%, tensile strength by 20%, shear strength by 15% and modulus of elasticity by 22%.

- The 18Ton mix showed a strain in the maximum stress of 0.0045, compared to 0.0035 for normal-weight concrete. Foamed concrete properties are more independently follow its density and the type of additives they consist of. Subsequently, the stress-strain relationship will have to be established for every type of FC, to be based on either the density or on the materials used.
- The tensile strength of foamed concrete is positively proportional to the density and strongly affected by additives. Indirect tensile strength, splitting and flexural strength are higher than direct tensile strength. More investigations might be needed to confirm the empirical equations for tensile strength, flexural strength and modulus of elasticity of FC of different densities, with the various strengths, and the different factors controlling the strength. The equations will have to adapt to all the conditions mentioned above.
- Experimentally, it was found that GFRP bars have 95% of the steel bond with FC and bond failure occurred partly on the surface between concrete and resin and partly near the surface between resin and glass fibres. The bond strength of steel/GFRP bars tended to increase when the compressive strength of concrete increased.
- The equations obtained from the theoretical derivations of the reinforced concrete beams in the current study to determine the ultimate moment showed a slight under-estimation compared to experimental results. The ACI-440 equations showed similarity with the experimental ultimate moment in both normal and foamed concrete beams reinforced with steel.
- Foamed concrete beams are found to have a higher cracking moment and few cracks compared to normal weight concrete beams. However, the cracks are bigger, which may be attributed to the shear effect combined with flexure at failure. Foamed concrete GFRP reinforced beams illustrated higher deflection than the steel-reinforced beams, owing to the lower elastic modulus of GFRP bars compared with steel. Nevertheless, they show a relatively higher ultimate moment capacity by almost 90% of that in normal-weight concrete beams reinforced with steel bars.
- Three-dimensional, nonlinear finite element models were developed to replicate four beams tested experimentally. The nonlinear model of normal and foamed concrete

reflects relatively well the behaviour of the actual concrete beam experimental results. However, the nonlinear finite element models showed no hair cracking propagation surrounding the beam model compared with beams in the experimental testing.

- As a final concluding remark, the FC as known today has only been used in non-structural applications, while with this research, the compressive strength has been upgraded to over  $25 \text{ N/mm}^2$ . Therefore, Waste Toner foamed concrete with a plastic density ranging between  $1600\text{-}1800 \text{ kg/m}^3$ , reinforced with GFRP is an eco-friendly material that has a great potential to be used in structural applications.

### 7.3 Recommendations for Future Work

Further research works can be carried out to advance the current state of this research project on the following subjects:

- Waste Toner and other waste materials can be further investigated in different ratios for densities from  $(1500 \text{ to } 1800) \text{ kg/m}^3$ , at  $100 \text{ kg/m}^3$  intervals, to find the trend of strength and other physical and mechanical and structural properties which haven't been investigated in this research. Carrying out a bigger project of this type could lead to the introduction of standard code for FC in structural applications.
- Steam curing method for the specimens can be examined for waste toner foamed concrete as this method showed good results with precast low-density lightweight concrete.
- Further investigation is required to improve the formulas for modulus of elasticity, tensile and flexural strength to predict the mechanical properties of foamed concrete from the compressive strength more accurately. The modification factor needs to be calculated for different concrete densities and materials used in the production of the FC.
- Further studies on different structural members such as slabs, columns or foundations made of waste toner foamed concrete reinforced with GFRP to investigate its structural behaviour.

- Waste Toner foamed concrete might be reinforced with different materials such as CFRP bars or CFRP textiles and exploring hybrid solutions which could combine GFRP bars with another reinforcing type, such as mild steel or other FRP bars.
- Further investigation is required regarding testing FC samples under other types of static load (axial compression, torsion, combined axial and bending). Also, study the durability, fire resistance and the behaviour of FC beams under dynamic loads.
- Further investigation is required regarding the long-term behaviour of GFRP bars. The effect of creep is the main uncertainty in GFRP reinforced concrete design. This provides designers with more certainty and contributes to GFRP bar products being a more reliable and competitive alternative for steel reinforcing.

## References

- Abbood, I.S., Odaa, S.A., Hasan, K.F., Jasim, M.A., 2021. Properties evaluation of fiber reinforced polymers and their constituent materials used in structures - A review. *Mater. Today Proc.* 43, 1003–1008. <https://doi.org/10.1016/j.matpr.2020.07.636>
- Abedini, M., Akhlaghi, E., Mehrmashhadi, J., Mussa, M.H., Ansari, M., Momeni, T., 2017. Evaluation of Concrete Structures Reinforced with Fiber Reinforced Polymers Bars: A Review. *J. Asian Sci. Res.* 7, 165–175. <https://doi.org/10.18488/journal.2.2017.75.165.175>
- ACI-440, 2006. State-of-the-Art Report on Fiber Reinforced Plastic ( FRP ) Reinforcement for Concrete Structures Repo rted by ACI Committee 440. *ACI Comm.* 96, 1–68.
- ACI-440, 2002. State-of-the-art report on fiber reinforced plastic (FRP) reinforcement for concrete structures 20, 1–68.
- ACI 318-05, 2004. Building code requirements for structural concrete and commentary (ACI 318R-05) report.
- ACI Committee 408, n.d. Bond and Development of Straight Reinforcing Bars in Tension.
- Aini, K., Sari, M., Rahim, A., Sani, M., 2017. Applications of Foamed Lightweight Concrete 01097, 1–5. <https://doi.org/10.1051/mateconf/20179701097>
- Akinpelu, M.A., Odeyemi, S.O., Olafusi, O.S., Muhammed, F.Z., 2018. Evaluation of splitting tensile and compressive strength relationship of self-compacting concrete. *J. King Saud Univ. - Eng. Sci.* <https://doi.org/10.1016/j.jksues.2017.01.002>
- Alhussainy, F., Hasan, H.A., Rogic, S., Neaz Sheikh, M., Hadi, M.N.S., 2016. Direct tensile testing of Self-Compacting Concrete. *Constr. Build. Mater.* 112, 903–906. <https://doi.org/10.1016/j.conbuildmat.2016.02.215>
- Alkurdi, N.M., Mohammad, F.A., Klalib, H.A., 2020. Mechanical properties and direct tensile strength of waste toner foamed concrete. *J. Adv. Civ. Eng. Pract. Res.* 11, 11.

- Alsubari, B., Shafigh, P., Jumaat, M., 2015. Development of Self-Consolidating High Strength Concrete Incorporating Treated Palm Oil Fuel Ash. *Materials (Basel)*. 8, 2154–2173. <https://doi.org/10.3390/ma8052154>
- Amran, Y.H.M., Farzadnia, N., Ali, A.A.A., 2015a. Properties and applications of foamed concrete; a review. *Constr. Build. Mater.* 101, 990–1005. <https://doi.org/10.1016/j.conbuildmat.2015.10.112>
- Amran, Y.H.M., Farzadnia, N., Ali, A.A.A., 2015b. Properties and applications of foamed concrete; A review. *Constr. Build. Mater.* 101, 990–1005. <https://doi.org/10.1016/j.conbuildmat.2015.10.112>
- Ashour, A.F., 2006. Flexural and shear capacities of concrete beams reinforced with GFRP bars. *Constr. Build. Mater.* 20, 1005–1015. <https://doi.org/10.1016/j.conbuildmat.2005.06.023>
- Ashrafian, A., Shokri, F., Taheri Amiri, M.J., Yaseen, Z.M., Rezaie-Balf, M., 2020. Compressive strength of Foamed Cellular Lightweight Concrete simulation: New development of hybrid artificial intelligence model. *Constr. Build. Mater.* 230, 117048. <https://doi.org/10.1016/j.conbuildmat.2019.117048>
- ASTM C496-96, 1996. Standard Test Method for Splitting Tensile Strength of Cylindrical Concrete Specimens. *ASTM Int.* West Conshohocken, PA 04, 1–4.
- Awang, H., Aljoumaily, Z.S., Noordin, N., 2014. The Mechanical Properties of Foamed Concrete containing Un-processed Blast Furnace Slag 4, 1–9. <https://doi.org/10.1051/mateconf/20141501034>
- Aydin, F., 2018. Experimental investigation of thermal expansion and concrete strength effects on FRP bars behavior embedded in concrete. *Constr. Build. Mater.* 163, 1–8. <https://doi.org/10.1016/j.conbuildmat.2017.12.101>
- Babbitt, F., Barnett, R.E., Cornelius, M.L., Dye, B.T., Liotti, D.L., 2014. Guide for Cellular Concretes. *ACI Comm.* 523 3.
- Babu, D.S., 2008a. Mechanical and deformational properties, and shrinkage cracking

- behaviour of lightweight concretes. *Natl. Univ. Singapore* 49, 69–73.
- Babu, D.S., 2008b. Mechanical and deformational properties, and shrinkage cracking behaviour of lightweight concretes. *Natl. Univ. Singapore*.
- Benmokrane, B., Mousa, S., Mohamed, K., Sayed-Ahmed, M., 2021. Physical, mechanical, and durability characteristics of newly developed thermoplastic GFRP bars for reinforcing concrete structures. *Constr. Build. Mater.* 276, 122200. <https://doi.org/10.1016/j.conbuildmat.2020.122200>
- Benzecry, V., Brown, J., Al-Khafaji, A., Haluza, R., Koch, R., Nagarajan, M., Bakis, C.E., Myers, J.J., Nanni, A., 2019. Durability of GFRP Bars Extracted from Bridges with 15 to 20 Years of Service Life. *Strateg. Dev. Counc. Am. Concr. Inst.*
- Bilek, V., Bonczková, S., Hurta, J., Pytlík, D., Mrovec, M., 2017. Bond Strength between Reinforcing Steel and Different Types of Concrete. *Procedia Eng.* 190, 243–247. <https://doi.org/10.1016/j.proeng.2017.05.333>
- Bing, C., Ph, D., Ning, L., Ph, D., 2014. Experimental Research on Properties of Fresh and Hardened Rubberized Concrete. *J. Mater. Civ. Eng.* 26, 1–8. [https://doi.org/10.1061/\(ASCE\)MT.1943-5533.0000353](https://doi.org/10.1061/(ASCE)MT.1943-5533.0000353).
- Bing, C., Zhen, W., Ning, L., 2012. Experimental Research on Properties of High-Strength Foamed Concrete. *J. Mater. Civ. Eng.* 24, 113–118. [https://doi.org/10.1061/\(asce\)mt.1943-5533.0000353](https://doi.org/10.1061/(asce)mt.1943-5533.0000353)
- Bitiusca, L.-F., Clausen, J., 2016. Finite Element Modelling: Analysis of Reinforced Concrete Elements. *Sch. Eng. Sci. M.Sc. in S*, 62.
- Boulekbache, B., Hamrat, M., Chemrouk, M., Amziane, S., 2012. Influence of yield stress and compressive strength on direct shear behaviour of steel fibre-reinforced concrete. *Constr. Build. Mater.* 27, 6–14. <https://doi.org/10.1016/j.conbuildmat.2011.07.015>
- Brady, K.C., Watts, G.R. a., Jones, M.R., 2001. Specification for Foamed Concrete 78.
- BS-EN-12350, 2000. Testing fresh concrete Đ Part 6 : Density. October.

- BS:EN:1008:2002, 2002. Mixing water for concrete. Specification for sampling, testing and assessing the suitability of water, including water recovered from processes in the concrete industry, as mixing water for concrete. BSI Stand. 3.
- BS 1881-121, 1983. Testing concrete- Part 121: Method of Determination of Static Modulus of Elasticity in Compression, British Standards.
- BS 8110, 1985. Structural use of concrete. Part 1: Code of practice for design and construction.
- BS EN-12390-5, 2000. Testing Hardened Concrete- Part 5: Flexural Strength of Test Specimens, British Standards Institution, London,.
- BS EN 12350-6, 2009. Testing fresh concrete - Part 6: Density.
- BS EN 12390-3, 2009. Testing hardened concrete- Part 3: Compressive strength of test specimens.
- BS EN 12390-5, 2009. Testing hardened concrete- part 5: Flexural Strength Test. Constr. Stand. 2, 1–14. <https://doi.org/10.1006/abio.1994.1569>
- BS EN 12390-6, 2009. Testing hardened concrete- Part 6: Tensile splitting strength of test specimens. Aberdeen's Concr. Constr. 38.
- BS EN 12620, 2009. Aggregates for concrete.
- BS EN 13263-1, 2009. Silica fume for concrete - Part 1: Definitions, requirements and conformity criteria 3.
- BS EN12390-3, 2002. Testing hardened concrete—Compressive strength of test specimens. British European Standards Specifications.
- Chai, H.W.D.P.L., 1999. Optimum mix proportioning of self-compacting concrete. Proceedings 37, 277–285.
- Ching, N.S., 2012. Potential Use of Aerated Lightweight Concrete for Energy Efficient Construction 470.
- Choi, S.-J., Yang, K.-H., Sim, J.-I., Choi, B.-J., 2014. Direct tensile strength of lightweight

- concrete with different specimen depths and aggregate sizes. *Constr. Build. Mater.* 63, 132–141. <https://doi.org/10.1016/j.conbuildmat.2014.04.055>
- Chun, Y., Claisse, P., Naik, T.R., Ganjian, E., 2007. Sustainable Construction Materials and Technologies, International Conference on Sustainable Construction Materials and Technologies, 11–13 June, 2007, Coventry, Uk.
- Committee, A., 2003. ACI 213R-03, Guide for Structural Lightweight-Aggregate Concrete, ACI COMMITTEE REPORT 1–4.
- Craeye, B., Van Itterbeeck, P., Desnerck, P., Boel, V., De Schutter, G., 2014. Modulus of elasticity and tensile strength of self-compacting concrete: Survey of experimental data and structural design codes. *Cem. Concr. Compos.* 54, 53–61. <https://doi.org/10.1016/j.cemconcomp.2014.03.011>
- Dassault Systèmes, 2014. Analysis User's Guide: Volume III: Materials. ABAQUS 6.14 Anal. User's Guid. III, 294.
- De Villiers, J., 2015. Bond behaviour of deformed steel in lightweight foamed concrete.
- Deolalkar, S.P., 2016. Green Buildings. *Des. Green Cem. Plants* 215–220. <https://doi.org/10.1016/B978-0-12-803420-0.00032-9>
- Dijk, S. Van, 2002. Foam concrete : A different kind of mix.
- Dong, S.F., Zhang, W., 2013. Study on Foaming Agent Foam Ability and Stability for Foam Concrete. *Appl. Mech. Mater.* 357–360, 1304–1307. <https://doi.org/10.4028/www.scientific.net/AMM.357-360.1304>
- El-Nemr, A., Ahmed, E.A., El-Safty, A., Benmokrane, B., 2018. Evaluation of the flexural strength and serviceability of concrete beams reinforced with different types of GFRP bars. *Eng. Struct.* 173, 606–619. <https://doi.org/10.1016/j.engstruct.2018.06.089>
- Engineering, S., 2005. Fibre-reinforced Concrete for Industrial Construction, Technology.
- Falade, F., Ikponmwosa, E., Fapohunda, C., 2014. Flexural performance of foam concrete containing pulverized bone as partial replacement of cement. *Maejo Int. J. Sci. Technol.*

8, 20–31.

- Falade, F., Ikponmwosa, E., Fapohunda, C., 2013. A Study on the Compressive and Tensile Strength of Foamed Concrete Containing Pulverized Bone as a Partial Replacement of Cement. *J. Engg. Appl. Sci* 13, 82–93.
- Falliano, D., Restuccia, L., Ferro, G.A., Gugliandolo, E., 2020. Strategies to increase the compressive strength of ultra-lightweight foamed concrete. *Procedia Struct. Integr.* 28, 1673–1678. <https://doi.org/10.1016/j.prostr.2020.10.141>
- Fico, R., Prota, A., Manfredi, G., 2008. Assessment of Eurocode-like design equations for the shear capacity of FRP RC members. *Compos. Part B Eng.* 39, 792–806. <https://doi.org/10.1016/j.compositesb.2007.10.007>
- Fouad H, 2007. What is Cellular Concrete... and if It is So Great, Why Doesn't Everyone Use it? *Smart Foam Liq. Conc. Solut. Ser.*
- GangaRao, H.V.S., Taly, N., Vijay, P. V., 2006. Reinforced Concrete Design with FRP Composites, Reinforced Concrete Design with FRP Composites. <https://doi.org/10.1201/9781420020199>
- Gangatire, O.S., Suryawanshi, Y.R., 2016. Structural Behaviour of Lightweight concrete with Conventional Concrete 6, 635–638.
- Ghorbani, Saeid, Sharifi, S., de Brito, J., Ghorbani, Sahar, Jalayer, M.A., Tavakkolizadeh, M., 2019. Using statistical analysis and laboratory testing to evaluate the effect of magnetized water on the stability of foaming agents and foam concrete. *Constr. Build. Mater.* 207, 28–40. <https://doi.org/10.1016/j.conbuildmat.2019.02.098>
- Habsya, C., Diharjo, K., Setyono, P., Satwiko, P., 2018. Study of Characteristic Physical and Mechanic of Foamed Lightweight Concrete with Fly Ash Added for Wall Materials 5, 27–33.
- Halverson, M, M.Rosenberg, W.Wang, J. Zhang, V.Mendon, R.Athalye, Y Xie, R.Hart, S.G., 2014. ANSI / ASHRAE / IES Standard 90.1-2013. Determination of Energy Savings : Quantitative Analysis.

- Hama, S.M., 2017. Improving mechanical properties of lightweight Porcelanite aggregate concrete using different waste material. *Int. J. Sustain. Built Environ.* 6, 81–90. <https://doi.org/10.1016/j.ijbsbe.2017.03.002>
- Hamad, A.J., 2014. Materials, Production, Properties and Application of Aerated Lightweight Concrete: Review. *Int. J. Mater. Sci. Eng.* 2, 152–157. <https://doi.org/10.12720/ijmse.2.2.152-157>
- Harmon, K., 2010. Engineering Properties Of Structural Lightweight Concrete 11.
- Hashim, A.A., 2014. The Preparation of Foam Cement and Determining Some of Its Properties 3, 61–69.
- Hashim, M., Tantray, M., 2021. Comparative study on the performance of protein and synthetic-based foaming agents used in foamed concrete. *Case Stud. Constr. Mater.* 14, e00524. <https://doi.org/10.1016/j.cscm.2021.e00524>
- Hendriks, M., Boer, A. de, Belletti, B., 2016. Guidelines for Nonlinear Finite Element Analysis of Concrete Structures 65.
- Hickinbotham, A., 2016. Bond Behaviour of Glass Fibre Reinforced Polymer ( GRP ) Reinforcing Bars Using the Pull-out Test.
- Hilal, A., Nicholas, H., Andrew, R., 2015. The Use of Additives to Enhance Properties of Pre-Formed Foamed Concrete. *Int. J. Eng. Technol.* 7. <https://doi.org/10.7763/IJET.2015.V7.806>
- Hilal, A.A., 2015a. Properties and Microstructure of Pre-formed Foamed Concretes Properties and Microstructure of Pre-formed Foamed Concretes By Thesis submitted to the University of Nottingham for the degree of Doctor of Philosophy. <https://doi.org/10.13140/RG.2.1.3983.3768>
- Hilal, A.A., 2015b. Properties and Microstructure of Pre-formed Foamed Concretes. <https://doi.org/10.13140/RG.2.1.3983.3768>
- Hoffmann, S.O., 2016. University of Bradford eThesis This thesis is hosted in Bradford Scholars – The University of Bradford Open Access.

- Hosen, M.A., Alengaram, U.J., Jumaat, M.Z., Sulong, N.H.R., Darain, K.M. ud, 2017. Glass Fiber Reinforced Polymer (GFRP) Bars for Enhancing the Flexural Performance of RC Beams Using Side-NSM Technique. *Polymers (Basel)*. 9, 180. <https://doi.org/10.3390/polym9050180>
- Hu, C., Li, H., Liu, Z., Wang, Q., 2016. Research on properties of foamed concrete reinforced with small sized glazed hollow beads. *Adv. Mater. Sci. Eng.* 2016. <https://doi.org/10.1155/2016/5820870>
- Huiskes, D.M.A., Keulen, A., Yu, Q.L., Brouwers, H.J.H., 2016. Design and performance evaluation of ultra-lightweight geopolymer concrete. *Mater. Des.* 89, 516–526. <https://doi.org/10.1016/j.matdes.2015.09.167>
- Hulusi, O., Gholampour, A., Gencel, O., Ozbakkaloglu, T., 2020. Physical and mechanical properties of foam concretes containing granulated blast furnace slag as fine aggregate. *Constr. Build. Mater.* 238, 117774. <https://doi.org/10.1016/j.conbuildmat.2019.117774>
- Ikponmwosa, E., Fapohunda, C., Kolajo, O., Eyo, O., 2017. Structural behaviour of bamboo-reinforced foamed concrete slab containing polyvinyl wastes (PW) as partial replacement of fine aggregate. *J. King Saud Univ. - Eng. Sci.* 29, 348–355. <https://doi.org/10.1016/j.jksues.2015.06.005>
- Iqbal, M., Zhang, D., Jalal, F.E., Faisal, M., 2021. Computational AI prediction models for residual tensile strength of GFRP bars aged in the alkaline concrete environment. *Ocean Eng.* 232, 109134. <https://doi.org/10.1016/j.oceaneng.2021.109134>
- Jalal, M., Tanveer, A., Jagdeesh, K., Ahmed., F., 2017. *Foam Concrete* 8.
- Johnson, D., 2009. Investigation of Glass Fibre Reinforced Polymer Reinforcing Bars as Internal Reinforcement for Concrete Structures. Thesis 1–174.
- Jones, M.R., McCarthy, A., 2005. Preliminary views on the potential of foamed concrete as a structural material. *Mag. Concr. Res.* 57, 21–31. <https://doi.org/10.1680/macrcr.2005.57.1.21>

- Jones, M.R., Ozlutas, K., Zheng, L., 2016. Stability and instability of foamed concrete. *Mag. Concr. Res.* 68, 542–549. <https://doi.org/10.1680/mac.15.00097>
- Jones, R., McCarthy, A., Kharidu, S., Nicol, L., 2005a. Foamed concrete developments and applications. *Concr.* 39, 41–43.
- Jones, R., McCarthy, A., Kharidu, S., Nicol, L., 2005b. Foamed concrete developments and applications. *Concr.* 39, 41–43.
- Jose, S.K., Soman, M., Evangeline, Y.S., 2021. Influence of mixture composition on the properties of foamed concrete. *Mater. Today Proc.* 42, 399–404. <https://doi.org/10.1016/j.matpr.2020.09.592>
- Junaid, M.T., Elbana, A., Altoubat, S., Al-Sadoon, Z., 2019. Experimental study on the effect of matrix on the flexural behavior of beams reinforced with Glass Fiber Reinforced Polymer (GFRP) bars. *Compos. Struct.* 222, 110930. <https://doi.org/10.1016/j.compstruct.2019.110930>
- Kara, I.F., Ashour, A.F., 2012. Flexural performance of FRP reinforced concrete beams. *Compos. Struct.* 94, 1616–1625. <https://doi.org/10.1016/j.compstruct.2011.12.012>
- Kearsley, E.P., Wainwright, P.J., 2001. Porosity and permeability of foamed concrete. *Cem. Concr. Res.* 31, 805–812. [https://doi.org/10.1016/S0008-8846\(01\)00490-2](https://doi.org/10.1016/S0008-8846(01)00490-2)
- Kemp, M., Blowes, D., 2011. Concrete reinforcement and glass fibre reinforced polymer. *Queensl. Roads* 40–48.
- Khan, Q.S., Sheikh, M.N., McCarthy, T.J., Robati, M., Allen, M., 2019. Experimental investigation on foam concrete without and with recycled glass powder: A sustainable solution for future construction. *Constr. Build. Mater.* 201, 369–379. <https://doi.org/10.1016/j.conbuildmat.2018.12.178>
- Khaw, Y.H., 2010. Performance of Lightweight Foamed Concrete Using Laterite as Sand Replacement. *Fac. Civ. Eng. Earth Resour. Univ. Malaysia Pahang* i–67. <https://doi.org/10.1017/CBO9781107415324.004>
- Kim, H., Kim, M.S., Ko, M.J., Lee, Y.H., 2015. Shear Behavior of Concrete Beams Reinforced

- with GFRP Shear Reinforcement. *Int. J. Polym. Sci.* 2015. <https://doi.org/10.1155/2015/213583>
- Kong, S.Y., Wong, L.S., Paul, S.C., Miah, M.J., 2020. Shear response of glass fibre reinforced polymer (Gfrp) built-up hollow and lightweight concrete filled beams: An experimental and numerical study. *Polymers (Basel)*. 12, 1–14. <https://doi.org/10.3390/polym12102270>
- Kong, S.Y., Yang, X., Lee, Z.Y., 2018. Mechanical performance and numerical simulation of GFRP-concrete composite panel with circular hollow connectors and epoxy adhesion. *Constr. Build. Mater.* 184, 643–654. <https://doi.org/10.1016/j.conbuildmat.2018.07.008>
- Kosmatka, 2015. Concrete reinforced with polypropylene fibers 4, 45–49.
- Krasniqi, C., Kabashi, N., Krasniqi, E., Kaqi, V., 2018. Comparison of the behavior of GFRP reinforced concrete beams with conventional steel bars. *Pollack Period.* 13, 141–150. <https://doi.org/10.1556/606.2018.13.3.14>
- Krishna, A.S., Siempu, R., Kumar, G.A.V.S.S., 2021. Materials Today : Proceedings Study on the fresh and hardened properties of foam concrete incorporating fly ash. *Mater. Today Proc.* <https://doi.org/10.1016/j.matpr.2021.03.599>
- Kudyakov, A.I., Kopanitsa, N.O., Sarkisov, J.S., Kasatkina, A. V, Prischepa, I.A., 2015. Foam concrete of increased strength with the thermomodified peat additives. *IOP Conf. Ser. Mater. Sci. Eng.* 71, 012012. <https://doi.org/10.1088/1757-899X/71/1/012012>
- KUM, Y., 2011. Cracking Mode and Shear Strength of Lightweight Concrete Beams.
- Kumar, R., Lakhani, R., Tomar, P., 2018. A simple novel mix design method and properties assessment of foamed concretes with limestone slurry waste. *J. Clean. Prod.* 171, 1650–1663. <https://doi.org/10.1016/j.jclepro.2017.10.073>
- Lee, H.-S., Ismail, M., Woo, Y.-J., Min, T.-B., Choi, H.-K., 2014. Fundamental Study on the Development of Structural Lightweight Concrete by Using Normal Coarse Aggregate and Foaming Agent. *Materials (Basel)*. 7, 4536–4554.

<https://doi.org/10.3390/ma7064536>

- Lee, Y.L., Tan, C.S., Saggaff, A., Md Tahir, M., Raupit, F., 2017. Splitting Tensile Strength of Lightweight Foamed Concrete with Polypropylene Fiber. *Int. J. Adv. Sci. Eng. Inf. Technol.* 7, 424. <https://doi.org/10.18517/ijaseit.7.2.2096>
- Lesovik, V., Voronov, V., Glagolev, E., Fediuk, R., Alaskhanov, A., Amran, Y.H.M., Murali, G., Baranov, A., 2020. Improving the behaviors of foam concrete through the use of composite binder. *J. Build. Eng.* 31, 101414. <https://doi.org/10.1016/j.jobbe.2020.101414>
- Marco, I.V., 2015. Bond-Slip and Cracking Behaviour of Glass Fibre Reinforced Polymer Reinforced Concrete Tensile Members B Ond - Slip and Cracking Behaviour of.
- Markin, V., Nerella, V.N., Schröfl, C., Guseynova, G., Mechtcherine, V., 2019. Material design and performance evaluation of foam concrete for digital fabrication. *Materials (Basel)*. 12. <https://doi.org/10.3390/ma12152433>
- Meera, M., Gupta, S., 2020. Development of a strength model for foam concrete based on water – Cement ratio. *Mater. Today Proc.* 32, 923–927. <https://doi.org/10.1016/j.matpr.2020.04.888>
- Mehta, M. and, 2017. Development of foamed concrete.
- Mohamad, N., Khalil, A.I., Abdul Samad, A.A., Goh, W.I., 2014. Structural behavior of precast lightweight foam concrete sandwich panel with double shear truss connectors under flexural load. *ISRN Civ. Eng.* 2014. <https://doi.org/10.1155/2014/317941>
- Mohammad, M., 2011. Development of foamed concrete : enabling and supporting design.
- Mohammed, J.H., Hamad, A.J., 2014. A classification of lightweight concrete : materials , properties and application review 7, 52–57.
- Muñoz, M.B., 2010. Study of bond behaviour between FRP reinforcement and concrete, Thesis.
- Nanni, A., De Luca, A., Zadeh, H., 2014. Reinforced Concrete with FRP Bars: Mechanics and

- Design, Reinforced Concrete with FRP Bars: Mechanics and Design.
- Neville, A., 2011. *Properties of Concrete*, 4th. London: Pitman Publishing.
- Ng, P.L., Barros, J.A.O., Kaklauskas, G., Lam, J.Y.K., 2020. Deformation analysis of fibre-reinforced polymer reinforced concrete beams by tension-stiffening approach. *Compos. Struct.* 234. <https://doi.org/10.1016/j.compstruct.2019.111664>
- Norasyikin Bt. Md., 2009. Production of foamed concrete with a method of mixing. *Prod. Foam. Concr. with a method Mix.*
- Othuman Mydin, M.A., 2010. Lightweight Foamed Concrete ( Lfc ) Thermal and Mechanical Properties At Elevated Temperatures and Its Application To Composite Walling System.
- Ozlutas, K., 2015. Behaviour of ultra - Low density foamed concrete 1.
- Pilakoutas, K., Neocleous, K., Guadagnini, M., 2002. Design Philosophy Issues of Fiber Reinforced Polymer Reinforced Concrete Structures. *J. Compos. Constr.* 6, 154–161. [https://doi.org/10.1061/\(asce\)1090-0268\(2002\)6:3\(154\)](https://doi.org/10.1061/(asce)1090-0268(2002)6:3(154))
- Pirela, S. V., Sotiriou, G.A., Bello, D., Shafer, M., Bunker, K.L., Castranova, V., Thomas, T., Demokritou, P., 2015. Consumer exposures to laser printer-emitted engineered nanoparticles: A case study of life-cycle implications from nano-enabled products. *Nanotoxicology* 9, 760–768. <https://doi.org/10.3109/17435390.2014.976602>
- Pour, S.M., Alam, M.S., Milani, A.S., 2016. Improved bond equations for fiber-reinforced polymer bars in concrete. *Materials (Basel)*. 9, 1–14. <https://doi.org/10.3390/ma9090737>
- Prabha, P., Palani, G.S., Lakshmanan, N., Senthil, R., 2017. Behaviour of steel-foam concrete composite panel under in-plane lateral load. *J. Constr. Steel Res.* 139, 437–448. <https://doi.org/10.1016/j.jcsr.2017.10.002>
- Quayyum, S., Rteil, A., 2012. Advances in FRP Composites in Civil Engineering. *Adv. FRP Compos. Civ. Eng.* <https://doi.org/10.1007/978-3-642-17487-2>
- Rafey, M. El, Mulhem, R. Al, 2016. Sustainable Construction Materials in ( Bait Al- Sha ' r )

and Modern Trends in Saudi Arabia.

- Raj, A., Sathyan, D., Mini, K.M., 2019. Physical and functional characteristics of foam concrete: A review. *Constr. Build. Mater.* 221, 787–799. <https://doi.org/10.1016/j.conbuildmat.2019.06.052>
- Ramamurthy, K., Nambiar, K., 2009. A classification of studies on properties of foam concrete. *Cem. Concr. Compos.* 31, 388–396. <https://doi.org/10.1016/j.cemconcomp.2009.04.006>
- Resan, S.F., Chassib, S.M., Zemam, S.K., Madhi, M.J., 2020. New approach of concrete tensile strength test. *Case Stud. Constr. Mater.* 12, 1–13. <https://doi.org/10.1016/j.cscm.2020.e00347>
- RILEM TC5-RC, 1982. Performance of glass fiber reinforced plastic bars as a reinforcing material for concrete structures. *CRILEM State-of-the-Art Reports* 31, 555–567. [https://doi.org/10.1016/S1359-8368\(99\)00049-9](https://doi.org/10.1016/S1359-8368(99)00049-9)
- RILEM TC9-RC, 1983. Introduction, *RILEM State-of-the-Art Reports*. [https://doi.org/10.1007/978-94-017-7336-2\\_1](https://doi.org/10.1007/978-94-017-7336-2_1)
- Roberts, G.D., 2015. Simplified Method To Nonlinear Analysis of Reinforced Concrete in Pure Flexure.
- Sabău, M., Oneț, T., 2011. Nonlinear concrete behaviour. *J. Appl. Eng. Sci.* 1, 55–60. <https://doi.org/10.6084/m9.figshare.3483020>
- Saidani, M., Ogbologugo, U., Coakley, E., George, S., 2016. Lightweight cementitious (GEM-TECH ) structural material. *Proc. Int. Congr. Technol. Concr. Durab.* 186–195.
- Sataloff, R.T., Johns, M.M., Kost, K.M., 2019. Nonlinear Finite Element Analysis of Composite and Reinforced Concrete Beams.
- Shakir Abbood, I., Odaa, S.A., Hasan, K.F., Jasim, M.A., 2020. Properties evaluation of fiber reinforced polymers and their constituent materials used in structures - A review. *Mater. Today Proc.* 43, 1003–1008. <https://doi.org/10.1016/j.matpr.2020.07.636>

- Shawnim, P.A., Mohammad, F., 2018. Toner Used in the Development of Foamed Concrete for structural use. 9, 27–33.
- Silva, B. V., Barbosa, M.P., Silva Filho, L.C.P.D., Lorrain, M.S., 2014. Experimental investigation on the use of steel-concrete bond tests for estimating axial compressive strength of concrete : Part 1. *Ibracon Struct. Mater. J.* 6, 715–725. <https://doi.org/10.1590/S1983-41952013000500003>
- Slag Cement Association, S., 2013. Compressive and Flexural Strength. *Concrete* 91, 489–493. <https://doi.org/10.4028/www.szent>
- Sldozian, R.J., Tkachev, A.G., Burakova, I. V., Mikhaleva, Z.A., 2021. Improve the mechanical properties of lightweight foamed concrete by using nanomodified sand. *J. Build. Eng.* 34. <https://doi.org/10.1016/j.jobee.2020.101923>
- Stoner, J.G., Polak, M.A., 2020. Finite element modelling of GFRP reinforced concrete beams. *Comput. Concr.* 25, 369–382. <https://doi.org/10.12989/cac.2020.25.4.369>
- Tan, J.H., Lim, S.K., Lim, J.H., Tunku, U., Rahman, A., Lumpur, K., 2013. Flexural Behaviour of Reinforced Lightweight Foamed Concrete Beams 1, 1–6.
- Thatcher, D.B., Heffington, J.A., Kolozs, R.T., Iii, G.S.S., Breen, J.E., Burns, N.H., River, R., 2002. Structural Lightweight Concrete Prestressed Girders and Panels September 2001 Revised January 2002 Research Report 1852-1 Center for Transportation Research The University of Texas at Austin Austin , TX 78705-2650 Research Project 0-1852 Texas Department 7.
- Trevor, Gideon, A., 2018. Investigating a reinforced lightweight foamed concrete walling system for low-rise residential buildings in moderate seismic regions. *J. Build. Eng.* 20, 663–670. <https://doi.org/10.1016/j.jobee.2018.09.011>
- Wahyuni, A.S., 2012. Structural Characteristics of Reinforced Concrete Beams and Slabs with Lightweight Blocks Infill.
- Wang, W.L., Kou, S.C., Xing, F., 2013. Deformation properties and direct shear of medium strength concrete prepared with 100% recycled coarse aggregates. *Constr. Build.*

- Mater. 48, 187–193. <https://doi.org/10.1016/j.conbuildmat.2013.06.065>
- Wang, X., Huang, J., Dai, S., Ma, B., Jiang, Q., 2020. Investigation of silica fume as foam cell stabilizer for foamed concrete. *Constr. Build. Mater.* 237, 117514. <https://doi.org/10.1016/j.conbuildmat.2019.117514>
- Warner, K.W.W.R.F., 1997. Non-linear Analysis of Concrete Frames using a Direct Stiffness Line Element Approach. Res. Rep. No. R 158 Novemb. 1997 ISBN 0-86396-599-7.
- World Steel Association, 2020. STEEL ' S CONTRIBUTION TO A LOW CARBON FUTURE AND CLIMATE RESILIENT SOCIETIES worldsteel position paper. World Steel Assoc. 1–6.
- Worner, V.J., 2015. Use of Glass Fibre Reinforced Polymer ( GFRP ) reinforcing bars for concrete bridge decks.
- Xingyu, G., Yiqing, D., Jiwang, J., 2020. Flexural behavior investigation of steel-GFRP hybrid-reinforced concrete beams based on experimental and numerical methods. *Eng. Struct.* 206, 110117. <https://doi.org/10.1016/j.engstruct.2019.110117>
- Yalciner, H., Eren, O., Sensoy, S., 2012. An experimental study on the bond strength between reinforcement bars and concrete as a function of concrete cover, strength and corrosion level. *Cem. Concr. Res.* 42, 643–655. <https://doi.org/10.1016/j.cemconres.2012.01.003>
- Yan, F., Lin, Z., Yang, M., 2016. Bond mechanism and bond strength of GFRP bars to concrete: A review. *Compos. Part B Eng.* 98, 56–69. <https://doi.org/10.1016/j.compositesb.2016.04.068>
- Yao, X., Wang, W., Liu, M., Yao, Y., Wu, S., 2019. Synergistic use of industrial solid waste mixtures to prepare ready-to-use lightweight porous concrete. *J. Clean. Prod.* 211, 1034–1043. <https://doi.org/10.1016/j.jclepro.2018.11.252>
- Yoo, S.Y., Lee, J.H., Shin, H.J., Park, C.G., 2019. Mechanical and fracture properties of steel/gfrp hybrid panels for an improved moveable weir after exposure to accelerated natural environmental conditions. *Appl. Sci.* 9, 8–11. <https://doi.org/10.3390/app9071423>

## References

---

Young, L.R., Darlington, S.J., 2016. MPhil / PhD Transfer Report. Computing 1–42.

Zhang, Y., Chen, D., Qu, K., Lu, K., Chen, S., Kong, M., 2020. Study on engineering properties of foam concrete containing waste seashell. *Constr. Build. Mater.* 260, 119896. <https://doi.org/10.1016/j.conbuildmat.2020.119896>

Zhuang, C., Chen, Y., 2019. The effect of nano-SiO<sub>2</sub> on concrete properties: A review. *Nanotechnol. Rev.* 8, 562–572. <https://doi.org/10.1515/ntrev-2019-0050>

## Appendix A: Foamed Concrete Mix Design

Mix number	Mix 1 -1600				
					for 70 L
Target Density	kg/m3	1200		Target plastic Density	1800 kg/m3
Cement (initail)	kg/m3	400			
% of replaced of silica fume from cement	%	10.00		CEMENT	25.2 KG
Silica Fume/toner (15% of Cement) replace	kg/m3	40		SAND	42 KG
Cement (final)	kg/m3	360		WATER	14 KG
Binder (Cement + Silica Fume)	kg/m3	400		FOAM NEEDED	31.4386 L
Water / Binder	Ratio	0.5		SF/MK/ Toner	2.8 KG
water	kg/m3	200			
% of Binder super plasticiser	%	0		1 to 1	
super plasticiser (1.5% of Binder)	kg/m3	0		cement	480
Sand (Initail)	kg/m3	600		sand	480
% of Fly Ash replacement of sand	%	0		water	240
	kg/m3	0			1200
Sand (Final)	kg/m3	600			
water added	kg/m3	0	Absorption	1 to 1.5	
Water Corrected	kg/m3	200		cement	400
Water / Binder (Final)	Ratio	0.5		sand	600
				water	200
					1200
Densities					
Specific Gravity of Cement	kg/m3	3150		1 to 2	
Specific Gravity of Silica Fume	kg/m3	2100		cement	342.8571
Specific Gravity of Sand	kg/m3	2500		sand	685.7143
Specific Gravity of Fly Ash	kg/m3	2090		water	171.4286
Unit weight of water	kg/m3	1000			1200
Specific Gravity of Foaming Agent	kg/m3	1050		1 to 0.5	
Unit weight of Foam	kg/m3	45		cement	600
super plasticiser	kg/m3	1100		sand	300
				water	300
					1200
Volumes					
Cement	m3	0.11428571			
Silica Fume	m3	0.01904762		1 to 1.5	
water	m3	0.2		cement	400
Sand	m3	0.24		sand	600
Fly Ash	m3	0		water	200
super plasticiser	m3	0			1200
Air Volume required	m3	0.42666667	426.666667	liter	
Total		1			

## Appendix

foam volume		m3	0.44912281		
foam needed		Liter	449.122807		
amount of foaming agent needed to produce x liter foam		ml	359.298246		
weight of the foaming agent (0.8* foam volume needed)		kg	0.35929825		
amount of water needed to foam		gram	20210.5263		
weight of the water needed to produce x liter foam		kg	20.2105263		
1 M3	mix	w/b	0.5		
Cement		kg	360		
Silica Fume		kg	40		
water		kg	200		
Sand		kg	600		
Fly Ash		kg	0		
super plasticiser		kg	0		
Foam		Liter	426.666667		
	0.004	mix volume m3			
Cement		kg	1		
Silica Fume		kg	0.16		
water		kg	0.8	0.31	w/b
Sand		kg	2.4		
Fly Ash		kg	0		
super plasticiser		kg	0		
Foam		Liter	1.70666667		
Design Density			1200		
Mix Volume	0.004 m3	w/b	0.5		
Cement		Gram	1000		
Silica Fume		Gram	160		
water		Gram	800		
Sand		Gram	2400		
Fly Ash		Gram	0	0.5	w/b
super plasticiser		Gram	0		
Foam		Liter	1.70666667		
measured density			1318		
design density			1200		

## Appendix B: Glass Fiber Reinforced Polymer GFRP Properties

Diameter (mm)	Cross Section (mm <sup>2</sup> )	Density (g/cm <sup>3</sup> )	Weight (g/m)	Ultimate Tensile(KN)	Ultimate Tensile Strength(Mpa)	Ultimate Shear Strength(Mpa)	E-modult (GPa)
3	7	2.2	18	13.5	1900	>150	>40
4	12	2.2	32	18	1500	>150	>40
6	28	2.2	51	36	1280	>150	>40
8	50	2.2	98	54	1080	>150	>40
10	73	2.2	150	72	980	>150	>40
12	103	2.1	210	99	870	>150	>40
14	134	2.1	275	117	764	>150	>40
16	180	2.1	388	149	752	>150	>40
18	248	2.1	485	189	744	>150	>40
20	278	2.1	570	225	716	>150	>40
22	355	2.1	700	270	695	>150	>40
25	478	2.1	970	342	675	>150	>40
28	590	2.1	1195	432	702	>150	>40
30	671	2.1	1350	450	637	>150	>40
32	740	2.1	1520	504	626	>150	>40
34	857	2.1	1800	540	595	>150	>40
36	961	2.1	2044	585	575	>150	>40
40	1190	2.1	2380	640	509	>150	>40



F-C 0.0045  
 N-C 0.0035  
 N-C=F-C 0.002  
 $\epsilon_s$   
 $0.85f_{ck}/1.5$   
 $\alpha_1 f_{ck}$   
 $\alpha_2 x$   
 $\alpha_3 x$   
 $d - \alpha_2 x$   
 $C = \alpha_1 f_{ck} b x$   
 $T = f_s * A_s$

$\epsilon_c/x = \epsilon_s/(d-x)$  Then  
 $\epsilon_s = (0.0035 * (192-x))/x$   
 $f_s = E_s * \epsilon_s$   $((d/x)-1) \epsilon_c * E_s$   $\leq f_y$   
 T=C Where:  
 $C = \alpha_1 * f_{ck} * b * x = 2534.3 x$   
 $T = f_s * A_s = ((d/x)-1) \epsilon_c * E_s * A_s = 162777.6 ((d/x)-1)$   
 $T=C$   
 $2534.25925925926x^2 + 162777.6x - 31253299.2 = 0$

lift	right
-5463816.91	0

$x = 73.7512$  mm ← by solver  
 Check  $f_s$   
 $f_s = 432.90$  If  $> 1000$  Take  $x = 237.892$  mm  
 $x = 73.751$   
 $C = 186904.64$   
 $T = 260989.10$  #  
 $M = (T \text{ or } C) * Z = 29.926$  kN.m  
 Ultimat Load = 105.0 kN

52.5 52.5

From strain digram at balance,